Multi-scale analysis of solute transport in steady and oscillatory flows with boundary reactions

by

Swarup Barik

DEPARTMENT OF MATHEMATICS
INDIAN INSTITUTE OF TECHNOLOGY GUWAHATI
GUWAHATI-781039, INDIA
May, 2019

Multi-scale analysis of solute transport in steady and oscillatory flows with boundary reactions

A Thesis Submitted in Partial Fulfillment of the Requirements for the Degree of

Doctor of Philosophy

by

Swarup Barik

(Roll No. - 126123016)

DEPARTMENT OF MATHEMATICS
INDIAN INSTITUTE OF TECHNOLOGY GUWAHATI
GUWAHATI-781039, INDIA

May, 2019

Dedicated To My Parents

Shri. Swapan Barik
&
Smt. Kalpana Barik

Declaration

I do hereby declare that this thesis entitled **Multi-scale analysis of solute transport in steady and oscillatory flows with boundary reactions** is a presentation of my original research work done under the supervision of **Dr. D. C. Dalal**, Professor, Department of Mathematics, Indian Institute of Technology Guwahati for the award of the degree of Doctor of Philosophy and this work has not been submitted elsewhere for a degree.

May, 2019

Swarup Barik
Roll No. 126123016
Department of Mathematics
Indian Institute of Technology Guwahati

Certificate

It is to certify that the work contained in this thesis entitled **Multi-scale analysis of solute transport in steady and oscillatory flows with boundary reactions** has been carried out by **Swarup Barik**, a student in the Department of Mathematics, Indian Institute of Technology Guwahati, under my supervision for the award of the degree of Doctor of Philosophy and this work has not been submitted elsewhere for a degree.

May, 2019

Dr. Durga Charan Dalal
Professor
Department of Mathematics
Indian Institute of Technology Guwahati

Acknowledgements

First and foremost, I am very grateful to my supervisor Prof. Durga Charan Dalal for his generous guidance throughout the years. Also I would like to express my deep appreciation for his patience, understanding and support. He helped me to overcome many obstacles that emerged while working on several problems. In a good way, he always used to push for better results. He was deeply involved and helped me in every possible way. His continuous encouragement and advice made it possible for me to work on this thesis. I could not have imagined having a better advisor and mentor for my Ph.D study.

I would like to express my gratitude to my doctoral committee members, Prof. Swaroop Nandan Bora, Prof. Natesan Srinivasan and Dr. Arnab Kumar De for their encouragement, precious comments to improve my research work.

I would also like to convey my sincere thanks to Dr. Zi Wu, Tsinghua University and Dr. Ping Wang, Beijing Forestry University for their several valuable suggestions, insightful comments and continuous encouragement during my research tenure.

I am highly grateful to the Ministry of Human Resource Development, Government of India for the necessary financial supports. I sincerely acknowledge Indian Institute of Technology Guwahati for providing a very nice educational environment and all kinds of support. I am also grateful to all the staff members of the Department of Mathematics for their assistance in various ways during my research period.

I would like to thank my friends and colleagues Anirudha, Balasubramani, Hiranmoy, Ankur, Anirban, Abhishek, Anand, Sougata, Swapnendu, Sonjoy, Debu, Madhu, Devanand, Chitralekha Di, Koyel, Nilay, Abhijit, Kuldeep and many others for all their encouragement and support during this period. My special appreciation goes to my close friends Anupama, Somnath, Amitava, Bapan, Shantanu, Sourav, Bikash, Avik, Debraj, Subhendu with whom I have shared some of the best moments of my life.

I am extremely grateful to my parents, my younger brother (Sudip Barik) and all other family members for their love, concern, care, encouragement and moral support throughout my life. I would like to express my deepest gratitude to them for staying besides me all the time. Finally, I would like to acknowledge everybody who is important to the successful completion of the thesis as well as express my apology that I could not mention each of them individually.

May, 2019 **Swarup Barik**

ABSTRACT

Transport of a solute through a flowing solvent has several important applications in diverse fields, such as biology, chemistry, chromatography, environment fluid mechanics etc. Due to its importance in different fields, it has been a topic of interest since mid of twentieth century. In the available literature on solute transport during the last decades, the main focus was either to obtain the dispersion coefficient or to address the mean concentration distribution rather than the transverse concentration distribution. In some environmental or industrial processes, we need information not only on dispersion coefficients or the longitudinal mean concentration, but also on the transverse concentration distribution and its uniformity over the cross-section. Study of the transverse concentration distribution in steady or oscillatory flows has a great significance in estuaries and other coastal regions. Prediction of accurate pollutant distribution and peak pollutant concentration are of matter of concern. Also knowledge of the transport coefficients of solute transport under oscillation of the boundary is very useful in the hydrodynamic theory of lubrication. The influence of chemical reaction on solute transport has a great significance in blood flow through human arteries. This study also has importance regarding the shear-driven flows encountered in micro motors, micro channels and other micro fluidic systems.

The thesis work is aimed to provide analytical expressions for transport coefficients, mean concentration and transverse real concentration. Detailed study on transverse concentration distribution and its uniformity throughout the channel cross-section is also carried out.

The present thesis begins with a brief introduction along with the overview and objective on its topic. A fundamental concept of Taylor dispersion process is discussed. Further, we include the basic information and procedure of multi-scale method. This is followed by a brief description of reversible and irreversible boundary reactions. A detailed literature review of the topic is also presented. Five problems are studied in this thesis.

In the first work, an analytical study is presented to explore two-dimensional concentration distribution in an open channel flow with absorbing channel bed. Simple analytical expressions are derived for transverse concentration distribution with the help of multi-scale method of homogenization. This study explores mean and real concentration distributions after an initial time when transient behaviour completely dies out. In this study, effects of bed absorption on solution dispersion as well as on transverse uniformity are discussed. Results reveal that transverse concentration of the solute should be preferred over the mean concentration to analyse the absorption effect more accurately.

The next study explores two-dimensional concentration distribution in an open channel flow with reversible phase exchange kinetics between the channel bed and fluid phase. Simple analytical expressions for transverse concentration distribution are obtained with the help of multi-scale method of homogenization. This work explains the pattern of transverse real concentration distribution and uniformity over the cross-section of the channel. Effects of phase exchange parameters on solute dispersion are discussed. It is found that for slow phase exchange kinetics with small retentive channel bed, solute concentration distribution becomes uniform faster.

In the third work, an attempt is made to find analytical expressions for mean and transverse real concentrations by using a multi-scale homogenization technique and to explore the evolution of transverse concentration distribution for oscillatory Couette flows for inert boundary walls. Effects of Stokes boundary layer thickness on dispersion coefficient and transverse variation of concentration distribution are observed. The study also suggests a time scale that would be more appropriate to characterize the initial transition stage of the transport process to approach transverse uniformity.

In the forth endeavour, the solute is assumed to undergo reversible and irreversible reactions at the channel bed. Simple analytical expressions are derived for steady and oscillatory components of dispersion coefficients. Absorption induced dispersion coefficients are also found. It is seen that absorption induced dispersion coefficient can be negative unlike the leading order dispersion coefficients. Study also discusses the effects of Stokes boundary layer thickness along with the chemical reaction parameters, i.e., bed absorption parameter, retention parameter, Damkohler number on the solute dispersion.

Finally, the present thesis deals with a problem that discusses the effects of nonlinear chemical reaction on dispersion coefficients for an oscillatory Couette flow. A two-dimensional mathematical model is formulated by taking into account the chemical decay and a phase exchange kinetics between bulk phase and sorbet boundaries. The main purpose of this work is to visualize the effects of nonlinear chemical decay reactions and the roles of different factors or parameters on transport coefficients. This work reveals that increase in order of nonlinearity in mobile phase decay reduces the mass depletion in the flow and increase in order of nonlinearity in the immobile phase decay enhances the advection speed for large retention parameter.

NOMENCLATURE

Superscript

$\widehat{\cdot}$	Dimensional quantity
$\cdot^*$	Complex conjugate
$\overline{\cdot}$	Time average

Symbol

$\langle\cdot\rangle$	Sectional average
$O(\cdot)$	Bachmann-Landau order notation

Notation

C	Concentration of the solute in the fluid phase
C_s	Concentration of the solute in the stationary phase
$C^{(i)}$, $i = 0, 1, 2, \ldots$	Developed terms of the asymptotic expansion of C
D	Molecular diffusivity
D_T	Dispersion coefficient
D_{Ta}	Apparent dispersion coefficient
D_{Ts}	Steady component of the dispersion coefficient
D_{Tw}	Oscillatory component of the dispersion coefficient
$D_{Ts}^{\beta_m}$	Steady component of the bed absorption induced dispersion coefficient
$D_{Tw}^{\beta_m}$	Oscillatory component of the bed absorption induced dispersion coefficient
Da	Damkohler number
Da_1, Da_2	Damkohler number for lower and upper boundaries
h	Channel width
k $(= k_b)$	Reversible (or backward) rate constant
k_f	Forward rate constant
k_1, k_2	Reversible reaction rates at lower and upper boundaries

K_0	Reaction coefficient for linear decay reaction
K_1	Advection coefficient for linear decay reaction
l	Characteristic longitudinal length
m	Order of non-linearity of decay reaction at the boundary
n	Order of non-linearity of decay reaction in the flow
Pe	Peclet number
Q_m	Released mass of the injected solute
R	Retardation factor
$\mathcal{R}$	Transverse concentration variation rate
Sc	Schmidt number
t	Time variable
t_0, t_1, t_2	Fast, medium, slow time variables
T_p	Flow period
T_0, T_1, T_2	Time scale for lateral diffusion (basic time scale), advection, longitudinal diffusion
T_r	Ratio of basic time scale to flow period
U	Steady component of the oscillatory plate velocity
u	Longitudinal flow velocity
u_s	Steady component of the velocity field
u_w	Oscillatory component of the velocity field
x, y	Spatial variables

Greek letters

α, α_1, α_2, α_m	Retention parameter or partition coefficient
β, β_m	Bed absorption parameters
δ	Dirac delta function
δ_s	Stokes boundary layer thickness
ϵ $(= \frac{h}{l})$	Perturbation parameter
ζ, ζ_1, ζ_2, ζ_3	Advection coefficients
η	Spatial variable
μ	Non-linear decay reaction rate occurring in the fluid phase
μ_{s1}, μ_{s2}	Non-linear decay reaction rates occurring at the lower and upper boundaries
ν	Kinematic viscosity
τ	Time variable
ξ, ξ_1, ξ_2, ξ_3	Reaction coefficients
Ψ	Ratio of the non-linear decay reaction rate occurring at the boundary to that of in the bulk flow
ω	Angular frequency of the oscillation
Ω	Dimensionless angular frequency of the oscillation

LIST OF FIGURES

LIST OF TABLES

CONTENTS

भारतीय प्रौद्योगिकी संस्थान गुवाहाटी
Indian Institute of Technology Guwahati

CHAPTER 1

INTRODUCTION

1.1 Overview

The solute dispersion in a fluid flow is an important topic of research in modern times and it has wide applications in diverse fields, such as biology [12, 23, 55], chromatography [56] and environment fluid mechanics [15–17, 62, 70–72]. These phenomena can be observed in daily life, for example, releasing a mass of chemical into a river, exhausting of air pollutants from plants, transport of dissolved chemicals through blood vessels and so on. Dispersion of solute in flowing fluid takes place due to the combined effects of molecular diffusion (longitudinal and lateral) and convection (forced and natural).

Theoretically as well as experimentally, the longitudinal dispersion of an inert (i.e., non-adsorbing) solute in an incompressible fluid flow through a tube of circular cross-section was first studied by G. I. Taylor [60]. Since then, this mechanism is termed as Taylor dispersion. Taylor dispersion resembles molecular diffusion, but it is indeed an outcome of the interaction between transverse variations of velocity shear and transverse diffusion of the solute, which raises the rate of spreading of the solute in a flowing fluid. He found an analytical expression for the dispersion coefficient by neglecting molecular diffusion in the direction of flow as $D_T = a^2\langle u\rangle^2/48D$, which is a measure of the rate at which the solute spreads out longitudinally in the flow geometry. Here D is the molecular diffusivity, a is the tube radius and $\langle u\rangle$ is the average velocity of the flow. Taylor [61] also obtained a condition $\frac{4l}{a} \gg \frac{a\langle u\rangle}{D} \gg 6.9$ for which the above expression for dispersion coefficient is valid, where l is the characteristic length of the pipe.

Bournia et al. [8] studied experimentally the longitudinal dispersion of a finite slug of a gas flowing through a circular tube. They showed that the condition $\frac{4l}{a} \gg \frac{a\langle u\rangle}{D}$, set by Taylor, could be relaxed but the condition $\frac{a\langle u\rangle}{D} \gg 6.9$ is very important.

Aris [2] extended the Taylor analysis for arbitrary cross-section and derived the effec-

tive expression of dispersion coefficient for circular pipe as a special case. He improved the Taylor′s expression by using the method of moments as $D_{\text{eff}} = D + a^2\langle u\rangle^2/48D$, where D_{eff} is termed as effective dispersion coefficient. This analysis also removed the validity condition $\frac{a\langle u\rangle}{D} \gg 6.9$, which was imposed by Taylor.

Numerically as well as experimentally Bailey and Gogarty [5] verified Taylor analysis without considering the longitudinal molecular diffusion. From their numerical results, it is possible to extract an expression for dispersion coefficient (D_T) as $D_T = t^{0.082}a^{1.836}\langle u\rangle^2/48D^{0.918}$, where t is the time. Despite a slight time dependence, the coefficient is quite similar to Taylor dispersion coefficient $a^2\langle u\rangle^2/48D$. Their experimental results also verified the fact that the dispersion coefficient increases with an increase in time, for a fixed velocity. However experimental results failed to agree with Taylor's results even for wide range of dimensionless time, $\tau(=\frac{Dt}{a^2}) > 2$.

Evans and Kenney [13] have analysed the gaseous flow through straight and curved tubes. They found that the experimental results for gas having velocities between 1 and 16 cm/s agree well with the analytical solution of this problem for a straight tube derived by Aris. In particular, at low velocities, the effective dispersion coefficients tend to the molecular diffusivities. They also showed that the presence of a bend in the tube slightly reduces the effective longitudinal dispersion coefficient.

Ananthakrishnan et al. [1] found the exact numerical solution for a laminar flow in a tube by finite difference method (alternating direction implicit method proposed by Peaceman and Rachford [46]). They considered both longitudinal and radial diffusion that can cover wide range of dimensionless time (0.01 to 30) and Peclet number (1 to 23000) for comparison with other analytical and experimental results. They showed that the effect of longitudinal molecular diffusion is negligible for high Peclet number ($Pe > 100$) and for $Pe < 100$ that effect is significant. They also showed that if the dimensionless time is sufficiently large then longitudinal molecular diffusion is negligible for all values of Peclet number and consequently satisfies the Taylor theory of dispersion.

Lighthill [26] derived a simple analytical solution applicable for very short time period after the release of solute in a Poiseuille flow. He also neglected the effect of longitudinal diffusion and studied the initial development of solute dispersion by solving the resulting equation with the help of Fourier transform. The solution of Lighthill [26] for initial spreading of solute concentration is a good approximation at dimensionless time $\tau < 0.1$.

Gill [18] proposed a series solution method for a fully developed laminar tube flow, which can predict local concentration distribution. The solution was accurate for a wide range of Peclet number. His analysis also included the analytical expression of mean concentration distribution for a large time. Dispersion coefficient obtained from his study is exactly same as of Aris [2] and reduced to Taylor dispersion coefficients as $Pe \to \infty$.

Gill and Sankarasubramanian [20] found analytical solutions of an unsteady convection diffusion problem by using series expansion method proposed by Gill [18]. They found a

time dependent dispersion coefficient that increases rapidly when the dimensionless time $\tau \leq 0.2$ and remains fixed after $\tau = 0.5$. The time dependent dispersion coefficient exactly becomes equal to that of Aris [2] after $\tau = 0.5$ and hence Taylor-Aris theory becomes applicable. Further, they also showed that at large time their solution for mean concentration distribution agreed well with the solution of Taylor and Aris works [2, 60].

Gill and Sankarasubramanian [21] studied dispersion of a non-uniform solute in fully developed laminar flow. They used series expansion method of Gill [18] to study the behaviour of transport coefficients (advection and dispersion coefficients) and mean concentration distribution of a solute, which had non-uniform initial distributions. They showed that for dimensionless time $\tau < 0.5$, the longitudinal dispersion coefficient decreased with the decrease in the initial slug radius. However, for $\tau > 0.5$ longitudinal dispersion coefficient was independent of slug radius and approached to Aris dispersion coefficient.

Several physical and chemical processes are responsible for solute transport in the flowing fluid. The physical processes affecting the solute concentrations include advection, diffusion, dispersion and flow geometry. The chemical processes affecting the solute concentrations include reaction in the flow and boundaries. Some important terminologies are required to discuss to proceed further.

1.2 Some useful terminologies

Some important terminologies that associated with solute dispersion are listed below:

- **Solute**

  Solute can be any substance that is transported downstream by a flowing fluid.

- **Diffusion**

  Diffusion is a process by which the mass of solute is transported from a region of high concentration to a region of low concentration as a result of random motion of molecules.

  Mathematically, diffusion can be described by Fick's law. It states that the rate of flow of the diffusing solute is proportional to the gradient of concentration of the solute. If q is the amount of solute passing through a reference surface of unit area per unit time (mass flux of the solute), if C is the concentration of the substance, then $q = -D\frac{\partial C}{\partial x}$, where D is the diffusion coefficient of the solute and x is the longitudinal coordinate, which is perpendicular to the surface area.

- **Advection**
  Advection is a process by which the mass of solute is transported from one place to another due to the surrounding medium.
  Mathematically, advection is represented by $u\frac{\partial C}{\partial x}$, where u is the advective velocity.

- **Dispersion**
  Dispersion is the mixing or spreading of the mass of a solute by the combined action of velocity gradient and diffusion.
  Dispersion along the direction of the flow is called longitudinal dispersion and along the lateral (radial) direction is known as transverse dispersion.

- **Mobile and immobile phases**
  The mobile phase is the fluid phase of the flow where the solute moves downstream. The immobile phase is the stationary phase where the solute can be retained or absorbed.

- **Adsorption and desorption**
  Adsorption is a surface process, where a gas or liquid is accumulated on a liquid or solid surface.
  Desorption is a reverse phenomenon, where a solute (gas or liquid) is released from or through a surface (liquid or solid).

- **Absorption**
  Absorption is a bulk phenomenon, where the solute absorbed in the sorbet boundaries.

- **Chemical reaction**
  Chemical reaction is a process in which one or more substances, the reactants, are converted to one or more different substances, the products. It can be homogeneous and heterogeneous.
  Homogeneous reaction is any of a class of chemical reactions that occur in a single phase (gaseous, liquid, or solid).
  Heterogeneous reaction is any of a class of chemical reactions in which the reactants are components of two or more phases (solid and gas, solid and liquid, two immiscible liquids). It can be reversible and irreversible. If a reaction proceeds in both the directions (forward and backward) simultaneously, then the reaction is called reversible reactions. If reaction proceeds to completion in one direction only and reactants are completely converted into products, then the reaction is termed as irreversible reaction.

- **Partition Coefficient**
  Partition coefficient or retention parameter is the ratio of the solute concentration

in immobile phase to the solute concentration in mobile phase for the equilibrium isotherm.

1.3 Basic transport equation

The continuity principle states that the rate of change of a scalar quantity in any differential control volume is the balance of the amount of quantity transported across the boundaries and the amount of quantity produced or removed in the volume. Therefore, mathematically the conservation equation for the scalar is defined as,

$$\frac{\partial C}{\partial t} = -\nabla \cdot q + S, \tag{1.1}$$

where C is the concentration of the scalar, t is the time, q is the total flux of the scalar through the boundaries and S is the source or sink term inside.

For mass transport phenomena, the total flux q is equal to the sum of advective mass flux (q_a) and diffusive mass flux (q_d). The advection of the scalar, caused by the movement of the fluid particles across the boundaries due to the flow, is depended on the velocity and the scalar concentration. Thus, the advective flux can be defined as,

$$q_a = uC, \tag{1.2}$$

where u is velocity relative to its coordinates. Diffusion of species, caused by random molecular motions, is governed by the Fick's Law as,

$$q_d = -D\nabla C, \tag{1.3}$$

where D is the molecular diffusion coefficient or the mass diffusivity and ∇C is the gradient of the scalar concentration.

Thus, by using Eqs. (1.2) and (1.3), the transport equation (1.1) can be rewritten as,

$$\frac{\partial C}{\partial t} + \nabla \cdot (uC) = \nabla \cdot (D\nabla C) + S. \tag{1.4}$$

1.4 Taylor dispersion model

The longitudinal dispersion of a solute in a solvent flowing through a tube of circular cross-section was first studied by Taylor [60]. He assumed that longitudinal diffusion was symmetrical about the central line of the tube and considered the transport equation (1.4) as,

$$\frac{\partial C}{\partial t} + u\frac{\partial C}{\partial x} = D\nabla^2 C, \tag{1.5}$$

where x is the axial distance.

He focused his analysis for sectionally averaged concentration ($\langle C \rangle$) and derived a simple one-dimensional diffusional like equation from Eq. (1.5), by neglecting the longitudinal diffusion term as,

$$\frac{\partial \langle C \rangle}{\partial t} = D_T \frac{\partial^2 \langle C \rangle}{\partial \eta^2}, \tag{1.6}$$

where η $(= x - \langle u \rangle t)$ is an axis of reference moving with the mean speed of the flow.

Here, D_T is the dispersion coefficient. Taylor provided an estimated analytical expression for the dispersion coefficient D_T, which was a measure of the rate of spreading out of the solute longitudinally in the flow geometry, as $D_T = a^2 \langle u \rangle^2 / 48D$. He observed that there was an increase in the diffusion along the flow direction due to velocity shear across the tube. This enhanced diffusion is known as "Taylor dispersion". Taylor dispersion resembles molecular diffusion but it is a combined action of lateral solute diffusion and transverse variations of velocity shear.

Taylor dispersion is basically an idea for the evolution of sectionally averaged or transverse mean concentration, which is leading to a Gaussian distribution. Taylor showed that after a transient initial stage ($t > 0.1\frac{a^2}{D}$) of the transport, Eq. (1.6) becomes valid, i.e., the transverse mean concentration satisfies a one-dimensional diffusion like equation.

1.5 Analytical Approaches

Solute dispersion in steady and oscillatory flows has been studied analytically with various techniques, adopted by researchers to find the dispersivity, mean and real concentration distributions.

- **Method of moment:** Aris [2, 4] first presented concentration moment method, which has the ability to capture temporal variation of solute dispersivity at the initial times. Concentration moments at different orders can give different statistical information for the solute. First, second, third and forth-order moments measure the transport velocity, dispersivity, skewness, kurtosis of the concentration cloud respectively. Although this method is unable to give a direct concentration distribution for the mean and real concentration distributions.

- **Mean concentration expansion method:** Mean concentration expansion method is first introduced by Gill [18, 20, 21]. In this method, concentration is expanded into mean concentration and its longitudinal derivatives. Substitution of expanded expression for concentration into the governing transport equation leads to a generalized dispersion model. This method derives the analytical expression for the mean and real concentration distributions.

- **Multi-scale method:** Expanding the solute concentration into multiple scales and performing a asymptotic analysis, this method gives a simplified advection diffusion equation for the dominant concentration. Once the dominant concentration is known, one can get the other order modification function and most importantly the mean and transverse concentrations. Although this is not an exact solution, but it gives a good approximation at large times.

In this thesis, we have applied multi-scale method to explore the evolutions of solute concentration distribution.

1.6 Multi-scale method

The multi-scale method of homogenization which is also called multi-scale perturbation analysis, was first proposed by Mei et al [32]. The method comprises of techniques used to construct effective macro-scale models from the complicated micro-scale models. Method is used to receive a sample of the same composition and structure in the whole volume. Generally at micro level a material (fluid) is inhomogeneous. Material properties are well defined and have rapid variation at micro level. Fundamental approach is to first construct micro-scale models, and then to deduce the macro-scale models by properly averaging over the micro-scale. Motive is to bypass the material properties from micro-level to macro-level and find an equation that governs the global variations of material properties at micro scale. The main idea here is to obtain effective equations for the slow time scale variable over long time scales by averaging over rapid variations of the fast variables.

1.6.1 Aim of this method

- To receive a sample of the same composition and structure in the whole volume.
- To derive simpler macroscopic models from complicated microscopic models.

1.6.2 Assumptions

- Material should change its physical properties without any changes in the chemistry of components.
- Material properties are periodic in micro scale.
- The perturbation or ordering parameter (ϵ) for asymptotic analysis is assumed to be too small ($\epsilon \ll 1$).

1.6.3 Procedure

The procedure of this method as follow:

- The physical properties are characterized by different length and time scales. First, one has to identify the micro and macro scales for both length and time scales.
- The small perturbation parameter (ϵ) has to be identified for asymptotic analysis.
- Multiple-scale variables (fast, slow) are introduced and expanded the original derivatives (spatial or time) in terms of newly introduced variables by chain rule.
- Need to expand the solute concentration by the asymptotic expansion, which was first introduced by Fife and Nicholes [14], into multiple scales.
- Deduce boundary value problems (BVP) for a typical period of successive orders. The leading order BVP ($O(1)$) is homogeneous. The solution for leading order unknown is indeterminate and independent of the micro-scale variables.
- Higher order problems ($O(\epsilon)$, $O(\epsilon^2)$, $\cdots$) are inhomogeneous. A solvability condition is required to solve it. Using the averaged equation as a solvability condition and assuming the linearity of the solution, express the higher order solution in terms of leading order solutions.
- Taking the average of the inhomogeneous micro-scale problem at the order $O(\epsilon^2)$, i.e., the solvability condition at second-order gives the equation, which governs the macro-scale behaviour of the leading order unknown. Also one can derive the effective constitutive coefficient in terms of micro-scale material properties.
- Finally, all the averaged equation (solvability conditions) of all order are added and the equation in original variable is rewritten. This equation leads to a one-dimensional advection diffusion equation.

The need of this technique lies with the fact that the traditional one scale approaches are not accurate enough at macro level and not efficient enough at micro level.

1.7 Reversible phase exchange kinetics

Dispersion affected by a reversible reaction has become a concern of many studies. Shankar and Lenhoff [56] studied the gas chromatography in a coated tube within a retentive layer. Phillips and Kaye [47] studied the effect of reversible phase exchange on the solute transport in a two-phase system. Ng and Yip [42] presented a theory for the transport in open-channel flow of a chemical species under the influence of kinetic sorptive exchange

between phases that are dissolved in water and sorbed onto suspended sediments. In a reversible reaction, the solute may chemically react to the channel boundaries. The solute is assumed to be completely miscible in the fluid. During the flow, a reversible exchange between different phases of the chemical species may take place across the interface. The reversible phase exchange consists of two physical processes, adsorption and desorption. In adsorption, a part of the solute is retained at the boundary and in desorption, the retained solute come back to flow again. If the solute undergoes a phase exchange with the lower channel boundary, then the rate of change of concentration of the stationary phase is balanced by the diffusive mass concentration flux in reversible reaction and is given by,

$$D\frac{\partial C}{\partial y} = \frac{\partial C_s}{\partial t}, \tag{1.7}$$

where C is the concentration of the fluid phase, C_s is the concentration of the stationary phase.

Phase exchange will take place in either forward or backward direction, which can be described by a first-order linear kinetics [42] as

$$\frac{\partial C_s}{\partial t} = k_f C - k_b C_s, \tag{1.8}$$

where k_f and k_b are the forward (adsorption) and backward (desorption) rate constants. At the equilibrium state, these two phases will have their concentrations in a fixed ratio

$$C_s/C = k_f/k_b = \alpha, \tag{1.9}$$

where α is the partition coefficient or retention parameter that relates the concentrations C and C_s.

Now, from Eqs. (1.7), (1.8) and (1.9) first-order kinetics reversible reactions at the channel bed can be expressed as

$$D\frac{\partial C}{\partial y} = \frac{\partial C_s}{\partial t} = k(\alpha C - C_s), \tag{1.10}$$

where $k = k_b$ is the reversible reaction rate constant.

1.8 Irreversible reaction

Beside boundary adsorption (retention) and desorption, a solute may absorbed irreversibly at the boundary interface. Gupta and Gupta [24] studied the phenomenon of dispersion of reactive contaminants in the bulk of the liquid flowing through a parallel channel in the presence of a first-order heterogeneous chemical reaction. Sankarasubramanian and

Gill [54] explored the study of a first-order inter-phase mass transfer in a tube by using the generalized dispersion model proposed by Gill and Sankarasubramanian [20, 22]. The effect of the boundary reaction on the longitudinal dispersion in shear flows was discussed by Smith [59], using the delay-diffusion equation.

If the solute absorbed at lower channel boundary, then the diffusive mass concentration flux in irreversible reaction is balanced by the rate of absorption, which is linearly proportional to the concentration at the channel bed. Mathematically, irreversible reaction can be described by

$$D\frac{\partial C}{\partial y} = \beta C, \tag{1.11}$$

where β is the absorption rate constant.

1.9 Objectives

The specific objectives of this work are:

- ★ To present a multi-scale analysis for the concentration distribution in laminar steady and oscillatory channel flows, where the solute may undergo reversible or irreversible chemical reaction with the channel boundaries.
- ★ To obtain analytical expressions for dispersion coefficient and both mean and transverse real concentrations up to certain order using multi-scale method of homogenization.
- ★ To observe the effects of flow and reaction parameters on dispersion coefficient, mean and two-dimensional transverse concentration distributions.
- ★ To discuss the uniformity in transverse real concentration over the channel cross-section.

1.10 Motivation and thesis contribution

In the available literature on solute transport during last decades, the main focus was either to obtain the dispersion coefficient or to address the mean concentration distribution rather than transverse concentration distribution. In some environmental or industrial processes, we need information not only on dispersion coefficients or the longitudinal mean concentration, but also on the transverse concentration distribution and its uniformity over the cross-section. Study of the transverse concentration distribution in steady or oscillatory flow has a great significance in estuaries and other coastal regions. Prediction of accurate pollutant distribution and peak pollutant concentration are of matter of concern.

The present work is to provide analytical expressions for dispersion coefficients, mean concentration and transverse real concentration. Also detailed study of transverse converse concentration distribution and its uniformity throughout the channel cross-section are given in this work.

- ♣ In first problem, an analytical study is presented to explore two-dimensional concentration distribution in an open channel flow with absorbing channel bed. Simple analytical expressions are derived for transverse concentration distribution with the help of multi-scale method of homogenization. This study explores mean and real concentration distributions after an initial time when transient behaviour completely dies out. This study also concerns about the non-uniformity of concentration variation over the channel cross-section and effects of bed absorption on it.

- ♣ The second study explores two-dimensional concentration distribution in an open channel flow with reversible phase exchange kinetics between the channel bed and the fluid phase. Simple analytical expressions are derived for transverse concentration distribution with the help of multi-scale method of homogenization. This work includes the pattern of transverse real concentration distribution and uniformity over the cross-section of the channel. Effects of phase exchange parameters on solute dispersion are discussed.

- ♣ In third problem, an attempt is made to find analytical expressions for mean and transverse real concentrations by using a multi-scale homogenization technique and to explore the evolution of transverse concentration distribution for oscillatory Couette flows between two infinite parallel inert walls. Effects of Stokes boundary layer thickness on dispersion coefficient and transverse variation of concentration distribution are observed. The study also suggests a time scale, which would be more appropriate to characterize the initial transition stage of the transport process to approach transverse uniformity.

- ♣ In fourth problem, we extended the previous work on chemical reactive boundaries. Here the solute undergoes reversible and irreversible reactions at the channel bed. Simple analytical expressions are derived for steady and oscillatory components of dispersion coefficients. Absorption induced dispersion coefficients are also found. Effects of Stokes boundary layer thickness along with the chemical reaction parameters, i.e., bed absorption parameter, retention parameter, Damkohler number on the solute dispersion are discussed.

- ♣ In last problem, the effects of non-linear chemical reaction on dispersion coefficients for an oscillatory Couette flow are discussed. A two-dimensional mathematical model is formulated by taking into account the chemical decay and a phase exchange

kinetics between bulk phase and sorbet boundaries. The main purpose of this work is to visualize the effects of nonlinear chemical decay reactions and the roles of different factors or parameters on transport coefficients.

1.11 Organization of the work

This thesis is organized as follows.

- In Chapter 2, solute dispersion in an open channel flow with absorbed bed is discussed.
- In Chapter 3, the effects of phase exchange kinetics on solute dispersion in an open channel flow are studied.
- Chapter 4 deals with the study of the two-dimensions solute concentration distribution in an oscillatory Couette flow between two infinite parallel plates.
- Effects of reversible and irreversible solute dispersion on oscillatory Couette flow are studied in Chapter 5.
- Chapter 6 discusses about the effects of non-linear chemical decay reactions in the flowing fluid and the channel boundaries on oscillatory Couette flow.
- In Chapter 7, conclusions of the thesis work and future directions are presented.

CHAPTER 2

SOLUTE DISTRIBUTION IN AN OPEN CHANNEL FLOW WITH BED ABSORPTION

2.1 Introduction

It is well known that the extensively applied Taylor dispersion model predicts the longitudinally distributed mean concentration. There are two fundamental issues which are equally important for the Taylor dispersion problem. Firstly, when does the mean concentration obey the dispersion model and how does the mean concentration approach to longitudinal Gaussian distribution? Secondly, how does the transverse real concentration approach transverse uniformity? Taylor first estimated the length of the initial stage, which is needed for the dispersion model to hold. In his pioneering work, Taylor showed that the time scale $0.1\, a^2/D$ (a was the tube radius and D was the molecular diffusivity) was characterized the initial stage of the dispersion. Chatwin [9] proposed an asymptotic series expansion of concentration and studied how the mean concentration approached to longitudinal normality. He proposed a time scale $1.0\, a^2/D$, which was an estimate of time scale for the mean concentration to reach longitudinal normality. Literature on solute transport, until last decade, mostly dealt with the first issue. However, the second issue has remained unexplored. Earlier, researchers believed that cross-sectional concentration variation was negligible for the Taylor dispersion stage of the transport process and mean concentration was enough to demonstrate the solute dispersion process. But, the recent study by Wu and Chen [67, 68] reveals that transverse variation is significant for a longer period of time. They derived the analytical expression for the two-dimensional transverse concentration distribution. In many environmental and industrial processes, transverse concentration distribution is very useful compared to the longitudinal mean concentra-

Content of this chapter is published in the journal *Communications in Nonlinear Science and Nonlinear Simulation*, **65** (2018), 1–19.

tion. They also analysed the transverse uniformity of concentration cloud for laminar steady flows and proposed a time scale $10\,a^2/D$, which was an estimate of time scale for the real concentration to reach transverse uniformity.

Taylor dispersion process in an open channel flow with boundary reaction has been studied extensively by many. However, efforts have been limited to determine the Taylor dispersion coefficients in the one-dimensional effective diffusion equation for the mean concentration [38, 42]. The exact peak position of real concentration distribution is a concern, rather than that of the mean concentration distribution. Wang and Chen [62] explored the transverse concentration distribution in an open channel flow with bed absorption by extending the Aris-Gill expansion method and analysed the initial skewed transient behaviours of the solute cloud. Sometimes, for a long channel, in order to study the solute concentration at locations far from the solute source, one does not need to know the initial transient behaviour of the solute cloud.

In this chapter, an analytical study is presented to explore two-dimensional concentration distribution in an open channel flow with absorbing channel bed. Analytical expressions are derived for transverse concentration distribution with the help of multi-scale method of homogenization. This study explores mean and real concentration distributions after an initial time when transient behaviour completely dies out. This study also concerns about the non-uniformity of concentration variation over the channel cross-section and the effects of bed absorption on it. The specific objectives of this work are: (I) to present a multi-scale analysis of the concentration distribution in an open channel flow with bed absorption, (II) to obtain analytical expressions for the transverse real concentrations up to third-order approximations, (III) to observe the effects of bed absorption on transverse variations of concentration distribution, (IV) to discuss the uniformity in transverse real concentration over the channel cross-section.

2.2 Formulation of the problem

A laminar, fully developed, unidirectional open channel flow with a separation width h is considered. A Cartesian coordinate system has been used assuming longitudinal direction as $\widehat{x}$-axis and vertical direction as $\widehat{y}$-axis. The solute is considered to undergo an irreversible bed absorption at the channel bed and to disperse throughout the channel under a flow velocity $\widehat{u}(\widehat{y})$, which is given by,

$$\widehat{u}(\widehat{y}) = u_0 \left(2\frac{\widehat{y}}{h} - \frac{\widehat{y}^2}{h^2} \right), \tag{2.1}$$

where u_0 is the flow velocity of the free surface. Schematic diagram of the flow geometry is given in Fig. (2.1).

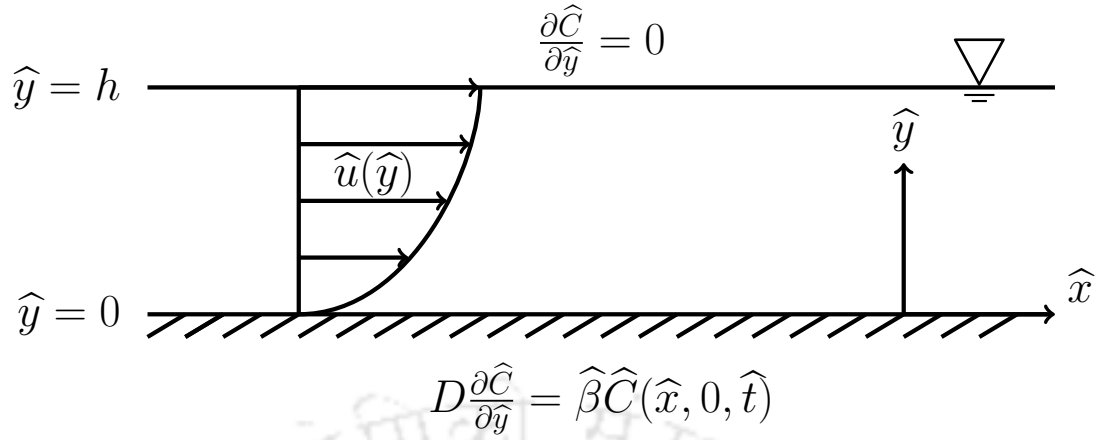

Figure 2.1: Sketch for the instantaneous release of solute in open channel flow with bed absorption.

The problem for the transport of the solute can be formulated as follows:

$$\frac{\partial \widehat{C}}{\partial \widehat{t}} + \widehat{u}\frac{\partial \widehat{C}}{\partial \widehat{x}} = D\left(\frac{\partial^2 \widehat{C}}{\partial \widehat{x}^2} + \frac{\partial^2 \widehat{C}}{\partial \widehat{y}^2}\right), \quad 0 < \widehat{y} < h, \tag{2.2}$$

where $\widehat{C}$ is the solute concentration, $\widehat{t}$ is the time, D the molecular diffusivity of the solute in the fluid is assumed to be constant.

The initial and boundary conditions are respectively given as,

$$\widehat{C}(\widehat{x}, \widehat{y}, \widehat{t})|_{\widehat{t}=0} = \frac{Q_m}{h}\delta(\frac{\widehat{x}}{h}), \tag{2.3}$$

$$D\frac{\partial \widehat{C}}{\partial \widehat{y}}\bigg|_{\widehat{y}=0} = \widehat{\beta}\widehat{C}(\widehat{x}, 0, \widehat{t}), \tag{2.4}$$

$$\frac{\partial \widehat{C}}{\partial \widehat{y}}\bigg|_{\widehat{y}=h} = 0, \tag{2.5}$$

and

$$\widehat{C}(\widehat{x}, \widehat{y}, \widehat{t})|_{\widehat{x}\to\pm\infty} = 0, \tag{2.6}$$

where Q_m is the released mass, $\delta(\cdot)$ the Dirac delta function and $\widehat{\beta}$ is the bed absorption parameter.

2.3 Multi-scale method of homogenization

2.3.1 Scales selection

Associated with two length scales h (channel width) and l (characteristic longitudinal length of the solute cloud), three distinct time scales for transport process are considered. These are T_0, T_1 and T_2, where, $T_0 = h^2/D$ as the diffusion time across the width of the channel h, $T_1 = l/\langle\widehat{u}\rangle$ as the advection time across the characteristic length l, and $T_2 = l^2/D$ as diffusion time across l. Their ratios are

$$T_0 : T_1 : T_2 = 1 : \frac{1}{\epsilon} : \frac{1}{\epsilon^2},$$

where $\epsilon = \frac{h}{l}$ ($\ll 1$) is used as the perturbation parameter.

2.3.2 Dimensionless governing equation and velocity profile

Dimensionless parameters are introduced as

$$x = \frac{\widehat{x}}{l},\ y = \frac{\widehat{y}}{h},\ u = \frac{\widehat{u}}{\langle\widehat{u}\rangle},\ t = \frac{\widehat{t}}{h^2/D},\ Pe = \frac{\langle\widehat{u}\rangle h}{D},\ C = \frac{\widehat{C}}{Q_m/h},\ \beta = \frac{\widehat{\beta} l}{D}, \tag{2.7}$$

where Pe is the Peclet number, β is the dimensionless absorption parameter and the angle bracket denotes section average defined as

$$\langle\widehat{u}\rangle = \int_0^1 \widehat{u}\, dy. \tag{2.8}$$

The non-dimensional forms of governing equation, initial and boundary conditions can be obtained as

$$\frac{\partial C}{\partial t} + \epsilon Pe\, u\frac{\partial C}{\partial x} = \epsilon^2\frac{\partial^2 C}{\partial x^2} + \frac{\partial^2 C}{\partial y^2}, \quad 0 < y < 1, \tag{2.9}$$

$$C(x, y, t)|_{t=0} = \delta(\frac{x}{\epsilon}), \tag{2.10}$$

$$\left.\frac{\partial C}{\partial y}\right|_{y=0} = \epsilon\beta C(x, 0, t), \tag{2.11}$$

$$\left.\frac{\partial C}{\partial y}\right|_{y=1} = 0, \tag{2.12}$$

$$C(x, y, t)|_{x=\pm\infty} = 0. \tag{2.13}$$

The dimensionless velocity profile becomes

$$u(y) = \frac{3}{2}(2y - y^2). \tag{2.14}$$

2.3.3 Asymptotic analysis

For the asymptotic analysis, the homogenization technique of Mei et al. [32] is employed. The concentrations C is expanded into multiple scales as:

$$C = C^{(0)} + \epsilon C^{(1)} + \epsilon^2 C^{(2)} + \epsilon^3 C^{(3)} + O(\epsilon^4). \tag{2.15}$$

Based on these time scales, fast, medium and slow time variables are introduced accordingly

$$t_0 = t,\ t_1 = \epsilon t,\ t_2 = \epsilon^2 t.$$

Now, the original time derivative, according to the chain rule, becomes

$$\frac{\partial}{\partial t} = \frac{\partial}{\partial t_0} + \epsilon \frac{\partial}{\partial t_1} + \epsilon^2 \frac{\partial}{\partial t_2}. \tag{2.16}$$

Substitution of Eqs. (2.16) and (2.15) into Eqs. (2.9), (2.11) and (2.12) results in

$$\begin{aligned}\left(\frac{\partial C^{(0)}}{\partial t_0} - \frac{\partial^2 C^{(0)}}{\partial y^2}\right) + \epsilon\left(\frac{\partial C^{(0)}}{\partial t_1} + \frac{\partial C^{(1)}}{\partial t_0} + Pe\, u\frac{\partial C^{(0)}}{\partial x} - \frac{\partial^2 C^{(1)}}{\partial y^2}\right) + \epsilon^2\left(\frac{\partial C^{(0)}}{\partial t_2}\right. \\ \left. + \frac{\partial C^{(1)}}{\partial t_1} + \frac{\partial C^{(2)}}{\partial t_0} + Pe\, u\frac{\partial C^{(1)}}{\partial x} - \frac{\partial^2 C^{(0)}}{\partial x^2} - \frac{\partial^2 C^{(2)}}{\partial y^2}\right) + \cdots = 0, \quad 0 < y < 1,\end{aligned} \tag{2.17}$$

$$\frac{\partial C^{(0)}}{\partial y} + \epsilon\left(\frac{\partial C^{(1)}}{\partial y} - \beta C^{(0)}\right) + \epsilon^2\left(\frac{\partial C^{(2)}}{\partial y} - \beta C^{(1)}\right) + \cdots = 0, \quad y = 0, \tag{2.18}$$

$$\frac{\partial C^{(0)}}{\partial y} + \epsilon\frac{\partial C^{(1)}}{\partial y} + \epsilon^2\frac{\partial C^{(2)}}{\partial y} + \cdots = 0, \quad y = 1. \tag{2.19}$$

For leading order ($O(1)$), Eqs. (2.17)–(2.19) give:

$$\frac{\partial C^{(0)}}{\partial t_0} = \frac{\partial^2 C^{(0)}}{\partial y^2}, \qquad 0 < y < 1, \tag{2.20}$$

$$\left.\frac{\partial C^{(0)}}{\partial y}\right|_{y=0} = \left.\frac{\partial C^{(0)}}{\partial y}\right|_{y=1} = 0. \tag{2.21}$$

The general solution of Eq. (2.20) is obtained as,

$$C^{(0)} = C_0^{(0)}(x, t_1, t_2) + \sum_{n=1}^{\infty} Re\left[C_n^{(0)}(x, t_1, t_2)e^{in\pi y}\right]e^{-n^2\pi^2 t_0}. \tag{2.22}$$

The channel is assumed to be shallow so that the transverse diffusion is accomplished within the first time scale, which is very small. The series part of Eq. (2.22) dies out exponentially with the fast time variable t_0 and is considered to be insignificant for the time variable $t_1 \geq O(1)$ [33], if we interested in long time behaviour.

So, the solution can be considered as,

$$C^{(0)} = C^{(0)}(x, t_1, t_2). \tag{2.23}$$

For first-order ($O(\epsilon)$), Eqs. (2.17)–(2.19) give:

$$\frac{\partial C^{(0)}}{\partial t_1} + \frac{\partial C^{(1)}}{\partial t_0} + Pe\, u \frac{\partial C^{(0)}}{\partial x} = \frac{\partial^2 C^{(1)}}{\partial y^2}, \quad 0 < y < 1, \tag{2.24}$$

$$\left.\frac{\partial C^{(1)}}{\partial y}\right|_{y=0} = \beta C^{(0)}, \tag{2.25}$$

$$\left.\frac{\partial C^{(1)}}{\partial y}\right|_{y=1} = 0. \tag{2.26}$$

As the time scale t_0 is much larger compared to t_1, the second term of the L.H.S. of equation (2.24) can be neglected. So, Eq. (2.24) becomes

$$\frac{\partial C^{(0)}}{\partial t_1} + Pe\, u \frac{\partial C^{(0)}}{\partial x} = \frac{\partial^2 C^{(1)}}{\partial y^2}, \quad 0 < y < 1. \tag{2.27}$$

Further, taking a section average of Eq. (2.27) w.r.t the spatial variable y subject to the conditions (2.25) and (2.26), we get

$$\frac{\partial C^{(0)}}{\partial t_1} + Pe\langle u\rangle \frac{\partial C^{(0)}}{\partial x} = -\beta C^{(0)}. \tag{2.28}$$

Subtracting (2.28) from (2.27), we get

$$Pe(u - \langle u\rangle)\frac{\partial C^{(0)}}{\partial x} - \beta C^{(0)} = \frac{\partial^2 C^{(1)}}{\partial y^2}, \quad 0 < y < 1. \tag{2.29}$$

This equation suggests the following substitution

$$C^{(1)} = Pe\, F(y)\frac{\partial C^{(0)}}{\partial x} + \beta M(y) C^{(0)}, \tag{2.30}$$

where the coefficients $F(y)$ and $M(y)$ are to be found by eliminating $C^{(1)}$ from Eqs. (2.29), (2.30), (2.25) and (2.26), and matching terms associated with $\frac{\partial C^{(0)}}{\partial x}$ and $C^{(0)}$ respectively.

On matching term associated with $\frac{\partial C^{(0)}}{\partial x}$, the function $F(y)$ is governed by

$$\frac{d^2 F}{dy^2} = u - \langle u\rangle, \quad 0 < y < 1, \tag{2.31}$$

with the following conditions

$$\left.\frac{dF}{dy}\right|_{y=0} = \left.\frac{dF}{dy}\right|_{y=1} = 0, \tag{2.32}$$

and

$$\langle F \rangle = 0. \tag{2.33}$$

Similarly, equating the terms associated with $C^{(0)}$, the function $M(y)$ is governed by

$$\frac{d^2M}{dy^2} = -1, \quad 0 < y < 1, \tag{2.34}$$

with the following conditions

$$\left.\frac{dM}{dy}\right|_{y=0} = 1, \tag{2.35}$$

$$\left.\frac{dM}{dy}\right|_{y=1} = 0, \tag{2.36}$$

and

$$\langle M \rangle = 0. \tag{2.37}$$

For second-order ($O(\epsilon^2)$), Eqs. (2.17)–(2.19) give:

$$\frac{\partial C^{(0)}}{\partial t_2} + \frac{\partial C^{(1)}}{\partial t_1} + \frac{\partial C^{(2)}}{\partial t_0} + Pe\, u\frac{\partial C^{(1)}}{\partial x} = \frac{\partial^2 C^{(0)}}{\partial x^2} + \frac{\partial^2 C^{(2)}}{\partial y^2}, \quad 0 < y < 1, \tag{2.38}$$

$$\left.\frac{\partial C^{(2)}}{\partial y}\right|_{y=0} = \beta C^{(1)}(x, 0, t), \tag{2.39}$$

$$\left.\frac{\partial C^{(2)}}{\partial y}\right|_{y=1} = 0. \tag{2.40}$$

Again, as the time scale t_0 is quite larger compared to both t_1 and t_2, the third term of L.H.S. of Eq. (2.38) can be neglected. So, Eq. (2.38) becomes

$$\frac{\partial C^{(0)}}{\partial t_2} + \frac{\partial C^{(1)}}{\partial t_1} + Pe\, u\frac{\partial C^{(1)}}{\partial x} = \frac{\partial^2 C^{(0)}}{\partial x^2} + \frac{\partial^2 C^{(2)}}{\partial y^2}. \tag{2.41}$$

On taking a section average of Eq. (2.41) w.r.t the spatial variable y subject to the conditions (2.39) and (2.40), we get

$$\frac{\partial C^{(0)}}{\partial t_2} + \frac{\partial \langle C^{(1)} \rangle}{\partial t_1} + Pe \left\langle u\frac{\partial C^{(1)}}{\partial x} \right\rangle = \frac{\partial^2 C^{(0)}}{\partial x^2} - \beta C^{(1)}(0). \tag{2.42}$$

Using Eqs. (2.30), (2.33) and (2.37), the following terms of Eq. (2.42) can be found

$$\frac{\partial \langle C^{(1)} \rangle}{\partial t_1} = 0, \tag{2.43}$$

$$\left\langle u \frac{\partial C^{(1)}}{\partial x} \right\rangle = Pe \, \langle uF \rangle \frac{\partial^2 C^{(0)}}{\partial x^2} + \beta \langle uM \rangle \frac{\partial C^{(0)}}{\partial x}, \tag{2.44}$$

and

$$C^{(1)}(0) = Pe \, F(0) \frac{\partial C^{(0)}}{\partial x} + \beta M(0) \, C^{(0)}. \tag{2.45}$$

Substituting of these terms in Eq. (2.42) gives

$$\frac{\partial C^{(0)}}{\partial t_2} + \beta Pe \Big(\langle uM \rangle + F(0) \Big) \frac{\partial C^{(0)}}{\partial x} = \Big(1 - Pe^2 \, \langle uF \rangle \Big) \frac{\partial^2 C^{(0)}}{\partial x^2} - \beta^2 M(0) C^{(0)}. \tag{2.46}$$

Multiplying Eq. (2.28) by ϵ, and Eq. (2.46) by ϵ^2 and adding together, we obtained,

$$\frac{\partial C^{(0)}}{\partial t_0} + \epsilon \frac{\partial C^{(0)}}{\partial t_1} + \epsilon^2 \frac{\partial C^{(0)}}{\partial t_2} + \Big(\epsilon Pe \, \langle u \rangle + \epsilon^2 \beta Pe \, \langle uM \rangle + \epsilon^2 \beta Pe \, F(0) \Big) \frac{\partial C^{(0)}}{\partial x} = \epsilon^2 \Big(1 - Pe^2 \langle uF \rangle \Big) \frac{\partial^2 C^{(0)}}{\partial x^2} - \Big(\epsilon \beta + \epsilon^2 \beta^2 M(0) \Big) C^{(0)}. \tag{2.47}$$

Rewriting Eq. (2.47), in original time variable, as

$$\frac{\partial C^{(0)}}{\partial t} + \Big(\epsilon Pe \, \langle u \rangle + \epsilon^2 \beta Pe \, \langle uM \rangle + \epsilon^2 \beta Pe \, F(0) \Big) \frac{\partial C^{(0)}}{\partial x} = \epsilon^2 \Big(1 - Pe^2 \langle uF \rangle \Big) \frac{\partial^2 C^{(0)}}{\partial x^2} - \Big(\epsilon \beta + \epsilon^2 \beta^2 M(0) \Big) C^{(0)}. \tag{2.48}$$

On solving the two systems of Eqs. (2.31)–(2.33) and Eqs. (2.34)–(2.37), one can get

$$F(y) = -\frac{y^4}{8} + \frac{y^3}{2} - \frac{y^2}{2} + \frac{1}{15}, \tag{2.49}$$

and

$$M(y) = -\frac{y^2}{2} + y - \frac{1}{3}. \tag{2.50}$$

Using Eqs. (2.49), (2.50), (2.8) and (2.14) one can find the followings

$$\langle uF \rangle = -\frac{2}{105}, \tag{2.51}$$

and

$$\langle uM \rangle = \frac{1}{15}. \tag{2.52}$$

Now, from Eq. (2.48) we get

$$\frac{\partial C^{(0)}}{\partial t}+\epsilon Pe\Big(1+\frac{2}{15}\epsilon\beta\Big)\frac{\partial C^{(0)}}{\partial x}=\epsilon^2\Big(1+\frac{2}{105}Pe^2\Big)\frac{\partial^2 C^{(0)}}{\partial x^2}-\Big(\epsilon\beta-\frac{1}{3}\epsilon^2\beta^2\Big)C^{(0)}. \quad (2.53)$$

Using dimensionless variable $\beta_m(\geq 0)=\frac{\widehat{\beta}h}{D}$, one can get

$$\frac{\partial C^{(0)}}{\partial t}+\epsilon Pe\Big(1+\frac{2}{15}\beta_m\Big)\frac{\partial C^{(0)}}{\partial x}=\epsilon^2\Big(1+\frac{2}{105}Pe^2\Big)\frac{\partial^2 C^{(0)}}{\partial x^2}-\Big(\beta_m-\frac{1}{3}\beta_m^2\Big)C^{(0)}. \quad (2.54)$$

For significant non-zero exponential decay occurring because of bed absorption, the term $(\beta_m-\frac{1}{3}\beta_m^2)$ should be increasing and greater than zero, which implies $0<\beta_m\leqslant 1.5$.

Using the transformation $C^{(0)}=we^{-\left(\beta_m-\frac{1}{3}\beta_m^2\right)\tau}$ and the initial and boundary condition given in Eqs. (2.3) and (2.6), the solution in new variable $\tau=t$ and $\eta=\frac{\widehat{x}}{h}-Pe(1+\frac{2}{15}\beta_m)t$ be

$$C^{(0)}=\frac{1}{\sqrt{4\pi D_T\tau}}\exp\Big(-\frac{\eta^2}{4D_T\tau}-(\beta_m-\frac{1}{3}\beta_m^2)\tau\Big), \quad (2.55)$$

where the effective dispersion coefficient

$$D_T=1+\frac{2}{105}Pe^2. \quad (2.56)$$

Subtract Eq. (2.42) from Eq. (2.41) one can get

$$\frac{\partial C^{(1)}}{\partial t_1}+Pe\,u\frac{\partial C^{(1)}}{\partial x}-Pe\left\langle u\frac{\partial C^{(1)}}{\partial x}\right\rangle=\frac{\partial^2 C^{(2)}}{\partial y^2}+\beta C^{(1)}(0). \quad (2.57)$$

Derivative of both sides of Eq. (2.30) with respect to t_1 gives

$$\frac{\partial C^{(1)}}{\partial t_1}=-Pe^2\langle u\rangle F\frac{\partial^2 C^{(0)}}{\partial x^2}-\beta Pe\,F\frac{\partial C^{(0)}}{\partial x}-\beta Pe\langle u\rangle M\frac{\partial C^{(0)}}{\partial x}-\beta^2 MC^{(0)}. \quad (2.58)$$

After using Eqs. (2.30), (2.58) and (2.44), in Eq. (2.57), it becomes

$$\Big(-Pe^2\langle u\rangle F+Pe^2\,uF-Pe^2\langle uF\rangle\Big)\frac{\partial^2 C^{(0)}}{\partial x^2}+\beta\Big(-Pe\,F-Pe\,F(0)-Pe\langle u\rangle M+Pe\,uM -Pe\langle uM\rangle\Big)\frac{\partial C^{(0)}}{\partial x}+\beta^2\Big(-M-M(0)\Big)C^{(0)}=\frac{\partial^2 C^{(2)}}{\partial y^2}. \quad (2.59)$$

The above equation suggests the following substitution,

$$C^{(2)}=Pe^2\,X(y)\frac{\partial^2 C^{(0)}}{\partial x^2}+\beta Pe\,Y(y)\frac{\partial C^{(0)}}{\partial x}+\beta^2 Z(y)C^{(0)}, \quad (2.60)$$

where the coefficients $X(y)$, $Y(y)$ and $Z(y)$ are to be found by eliminating $C^{(2)}$ from

Eqs. (2.60), (2.59), (2.39) and (2.40) and matching terms associated with $\frac{\partial^2 C^{(0)}}{\partial x^2}$, $\frac{\partial C^{(0)}}{\partial x}$ and $C^{(0)}$ respectively.

On matching terms associated with $\frac{\partial^2 C^{(0)}}{\partial x^2}$, the function $X(y)$ is governed by

$$\frac{d^2X}{dy^2} = uF - \langle u\rangle F - \langle uF\rangle, \quad 0 < y < 1, \tag{2.61}$$

with the following conditions

$$\left.\frac{dX}{dy}\right|_{y=0} = \left.\frac{dX}{dy}\right|_{y=1} = 0, \tag{2.62}$$

and

$$\langle X\rangle = 0. \tag{2.63}$$

Similarly, matching terms associated with $\frac{\partial C^{(0)}}{\partial x}$, the function $Y(y)$ is governed by

$$\frac{d^2Y}{dy^2} = uM - \langle u\rangle M - \langle uM\rangle - F - F(0), \quad 0 < y < 1, \tag{2.64}$$

with the following conditions

$$\left.\frac{dY}{dy}\right|_{y=0} = F(0), \tag{2.65}$$

$$\left.\frac{dY}{dy}\right|_{y=1} = 0, \tag{2.66}$$

and

$$\langle Y\rangle = 0. \tag{2.67}$$

Similarly, matching terms associated with $C^{(0)}$, the function $Z(y)$ is governed by

$$\frac{d^2Z}{dy^2} = -M - M(0), \quad 0 < y < 1, \tag{2.68}$$

with the following conditions

$$\left.\frac{dZ}{dy}\right|_{y=0} = M(0), \tag{2.69}$$

$$\left.\frac{dZ}{dy}\right|_{y=1} = 0, \tag{2.70}$$

and

$$\langle Z\rangle = 0. \tag{2.71}$$

On solving three consecutive systems of equations (given in Eqs. (2.61)–(2.71)) one

can get

$$X(y) = \frac{3}{896}y^8 - \frac{3}{112}y^7 + \frac{19}{240}y^6 - \frac{1}{10}y^5 + \frac{1}{30}y^4 + \frac{1}{30}y^3 - \frac{1}{42}y^2 + \frac{2}{1575}, \tag{2.72}$$

$$Y(y) = \frac{7}{240}y^6 - \frac{7}{40}y^5 + \frac{3}{8}y^4 - \frac{1}{3}y^3 + \frac{1}{15}y^2 + \frac{1}{15}y - \frac{1}{45}, \tag{2.73}$$

and

$$Z(y) = \frac{1}{24}y^4 - \frac{1}{6}y^3 + \frac{1}{3}y^2 - \frac{1}{3}y + \frac{4}{45}. \tag{2.74}$$

For third-order ($O(\epsilon^3)$), Eqs. (2.17)–(2.19) give:

$$\frac{\partial C^{(1)}}{\partial t_2} + \frac{\partial C^{(2)}}{\partial t_1} + \frac{\partial C^{(3)}}{\partial t_0} + Pe\, u\frac{\partial C^{(2)}}{\partial x} = \frac{\partial^2 C^{(1)}}{\partial x^2} + \frac{\partial^2 C^{(3)}}{\partial y^2}, \quad 0 < y < 1, \tag{2.75}$$

$$\left.\frac{\partial C^{(3)}}{\partial y}\right|_{y=0} = \beta C^{(2)}(x, 0, t), \tag{2.76}$$

$$\left.\frac{\partial C^{(3)}}{\partial y}\right|_{y=1} = 0. \tag{2.77}$$

The time scale t_0 is much larger compared to t_1 and t_2, so the third term of L.H.S. of Eq. (2.75) can be neglected. Equation (2.75) becomes

$$\frac{\partial C^{(1)}}{\partial t_2} + \frac{\partial C^{(2)}}{\partial t_1} + Pe\, u\frac{\partial C^{(2)}}{\partial x} = \frac{\partial^2 C^{(1)}}{\partial x^2} + \frac{\partial^2 C^{(3)}}{\partial y^2}, \quad 0 < y < 1. \tag{2.78}$$

Further on taking a section average of Eq. (2.78) w.r.t. the spatial variable y subject to the conditions (2.76) and (2.77), we get

$$Pe\Big\langle u\frac{\partial C^{(2)}}{\partial x}\Big\rangle = -\beta C^{(2)}(0). \tag{2.79}$$

Subtracting Eq. (2.79) from Eq. (2.78), we get

$$\frac{\partial C^{(1)}}{\partial t_2} + \frac{\partial C^{(2)}}{\partial t_1} + Pe\Big(u\frac{\partial C^{(2)}}{\partial x} - \Big\langle u\frac{\partial C^{(2)}}{\partial x}\Big\rangle\Big) = \frac{\partial^2 C^{(1)}}{\partial x^2} + \frac{\partial^2 C^{(3)}}{\partial y^2} + \beta C^{(2)}(0). \tag{2.80}$$

The first two terms of Eq. (2.80) can be found as

$$\begin{aligned}\frac{\partial C^{(1)}}{\partial t_2} = {} & Pe\, F(1 - Pe^2\langle uF\rangle)\frac{\partial^3 C^{(0)}}{\partial x^3} + \beta\Big(M(1 - Pe^2\langle uF\rangle) - Pe^2 F(\langle uM\rangle + F(0))\Big) \\ & \times\frac{\partial^2 C^{(0)}}{\partial x^2} - \beta^2 Pe\Big(M(\langle uM\rangle + F(0)) + FM(0)\Big)\frac{\partial C^{(0)}}{\partial x} - \beta^3 MM(0)C^{(0)},\end{aligned} \tag{2.81}$$

$$\frac{\partial C^{(2)}}{\partial t_1} = -Pe^3\langle u\rangle X\frac{\partial^3 C^{(0)}}{\partial x^3} - \beta Pe^2(\langle u\rangle Y + X)\frac{\partial^2 C^{(0)}}{\partial x^2} - \beta^2 Pe(Y + \langle u\rangle Z)\frac{\partial C^{(0)}}{\partial x} - \beta^3 Z C^{(0)}. \tag{2.82}$$

Following similar process like previous order, we may express

$$C^{(3)} = Pe^3\, I(y)\frac{\partial^3 C^{(0)}}{\partial x^3} + \beta Pe^2\, J(y)\frac{\partial^2 C^{(0)}}{\partial x^2} + \beta^2 Pe\, K(y)\frac{\partial C^{(0)}}{\partial x} + \beta^3 L(y) C^{(0)}, \tag{2.83}$$

where the coefficients $I(y)$, $J(y)$, $K(y)$ and $L(y)$ are to be found as follows.

On matching with terms associated with $\frac{\partial^3 C^{(0)}}{\partial x^3}$, the function $I(y)$ is governed by

$$\frac{d^2 I}{dy^2} = uX - \langle u\rangle X - \langle uX\rangle - F\langle uF\rangle, \quad 0 < y < 1, \tag{2.84}$$

with the following conditions

$$\left.\frac{dI}{dy}\right|_{y=0} = \left.\frac{dI}{dy}\right|_{y=1} = 0, \tag{2.85}$$

and

$$\langle I\rangle = 0. \tag{2.86}$$

Similarly, equating the terms associated with $\frac{\partial^2 C^{(0)}}{\partial x^2}$, the function $J(y)$ is governed by

$$\frac{d^2 J}{dy^2} = uY - \langle u\rangle Y - \langle uY\rangle - X - X(0) - F\langle uM\rangle - M\langle uF\rangle - FF(0), \quad 0 < y < 1, \tag{2.87}$$

with the following conditions

$$\left.\frac{dJ}{dy}\right|_{y=0} = X(0), \tag{2.88}$$

$$\left.\frac{dJ}{dy}\right|_{y=1} = 0, \tag{2.89}$$

and

$$\langle J\rangle = 0. \tag{2.90}$$

Equating the terms associated with $\frac{\partial C^{(0)}}{\partial x}$, the function $K(y)$ is governed by

$$\frac{d^2 K}{dy^2} = uZ - \langle u\rangle Z - \langle uZ\rangle - Y - Y(0) - M\langle uM\rangle - FM(0) - MF(0), \quad 0 < y < 1, \tag{2.91}$$

with the following conditions

$$\left.\frac{dK}{dy}\right|_{y=0} = Y(0), \tag{2.92}$$

$$\left.\frac{dK}{dy}\right|_{y=1} = 0, \tag{2.93}$$

and

$$\langle K \rangle = 0. \tag{2.94}$$

Equating the terms associated with $C^{(0)}$, the function $L(y)$ is governed by

$$\frac{d^2L}{dy^2} = -Z - Z(0) - MM(0), \quad 0 < y < 1, \tag{2.95}$$

with the following conditions

$$\left.\frac{dL}{dy}\right|_{y=0} = Z(0), \tag{2.96}$$

$$\left.\frac{dL}{dy}\right|_{y=1} = 0, \tag{2.97}$$

and

$$\langle L \rangle = 0. \tag{2.98}$$

On solving four consecutive system of equations, one can get

$$I(y) = -\frac{3}{78848}y^{12} + \frac{9}{19712}y^{11} - \frac{907}{403200}y^{10} + \frac{29}{5040}y^9 - \frac{103}{13440}y^8 + \frac{1}{280}y^7 + \frac{1}{300}y^6 - \frac{1}{210}y^5 + \frac{13}{12600}y^4 + \frac{1}{1575}y^3 + \frac{2}{17325}y^2 - \frac{14}{160875}, \tag{2.99}$$

$$J(y) = -\frac{211}{403200}y^{10} + \frac{211}{40320}y^9 - \frac{41}{1920}y^8 + \frac{19}{420}y^7 - \frac{179}{3600}y^6 + \frac{1}{60}y^5 + \frac{13}{630}y^4 - \frac{2}{105}y^3 + \frac{1}{3150}y^2 + \frac{2}{1575}y + \frac{8}{17325}, \tag{2.100}$$

$$K(y) = -\frac{11}{6720}y^8 + \frac{11}{840}y^7 - \frac{7}{144}y^6 + \frac{13}{120}y^5 - \frac{49}{360}y^4 + \frac{1}{15}y^3 + \frac{2}{105}y^2 - \frac{1}{45}y + \frac{13}{4725}, \tag{2.101}$$

$$L(y) = -\frac{1}{720}y^6 + \frac{1}{120}y^5 - \frac{1}{24}y^4 + \frac{1}{9}y^3 - \frac{13}{90}y^2 + \frac{4}{45}y - \frac{16}{945}. \tag{2.102}$$

In a similar way, one can find the further terms C_n, $(n = 4, 5, 6, \ldots)$, whose expressions are too long and cumbersome, and therefore omitted here. Without bed absorption effect, the functions $F(y)$, $X(y)$ and $I(y)$ are similar to the functions obtained in the work of Wu and Chen [67].

2.4 Results and discussion

In the following subsections, distributions of mean and transverse concentrations and their dependence primarily on the parameters Pe and β_m are discussed. The mean concentration distribution can be obtained from Eqs. (2.15) and (2.55) as

$$\langle C\rangle = C^{(0)} = \frac{1}{\sqrt{4\pi D_T \tau}}\ \exp\Big(-\frac{\eta^2}{4D_T\tau} - (\beta_m - \frac{1}{3}\beta_m^2)\tau\Big). \tag{2.103}$$

According to the asymptotic expansion given in Eq. (2.15), the two-dimensional concentration distribution up to third-order is derived as

$$\begin{aligned} C &= C^{(0)} + \epsilon C^{(1)} + \epsilon^2 C^{(2)} + \epsilon^3 C^{(3)} \\ &= (1 + \beta_m M + \beta_m^2 Z + \beta_m^3 L)C^{(0)} + Pe(F + \beta_m Y + \beta_m^2 K)\frac{\partial C^{(0)}}{\partial \eta} \\ &\qquad + Pe^2(X + \beta_m J)\frac{\partial^2 C^{(0)}}{\partial \eta^2} + Pe^3\, I\, \frac{\partial^3 C^{(0)}}{\partial \eta^3}. \end{aligned} \tag{2.104}$$

This expression is much simpler and relatively easier to deal with compared to the analytical results obtained by others, such as Wang and Chen [62]. In order to verify accuracy of the above analytical solution, the transverse concentration distribution is compared with the results of existing studies [62, 67]. We also performed numerical simulation for the above advection-diffusion problem governed by the differential equation with the initial and boundary conditions as given by Eqs. (2.2)–(2.6).

One can rewrite Eq. (2.9) in dimensionless form with the help of dimensionless space and time variables $\{\eta, \tau\}$, as

$$\frac{\partial C}{\partial \tau} + Pe(u - 1 - \frac{2}{15}\beta_m)\frac{\partial C}{\partial \eta/Pe} = \frac{1}{Pe^2}\frac{\partial^2 C}{\partial(\eta/Pe)^2} + \frac{\partial^2 C}{\partial y^2}. \tag{2.105}$$

The longitudinal diffusion term (first term of R.H.S. of the above equation), whose effect is insignificant for large value of Pe, can be neglected and the equation finally becomes

$$\frac{\partial C}{\partial \tau} + Pe(u - 1 - \frac{2}{15}\beta_m)\frac{\partial C}{\partial \eta/Pe} = \frac{\partial^2 C}{\partial y^2}. \tag{2.106}$$

Now, by solving the above equation numerically, results are presented in Pe independent system $\{\eta/Pe, C\ Pe\}$. Figures (2.2) and (2.3) show the comparison between analytical and numerical results of the present work and results of Wu and Chen [67] and Wang and Chen [62]. Results are compared at the channel bed for $\beta_m = 0$ and $\beta_m = 1$. Following the figures, it can be claimed that our analytical results show a very good agreement with our numerical results as well as the already existing analytical results. However, the comparison shows a slight discrepancy at the initial stage, as our analytical study suggests that results may not be fully reliable at the initial period of time.

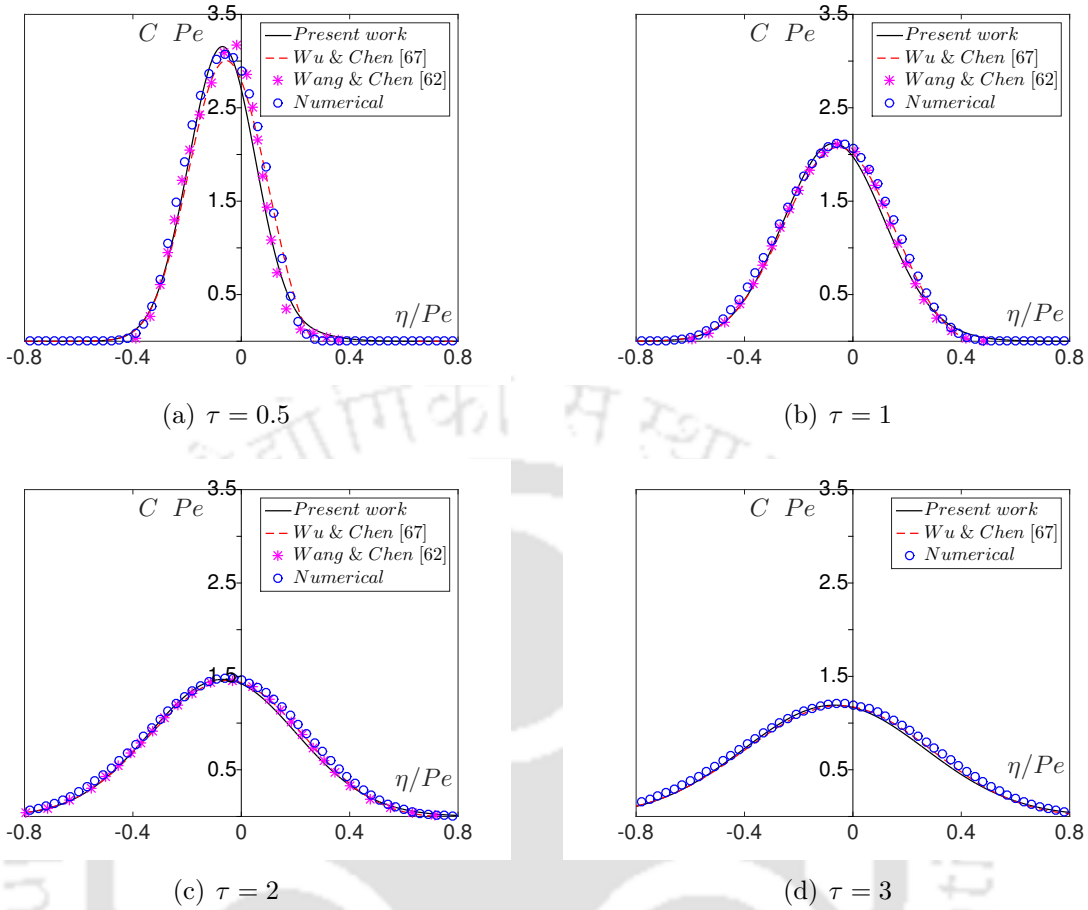

(a) $\tau = 0.5$ (b) $\tau = 1$

(c) $\tau = 2$ (d) $\tau = 3$

Figure 2.2: Comparison of transverse concentration distributions between present and previous results at different times for $y = 0$ and $\beta_m = 0$.

2.4.1 Mean concentration distribution

Effects of Pe on mean concentration can be observed from Fig. (2.4). The graphs show that with the increase of Pe, the peak of mean concentration gradually decreases and become flatter. As Pe increases, molecular diffusion also increases, which helps the solute to spread longitudinally.

In the expression of effective dispersion coefficient D_T (Eq. (2.56), the first term on the R.H.S. (i.e., the constant 1) represents the effects of longitudinal diffusion. The term usually is neglected when compared with the last term of the expression for $Pe > 100$ [18]. Consequently, one can obtain expressions independent of Pe for mean concentration in a new system $\{\eta/Pe, \langle C \rangle Pe\}$ as

$$\langle C \rangle Pe = \sqrt{\frac{105}{8\pi\tau}} \exp\Big(- \frac{105}{8\tau}\Big(\frac{\eta}{Pe}\Big)^2 - (\beta_m - \frac{1}{3}\beta_m^2)\tau\Big). \tag{2.107}$$

Longitudinal distributions of mean concentration in the channel are shown in Fig. (2.5). Absorption at channel bed mainly depletes solute concentration, which causes reduction

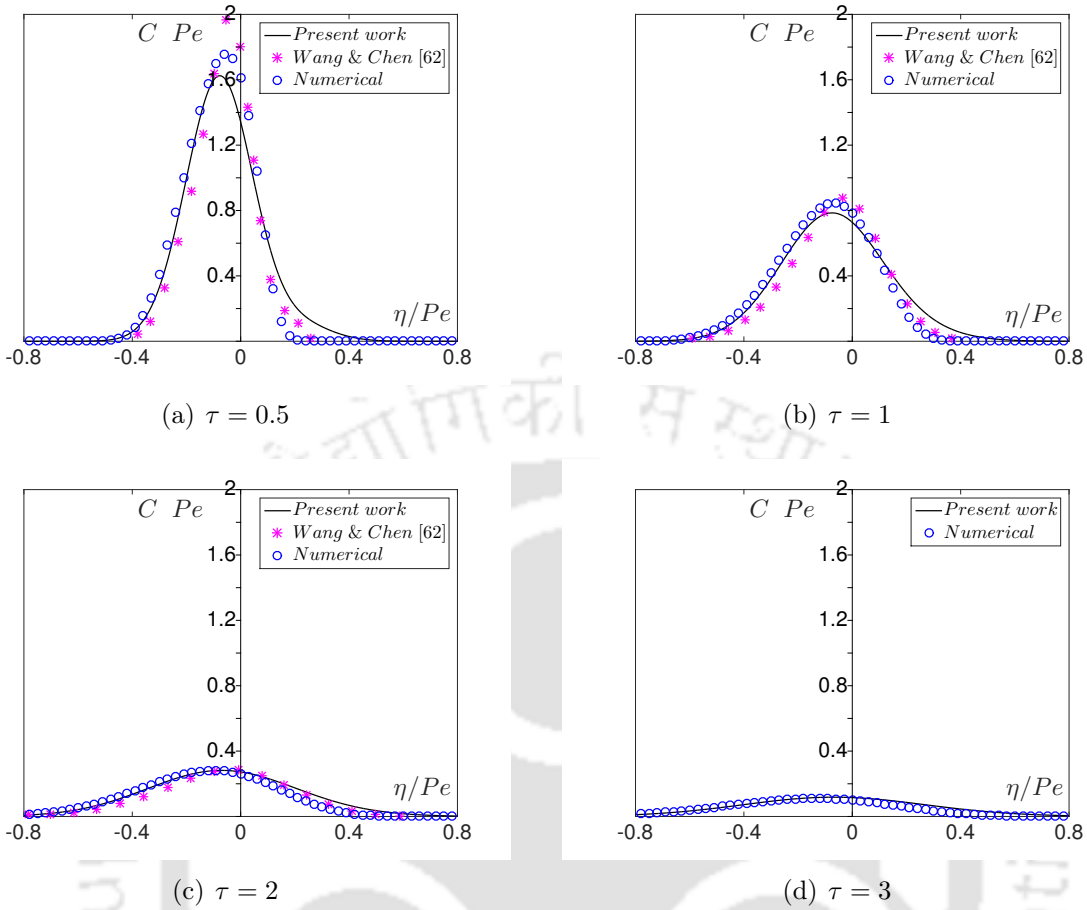

Figure 2.3: Comparison of transverse concentration distributions between present and previous results at different times for $y = 0$ and $\beta_m = 1$.

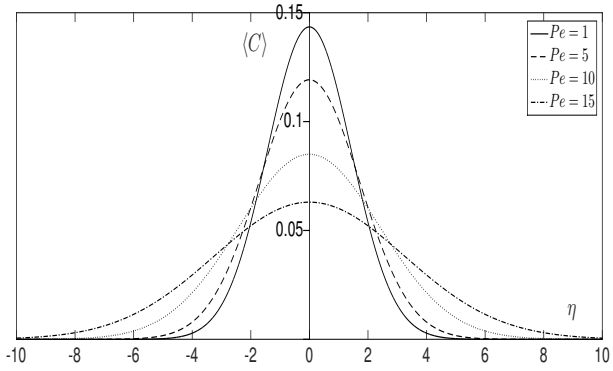

Figure 2.4: Longitudinal distributions of the mean concentrations for different Pe, where $\beta_m = 1$.

in mean concentration distribution as well. Figure (2.5a) shows that the bed absorption significantly decreases the overall mean concentration distribution with the increase of β_m. Temporal evolutions of mean concentration distribution are depicted in Fig. (2.5b)

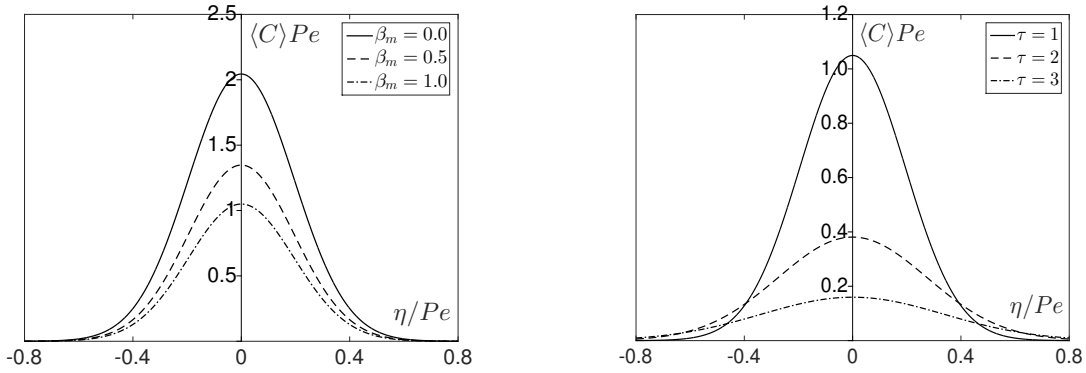

(a) $\tau = 1.0$ (b) $\beta_m = 1.0$

Figure 2.5: Longitudinal distributions of mean concentration.

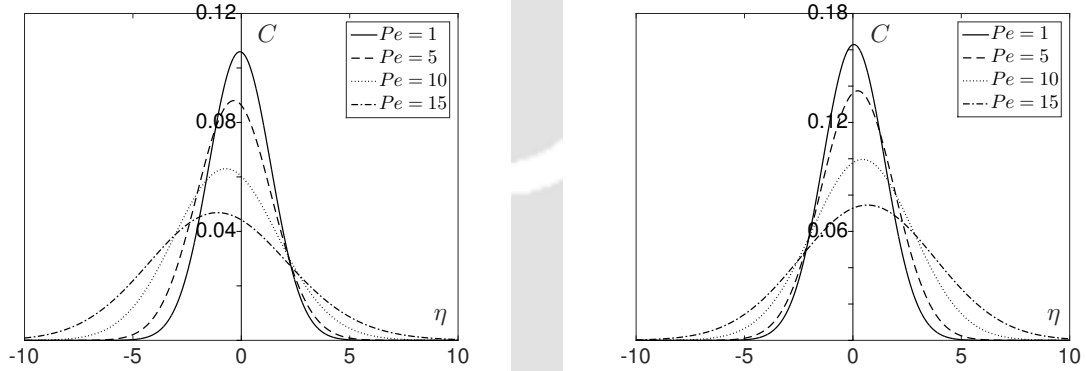

(a) $y = 0$ (b) $y = 1$

Figure 2.6: Transverse concentration distribution at $\tau = 1$ for different Pe, where $\beta_m = 1$.

for β_m. Figure shows that the mean concentration reduces with time in the central region of the moving solute. However, concentration away from the centroid increases with time due to diffusion.

2.4.2 Transverse concentration distribution

The variation of transverse concentration distribution with Pe is illustrated in Fig. (2.6). Figure (2.6a) shows that peak of the solute concentration at channel bed moves upstream with the increase of Pe. Near the channel bed, the flow becomes diffusion dominated as velocity is very low there. In addition, at higher Pe, the diffusion rate goes down, as molecular diffusivity D is inversely proportional to Pe. So, near the bed and at higher Pe, solute does not move much compared to the flow near the surface and solute stays at the upstream with respect to moving coordinate. On the other hand, peak of the solute concentration moves downstream at free surface. As the flow is advection dominated at the free surface, solute is carried away by the flow and spread longitudinally.

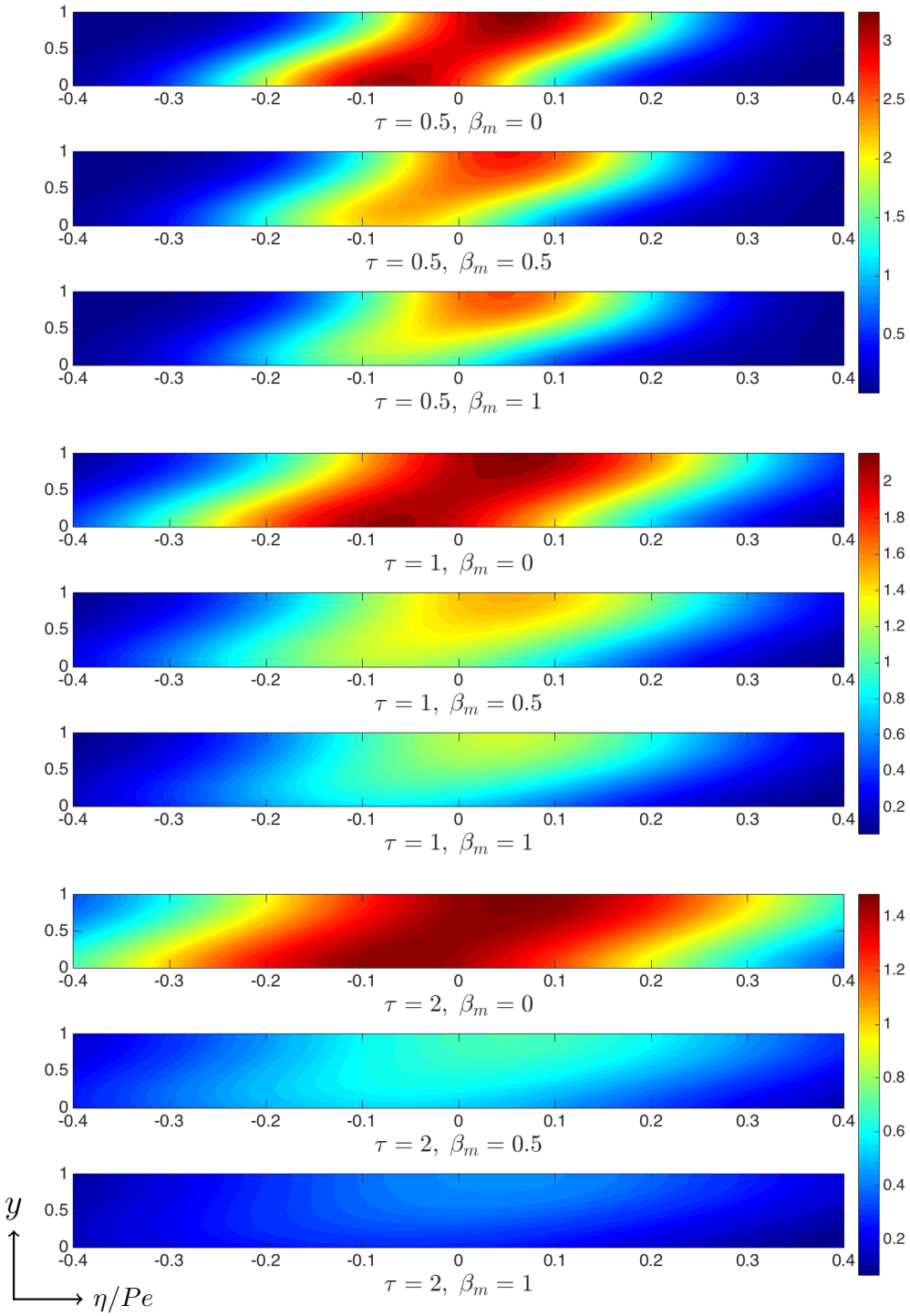

Figure 2.7: Concentration contours: horizontal coordinate represents as η/Pe and the vertical one as y.

As discussed above, for $Pe > 100$, one can easily get a Pe independent expression for transverse concentration distribution in the new coordinate system $\{\eta/Pe, C\ Pe\}$.

Equation (2.104) gives,

$$C\,Pe = \sqrt{\frac{105}{8\pi\tau}}\Bigg[(1+\beta_m M+\beta_m^2 Z+\beta_m^3 L)+(F+\beta_m Y+\beta_m^2 K)\frac{\partial}{\partial(\eta/Pe)}+(X+\beta_m J)\frac{\partial^2}{\partial(\eta/Pe)^2}+I\,\frac{\partial^3}{\partial(\eta/Pe)^3}\Bigg]\exp\Big(-\frac{105}{8\tau}\Big(\frac{\eta}{Pe}\Big)^2-(\beta_m-\frac{1}{3}\beta_m^2)\tau\Big). \tag{2.108}$$

In order to intuitively demonstrate the solute concentration transport process in an open channel flow, the concentration contours are plotted in Fig. (2.7) for different β_m and τ. Initially, the solute is injected across the line $\eta = 0$ and dispersed through the channel under the effects of advection and lateral diffusion. The coordinate system in the figures is allowed to move longitudinally with velocity $Pe(1+\frac{2}{15}\beta_m)$ to ensure that the centroid of the concentration cloud remains at the origin in each case. Figures show that in the absence of absorption at the channel bed, the solute with higher concentration is found at the free surface in the downstream and near the bed in the upstream. This is because of different combinations of scalar diffusion and advection effects. Near the free-surface, advection process is dominant and combination of this with the diffusion results in higher concentration of solute in the downstream region compared to that in the upstream region. Whereas, near the bed, the flow is diffusion dominated and advection process is not that significant. So, the solute will be diffused in the downstream as well as in the upstream region and high concentration of solute will be found in the upstream region near the origin. When absorption takes place at channel bed, it depletes the solute concentration near the channel bed and consequently the overall concentration in the channel gradually decreases. The remaining solute cloud moves with the free surface.

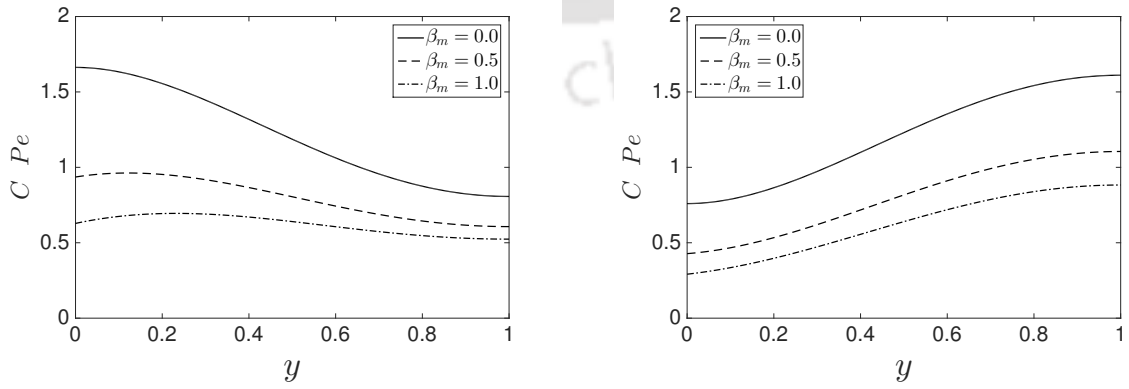

(a) $\eta/Pe = -0.2$ (b) $\eta/Pe = 0.2$

Figure 2.8: Transverse concentration distribution for different β_m at $\tau = 1$.

Figure (2.8) illustrates the transverse variation of concentration distribution for different β_m at $\tau = 1$. In order to discuss the concentration variations in the upstream and downstream sections, two typical cross-sections at $\eta/Pe = -0.2$ and at $\eta/Pe = 0.2$ are chosen. In this study, a parabolic flow profile is considered throughout the channel where the flow attains its maximum velocity at the free surface and minimum velocity at the channel bed. Figure (2.8a) reveals that in the upstream cross-section at $\eta/Pe = -0.2$, the concentration increases in the lateral direction from free surface to the channel bed and becomes maximum at the bed. The released slug moves towards the upstream through diffusion and simultaneously gets advected by the flow at a faster rate near the free surface and relatively at much slower rate near the bed. This leads to form a higher concentration zone near the channel bed. The case is reverse across a typical downstream section at $\eta/Pe = 0.2$ as plotted in Fig. (2.8b), the concentration decreases in the vertically downward direction having its maximum at the free surface. Flow velocity is higher near the free surface where longitudinal spreading of the scalar substance is fast, which causes higher concentration zone near the free surface. Such phenomena have also been discussed by Wu and Chen [67], and Wang and Chen [62]. Figures also show that concentration of the solute reduces with the increase in bed absorption (β_m).

Concentration distribution over typical upstream and downstream cross-sections can be seen from Fig. (2.9). In the absence of bed absorption, transverse concentration variation first increases up to a certain value and then decreases with the chosen section plane moving away from the centroid in both downstream and upstream directions. When bed absorption takes place, it depletes the solute near the channel bed and the concentration variation gets reduced in the upstream whereas it increases in the downstream at each cross-section. Temporal evolutions of cross-section distribution of the solute are plotted in Fig. (2.10). The graphs show that non-uniformity in the concentration distributions over the channel cross-section decrease with time in the upstream as well as in the downstream region.

Concentration distributions at different heights along with the mean concentration for various combinations of β_m and τ are shown in Fig. (2.11). Figures show that concentration curves at different heights become closer to the mean with increasing time. It concludes that non-uniformity of transverse concentration distribution reduces with time due to the effect of lateral diffusion. When bed absorption takes place, it depletes solute concentration near the upstream bed. It also reduces the concentration variation and makes the distribution uniform over the upstream cross-section. Concentration at the bed over the mean concentration should be preferred to analyse the bed absorption effects more accurately, as there is a difference between the concentration profiles at the bed and that of the mean concentration (as seen in Fig. (2.11)) and may generate significant errors in the results.

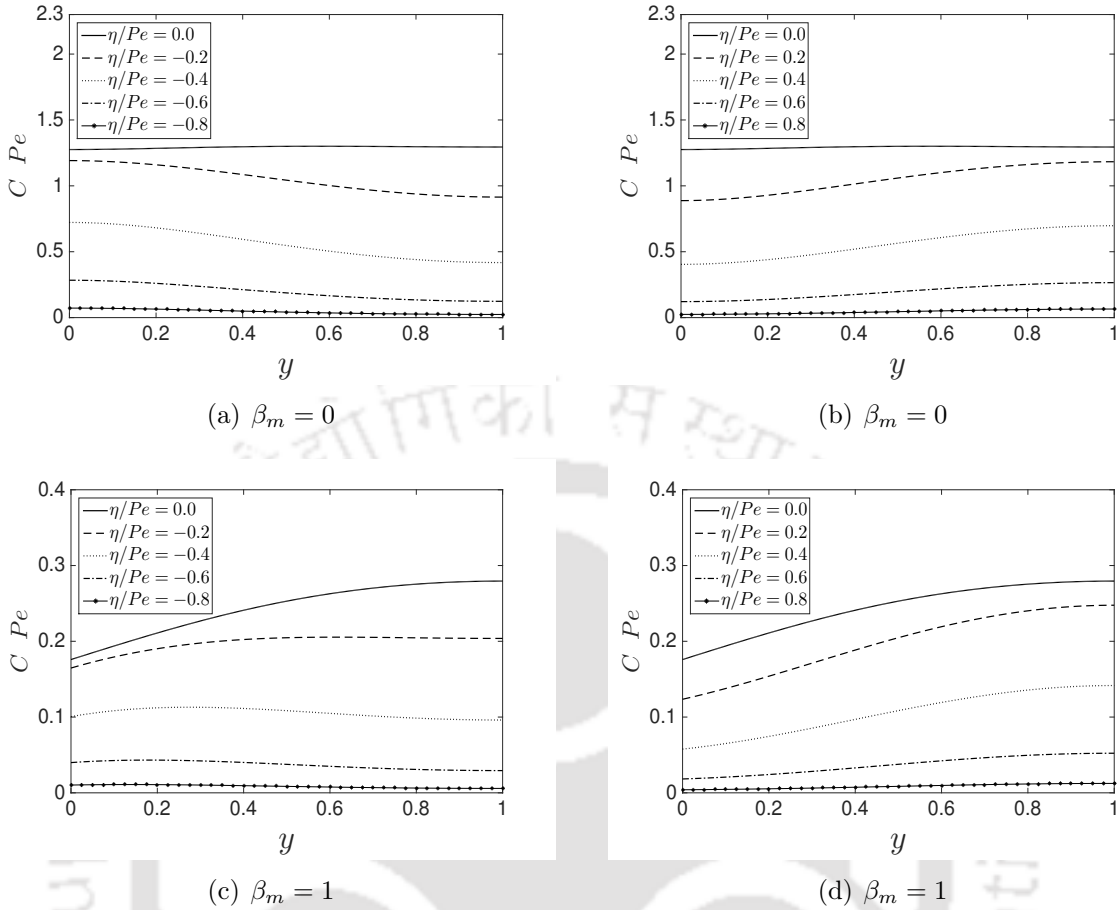

(a) $\beta_m = 0$ (b) $\beta_m = 0$

(c) $\beta_m = 1$ (d) $\beta_m = 1$

Figure 2.9: Concentration distribution over typical cross-sections for different β_m at time $\tau = 2.5$.

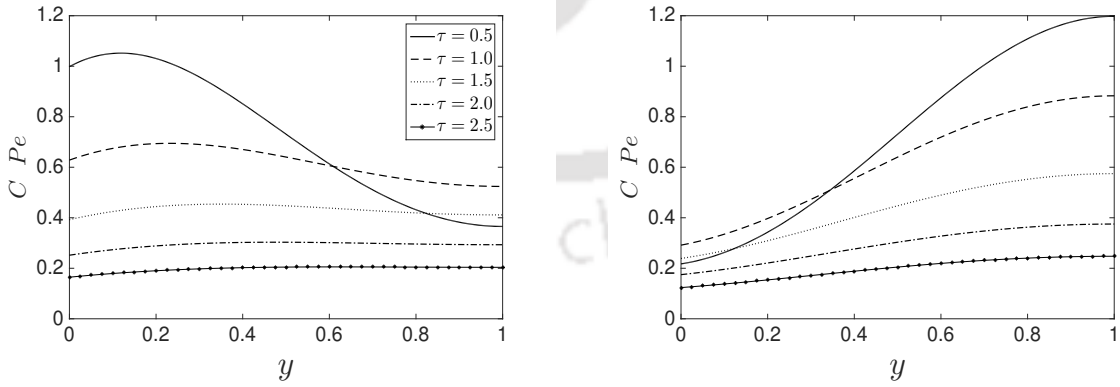

(a) $\eta/Pe = -0.2$ (b) $\eta/Pe = 0.2$

Figure 2.10: Concentration distributions for different dimensionless times at $\eta/Pe = -0.2$ and 0.2, where $\beta_m = 1.0$.

In order to discuss the uniformity of transverse concentration variations, an indicator

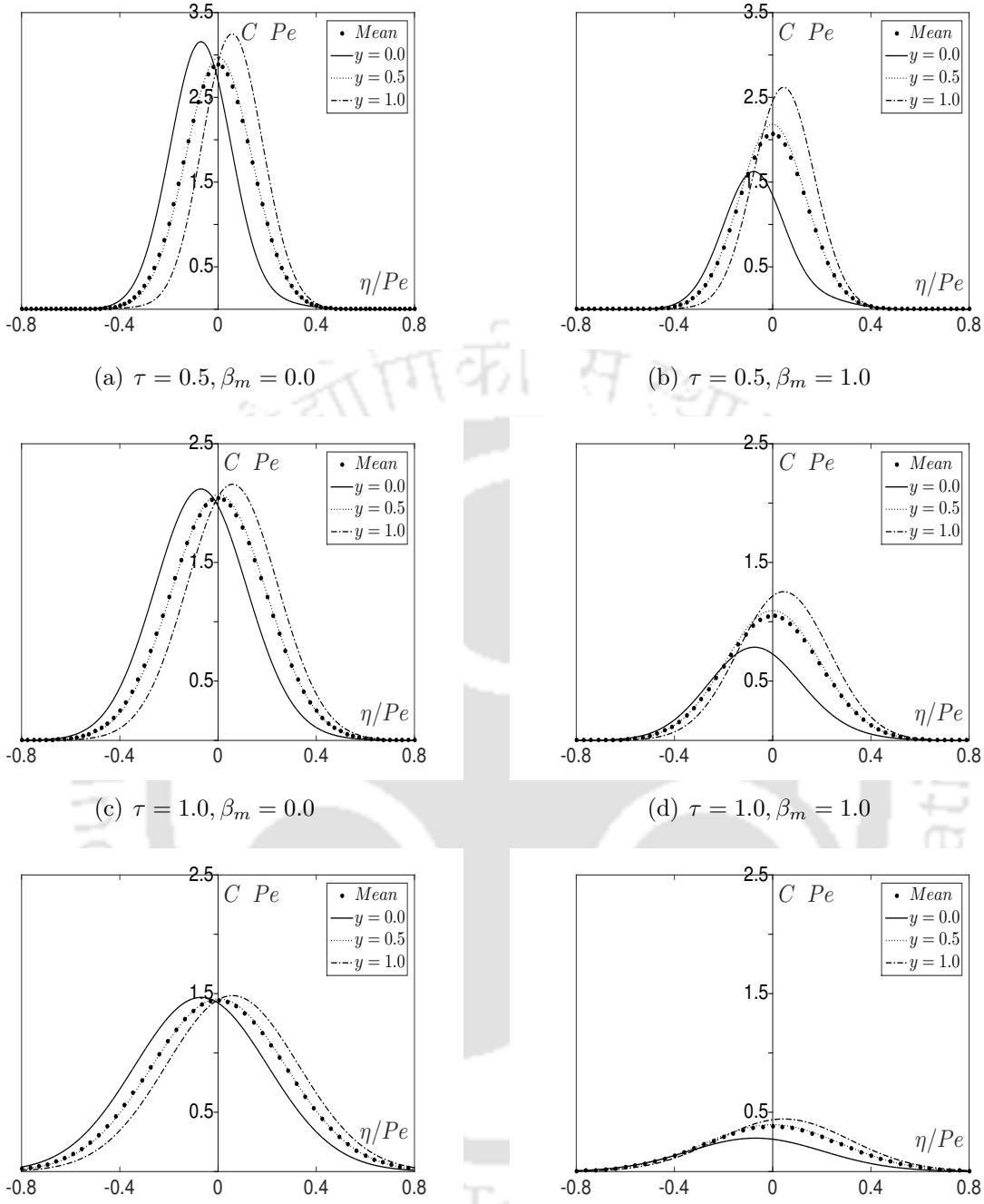

(a) $\tau = 0.5, \beta_m = 0.0$ (b) $\tau = 0.5, \beta_m = 1.0$

(c) $\tau = 1.0, \beta_m = 0.0$ (d) $\tau = 1.0, \beta_m = 1.0$

(e) $\tau = 2.0, \beta_m = 0.0$ (f) $\tau = 2.0, \beta_m = 1.0$

Figure 2.11: Concentration distribution at different heights for different combinations of β_m and τ.

$\mathcal{R}$ is adopted [68] as

$$\mathcal{R}(\eta, \tau) = \frac{\max\limits_{0 \le y \le 1} C(\eta, y, \tau) - \min\limits_{0 \le y \le 1} C(\eta, y, \tau)}{C(0, 0, \tau)} \times 100\%,$$

which is the transverse variation in the cross-section against the centroid of the concentration cloud.

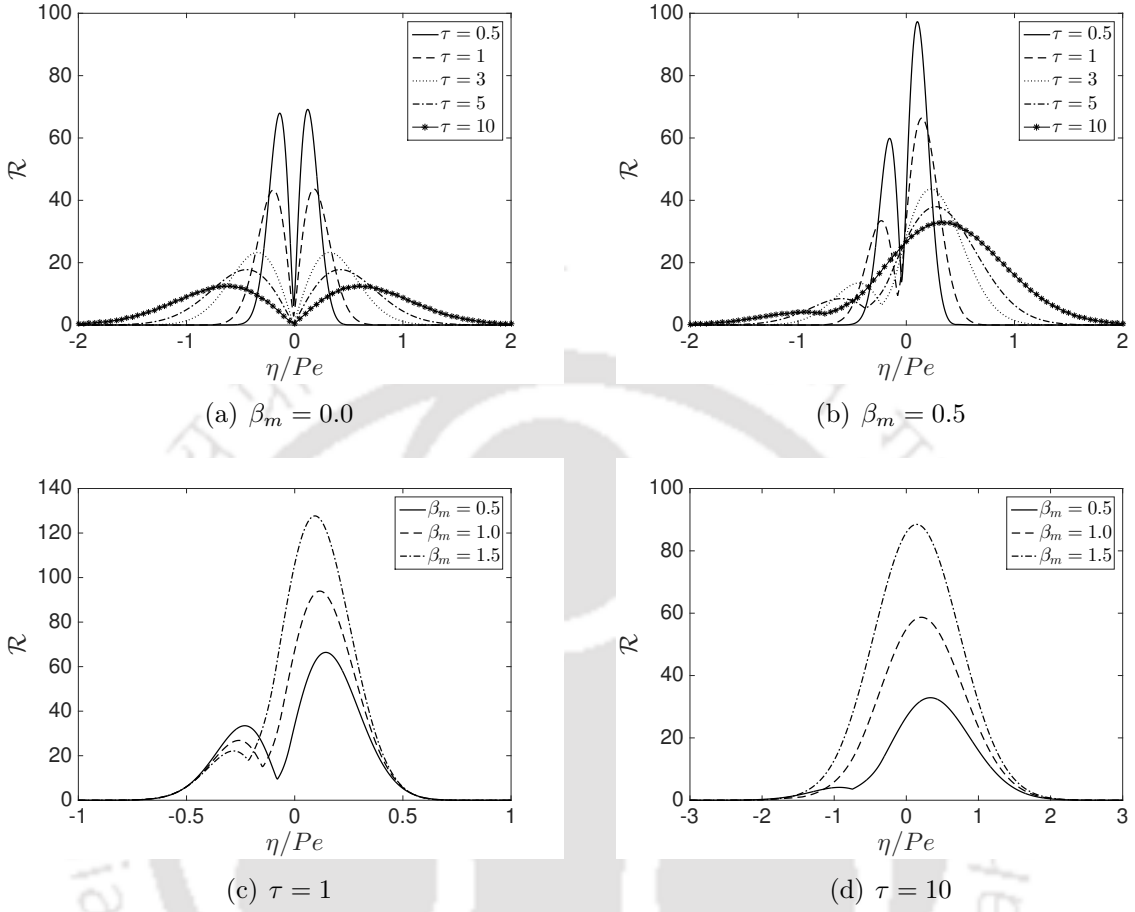

(a) $\beta_m = 0.0$ (b) $\beta_m = 0.5$

(c) $\tau = 1$ (d) $\tau = 10$

Figure 2.12: Longitudinal distributions of the vertical concentration variation rates.

Figure (2.12) demonstrates the longitudinal distribution of the transverse concentration variation rate for open channel flow. Figure (2.12a) shows the transverse concentration variation rate of the solute in a flow without bed absorption. The graph shows that variation rates are symmetrical about the centroid of the solute cloud and maximum variation rate moves away with times from solute centroid. This feature is similar to the results obtained by Wu and Chen [67] for open channel flow without bed absorption effect. Effects of bed absorption on concentration variation rate are plotted in Fig. (2.12b). Figure shows that concentration variation rate increases in the downstream. It can be added that the variation rate becomes higher in the downstream when bed absorption takes place. In downstream location, higher concentration appears near the free surface and concentration reduces at the channel bed due to bed absorption. This increases the concentration variation rate in the downstream, consequently increases the non-uniformity in concentration distribution. On the other hand, in the upstream, initially concentration is high at upstream bed but when bed absorption takes place it reduces the solute concentra-

tion near the channel bed and consequently reduces the non-uniformity in the upstream. As time increases, peak concentration value at upstream decreases and the bimodal graph becomes unimodal. Maximum concentration rate always remains in downstream region. Comparing with Fig. (2.12a), it can be concluded that bed absorption increases the non-uniformity over the channel cross-section in the downstream location of channel centroid. Figures (2.12c) and (2.12d) show the concentration variation rate for different β_m at the time $\tau = 1$ and 10 receptively. With the increase in β_m, maximum concentration variation rate increases in the downstream and consequently increases the non-uniformity. At large time $\tau = 10$, the maximum peak in the upstream almost vanishes.

2.5 Conclusions

Multi-scale method of homogenization is used to study two-dimensional transport phenomena of a solute in an open channel flow having absorbing bed. Analytical solutions are obtained for transverse real concentrations up to third-order approximations. This work presents the patterns of transverse real concentration distribution and uniformity over the cross-section of the channel. An indicator is adopted that measures the concentration variation rate over the channel cross-section. Some important observations are as follows:

1. Mean and transverse real concentrations decrease with the increase of bed absorption parameter (β_m) value.

2. Bed absorption generates large non-uniformity in transverse concentration over the channel cross-section, especially in the downstream.

3. Real concentration of the solute over the mean concentration should be preferred to analyse the bed absorption effects more accurately.

4. Our analytical solutions are relatively simpler and easier for post-processing. Results obtained through our analytical solutions agree well with the existing analytic solutions of other studies.

CHAPTER 3

SOLUTE DISPERSION IN AN OPEN CHANNEL FLOW WITH SORPTIVE CHANNEL BED

In the previous chapter, the effects of irreversible boundary reaction for an open channel flow are discussed. Boundary reaction can be reversible in nature. We discuss about the effects of reversible reaction in this chapter.

3.1 Introduction

Effect of partitioning between phases on axial dispersion behaviour was initially analysed by Westhaver [66]. Since the pioneering work of Taylor [60], the study of solute dispersion has been extended in various ways to account for partitioning effects [3]. Reversible phase exchange and partitioning is important to different applications in chromatography [56], physiological transport [12, 47, 48], and also in environmental contaminant transport [35, 36, 49].

Purnama [49] generalized the work of Taylor [60] to account for dispersion of contaminant in the presence of both reactions and retention at the flow boundary. Expressions are derived for the longitudinal shear dispersion coefficient. For turbulent flow in an open-channel, the dispersion of a passive contaminant is significantly increased by the presence of the bed retention. Purnama [50] also generalized the method of moments to account for dispersion of chemically active solutes in the presence of both reactions and retention at the flow boundary. He showed that the longitudinal shear dispersion coefficient increases and the skewness decreases as the retentive layer width increases, provided that the effect of chemical reaction at the flow boundary is not very large.

Ng [35] presented an analytical study on the transport of a chemical contaminant resulting from the discharge of contaminated fine solid particles into a turbulent open-channel flow. He found that the advection velocity and dispersion coefficient for the

chemical transport will change with space and time according to the local sediment concentration. Because of sorptive exchange between dissolved and sorbed phases, the transport of the dissolved phase is affected by the suspended particulates. Moreover, he showed that the dispersion of the dissolved chemical was higher for larger particulates. Similar observation was experimented by him while investigating the effects of kinetic sorptive exchange on the dispersion of a sorbing solute in a sediment-laden open-channel flow [36]. Following this work, Ng and Yip [42] studied a more general problem by taking a finite fall velocity of particulates, which will lead to non-trivial effects on the transport of the solute. Although the widely used method of moments gives a great deal of information about the distribution of solute concentration across the flow as it disperses, it has the disadvantage that it does not give a direct expression for real concentration distribution. Applications in the risk assessment for toxic pollutant transport in environmental fluid flows require detailed information on the transverse real concentration distribution.

In this chapter, an analytical study is presented to explore two-dimensional concentration distribution for an open channel flow with reversible phase exchange kinetics between the channel bed (immobile phase) and fluid phase (mobile phase). Analytical expressions are derived for transverse concentration distribution with the help of multi-scale method of homogenization. This study explores mean and real concentration distributions after an initial time when transient behaviour completely dies out. This study also concerns about the non-uniformity of concentration variation over the channel cross-section and effects of bed absorption on it. The specific objectives of this work are: (I) to present a multi-scale analysis for the concentration distribution in an open channel flow with sorptive channel bed, (II) to obtain analytical expressions for dispersion coefficient as well as for mean and transverse real concentrations up to second-order approximation, (III) to observe the effects of phase exchange kinetics on dispersion coefficient and two-dimensional transverse concentration distribution, (IV) to discuss the uniformity in transverse real concentration over the channel cross-section.

3.2 Formulation of the problem

A laminar, fully developed, unidirectional open channel flow with a separation width h in a Cartesian coordinate system (longitudinal $\widehat{x}$-axis and vertical $\widehat{y}$-axis) is considered. The solute is assumed to undergo an reversible phase exchange with the channel bed and disperse throughout the channel under the flow velocity $\widehat{u}$, which is given as

$$\widehat{u}(\widehat{y}) = u_0\Big(2\frac{\widehat{y}}{h} - \frac{\widehat{y}^2}{h^2}\Big), \tag{3.1}$$

where u_0 is the flow velocity of the free surface. Schematic diagram of the flow geometry is shown in Fig. (3.1).

Consider the transport of a reactive solute through the flow mentioned above. The solute is assumed to be completely miscible in the fluid. During the flow, a part of the solute is retained at the boundary and the rest moves with the fluid. In the phase where solute flows with the flowing fluid is termed as mobile or fluid phase and the phase in which the solute retains at the boundary is called immobile phase.

It is also assumed that the solute undergoes a reversible phase exchange between mobile and immobile phases. Phase exchange will take place in either forward or backward direction, which can be described by a first-order linear kinetics [42], as

$$\frac{\partial \widehat{C}_s}{\partial t} = k_f \widehat{C} - k_b \widehat{C}_s, \tag{3.2}$$

where $\widehat{C}$ is the concentration (mass of solute per bulk volume of fluid) of the mobile phase, $\widehat{C}_s$ is the concentration (mass of solute per surface area of the channel bed) of the immobile phase. The terms k_f and k_b are the forward and backward rate constants for the sorption reaction respectively. At the equilibrium state, these two phases will have their concentrations in a fixed ratio as,

$$\widehat{C}_s/\widehat{C} = k_f/k_b = \widehat{\alpha}, \tag{3.3}$$

where $\widehat{\alpha}$ is the partition coefficient or retention parameter that relates the concentrations $\widehat{C}$ and $\widehat{C}_s$. From Eqs. (3.2) and (3.3), first-order kinetics reversible reaction at the channel bed can be expressed as,

$$\frac{\partial \widehat{C}_s}{\partial t} = k(\widehat{\alpha}\widehat{C} - \widehat{C}_s),$$

where $k = k_b$ is the reversible reaction rate constant.

The problem for transport of the solute can be formulated as follows:

$$\frac{\partial \widehat{C}}{\partial \widehat{t}} + \widehat{u}\frac{\partial \widehat{C}}{\partial \widehat{x}} = D\frac{\partial^2 \widehat{C}}{\partial \widehat{x}^2} + D\frac{\partial^2 \widehat{C}}{\partial \widehat{y}^2}, \quad 0 < \widehat{y} < h, \tag{3.4}$$

where $\widehat{t}$ is the time, D is the molecular diffusivity of the solute in the fluid assumed to be constant.

The initial and boundary conditions are respectively given as

$$\widehat{C}(\widehat{x}, \widehat{y}, \widehat{t})|_{\widehat{t}=0} = \frac{Q_m}{h}\delta(\frac{\widehat{x}}{h}), \tag{3.5}$$

$$D\frac{\partial \widehat{C}}{\partial \widehat{y}} = 0, \quad \widehat{y} = h, \tag{3.6}$$

$$D\frac{\partial \widehat{C}}{\partial \widehat{y}} = \frac{\partial \widehat{C}_s}{\partial \widehat{t}} = k(\widehat{\alpha}\widehat{C} - \widehat{C}_s), \quad \widehat{y} = 0, \tag{3.7}$$

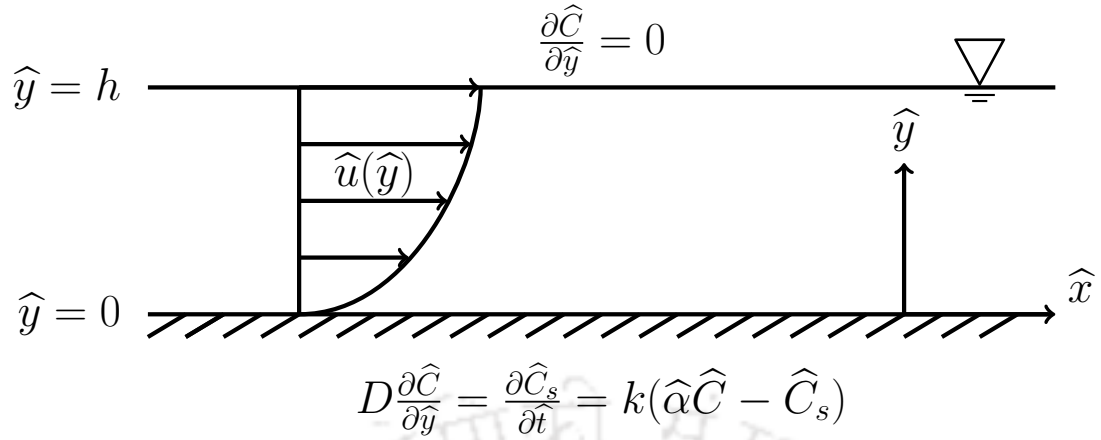

Figure 3.1: Sketch for the instantaneous release of solute in open channel flow with sorptive channel bed.

and

$$\widehat{C}(\widehat{x}, \widehat{y}, \widehat{t})|_{\widehat{x}\to\pm\infty} = 0, \tag{3.8}$$

where Q_m is the released mass and $\delta(\cdot)$ is the Dirac delta function.

3.3 Multi-scale Method of Homogenization

3.3.1 Scales selection

Associated with two length scales h (channel width) and l (characteristic longitudinal length of the solute cloud), there are three distinct time scales for transport process. The basic time scale is taken as the diffusion time across the width of the channel h. The reversible phase exchange is assumed to achieve equilibrium locally within this basic time scale. Therefore, basic time scale can be written as,

$$T_0 = O(h^2/D) = O(k^{-1}).$$

Time scale for advection down the channel is one order of magnitude longer than T_0:

$$T_1 = l/\langle \widehat{u} \rangle = T_0/\epsilon.$$

Time scale for axial diffusion is two order of magnitude longer than T_0:

$$T_2 = l^2/D = T_0/\epsilon^2.$$

Their ratios are

$$T_0 : T_1 : T_2 = 1 : \frac{1}{\epsilon} : \frac{1}{\epsilon^2},$$

where $\epsilon = \frac{h}{l}$ $(\ll 1)$ is used as the perturbation parameter.

3.3.2 Dimensionless governing equation and velocity profile

Dimensionless parameters are introduced as

$$x = \frac{\widehat{x}}{l},\ y = \frac{\widehat{y}}{h},\ u = \frac{\widehat{u}}{\langle\widehat{u}\rangle},\ t = \frac{\widehat{t}}{h^2/D},\ Pe = \frac{\langle\widehat{u}\rangle h}{D},\ C = \frac{\widehat{C}}{Q_m/h},\ C_s = \frac{\widehat{C}_s}{Q_m},$$
$$,\ Da = \frac{kh^2}{D},\ \alpha = \frac{\widehat{\alpha}}{h}, \tag{3.9}$$

where Pe is the Peclet number, Da is the Damkohler number, α is the dimensionless retention parameter and the angle brackets denote section average defined as

$$\langle\widehat{u}\rangle = \int_0^1 \widehat{u}\, dy. \tag{3.10}$$

Then the governing equation and boundary conditions can be rewritten as

$$\frac{\partial C}{\partial t} + \epsilon Pe\, u\frac{\partial C}{\partial x} = \epsilon^2\frac{\partial^2 C}{\partial x^2} + \frac{\partial^2 C}{\partial y^2}, \quad 0 < y < 1, \tag{3.11}$$

$$\frac{\partial C}{\partial y} = 0, \quad y = 1, \tag{3.12}$$

$$\frac{\partial C}{\partial y} = \frac{\partial C_s}{\partial t} = Da(\alpha C - C_s), \quad y = 0. \tag{3.13}$$

The dimensionless velocity profile is

$$u(y) = \frac{3}{2}(2y - y^2). \tag{3.14}$$

3.3.3 Asymptotic analysis

For the asymptotic analysis, the homogenization technique of Mei et al. [32] is employed. The concentrations C and C_s are expanded into multiple scales as:

$$C = C^{(0)} + \epsilon C^{(1)} + \epsilon^2 C^{(2)} + O(\epsilon^3), \tag{3.15}$$

and

$$C_s = C_s^{(0)} + \epsilon C_s^{(1)} + \epsilon^2 C_s^{(2)} + O(\epsilon^3). \tag{3.16}$$

Based on these time scales, fast, medium and slow time variables are introduced accordingly

$$t_0 = t,\ t_1 = \epsilon t,\ t_2 = \epsilon^2 t.$$

The original time derivative becomes, according to the chain rule

$$\frac{\partial}{\partial t} = \frac{\partial}{\partial t_0} + \epsilon\frac{\partial}{\partial t_1} + \epsilon^2\frac{\partial}{\partial t_2}. \tag{3.17}$$

Substitution of Eqs. (3.17) and (3.15) into Eqs. (3.11)–(3.13) results in

$$\left(\frac{\partial C^{(0)}}{\partial t_0} - \frac{\partial^2 C^{(0)}}{\partial y^2}\right) + \epsilon\left(\frac{\partial C^{(0)}}{\partial t_1} + \frac{\partial C^{(1)}}{\partial t_0} + Pe\,u\frac{\partial C^{(0)}}{\partial x} - \frac{\partial^2 C^{(1)}}{\partial y^2}\right) + \epsilon^2\left(\frac{\partial C^{(0)}}{\partial t_2} + \frac{\partial C^{(1)}}{\partial t_1} + \frac{\partial C^{(2)}}{\partial t_0} + Pe\,u\frac{\partial C^{(1)}}{\partial x} - \frac{\partial^2 C^{(0)}}{\partial x^2} - \frac{\partial^2 C^{(2)}}{\partial y^2}\right) + \cdots = 0, \quad 0 < y < 1, \tag{3.18}$$

$$\frac{\partial C^{(0)}}{\partial y} + \epsilon\frac{\partial C^{(1)}}{\partial y} + \epsilon^2\frac{\partial C^{(2)}}{\partial y} + \cdots = 0, \quad y = 1, \tag{3.19}$$

$$\frac{\partial C^{(0)}}{\partial y} + \epsilon\frac{\partial C^{(1)}}{\partial y} + \epsilon^2\frac{\partial C^{(2)}}{\partial y} + \cdots = \frac{\partial C_s^{(0)}}{\partial t_0} + \epsilon\left(\frac{\partial C_s^{(0)}}{\partial t_1} + \frac{\partial C_s^{(1)}}{\partial t_0}\right) + \epsilon^2\left(\frac{\partial C_s^{(0)}}{\partial t_2} + \frac{\partial C_s^{(1)}}{\partial t_1} + \frac{\partial C_s^{(2)}}{\partial t_0}\right) + \cdots = Da(\alpha C^{(0)} - C_s^{(0)}) + \epsilon\Big(Da(\alpha C^{(1)} - C_s^{(1)})\Big) + \epsilon^2\Big(Da(\alpha C^{(2)} - C_s^{(2)})\Big) + \cdots, \quad y = 0. \tag{3.20}$$

For leading order ($O(1)$), Eqs. (3.18)–(3.20) give:

$$\frac{\partial C^{(0)}}{\partial t_0} = \frac{\partial^2 C^{(0)}}{\partial y^2}, \quad 0 < y < 1, \tag{3.21}$$

$$\frac{\partial C^{(0)}}{\partial y} = 0, \quad y = 1, \tag{3.22}$$

$$\frac{\partial C^{(0)}}{\partial y} = \frac{\partial C_s^{(0)}}{\partial t_0} = Da(\alpha C^{(0)} - C_s^{(0)}), \quad y = 0. \tag{3.23}$$

The general solution of Eq. (3.21) becomes

$$C^{(0)} = C_0^{(0)}(x, t_1, t_2) + \sum_{n=1}^{\infty} Re\left[C_n^{(0)}(x, t_1, t_2)e^{in\pi y}\right]e^{-n^2\pi^2 t_0}. \tag{3.24}$$

The width of the channel is considered to be narrow enough so that transverse diffusion takes place almost immediately (within the first time scale) after the release. It is observed from the equation that the numerical value of the series part decreases exponentially with fast time variable, and it become insignificant for $t_1 \geq O(1)$ [33]. Considering above facts, dependency of $C^{(0)}$ on y and t_0 in a larger time may be neglected. So, the solution can

be considered as

$$C^{(0)} = C^{(0)}(x, t_1, t_2). \tag{3.25}$$

Evidently, for long time evolution, diffusion has enough time to smooth out lateral variations. Therefore, the leading order concentration is independent of y across the channel section [40]. On removing the dependence of $C^{(0)}$ on y, the boundary condition (3.23) gives

$$C_s^{(0)} = \alpha C^{(0)}. \tag{3.26}$$

For first-order ($O(\epsilon)$), Eqs. (3.18)–(3.20) give:

$$\frac{\partial C^{(0)}}{\partial t_1} + \frac{\partial C^{(1)}}{\partial t_0} + Pe\, u \frac{\partial C^{(0)}}{\partial x} = \frac{\partial^2 C^{(1)}}{\partial y^2}, \quad 0 < y < 1, \tag{3.27}$$

$$\frac{\partial C^{(1)}}{\partial y} = 0, \quad y = 1, \tag{3.28}$$

$$\frac{\partial C^{(1)}}{\partial y} = \frac{\partial C_s^{(0)}}{\partial t_1} + \frac{\partial C_s^{(1)}}{\partial t_0} = Da(\alpha C^{(1)} - C_s^{(1)}), \quad y = 0. \tag{3.29}$$

As the time scale t_0 is much larger compared to the time scale t_1, the partial derivative terms w.r.t. t_0 can be neglected [70]. So, Eq. (3.27) becomes

$$\frac{\partial C^{(0)}}{\partial t_1} + Pe\, u \frac{\partial C^{(0)}}{\partial x} = \frac{\partial^2 C^{(1)}}{\partial y^2}, \quad 0 < y < 1. \tag{3.30}$$

Taking a section average of Eq. (3.30) w.r.t. the spatial variable y subject to the conditions (3.28) and (3.29), we get

$$\frac{\partial C^{(0)}}{\partial t_1} + Pe \frac{\langle u \rangle}{R} \frac{\partial C^{(0)}}{\partial x} = 0, \tag{3.31}$$

where $R = 1 + \alpha$ is the retardation factor.

Subtracting (3.31) from (3.30), we get

$$Pe\Big(u - \frac{\langle u \rangle}{R}\Big) \frac{\partial C^{(0)}}{\partial x} = \frac{\partial^2 C^{(1)}}{\partial y^2}, \quad 0 < y < 1. \tag{3.32}$$

These equation suggest the following substitutions

$$C^{(1)} = Pe\, F(y) \frac{\partial C^{(0)}}{\partial x}, \tag{3.33}$$

$$C_s^{(1)} = Pe\, F_s \frac{\partial C^{(0)}}{\partial x}, \tag{3.34}$$

where the coefficients $F(y)$ and F_s are to be found as follows. On matching terms asso-

ciated with $\frac{\partial C^{(0)}}{\partial x}$, the function $F(y)$is found to be governed by

$$\frac{d^2F}{dy^2} = u - \frac{\langle u \rangle}{R}, \quad 0 < y < 1, \tag{3.35}$$

with the following conditions

$$\frac{dF}{dy} = 0, \quad y = 1, \tag{3.36}$$

$$\frac{dF}{dy} = -\frac{\alpha\langle u \rangle}{R} = Da(\alpha F - F_s), \quad y = 0, \tag{3.37}$$

and

$$\langle F \rangle = 0. \tag{3.38}$$

For second-order ($O(\epsilon^2)$), Eqs. (3.18)–(3.20) give:

$$\frac{\partial C^{(0)}}{\partial t_2} + \frac{\partial C^{(1)}}{\partial t_1} + \frac{\partial C^{(2)}}{\partial t_0} + Pe\, u\frac{\partial C^{(1)}}{\partial x} = \frac{\partial^2 C^{(0)}}{\partial x^2} + \frac{\partial^2 C^{(2)}}{\partial y^2}, \quad 0 < y < 1, \tag{3.39}$$

$$\frac{\partial C^{(2)}}{\partial y} = 0, \quad y = 1, \tag{3.40}$$

$$\frac{\partial C^{(2)}}{\partial y} = \frac{\partial C_s^{(0)}}{\partial t_2} + \frac{\partial C_s^{(1)}}{\partial t_1} + \frac{\partial C_s^{(2)}}{\partial t_0} = Da(\alpha C^{(2)} - C_s^{(2)}), \quad y = 0. \tag{3.41}$$

The time scale t_0 is much larger time scale compared to t_1 and t_2, the partial derivative terms w.r.t. t_0 can be neglected. So, equation (3.39) becomes

$$\frac{\partial C^{(0)}}{\partial t_2} + \frac{\partial C^{(1)}}{\partial t_1} + Pe\, u\frac{\partial C^{(1)}}{\partial x} = \frac{\partial^2 C^{(0)}}{\partial x^2} + \frac{\partial^2 C^{(2)}}{\partial y^2}, \quad 0 < y < 1. \tag{3.42}$$

On taking a section average of Eq. (3.42) w.r.t. the spatial variable y subject to the conditions (3.40) and (3.41), we get

$$R\frac{\partial C^{(0)}}{\partial t_2} + \frac{\partial \langle C^{(1)} \rangle}{\partial t_1} + \frac{\partial C_s^{(1)}}{\partial t_1} + Pe\left\langle u\frac{\partial C^{(1)}}{\partial x}\right\rangle = \frac{\partial^2 C^{(0)}}{\partial x^2}. \tag{3.43}$$

Using Eqs. (3.31), (3.33), (3.34) and (3.38), one can get the following

$$\frac{\partial C^{(1)}}{\partial t_1} = -Pe^2\frac{\langle u \rangle F}{R}\frac{\partial^2 C^{(0)}}{\partial x^2}, \tag{3.44}$$

$$\frac{\partial \langle C^{(1)} \rangle}{\partial t_1} = 0, \tag{3.45}$$

$$\frac{\partial C_s^{(1)}}{\partial t_1} = -Pe^2\frac{\langle u \rangle F_s}{R}\frac{\partial^2 C^{(0)}}{\partial x^2}, \tag{3.46}$$

$$u\frac{\partial C^{(1)}}{\partial x} = Pe\ uF\ \frac{\partial^2 C^{(0)}}{\partial x^2}, \tag{3.47}$$

and

$$\left\langle u\frac{\partial C^{(1)}}{\partial x}\right\rangle = Pe\ \langle uF\rangle \frac{\partial^2 C^{(0)}}{\partial x^2}. \tag{3.48}$$

Substitution of Eqs. (3.45), (3.46) and (3.48) in Eq. (3.43), we get

$$\frac{\partial C^{(0)}}{\partial t_2} = \left(\frac{1}{R} - Pe^2\frac{\langle uF\rangle}{R} + Pe^2\frac{\langle u\rangle F_s}{R^2}\right)\frac{\partial^2 C^{(0)}}{\partial x^2}. \tag{3.49}$$

Multiplying Eq. (3.31) by ϵ and Eq. (3.49) by ϵ^2 and adding together one obtains,

$$\frac{\partial C^{(0)}}{\partial t_0}+\epsilon\frac{\partial C^{(0)}}{\partial t_1}+\epsilon^2\frac{\partial^2 C^{(0)}}{\partial t_2}+\epsilon Pe\frac{\langle u\rangle}{R}\frac{\partial C^{(0)}}{\partial x} = \epsilon^2\left(\frac{1}{R}-Pe^2\frac{\langle uF\rangle}{R}+Pe^2\frac{\langle u\rangle F_s}{R^2}\right)\frac{\partial^2 C^{(0)}}{\partial x^2}. \tag{3.50}$$

Rewrite Eq. (3.50) in original time variable as

$$\frac{\partial C^{(0)}}{\partial t} + \epsilon Pe\frac{\langle u\rangle}{R}\frac{\partial C^{(0)}}{\partial x} = \epsilon^2\left(\frac{1}{R} - Pe^2\frac{\langle uF\rangle}{R} + Pe^2\frac{\langle u\rangle F_s}{R^2}\right)\frac{\partial^2 C^{(0)}}{\partial x^2}. \tag{3.51}$$

On solving the two system of Eqs. (3.35)–(3.38), one can get

$$F(y) = -\frac{1}{8}y^4 + \frac{1}{2}y^3 - \frac{1}{2R}y^2 - \left(1-\frac{1}{R}\right)y + \frac{2}{5} - \frac{1}{3R}, \tag{3.52}$$

$$F_s = \frac{2}{5}R - \frac{11}{15} + \frac{1}{3R} + \left(1-\frac{1}{R}\right)\frac{1}{Da}, \tag{3.53}$$

and using Eqs. (3.14) and (3.52) one can find

$$\langle uF\rangle = -\frac{3}{35} + \frac{1}{15R}. \tag{3.54}$$

With the help of the initial and boundary conditions given in equations (3.5) and (3.8), the solution of (3.51) in terms of the new variable $\tau = t$ and $\eta = \frac{\widehat{x}}{h} - Pe\frac{\langle u\rangle}{R}t$, can be obtained as,

$$C^{(0)} = \frac{1}{\sqrt{4\pi D_T\tau}}\ \exp\Big(-\frac{\eta^2}{4D_T\tau}\Big), \tag{3.55}$$

where

$$D_T = \frac{1}{R} - Pe^2\frac{\langle uF\rangle}{R} + Pe^2\frac{\langle u\rangle F_s}{R^2}, \tag{3.56}$$

is the effective diffusive coefficient or dispersion coefficient.

Eliminating $\frac{\partial C^{(0)}}{\partial t_2}$ from Eqs. (3.42) and (3.43), one can get

$$\frac{\partial C^{(1)}}{\partial t_1} + Pe\, u\frac{\partial C^{(1)}}{\partial x} - Pe\frac{1}{R}\left\langle u\frac{\partial C^{(1)}}{\partial x}\right\rangle - \frac{1}{R}\frac{\partial C_s^{(1)}}{\partial t_1} = \frac{\alpha}{R}\frac{\partial^2 C^{(0)}}{\partial x^2} + \frac{\partial^2 C^{(2)}}{\partial y^2}. \tag{3.57}$$

After substituting Eqs. (3.44), (3.46), (3.47) and (3.48) in Eq. (3.57), we get

$$\frac{\partial^2 C^{(2)}}{\partial y^2} = \left\{ -\frac{\alpha}{R} + Pe^2\left(\left(u - \frac{\langle u\rangle}{R}\right)F - \frac{\langle uF\rangle}{R} + \frac{\langle u\rangle F_s}{R^2}\right)\right\}\frac{\partial^2 C^{(0)}}{\partial x^2}. \tag{3.58}$$

The time scale t_0 is much larger time scale compared to t_1 and t_2, the boundary condition at channel bed, Eq. (3.41) becomes (taking first equality of Eq. (3.41))

$$\frac{\partial C^{(2)}}{\partial y} = \frac{\partial C_s^{(0)}}{\partial t_2} + \frac{\partial C_s^{(1)}}{\partial t_1}, \quad y = 0. \tag{3.59}$$

Using Eqs. (3.26), (3.49) and (3.46), Eq. (3.59) becomes

$$\frac{\partial C^{(2)}}{\partial y} = \left\{\frac{\alpha}{R} - Pe^2\left(\frac{\alpha\langle uF\rangle}{R} + \frac{\langle u\rangle F_s}{R^2}\right)\right\}\frac{\partial^2 C^{(0)}}{\partial x^2}, \quad y = 0. \tag{3.60}$$

In the equations (3.58) and (3.60), one may neglect the first term associated with $\frac{\partial^2 C^{(0)}}{\partial x^2}$ on R.H.S for large Pe (usually Pe is very large for practical purpose). Hence one can take the substitution for the equation as

$$C^{(2)} = Pe^2 X(y)\frac{\partial^2 C^{(0)}}{\partial x^2}, \tag{3.61}$$

$$C_s^{(2)} = Pe^2 X_s\frac{\partial^2 C^{(0)}}{\partial x^2}, \tag{3.62}$$

where the coefficients are to be found as follows. On matching the terms associated with $\frac{\partial^2 C^{(0)}}{\partial x^2}$, one can get

$$\frac{d^2X}{dy^2} = \left(u - \frac{\langle u\rangle}{R}\right)F - \frac{\langle uF\rangle}{R} + \frac{\langle u\rangle F_s}{R^2}, \quad 0 < y < 1, \tag{3.63}$$

with the following conditions

$$\frac{dX}{dy} = 0, \quad y = 1, \tag{3.64}$$

$$\frac{dX}{dy} = -\frac{\alpha\langle uF\rangle}{R} - \frac{\langle u\rangle F_s}{R^2} = Da(\alpha X - X_s), \quad y = 0, \tag{3.65}$$

and

$$\langle X\rangle = 0. \tag{3.66}$$

On solving Eqs. (3.63)–(3.66), one can get

$$X(y) = \frac{3}{896}y^8 - \frac{3}{112}y^7 + \left(\frac{1}{20} + \frac{7}{240R}\right)y^6 + \left(\frac{3}{40} - \frac{7}{40R}\right)y^5 + \left(-\frac{3}{10} + \frac{7}{24R} + \frac{1}{24R^2}\right) \times y^4 + \left(\frac{1}{5} - \frac{1}{6R^2}\right)y^3 + \left(\frac{3}{70R} - \frac{7}{30R^2} + \frac{1}{6R^3} + \frac{1}{2R^2Da} - \frac{1}{2R^3Da}\right)y^2 + \left(\frac{3}{35} - \frac{58}{105R} + \frac{4}{5R^2} - \frac{1}{3R^3} - \frac{1}{R^2Da} + \frac{1}{R^3Da}\right)y - \frac{26}{525} + \frac{8}{35R} - \frac{13}{45R^2} + \frac{1}{9R^3} + \frac{1}{3R^2Da} - \frac{1}{3R^3Da}, \tag{3.67}$$

and

$$X_s = -\frac{26}{525}R + \frac{146}{525} - \frac{163}{315R} + \frac{2}{5R^2} - \frac{1}{9R^3} - \frac{3}{35Da} + \frac{31}{35RDa} - \frac{22}{15R^2Da} + \frac{2}{3R^3Da} + \frac{1}{R^2Da^2} - \frac{1}{R^3Da^2}. \tag{3.68}$$

In a similar way, one can find the further terms C_n, $(n = 3, 4, 5, \ldots)$, whose expressions are too long and cumbersome, and therefore omitted here. Without phase exchange effect ($\alpha = 0$ or $R = 1$), the functions $F(y)$ and $X(y)$ becomes

$$F(y)\Big|_{\alpha=0} = -\frac{1}{8}y^4 + \frac{1}{2}y^3 - \frac{1}{2}y^2 + \frac{1}{15}, \tag{3.69}$$

$$X(y)\Big|_{\alpha=0} = \frac{3}{896}y^8 - \frac{3}{112}y^7 + \frac{19}{240}y^6 - \frac{1}{10}y^5 + \frac{1}{30}y^4 + \frac{1}{30}y^3 - \frac{1}{42}y^2 + \frac{2}{1575}, \tag{3.70}$$

which are similar to those obtained in the work of Wu and Chen [67].

3.4 Results and discussion

In the following subsections, Taylor dispersivity, distributions of mean and of transverse concentrations are discussed. Taylor dispersivity and the concentrations depend on the parameters α and Da. While the parameter α is the normalized partition coefficient or retention parameter, which is in other word, the ratio of solute distributed between the phase sorbed at channel bed and that dissolved in the fluid. The parameter Da, which is the ratio of the reversible reaction rate to the molecular diffusion rate, represents the significance of the kinetics of the phase exchange. Smaller and larger Da's imply slower and faster phase exchange kinetics respectively.

In the expression of effective dispersion coefficient D_T (Eq. (3.56)), the first term on the R.H.S. (i.e., the constant $1/R$) represents the effects of longitudinal diffusion. The term

usually is neglected when compared with the last term of the expression for $Pe > 100$ [18]. Hence, dispersion coefficient becomes

$$D_T \approx Pe^2\, D_{Ta}, \tag{3.71}$$

where

$$D_{Ta} = -\frac{\langle uF\rangle}{R} + \frac{\langle u\rangle F_s}{R^2}, \tag{3.72}$$

is the apparent dispersion coefficient, depends on α and Da.

The mean concentration distribution can be obtained from Eqs. (3.15) and (3.55) in a new Pe independent system $\{\eta/Pe, \langle C\rangle Pe\}$ as

$$\langle C\rangle Pe = C^{(0)}\, Pe = \frac{1}{\sqrt{4\pi D_{Ta}\tau}}\, \exp\Big(-\frac{(\eta/Pe)^2}{4D_{Ta}\tau}\Big). \tag{3.73}$$

According to the asymptotic expansion given in Eq. (3.15), the two-dimensional concentration distribution up to second-order is derived as

$$C\, Pe = \langle C\rangle Pe + F\frac{\partial(\langle C\rangle Pe)}{\partial(\eta/Pe)} + X\frac{\partial^2(\langle C\rangle Pe)}{\partial(\eta/Pe)^2}. \tag{3.74}$$

As we have not come across any literature that can be used directly to compare with the solution of the present problem, so results of the present study for $\alpha = 0$ (ie. without phase exchange) are compared with the results of Wu and Chen [67] and also with our previous study (in Chapter 2) without considering bed absorption effects in Fig. (3.2). Figure shows an excellent agreement, which, in turn, ensures the accuracy and reliability of the present solution.

3.4.1 Dispersivity

The explicit form of the apparent dispersion coefficient can be derived from Eqs. (3.53), (3.54) and (3.72) as

$$D_{Ta} = \frac{1}{R}\Big\{\frac{17}{35} - \frac{4}{5R} + \frac{1}{3R^2} + \frac{1}{RDa} - \frac{1}{R^2 Da}\Big\}. \tag{3.75}$$

In the inert case (when $\alpha = 0$ or $R = 1$), the dispersion coefficient becomes

$$D_{Ta}\Big|_{\alpha=0} = \frac{2}{105}, \tag{3.76}$$

which is same as the one obtained by Wu and Chen [67].

Effects of partition coefficient (α) and kinetics (depends on Da) on dispersion coefficient are shown in Fig. (3.3). Figure shows that dispersion coefficient increases with the

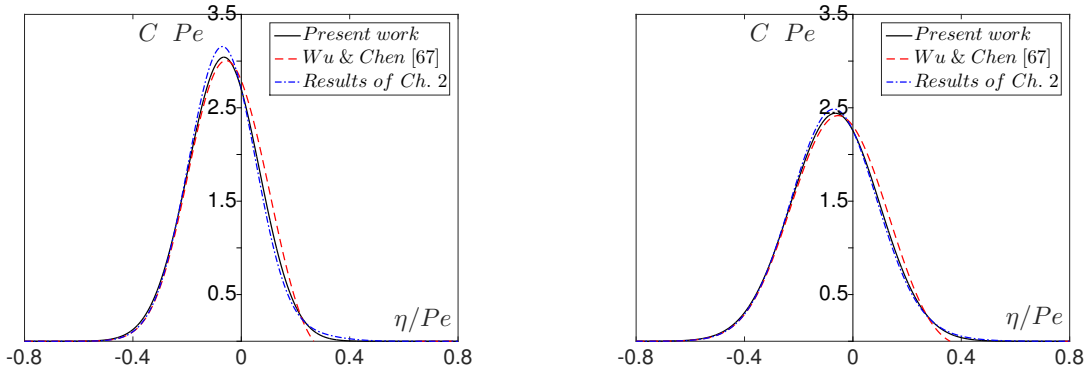

(a) $\tau = 0.5$ (b) $\tau = 0.75$

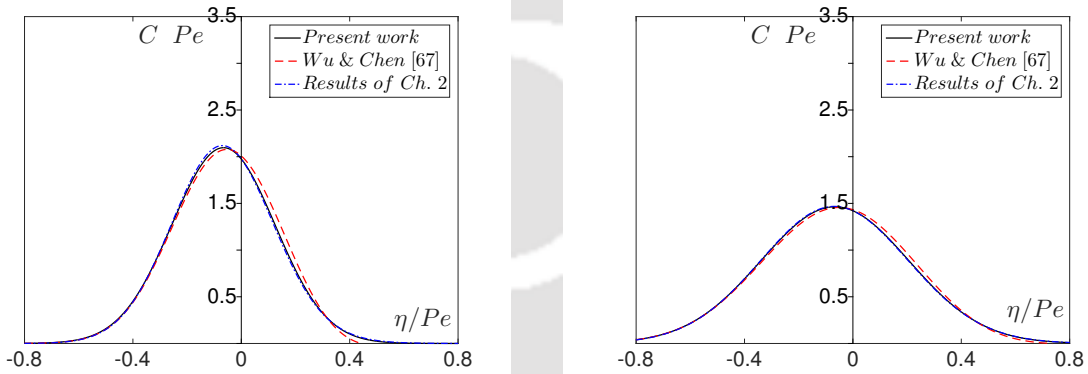

(c) $\tau = 1$ (d) $\tau = 2$

Figure 3.2: Comparison of transverse concentration distributions between present and previous results at different times, where $y = 0$ and $\alpha = 0$.

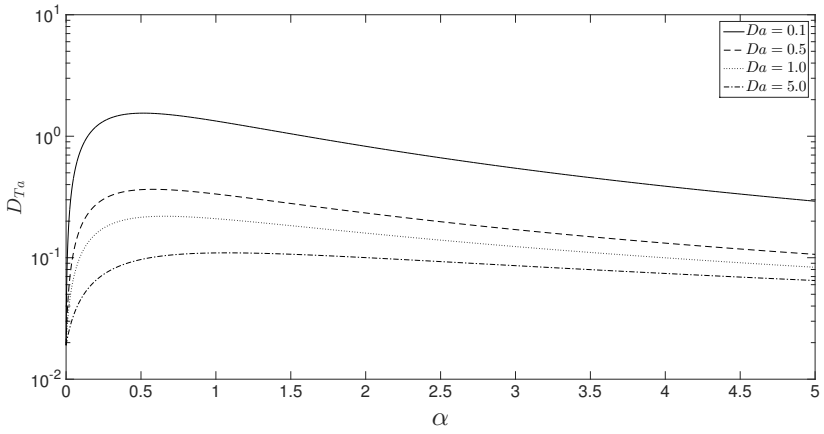

Figure 3.3: Variations of dispersion coefficient with α for different Da.

initial increase of α up to a certain value and then decreases for further increase of α. The occurrence of this maximum value may be due to bed retention that allows solute to retain at the channel bed and after a while (depending on Da) it is released back into

Da	Max$\{D_{Ta}\}$	α_m	$\frac{Max\{D_{Ta}\}}{D_{Ta}\|_{\alpha=0}}$
0.1	1.5490	0.5154	81.3225
1	0.2194	0.6588	11.5185
10	0.0981	1.2386	5.1502
100	0.0886	1.4317	4.6515
...	...	...	...
∞	0.0876	1.4557	4.5990

Table 3.1: Values of maximum dispersion coefficients at maximum α for different Da.

the flow at the upstream side, by that time the maximum concentration cloud moves from its original position. This creates a long tail of the solute cloud and consequently increases solute dispersion through the channel, as also discussed in the work of Ng and Rudraiah [41]. Further increase of α beyond a critical value will decrease the dispersion coefficient value due to the higher retardation factor, which drag down the ability of solute spreading along the concentration gradient. It is also observed that slow phase exchange kinetics ($Da \ll 1$) gives rise to larger values of dispersion coefficients than the fast kinetics ($Da > 1$) as solute is retained for a longer time in the former case and is slowly released into the flow that enhances the solute dispersion. Such a phenomenon is reported in Ng and Yip [42]. Also it is noticed that increase in dispersion coefficient is very sharp when channel bed just turned from perfectly inert to slightly retentive. These observations can be verified mathematically.

From Eq. (3.75), the gradient of D_{Ta} at $\alpha = 0$ is

$$\left.\frac{dD_{Ta}}{d\alpha}\right|_{\alpha=0} = \frac{4}{35} + \frac{1}{Da}, \tag{3.77}$$

which is always positive and is large for small Da. This fact indicates that the curve has a very steep gradient for $Da \ll 1$, which causes sharp increase in dispersion coefficient. The dispersion coefficient can reach at the maximum value at $\alpha = \alpha_m$, where

$$\alpha_m = \frac{1}{17}\left(11 - \frac{35}{Da} + \sqrt{189 - \frac{175}{Da} + \frac{1225}{Da^2}}\right). \tag{3.78}$$

The values of maximum D_{Ta} for different Da are listed in table 3.1. The dispersion coefficients reach their maximum values when the phase exchange coefficient or retention parameter is in the range of 0.5–1.5 (as Da tends to 0, limiting value of α_m approaches 0.5). Further increase in α will cause dispersion coefficient to decrease as reversible phase exchange process retards the advection speed $1/R$, which is always smaller than the initial velocity. It can be observed from the table 3.1, that for $Da = 0.1$, the maximum dispersion

coefficient value is more than 81 times the value of the coefficient (2/105) for the inert case ($\alpha = 0$). Such a huge impact of phase exchange kinetics on dispersion coefficient is extremely remarkable.

3.4.2 Mean concentration distributions

From Eq. (3.73), the explicit form of the mean concentration distribution can be written as

$$\langle C\rangle Pe = \frac{\exp\left[-(\eta/Pe)^2 \Big/ \frac{4}{R}\left\{\frac{17}{35} - \frac{4}{5R} + \frac{1}{3R^2} + \frac{1}{RDa} - \frac{1}{R^2 Da}\right\}\tau\right]}{\sqrt{\frac{4\pi}{R}\left\{\frac{17}{35} - \frac{4}{5R} + \frac{1}{3R^2} + \frac{1}{RDa} - \frac{1}{R^2 Da}\right\}\tau}}. \tag{3.79}$$

The present study is not intended to focus on the longitudinal skewness of concentration cloud at initial times. The expression for mean concentration becomes exactly similar to that of Taylor dispersion model. The expression of mean (Eq. (3.79)) can give an excellent result after some initial time when the longitudinal skewness completely dies out.

Da	α_m	$\alpha = 0.001$	$\alpha = 0.01$	$\alpha = 0.1$	$\alpha = 0.3$	$\alpha = 0.5$	$\alpha = 1$	$\alpha = 3$	$\alpha = 5$	$\alpha = 10$
0.1	0.5154	1.6528	0.8238	0.3190	0.2369	0.2267	0.2442	0.3820	0.5223	0.8395
1	0.6588	1.9868	1.6313	0.8666	0.6497	0.6081	0.6163	0.8027	0.9767	1.3253
10	1.2386	2.0326	1.9389	1.4404	1.1011	0.9861	0.9056	0.9892	1.1276	1.4368

Table 3.2: Peak values of mean concentration distributions for different values of α and Da at $\tau = 1$.

Longitudinal distribution of mean concentration in the channel are shown in Fig. (3.4). Figure (3.4a) shows the distribution curves of mean for different values of α. Figure shows that peak value of the mean concentration distribution decreases with the increase of α up to a maximum value $\alpha_m \approx 0.6588$ (graph not shown) as dispersion coefficient increases in that range. Further increase of α causes the peak value to increase. As large α delays the solute transport by slowing down the transport velocity. The result is reported in table 3.2. Variations of longitudinal distribution of mean concentration with Da can be observed from Fig. (3.4b). Figure shows that for a fixed value of α, peak value of the mean concentration increases as Da increases. For $Da \gg 1$, the reversible reaction rate is much faster than the diffusion rate. Solute moves back quickly to the fluid from the immobile phase (i.e., the channel bed) and increases the solute concentration in the mobile phase. The result is reverse in the case of $Da \ll 1$, as molecular diffusion rate dominates the reversible reaction rate and makes the mean concentration distribution more blunt and flatter.

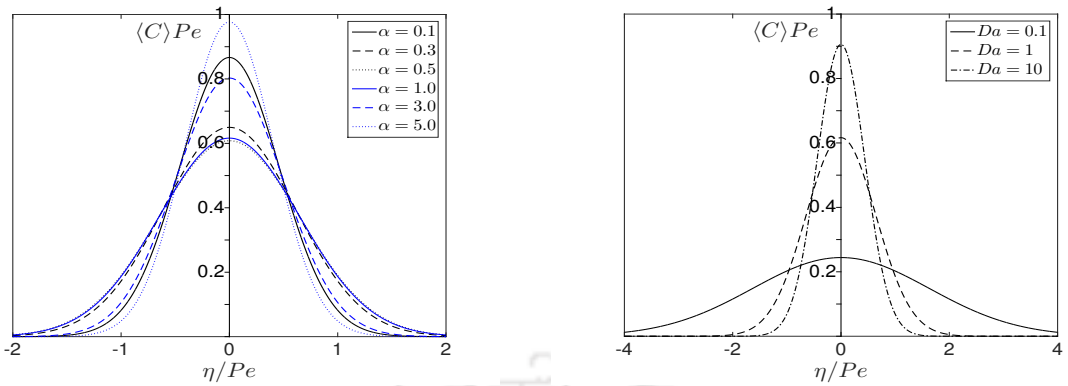

(a) $Da = 1$ (b) $\alpha = 1$

Figure 3.4: Longitudinal distribution of mean concentration at $\tau = 1$.

3.4.3 Transverse real concentration distribution

The two-dimensional concentration distributions for mobile and immobile phases can be written explicitly up to second-order as

$$C\,Pe = \frac{\left\{1 + F\frac{\partial}{\partial(\eta/Pe)} + X\frac{\partial^2}{\partial(\eta/Pe)^2}\right\}\exp\left[-\frac{(\eta/Pe)^2}{\frac{4}{R}\left\{\frac{17}{35} - \frac{4}{5R} + \frac{1}{3R^2} + \frac{1}{RDa} - \frac{1}{R^2Da}\right\}\tau}\right]}{\sqrt{\frac{4\pi}{R}\left\{\frac{17}{35} - \frac{4}{5R} + \frac{1}{3R^2} + \frac{1}{RDa} - \frac{1}{R^2Da}\right\}\tau}}, \tag{3.80}$$

$$C_s\,Pe = \frac{\left\{\alpha + F_s\frac{\partial}{\partial(\eta/Pe)} + X_s\frac{\partial^2}{\partial(\eta/Pe)^2}\right\}\exp\left[-\frac{(\eta/Pe)^2}{\frac{4}{R}\left\{\frac{17}{35} - \frac{4}{5R} + \frac{1}{3R^2} + \frac{1}{RDa} - \frac{1}{R^2Da}\right\}\tau}\right]}{\sqrt{\frac{4\pi}{R}\left\{\frac{17}{35} - \frac{4}{5R} + \frac{1}{3R^2} + \frac{1}{RDa} - \frac{1}{R^2Da}\right\}\tau}}. \tag{3.81}$$

In order to intuitively demonstrate the effects of reversible phase exchange in the solute transport process in an open channel flow, the concentration contours are plotted in Figs. (3.5) and (3.6). Initially, the solute is injected across the line $\eta = 0$ and dispersed throughout the channel under the effects of advection and lateral diffusion. The coordinate systems in the figures are allowed to move longitudinally with velocity Pe/R to ensure that the centroid of the concentration cloud always remains at the origin in each case. From Fig. (3.5), it can be seen that how reversible phase exchange affects the solute dispersion compared to its inert counterpart. When the channel bed just changes from inert to slightly retentive (say, $\alpha = 0.01$) and $Da = 0.1$, concentration distribution becomes more dispersed due to slow kinetics, which increases the solute dispersion in the flow. Further increase of Da increases the solute concentration in the channel as the faster rate of exchange between the channel bed and fluid phase increases solute concentration in the fluid phase. It is possible that for a slightly retentive channel bed ($\alpha \ll 1$), the dis-

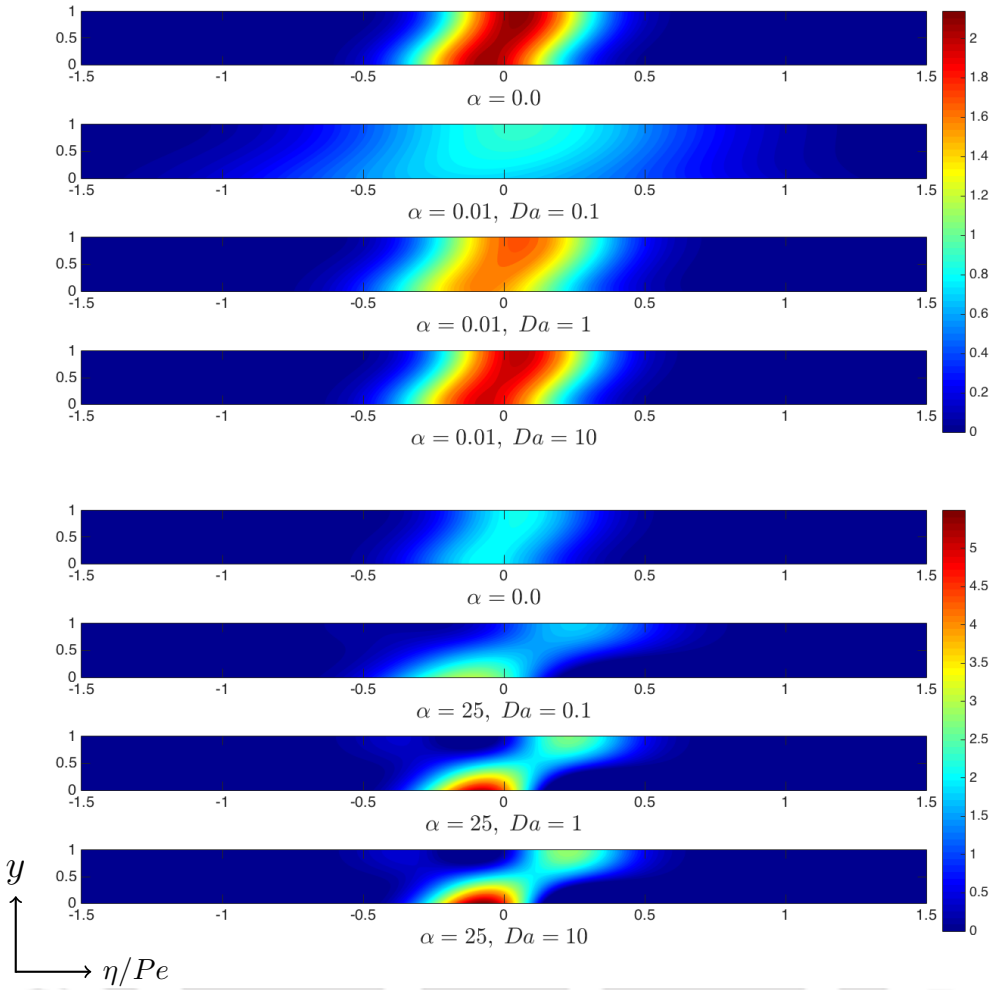

Figure 3.5: Mobile phase concentration contours at $\tau = 1$: horizontal coordinate represents η/Pe, vertical coordinate represents y.

persion process is more akin to the inert boundary case subject to a fast phase exchange ($Da \gg 1$) between mobile and immobile phases. The maximum concentration of the solute after $\tau = 1$ for $\alpha = 0$ is 2.1367 and for $\alpha = 0.01$ the maximum concentrations are 0.8865, 1.7237 and 2.0307 for $Da = 0.1$, 1 and 10, respectively. From the figure it is also observed that for large α (say, $\alpha = 25$), concentration is higher than with inert channel bed because of higher retention capacity of the channel bed. As bed retention increases, retardation factor reduces the ability of the solute to move along the concentration gradient, which was also reported by Ramon et al. [51]. The maximum concentrations of the solute after $\tau = 1$ for $\alpha = 25$ are 3.0753, 5.1054 and 5.4903 for $Da = 0.1$, 1 and 10, respectively. Plots in Fig. (3.6) show the two-dimensional concentration distributions for different combinations of τ and α. It is observed that for a smaller bed retention, higher concentration zone appears in the downstream free surface due to flow advection, and with

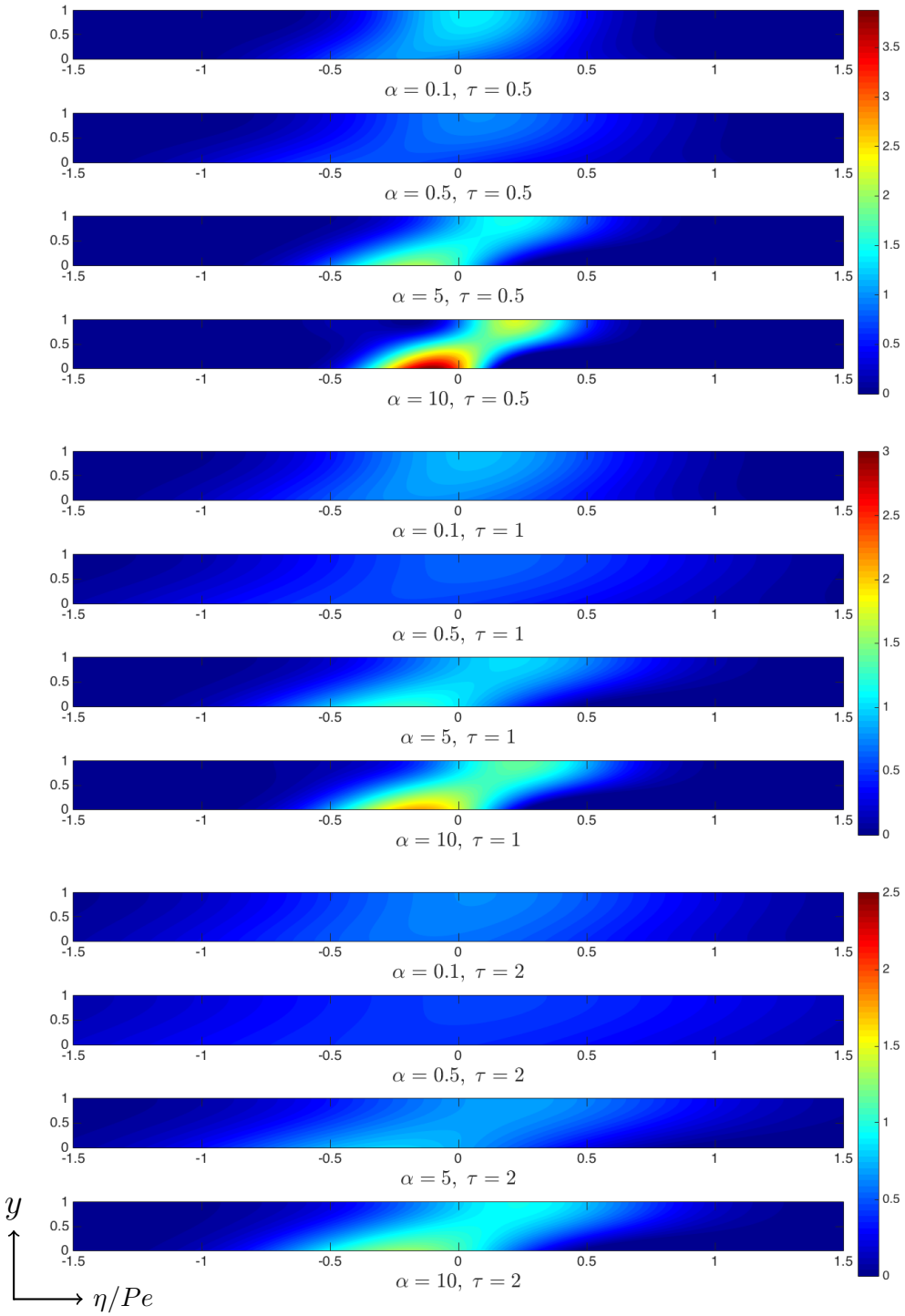

Figure 3.6: Mobile phase concentration contours for $Da = 1$: horizontal coordinate represents η/Pe, vertical coordinate represents y.

the increase in retention parameter, the solute concentration decreases as the channel bed holds some fraction of solute temporally which allows to enhances the solute dispersion.

Further increase of α will retard the flow advection, consequently will cause the higher concentrations zone in both downstream and upstream sides. It is also noticeable that concentration is higher in the upstream channel bed than that in the downstream free surface for large value of α. The maximum solute concentration of upstream and downstream sides at $\tau = 0.5$ are 3.8724 and 3.0550 respectively for $\alpha = 10$.

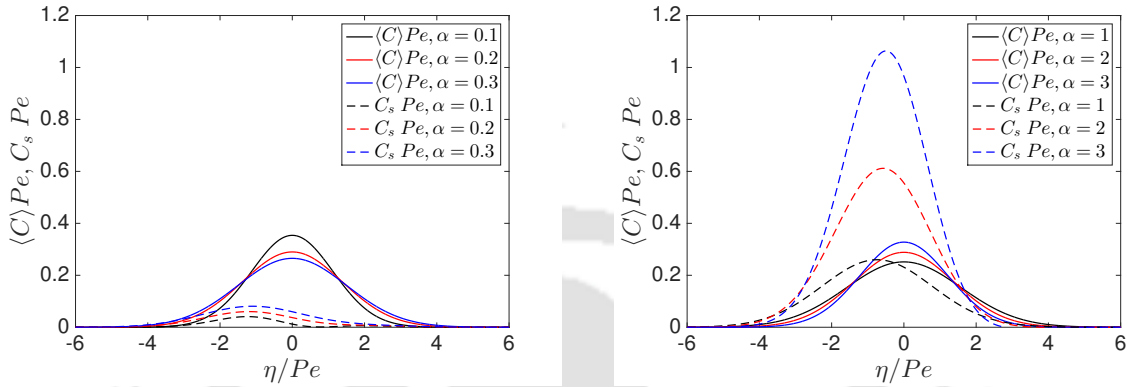

(a) (b)

Figure 3.7: Mean concentration with immobile phase concentration for different α at $\tau = 6$, where $Da = 1$.

Variation of immobile phase concentration distribution is depicted in Fig. (3.7). As a comparison, mean concentration in the mobile phase is shown in the figure. Figure reveals that increase in retention parameter always increases the immobile flow concentration as retention capacity of the channel bed increases with the increase in α. It is also observed from the figure that for large value of α ($\alpha \geq 1$), immobile phase concentration can be higher compared to the mean concentration in the fluid phase.

In order to discuss the uniformity in transverse concentration variations of the mobile flow, an indicator $\mathcal{R}$ is adopted [68] as

$$\mathcal{R}(\eta, \tau) = \frac{\max\limits_{0\leq y\leq 1} C(\eta, y, \tau) - \min\limits_{0\leq y\leq 1} C(\eta, y, \tau)}{C(0, 0, \tau)} \times 100\%,$$

which is the transverse variation in the cross-section against the centroid of the concentration cloud.

Figure (3.8) demonstrates longitudinal distributions of the transverse concentration variation rate for open channel flow. Figure (3.8a) shows the transverse concentration variation rate of the solute in a flow for inert channel bed. The graph shows that variation rates are symmetrical about the centroid of the solute cloud and peak of the maximum variation rate moves away with times from the solute centroid. Effects of retention parameter on concentration variation rate are plotted in Figs. (3.8b)–(3.8d). Figures show that for $\alpha = 0.1$, initially variation rate higher at some downstream locations. In downstream

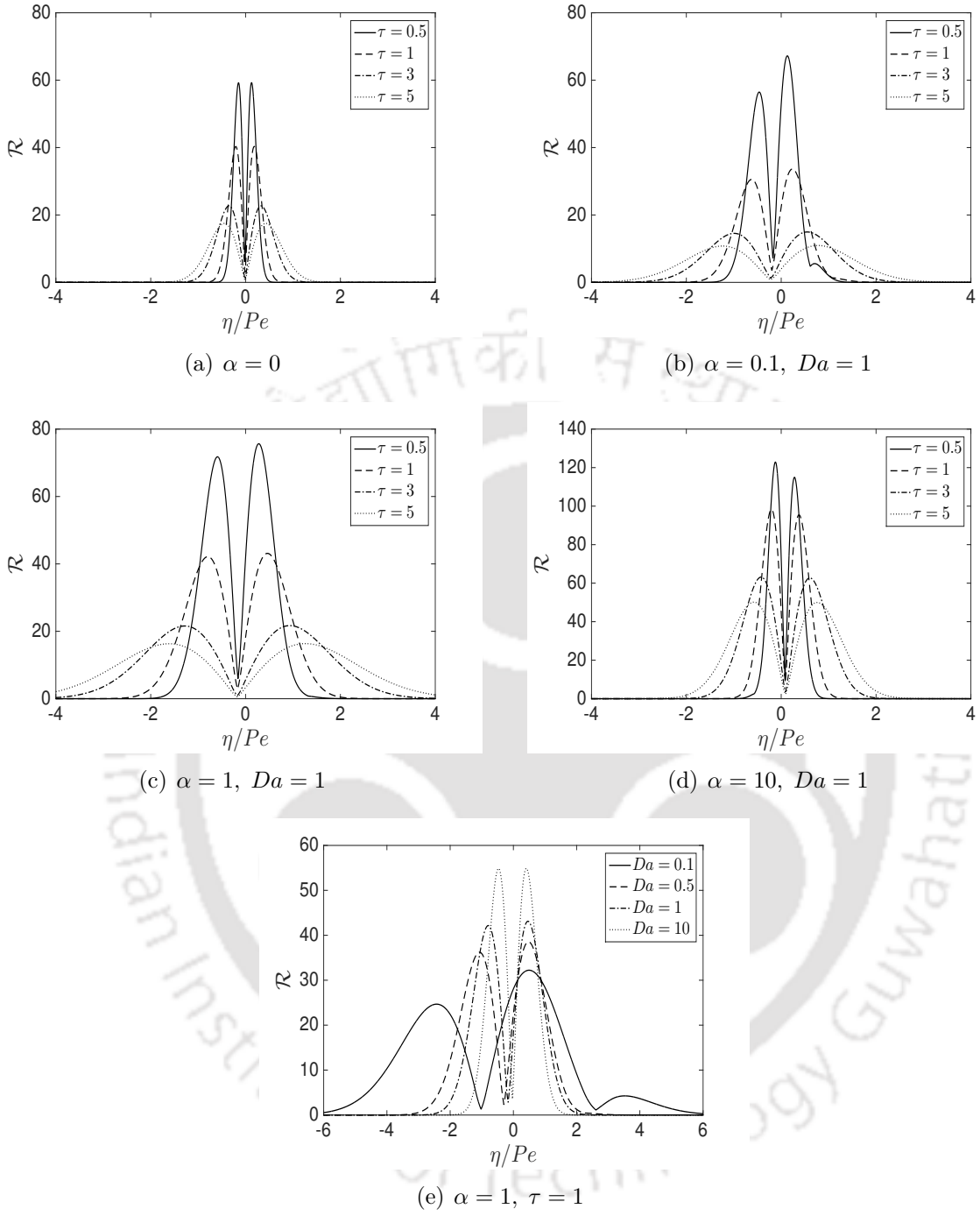

(a) $\alpha = 0$

(b) $\alpha = 0.1,\ Da = 1$

(c) $\alpha = 1,\ Da = 1$

(d) $\alpha = 10,\ Da = 1$

(e) $\alpha = 1,\ \tau = 1$

Figure 3.8: Longitudinal distribution of the transverse concentration variation rate.

location, higher concentration appears near the free surface and concentration reduces at the channel bed due to bed retention. This increases the concentration variation rate in the downstream, consequently increases the non-uniformity in concentration distribution. On the other hand, in the upstream, initially concentration is high at upstream bed but when phase exchange takes place it reduces the solute concentration near the channel

bed and consequently reduces the non-uniformity in the upstream. When bed retention increases variation rate also increases in both upstream and downstream sides. But maximum variation rate appears at upstream bed due to slow advection and strong retention effects. Influences of Da on transverse variation rate are displayed in Fig. (3.8e). It is shown from the figure that as Da increases, maximum variation rates on both upstream and downstream increase. When $Da \ll 1$, molecular diffusion rate dominates the reversible reaction rate and consequently the maximum variation rate is reduced. But the result is reverse for the case of $Da \gg 1$, where the reversible reaction rate dominates over diffusion and increases the solute concentration in the flow and also the maximum variation rate. With the increase of Da, maximum variation rate in upstream increases faster than that in the downstream and for fast kinetics ($Da = 10$), the maximum variation rates in both sides are almost equal to each other (Variation rates for $Da = 10$ in upstream and downstream sides are 54.86% and 54.88% respectively). Maximum variation rates for different combinations of α and Da are reported in table 3.3. It can be noted that for slow kinetics ($Da = 0.1$), subject to small retention capacity of the channel bed, variation rates are smaller than that in the inert case ($\alpha = 0$). So, it can be concluded from the table that for small values of α and Da, i.e., for slow kinetics with small retentive channel bed, solute concentration distribution will become uniform at a faster rate.

Da	$\alpha = 0$	$\alpha = 0.001$	$\alpha = 0.01$	$\alpha = 0.1$	$\alpha = 0.3$	$\alpha = 0.5$	$\alpha = 1$	$\alpha = 3$	$\alpha = 5$	$\alpha = 10$
0.1	40.32	35.94	30.97	30.42	30.69	31.05	32.22	39.82	49.62	72.45
1	40.32	39.74	36.55	33.64	35.33	37.47	43.12	62.78	76.52	98.33
10	40.32	40.31	40.22	41.26	44.94	48.18	54.88	72.71	84.41	103.34
15	40.32	40.33	40.41	42.08	45.94	49.16	55.72	73.20	84.77	103.55

Table 3.3: Peak values of $\mathcal{R}$ with increasing α, where $\tau = 1$.

3.5 Conclusions

The solute dispersion in an open channel flow that involves phase exchange between mobile and immobile phases is studied using multi-scale method of homogenization. Effects of retention parameter and phase exchange kinetics on dispersion coefficient, mean and transverse real concentrations are discussed. Analytical solutions are obtained for transverse real concentration up to second-order approximation. This work includes the pattern of transverse real concentration distribution and uniformity over the cross-section of the channel. An indicator for characterizing the transverse concentration variation rate is adopted, which measures the concentration variation rate over the channel cross-section. Some important conclusions are as follows:

1. As Da increases, the dispersion coefficient decreases.

2. With the increase of α, dispersion coefficient increases up to some maximum value α_m and later it decreases.

3. If the channel bed is slight retentive and the phase exchange kinetics is very slow then solute disperses very fast owing to higher value of dispersion coefficient. Whereas, if the channel bed is highly retentive and the phase exchange kinetics is very fast, then the solute disperses slowly as large values of α retard the flow advection and also the solute releases faster from the channel bed to the flowing fluid owing to the higher value of Da.

4. For smaller values of α and Da, solute concentration distribution becomes uniform faster. It is possible that for slow kinetics subject to small retentive channel bed, transverse concentration distribution becomes uniform more quickly than their inert counterpart.

CHAPTER 4

CONCENTRATION DISTRIBUTION IN AN OSCILLATORY COUETTE FLOW

In the previous two chapters, we have studied the solute transport in a steady open channel flow, where the solute may undergo reversible or irreversible boundary reaction with the channel wall. Analytical solutions are obtained for transverse real concentration up to certain order of approximation by multi-scale method of homogenization. In this chapter, we are going to study the solute dispersion in an oscillatory Couette flow. Analytical expressions for mean and transverse concentration distribution are derived.

4.1 Introduction

The study of dispersion in oscillatory flows is important to model shear-driven flows encountered in micro motors, micro channels and other micro fluidic systems. Knowledge of solute dispersion under oscillation of boundary is important in the hydrodynamic theory of lubrication. Aris [4] analysed the longitudinal dispersion coefficient of solute in an oscillatory flow through a circular tube under a periodic pressure gradient by using his method of moments. He concluded that if the amplitude of the fluctuations in the pressure gradient is larger than the mean pressure gradient, then the contribution of the flow oscillation in solute dispersion will be significant. Chatwin [10] derived the explicit expressions for dispersion coefficient for a tube. He also showed the effects of oscillatory flow parameters on solute dispersion coefficient and concluded that the effects are prominent at low frequency of the flow oscillation. Watson [65] used the concept proposed by Chatwin to study the passive contaminant dispersion in an oscillatory pressure-driven flow in a tube with arbitrary cross-section. He showed that, for a given tidal volume, the flux of the solute increase significantly for high frequency of oscillation.

Content of this chapter is published in the journal *Proceedings of the Royal Society A*, **475** (2019) 20180483.

In the available literature on solute transport during last decades, the main focus was either to obtain the dispersion coefficient or to address the mean concentration distribution [9,11,19,35,69,76,77] rather than transverse concentration distribution. Smith [57,58] analysed the variance of the solute cloud and derived the time averaged dispersion coefficient during the initial time in an oscillatory flow. He showed that the concentration cloud might contract and expand periodically as the dispersion coefficient sometimes could be negative due to the reversing flow. Yasuda [74, 75] analysed the longitudinal dispersion in an oscillatory flow forming a boundary layer during the initial stages, and studied how the longitudinal dispersion was generated by the shear effect of the oscillatory flow. A new definition of the vertical average of the dispersion was proposed to get rid of the negativity of the dispersion coefficients. Though two-dimensional concentration distributions had been considered in the above studies, main focus was only on the dispersion coefficient. In some environmental or industrial processes, we need information not only on dispersion coefficients or the longitudinal mean concentration, but also on the transverse concentration distribution and its uniformity over the cross-section. Wu and Chen [67,68] systemically analysed the transverse uniformity of concentration cloud for laminar steady flows by extending the homogenization technique of Mei et al. [32]. They showed that the approach to the transverse uniformity of the concentration was much slower than the approach to the longitudinal normality of the mean concentration. Study of the transverse concentration distribution in an oscillatory flow has a great significance in estuaries and other coastal regions. Prediction of accurate pollutant distribution and peak pollutant concentration are of matter of concern. In recent progress, Wang and Chen [64] illustrated the evolution of transverse concentration distribution in an oscillatory flow by their simplified Aris-Gill expansion technique [63]. They derived transverse concentration distribution up to first-order approximation and described its approach to uniformity. They also showed that the approach to the transverse uniformity of the concentration for reversal laminar flows was slower than that in steady flows [67, 68].

Dispersion of inert matter in oscillatory flows has been studied in the classical works of Aris [4] and Watson [65]. Effects of different flow parameters on transport coefficients in oscillatory flows with linear boundary chemical reactions have been explored analytically with the help of homogenization technique in many existing studies [38–40, 44]. Paul and Mazumder [45] analysed effects of nonlinear chemical reaction on transport coefficients in steady and oscillatory flows. Evolution of mean concentration for oscillatory flows has been studied by Mazumder and his co-workers using a modified moments method [6, 27, 29, 30, 34]. Their focus was more on an early period of the dispersion process. As mentioned earlier, concerns are so far mainly on distribution of mean concentration, transverse concentration distribution of solute cloud and its dependence on different flow parameters are yet to be explored.

The aim of this chapter is to find the analytical expressions for mean and transverse real concentrations by multi-scale homogenization technique and to explore the evolution of transverse concentration distribution for oscillatory Couette flows. The specific objectives of this work are: (I) to present a multi-scale analysis for the determination of the Taylor dispersivity for the oscillatory Couette flow, (II) to obtain analytical expressions for mean and transverse real concentrations up to third-order approximation, (III) to discuss the validity of Taylor dispersion model by obtaining analytical solutions for mean concentration, (IV) to observe the effects of Stokes boundary layer thickness on dispersion coefficient and transverse variation of concentration distribution, (V) to discuss the uniformity in transverse real concentration over the channel cross-section.

4.2 Formulation of the problem

A laminar, one-dimensional plane Couette flow of an incompressible viscous fluid between two infinite parallel flat plates with a separation width h is considered. A Cartesian coordinate system is used in which the longitudinal and transverse coordinates are $\widehat{x}$ and $\widehat{y}$ respectively. The lower plate at $\widehat{y} = 0$ is assumed to be stationary, whereas the upper one at $\widehat{y} = h$ oscillates in its own plane with a prescribed velocity

$$\widehat{u}(h, \widehat{t}) = U[1 + \phi Re(e^{-i\omega\widehat{t}})],$$

where U is the steady component of the velocity of the upper plate, ϕ is a factor such that ϕU represents the amplitude of the oscillatory velocity component, ω is the angular frequency of the oscillation, $\widehat{t}$ is time and Re stands for real part. As the flow is influenced by the oscillation of the upper plate, the velocity profile of the flow can be considered as,

$$\widehat{u}(\widehat{y}, \widehat{t}) = \widehat{u}_s + Re(\widehat{u}_w e^{-i\omega\widehat{t}}), \tag{4.1}$$

where $\widehat{u}_s(\widehat{y}) = U\widehat{y}/h$ and $\widehat{u}_w(\widehat{y}) = U\phi\frac{\sin\widehat{\sigma}\widehat{y}}{\sin\widehat{\sigma}h}$ are the steady and oscillatory components of the velocity field respectively. Here $\widehat{\sigma}^2 = i\omega/\nu$ or $\widehat{\sigma} = (1+i)/\widehat{\delta}_s$ and $\widehat{\delta}_s = \sqrt{2\nu/\omega}$ is the thickness of the Stokes boundary layer resulting from the oscillation of the upper plate, where ν is the kinematic viscosity of the fluid. Schematic diagram of flow geometry is given in Fig. (4.1).

Associated with oscillatory Couette flow, the problem of transport of the substance can be formulated as follows:

$$\frac{\partial\widehat{C}}{\partial\widehat{t}} + \widehat{u}\frac{\partial\widehat{C}}{\partial\widehat{x}} = D\left(\frac{\partial^2\widehat{C}}{\partial\widehat{x}^2} + \frac{\partial^2\widehat{C}}{\partial\widehat{y}^2}\right), \quad 0 < \widehat{y} < h, \tag{4.2}$$

where D, the molecular diffusivity of the substance in the fluid, is assumed to be constant.

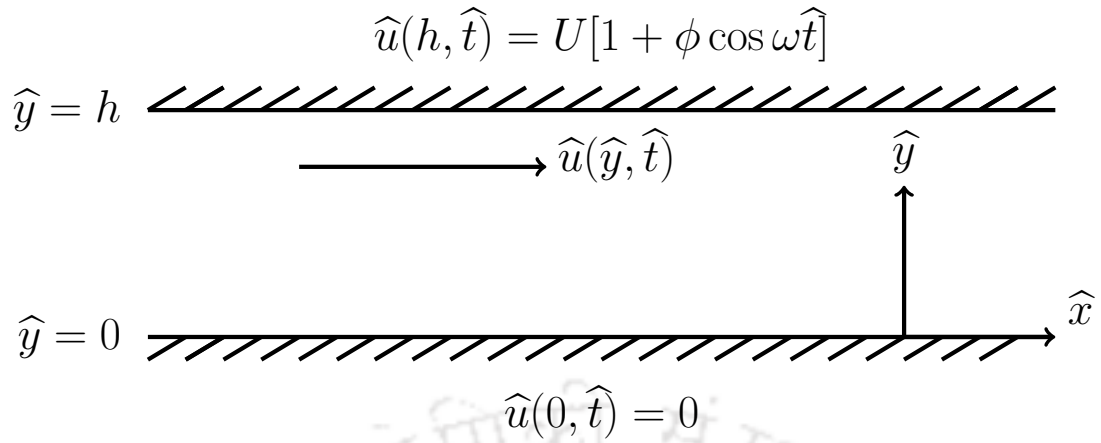

Figure 4.1: Sketch for Couette flow with stationary lower boundary and oscillatory upper boundary.

The initial and boundary conditions are respectively given as,

$$\widehat{C}(\widehat{x},\widehat{y},\widehat{t})|_{\widehat{t}=0} = \frac{Q_m}{h}\delta\Big(\frac{\widehat{x}}{h}\Big), \tag{4.3}$$

$$\left.\frac{\partial\widehat{C}}{\partial\widehat{y}}\right|_{\widehat{y}=0} = \left.\frac{\partial\widehat{C}}{\partial\widehat{y}}\right|_{\widehat{y}=h} = 0, \tag{4.4}$$

and

$$\widehat{C}(\widehat{x},\widehat{y},\widehat{t})|_{\widehat{x}\to\pm\infty} = 0, \tag{4.5}$$

where Q_m is the released mass and $\delta(\cdot)$ the Dirac delta function.

4.3 Multi-scale Analysis

4.3.1 Scales selection

Associated with two length scales h (channel width) and l (characteristic axial length of the solute cloud), there are three distinct time scales for transport process, i.e., $T_0 = 2\pi/\omega = h^2/D$ as the diffusion time across the width of the channel h, $T_1 = l/U$ as the advection time across the characteristic length l, and $T_2 = l^2/D$ as diffusion time across l. Their ratios are

$$T_0 : T_1 : T_2 = 1 : \frac{1}{\epsilon} : \frac{1}{\epsilon^2},$$

where $\epsilon = \frac{h}{l}$ ($\ll 1$) used as the perturbation parameter.

4.3.2 Dimensionless governing equation and velocity profile

Dimensionless parameters are introduced as

$$x = \frac{\widehat{x}}{l},\ y = \frac{\widehat{y}}{h},\ u = \frac{\widehat{u}}{U},\ t = \frac{\widehat{t}}{h^2/D},\ Pe = \frac{Uh}{D},\ C = \frac{\widehat{C}}{Q_m/h},\ \Omega = \frac{\omega h^2}{\nu},\ Sc = \frac{\nu}{D},$$

where Pe is the Peclet number, Ω is the dimensionless frequency parameter and Sc is the Schmidt number.

The Peclet number Pe is a ratio of the relative characteristic time of diffusion process (h^2/D) to the convection process (h/U) across the channel width. Alternatively, it can be defined as the ratio of the rate of advection $(\frac{1}{h/U})$ to the rate of diffusion $(\frac{1}{h^2/D})$. The parameter Ω is the ratio of time (h^2/ν) taken by viscosity for smoothing out the vorticity variation in the transverse direction to the flow period $(1/\omega)$. The Schmidt number Sc is the ratio of viscous diffusion to the molecular diffusion [6].

The non-dimensional governing equation and boundary conditions can be rewritten as

$$\frac{\partial C}{\partial t} + \epsilon Pe\, u\frac{\partial C}{\partial x} = \epsilon^2\frac{\partial^2 C}{\partial x^2} + \frac{\partial^2 C}{\partial y^2}, \quad 0 < y < 1, \tag{4.6}$$

$$\left.\frac{\partial C}{\partial y}\right|_{y=0} = \left.\frac{\partial C}{\partial y}\right|_{y=1} = 0. \tag{4.7}$$

The dimensionless velocity profile is

$$u(y,t) = u_s + Re(u_w e^{-i\Omega Sc\, t}), \tag{4.8}$$

where $u_s(y) = y$ and $u_w(y) = \phi\frac{\sin\sigma y}{\sin\sigma}$ are the steady and oscillatory components of the velocity field, respectively. In the expression of u_w, $\sigma = \sqrt{i\Omega}$ or $\sigma = (1+i)/\delta_s$, where $\delta_s = \widehat{\delta}_s/h = \sqrt{2/\Omega}$ is the dimensionless Stokes boundary layer thickness. So, $\Omega\ (= 2/\delta_s^2)$ is inversely proportional to the square of the dimensionless Stokes boundary layer thickness. Therefore, a small value of Ω implies a large viscous layer near the oscillatory upper wall and vice versa for large Ω.

4.3.3 Homogenization

For the asymptotic analysis, the homogenization technique of Mei et al. [32] is employed. Based on the time scales mentioned before fast, medium and slow time variables are introduced accordingly,

$$t_0 = t,\ t_1 = \epsilon t,\ t_2 = \epsilon^2 t.$$

According to the chain rule, the original time derivative becomes

$$\frac{\partial}{\partial t} = \frac{\partial}{\partial t_0} + \epsilon \frac{\partial}{\partial t_1} + \epsilon^2 \frac{\partial}{\partial t_2}. \tag{4.9}$$

The concentration C is expanded by the asymptotic expansion, which was first introduced by Fife and Nicholes [14], into multiple scales as,

$$\begin{aligned} C(x,y,t) = C^{(0)}(x,y,t_0,t_1,t_2) + \epsilon C^{(1)}(x,y,t_0,t_1,t_2) + \epsilon^2 C^{(2)}(x,y,t_0,t_1,t_2) \\ + \epsilon^3 C^{(3)}(x,y,t_0,t_1,t_2) + O(\epsilon^4), \end{aligned} \tag{4.10}$$

where $C^{(n)}$,$(n = 1, 2, 3, \ldots)$ are the developed terms, which are purely oscillatory functions of the short time variable t_0.

Substitution of (4.9) and (4.10) into (4.6) and (4.7) results in

$$\begin{aligned} &\left(\frac{\partial C^{(0)}}{\partial t_0} - \frac{\partial^2 C^{(0)}}{\partial y^2}\right) + \epsilon\left(\frac{\partial C^{(0)}}{\partial t_1} + \frac{\partial C^{(1)}}{\partial t_0} + Pe\, u\frac{\partial C^{(0)}}{\partial x} - \frac{\partial^2 C^{(1)}}{\partial y^2}\right) + \epsilon^2\left(\frac{\partial C^{(0)}}{\partial t_2}\right. \\ &\left. + \frac{\partial C^{(1)}}{\partial t_1} + \frac{\partial C^{(2)}}{\partial t_0} + Pe\, u\frac{\partial C^{(1)}}{\partial x} - \frac{\partial^2 C^{(0)}}{\partial x^2} - \frac{\partial^2 C^{(2)}}{\partial y^2}\right) + \cdots = 0, \quad 0 < y < 1, \end{aligned} \tag{4.11}$$

$$\frac{\partial C^{(0)}}{\partial y} + \epsilon \frac{\partial C^{(1)}}{\partial y} + \epsilon^2 \frac{\partial C^{(2)}}{\partial y} + \ldots = 0, \quad y = 0, 1. \tag{4.12}$$

For the leading order $(O(1))$, Eqs. (4.11) and (4.12) give:

$$\frac{\partial C^{(0)}}{\partial t_0} = \frac{\partial^2 C^{(0)}}{\partial y^2}, \quad 0 < y < 1, \tag{4.13}$$

$$\left.\frac{\partial C^{(0)}}{\partial y}\right|_{y=0} = \left.\frac{\partial C^{(0)}}{\partial y}\right|_{y=1} = 0. \tag{4.14}$$

The general solution of Eq. (4.13) becomes

$$C^{(0)} = C_0^{(0)}(x, t_1, t_2) + \sum_{n=1}^{\infty} Re\left[C_n^{(0)}(x, t_1, t_2) e^{in\pi y}\right] e^{-n^2\pi^2 t_0}. \tag{4.15}$$

Clearly, for long time evolution, since the series terms die out quickly because of the exponential decay, $C^{(0)}$ becomes independent of t_0; thus, one can omit the series part and take the solution to be

$$C^{(0)} = C^{(0)}(x, t_1, t_2). \tag{4.16}$$

For the first order $(O(\epsilon))$, Eqs. (4.11) and (4.12) give:

$$\frac{\partial C^{(0)}}{\partial t_1} + \frac{\partial C^{(1)}}{\partial t_0} + Pe\, u\frac{\partial C^{(0)}}{\partial x} = \frac{\partial^2 C^{(1)}}{\partial y^2}, \quad 0 < y < 1, \tag{4.17}$$

$$\left.\frac{\partial C^{(1)}}{\partial y}\right|_{y=0} = \left.\frac{\partial C^{(1)}}{\partial y}\right|_{y=1} = 0. \tag{4.18}$$

On taking time average of these equations w.r.t. the fast time variable t_0, we get

$$\frac{\partial C^{(0)}}{\partial t_1} + Pe\, u_s \frac{\partial C^{(0)}}{\partial x} = \frac{\partial^2 \overline{C^{(1)}}}{\partial y^2}, \quad 0 < y < 1, \tag{4.19}$$

$$\left.\frac{\partial \overline{C^{(1)}}}{\partial y}\right|_{y=0} = \left.\frac{\partial \overline{C^{(1)}}}{\partial y}\right|_{y=1} = 0, \tag{4.20}$$

where overbar denotes time average w.r.t. t_0. The time average of a function f defined by $\overline{f}$ [33, 37] as,

$$\overline{f} = \frac{\Omega Sc}{2\pi} \int_{t_0}^{t_0 + \frac{2\pi}{\Omega Sc}} f dt_0, \tag{4.21}$$

where $\frac{2\pi}{\Omega Sc}$ is the dimensionless flow period. Here $C^{(0)}$ is invariant under t_0 and $C^{(n)}$, $(n = 1, 2, 3, \ldots)$ are purely oscillatory functions of t_0, i.e., $C^{(n)}(t_0) = C^{(n)}(t_0 + \frac{2\pi}{\Omega Sc})$. Hence, from Eq. (4.21) one can get, $\overline{C^{(0)}} = C^{(0)}$ and $\frac{\partial \overline{C^{(n)}}}{\partial t_0} = 0$, for $n = 1, 2, 3, etc$.

Further, taking a section average of Eq. (4.19) w.r.t. the spatial variable y subject to the conditions (4.20), we get

$$\frac{\partial C^{(0)}}{\partial t_1} + Pe\langle u_s \rangle \frac{\partial C^{(0)}}{\partial x} = 0, \tag{4.22}$$

where angle brackets denote section average w.r.t. y. The section average of a function v defined by $\langle v \rangle$ [33] as

$$\langle v \rangle = \int_0^1 v dy. \tag{4.23}$$

Here, $C^{(0)}$ is invariant under y, that implies $\langle C^{(0)} \rangle = C^{(0)}$ and also one can get by using the above definition, $\left\langle \frac{\partial^2 \overline{C^{(n)}}}{\partial y^2} \right\rangle = \left.\frac{\partial \overline{C^{(n)}}}{\partial y}\right|_{y=1} - \left.\frac{\partial \overline{C^{(n)}}}{\partial y}\right|_{y=0}$, for $n = 1, 2, 3,$ etc.

Subtracting (4.17) from (4.22), we get

$$\frac{\partial C^{(1)}}{\partial t_0} + Pe\left[(u_s - \langle u_s \rangle) + Re(u_w e^{-i\Omega Sc t_0})\right] \frac{\partial C^{(0)}}{\partial x} = \frac{\partial^2 C^{(1)}}{\partial y^2}, \quad 0 < y < 1. \tag{4.24}$$

This equation suggests the following substitution:

$$C^{(1)} = Pe[F(y) + Re(G(y)e^{-i\Omega Sc t_0})] \frac{\partial C^{(0)}}{\partial x}, \tag{4.25}$$

where the coefficients $F(y), G(y)$ are to be found as follows. On matching with the steady

terms associated with $\frac{\partial C^{(0)}}{\partial x}$, the function $F(y)$ will be governed by

$$\frac{d^2F}{dy^2} = u_s - \langle u_s \rangle, \quad 0 < y < 1, \tag{4.26}$$

with the boundary conditions

$$\left.\frac{dF}{dy}\right|_{y=0} = \left.\frac{dF}{dy}\right|_{y=1} = 0, \tag{4.27}$$

and

$$\langle F \rangle = 0. \tag{4.28}$$

Similarly, equating the oscillatory terms associated with $\frac{\partial C^{(0)}}{\partial x}$, one can get

$$\frac{d^2G}{dy^2} + \lambda^2 G = u_w, \quad 0 < y < 1, \tag{4.29}$$

and

$$\left.\frac{dG}{dy}\right|_{y=0} = \left.\frac{dG}{dy}\right|_{y=1} = 0, \tag{4.30}$$

where

$$\lambda^2 = i\Omega Sc, \quad or \quad \lambda = Sc^{1/2}\sigma. \tag{4.31}$$

For the second order ($O(\epsilon^2)$), Eqs. (4.11)–(4.12) give

$$\frac{\partial C^{(0)}}{\partial t_2} + \frac{\partial C^{(1)}}{\partial t_1} + \frac{\partial C^{(2)}}{\partial t_0} + Pe\, u\frac{\partial C^{(1)}}{\partial x} = \frac{\partial^2 C^{(0)}}{\partial x^2} + \frac{\partial^2 C^{(2)}}{\partial y^2}, \quad 0 < y < 1, \tag{4.32}$$

and

$$\left.\frac{\partial C^{(2)}}{\partial y}\right|_{y=0} = \left.\frac{\partial C^{(2)}}{\partial y}\right|_{y=1} = 0. \tag{4.33}$$

On taking time average of these equations w.r.t. the fast time variable t_0 (as defined in Eq. (4.21)), we get

$$\frac{\partial C^{(0)}}{\partial t_2} + \frac{\partial \overline{C^{(1)}}}{\partial t_1} + Pe\ \overline{u\frac{\partial C^{(1)}}{\partial x}} = \frac{\partial^2 C^{(0)}}{\partial x^2} + \frac{\partial^2 \overline{C^{(2)}}}{\partial y^2}, \quad 0 < y < 1, \tag{4.34}$$

and

$$\left.\frac{\partial \overline{C^{(2)}}}{\partial y}\right|_{y=0} = \left.\frac{\partial \overline{C^{(2)}}}{\partial y}\right|_{y=1} = 0. \tag{4.35}$$

Averaging Eq. (4.34) w.r.t. space variable y (as defined in Eq. (4.23)) subject to the

boundary conditions (4.35), the equation becomes

$$\frac{\partial C^{(0)}}{\partial t_2} + \frac{\partial \langle \overline{C^{(1)}} \rangle}{\partial t_1} + Pe \left\langle \overline{u \frac{\partial C^{(1)}}{\partial x}} \right\rangle = \frac{\partial^2 C^{(0)}}{\partial x^2}. \tag{4.36}$$

Subtracting Eq. (4.36) from Eq. (4.32) one can get

$$\frac{\partial C^{(2)}}{\partial t_0} + \frac{\partial C^{(1)}}{\partial t_1} + Pe\left(u\frac{\partial C^{(1)}}{\partial x} - \left\langle \overline{u\frac{\partial C^{(1)}}{\partial x}} \right\rangle \right) - \frac{\partial \langle \overline{C^{(1)}} \rangle}{\partial t_1} = \frac{\partial^2 C^{(2)}}{\partial y^2}, \quad 0 < y < 1. \tag{4.37}$$

With the help of Eqs. (4.8), (4.22), (4.25) and (4.28), one can get the following

$$\frac{\partial \langle \overline{C^{(1)}} \rangle}{\partial t_1} = 0, \tag{4.38}$$

$$\frac{\partial C^{(1)}}{\partial t_1} = -Pe^2 \langle u_s \rangle \Big[F(y) + Re(G(y)e^{-i\Omega Sc t_0}) \Big] \frac{\partial^2 C^{(0)}}{\partial x^2}, \tag{4.39}$$

$$u\frac{\partial C^{(1)}}{\partial x} = Pe\Big[u_s F + \frac{1}{2}Re(u_w G^*) + Re\{(u_w F + u_s G)e^{-i\Omega Sc t_0}\} + \frac{1}{2}Re(u_w G e^{-2i\Omega Sc t_0}) \Big] \times \frac{\partial^2 C^{(0)}}{\partial x^2}, \tag{4.40}$$

and

$$\left\langle \overline{u\frac{\partial C^{(1)}}{\partial x}} \right\rangle = Pe\Big[\langle u_s F \rangle + \frac{1}{2}Re\langle u_w G^* \rangle \Big] \frac{\partial^2 C^{(0)}}{\partial x^2}, \tag{4.41}$$

where * denotes the complex conjugate.

Substitution of terms (4.38) and (4.41) in (4.36) gives

$$\frac{\partial C^{(0)}}{\partial t_2} = \Big(1 - Pe^2[\langle u_s F \rangle + \frac{1}{2}Re\langle u_w G^* \rangle] \Big) \frac{\partial^2 C^{(0)}}{\partial x^2}. \tag{4.42}$$

Multiplying Eq. (4.22) by ϵ, Eq. (4.42) by ϵ^2 and adding together we get

$$\frac{\partial C^{(0)}}{\partial t_0} + \epsilon\frac{\partial C^{(0)}}{\partial t_1} + \epsilon^2\frac{\partial C^{(0)}}{\partial t_2} + \epsilon Pe\, \langle u_s \rangle \frac{\partial C^{(0)}}{\partial x} = \epsilon^2 \Big(1 - Pe^2[\langle u_s F \rangle + \frac{1}{2}Re\langle u_w G^* \rangle] \Big) \frac{\partial^2 C^{(0)}}{\partial x^2}. \tag{4.43}$$

Rewriting Eq. (4.43) in original time variable the equation becomes,

$$\frac{\partial C^{(0)}}{\partial t} + \epsilon Pe\, \langle u_s \rangle \frac{\partial C^{(0)}}{\partial x} = \epsilon^2 \Big(1 - Pe^2[\langle u_s F \rangle + \frac{1}{2}Re\langle u_w G^* \rangle] \Big) \frac{\partial^2 C^{(0)}}{\partial x^2}. \tag{4.44}$$

In order to get an one-dimensional diffusion like equation from the above equation, we use new variables (as in [70]), $\tau = t$ and $\eta = \frac{\hat{x}}{h} - Pe\, \langle u_s \rangle t$. Hence, the above equation

becomes

$$\frac{\partial C^{(0)}}{\partial \tau} = D_T \frac{\partial^2 C^{(0)}}{\partial \eta^2}, \tag{4.45}$$

where

$$D_T = 1 + Pe^2(D_{Ts} + D_{Tw}) \tag{4.46}$$

is the Taylor dispersivity. The constant 1 represents the contribution of the effective longitudinal diffusion to Taylor dispersion. The terms D_{Ts} and D_{Tw} are, respectively, the dispersion coefficient components due to the steady and oscillatory flows, respectively:

$$D_{Ts} = -\langle u_s F \rangle, \tag{4.47}$$

and

$$D_{Tw} = -\frac{1}{2} Re \langle u_w G^* \rangle. \tag{4.48}$$

Here, the new coordinate system $\{\eta, \tau\}$ allows to view the mass transport from an observer moving at a speed of $Pe\,\langle u_s \rangle$.

The solution of Eq. (4.45) with the initial and boundary conditions given in equations (4.3) and (4.5) is

$$C^{(0)} = \frac{1}{\sqrt{4\pi D_T \tau}} \exp\left(\frac{-\eta^2}{4 D_T \tau}\right), \tag{4.49}$$

which is a longitudinal Gaussian distribution.

Using Eqs. (4.38)–(4.41) in (4.37), we get

$$\frac{\partial C^{(2)}}{\partial t_0} + Pe^2 \Big[\{(u_s - \langle u_s \rangle) F - \langle u_s F \rangle\} + \frac{1}{2} Re(u_w G^* - \langle u_w G^* \rangle) + Re[\{(u_s - \langle u_s \rangle) G + u_w F\} e^{-i\Omega Sc t_0}] + \frac{1}{2} Re(u_w G e^{-2i\Omega Sc t_0}) \Big] \frac{\partial^2 C^{(0)}}{\partial x^2}. \tag{4.50}$$

This equation suggests the following substitution:

$$C^{(2)} = Pe^2 [P(y) + Re(Q(y) + T(y) e^{-i\Omega Sc t_0} + S(y) e^{-2i\Omega Sc t_0})] \frac{\partial^2 C^{(0)}}{\partial x^2}. \tag{4.51}$$

On matching with the steady terms associated with $\frac{\partial^2 C^{(0)}}{\partial x^2}$, the function $P(y)$ is governed by

$$\frac{d^2 P}{dy^2} = (u_s - \langle u_s \rangle) F - \langle u_s F \rangle, \quad 0 < y < 1, \tag{4.52}$$

with the following conditions

$$\left.\frac{dP}{dy}\right|_{y=0} = \left.\frac{dP}{dy}\right|_{y=1} = 0, \tag{4.53}$$

and

$$\langle P \rangle = 0. \tag{4.54}$$

Similarly, matching with oscillatory non-exponential terms, the function $Q(y)$ will be governed by

$$\frac{d^2Q}{dy^2} = \frac{1}{2}(u_w G^* - \langle u_w G^* \rangle), \quad 0 < y < 1, \tag{4.55}$$

with the following conditions

$$\left.\frac{dQ}{dy}\right|_{y=0} = \left.\frac{dQ}{dy}\right|_{y=1} = 0, \tag{4.56}$$

and

$$\langle Q \rangle = 0. \tag{4.57}$$

Similarly, the function $T(Y)$ satisfies the boundary value problem,

$$\frac{d^2T}{dy^2} + \lambda^2 T = (u_s - \langle u_s \rangle)G + u_w F, \quad 0 < y < 1, \tag{4.58}$$

and

$$\left.\frac{dT}{dy}\right|_{y=0} = \left.\frac{dT}{dy}\right|_{y=1} = 0. \tag{4.59}$$

While $S(y)$ satisfies

$$\frac{d^2S}{dy^2} + 2\lambda^2 S = \frac{1}{2}u_w G, \quad 0 < y < 1, \tag{4.60}$$

and

$$\left.\frac{dS}{dy}\right|_{y=0} = \left.\frac{dS}{dy}\right|_{y=1} = 0. \tag{4.61}$$

For the third-order ($O(\epsilon^3)$), Eqs. (4.11)–(4.12) give

$$\frac{\partial C^{(1)}}{\partial t_2} + \frac{\partial C^{(2)}}{\partial t_1} + \frac{\partial C^{(3)}}{\partial t_0} + Pe\, u\frac{\partial C^{(2)}}{\partial x} = \frac{\partial^2 C^{(1)}}{\partial x^2} + \frac{\partial^2 C^{(3)}}{\partial y^2}, \quad 0 < y < 1, \tag{4.62}$$

and

$$\left.\frac{\partial C^{(3)}}{\partial y}\right|_{y=0} = \left.\frac{\partial C^{(3)}}{\partial y}\right|_{y=1} = 0. \tag{4.63}$$

Averaging Eq. (4.32) w.r.t. time variable t_0 followed by space variable y subject to the boundary conditions (4.33), the equation becomes

$$\frac{\partial \langle \overline{C^{(1)}} \rangle}{\partial t_2} + \frac{\partial \langle \overline{C^{(2)}} \rangle}{\partial t_1} + Pe \left\langle \overline{u\frac{\partial C^{(2)}}{\partial x}} \right\rangle = \frac{\partial^2 \langle \overline{C^{(1)}} \rangle}{\partial x^2}. \tag{4.64}$$

Subtracting Eq. (4.64) from Eq. (4.62) one can get

$$\frac{\partial C^{(1)}}{\partial t_2}+\frac{\partial C^{(2)}}{\partial t_1}+\frac{\partial C^{(3)}}{\partial t_0}+Pe\left(u\frac{\partial C^{(2)}}{\partial x}-\left\langle\overline{u\frac{\partial C^{(2)}}{\partial x}}\right\rangle\right)-\frac{\partial\langle\overline{C^{(1)}}\rangle}{\partial t_2}-\frac{\partial\langle\overline{C^{(2)}}\rangle}{\partial t_1}+\frac{\partial^2\langle\overline{C^{(1)}}\rangle}{\partial x^2}=\frac{\partial^2 C^{(3)}}{\partial y^2},\quad 0<y<1. \tag{4.65}$$

Using (4.8) and (4.51), one can get the following

$$\frac{\partial\langle\overline{C^{(1)}}\rangle}{\partial t_2}=\frac{\partial\langle\overline{C^{(2)}}\rangle}{\partial t_1}=\frac{\partial^2\langle\overline{C^{(1)}}\rangle}{\partial x^2}=0, \tag{4.66}$$

$$\frac{\partial C^{(1)}}{\partial t_2}=Pe\{1+Pe^2(D_{Ts}+D_{Tw})\}\Big[F+Re(Ge^{-i\Omega Sct_0})\Big]\frac{\partial^3 C^{(0)}}{\partial x^3}, \tag{4.67}$$

$$\frac{\partial C^{(2)}}{\partial t_1}=-Pe^3\langle u_s\rangle\Big[P+Re(Q+Te^{-i\Omega Sct_0}+Se^{-2i\Omega Sct_0})\Big]\frac{\partial^3 C^{(0)}}{\partial x^3}, \tag{4.68}$$

$$u\,\frac{\partial C^{(2)}}{\partial x}=Pe^2\Big[u_sP+Re(u_sQ+\frac{1}{2}u_wT^*)+Re\{(u_wP+u_wRe(Q)+u_sT+\frac{1}{2}u_w^*S)\times e^{-i\Omega Sct_0}\}+Re\{(\frac{1}{2}u_wT+u_sS)e^{-2i\Omega Sct_0}\}+\frac{1}{2}Re(u_wSe^{-3i\Omega Sct_0})\Big]\frac{\partial^3 C^{(0)}}{\partial x^3}, \tag{4.69}$$

and

$$\left\langle\overline{u\frac{\partial C^{(2)}}{\partial x}}\right\rangle=Pe^2\Big[\langle u_sP\rangle+Re\{\langle u_sQ\rangle+\frac{1}{2}\langle u_wT^*\rangle\}\Big]\frac{\partial^3 C^{(0)}}{\partial x^3}. \tag{4.70}$$

Substitution of these terms in (4.65) gives

$$\frac{\partial C^{(3)}}{\partial t_0}+Pe^3\Big[\{(u_s-\langle u_s\rangle)P-\langle u_sP\rangle+D_{Ts}F\}+Re\{(u_s-\langle u_s\rangle)Q-\langle u_sQ\rangle-\frac{1}{2}F\langle u_wG^*\rangle+\frac{1}{2}(u_wT^*-\langle u_wT^*\rangle)\}+Re[\{(u_s-\langle u_s\rangle)T+(D_{Ts}+D_{Tw})G+u_wP+u_wRe(Q)+\frac{1}{2}u_w^*S\}e^{-i\Omega Sct_0}]+Re[\{(u_s-\langle u_s\rangle)S+\frac{1}{2}u_wT\}e^{-2i\Omega Sct_0}]+\frac{1}{2}Re(u_wSe^{-3i\Omega Sct_0})\Big]\frac{\partial^3 C^{(0)}}{\partial x^3}. \tag{4.71}$$

This equation suggests the following substitution:

$$C^{(3)}=Pe^3[H(y)+Re(I(y)+J(y)e^{-i\Omega Sct_0}+K(y)e^{-2i\Omega Sct_0}+L(y)e^{-3i\Omega Sct_0})]\frac{\partial^3 C^{(0)}}{\partial x^3}. \tag{4.72}$$

On matching with the steady terms associated with $\frac{\partial^3 C^{(0)}}{\partial x^3}$, the function $H(y)$ is governed by

$$\frac{d^2H}{dy^2} = (u_s - \langle u_s \rangle)P - \langle u_s P \rangle - \langle u_s F \rangle F, \quad 0 < y < 1, \tag{4.73}$$

with the following conditions

$$\left.\frac{dH}{dy}\right|_{y=0} = \left.\frac{dH}{dy}\right|_{y=1} = 0, \tag{4.74}$$

and

$$\langle H \rangle = 0. \tag{4.75}$$

Similarly, matching with oscillatory non-exponential terms, the function $I(y)$ will be governed by

$$\frac{d^2I}{dy^2} = (u_s - \langle u_s \rangle)Q - \langle u_s Q \rangle - \frac{1}{2}\langle u_w G^* \rangle F + \frac{1}{2}(u_w T^* - \langle u_w T^* \rangle), \quad 0 < y < 1, \tag{4.76}$$

with the following conditions

$$\left.\frac{dI}{dy}\right|_{y=0} = \left.\frac{dI}{dy}\right|_{y=1} = 0, \tag{4.77}$$

and

$$\langle I \rangle = 0. \tag{4.78}$$

The function $J(y)$ is governed by

$$\frac{d^2J}{dy^2} + \lambda^2 J = (u_s - \langle u_s \rangle)T + (D_{Ts} + D_{Tw})G + u_w P + u_w Re(Q) + \frac{1}{2}u_w^* S, \quad 0 < y < 1, \tag{4.79}$$

and

$$\left.\frac{dJ}{dy}\right|_{y=0} = \left.\frac{dJ}{dy}\right|_{y=1} = 0. \tag{4.80}$$

Similarly, the function $K(y)$ satisfies the boundary value problem,

$$\frac{d^2K}{dy^2} + 2\lambda^2 K = (u_s - \langle u_s \rangle)S + \frac{1}{2}u_w T, \quad 0 < y < 1, \tag{4.81}$$

and

$$\left.\frac{dK}{dy}\right|_{y=0} = \left.\frac{dK}{dy}\right|_{y=1} = 0, \tag{4.82}$$

while $L(y)$ satisfies

$$\frac{d^2L}{dy^2} + 3\lambda^2 L = \frac{1}{2}u_w S, \quad 0 < y < 1, \tag{4.83}$$

and

$$\left.\frac{dL}{dy}\right|_{y=0} = \left.\frac{dL}{dy}\right|_{y=1} = 0. \tag{4.84}$$

On solving the system of equations (4.26)–(4.30), one gets,

$$F(y) = \frac{y^3}{6} - \frac{y^2}{4} + \frac{1}{24}, \tag{4.85}$$

and

$$G(y) = -\frac{i\phi\delta_s^2}{2(Sc-1)}\left[d_1 \sin\lambda y + d_2 \cos\lambda y + \frac{\sin\sigma y}{\sin\sigma}\right], \tag{4.86}$$

where, $d_1 = -\frac{\sigma}{\lambda \sin\sigma}$, and $d_2 = \frac{\sigma(\cos\sigma - \cos\lambda)}{\lambda \sin\lambda \sin\sigma}$.

Using (4.85) and (4.86), one can find the following

$$\langle u_s F\rangle = -\frac{1}{120}, \tag{4.87}$$

$$\begin{aligned}\langle u_w G^*\rangle = \frac{i\phi^2\delta_s^2}{2(Sc-1)}\Bigg\{&\frac{\sigma^*}{\lambda^* \sin\sigma^* \sin\sigma}\left(\frac{\sin(\sigma+\lambda^*)}{2(\sigma+\lambda^*)} - \frac{\sin(\sigma-\lambda^*)}{2(\sigma-\lambda^*)}\right)\\ &+\frac{\sigma^*(\cos\sigma^* - \cos\lambda^*)}{\lambda^* \sin\lambda^* \sin\sigma^* \sin\sigma}\left(\frac{1-\cos(\sigma+\lambda^*)}{2(\sigma+\lambda^*)} + \frac{1-\cos(\sigma-\lambda^*)}{2(\sigma-\lambda^*)}\right)\\ &+\frac{1}{\sin\sigma^* \sin\sigma}\left(\frac{\sin(\sigma-\sigma^*)}{2(\sigma-\sigma^*)} - \frac{\sin(\sigma+\sigma^*)}{2(\sigma+\sigma^*)}\right)\Bigg\},\end{aligned} \tag{4.88}$$

and

$$\langle G(y)\rangle = -\frac{i\phi\delta_s^2}{2(Sc-1)}\left[-\frac{\sigma(1-\cos\lambda)}{\lambda^2 \sin\sigma} + \frac{\sigma(\cos\sigma - \cos\lambda)}{\lambda^2 \sin\sigma} + \frac{1-\cos\sigma}{\sigma \sin\sigma}\right]. \tag{4.89}$$

On solving the system of equations (4.52)–(4.61), one gets,

$$P(y) = \frac{y^6}{180} - \frac{y^5}{60} + \frac{y^4}{96} + \frac{y^3}{144} - \frac{y^2}{160} + \frac{1}{4032}, \tag{4.90}$$

$$\begin{aligned}Q(y) = -\frac{1}{2}\Bigg[\frac{\phi^2}{(\lambda^2-\sigma^2)\sin\sigma}\Bigg\{\frac{d_1^*}{2}\left(\frac{\cos(\sigma+\lambda^*)y}{(\sigma+\lambda^*)^2} - \frac{\cos(\sigma-\lambda^*)y}{(\sigma-\lambda^*)^2}\right) + \frac{d_2^*}{2}\Bigg(\frac{y}{\sigma+\lambda^*} + \frac{y}{\sigma-\lambda^*}\\ -\frac{\sin(\sigma+\lambda^*)y}{(\sigma+\lambda^*)^2} - \frac{\sin(\sigma-\lambda^*)y}{(\sigma-\lambda^*)^2}\Bigg)\Bigg\}\Bigg] - \frac{1}{4}\langle u_w G^*\rangle y^2 + e_1,\end{aligned} \tag{4.91}$$

$$T(y) = e_2 \cos\lambda y + e_3 \sin\lambda y + A_1(y) + A_2(y), \tag{4.92}$$

$$S(y) = e_4 \cos(\sqrt{2}\lambda)y + e_5 \sin(\sqrt{2}\lambda)y + A_3(y), \tag{4.93}$$

where the functions $A_1(y)$,$A_2(y)$ and $A_3(y)$ are

$$A_1(y) = \frac{\phi}{\sin\sigma}\Bigg[\Bigg\{-\frac{\sigma}{(\lambda^2-\sigma^2)^2}y^2+\frac{\sigma}{(\lambda^2-\sigma^2)^2}y+\frac{8\sigma^3}{(\lambda^2-\sigma^2)^4}+\frac{4\sigma}{(\lambda^2-\sigma^2)^3}\Bigg\}\cos\sigma y + \Bigg\{\frac{1}{6(\lambda^2-\sigma^2)}y^3-\frac{1}{4(\lambda^2-\sigma^2)}y^2-\left(\frac{4\sigma^2}{(\lambda^2-\sigma^2)^3}+\frac{1}{(\lambda^2-\sigma^2)^2}\right)y+\frac{2\sigma^2}{(\lambda^2-\sigma^2)^3} + \frac{1}{2(\lambda^2-\sigma^2)^2}+\frac{1}{24(\lambda^2-\sigma^2)}\Bigg\}\sin\sigma y\Bigg], \tag{4.94}$$

$$A_2(y) = \frac{\phi}{\lambda^2-\sigma^2}\Bigg[d_1\Bigg\{\left(-\frac{y^2}{4\lambda}+\frac{y}{4\lambda}\right)\cos\lambda y+\frac{y}{4\lambda^2}\sin\lambda y\Bigg\}+d_2\Bigg\{\frac{y}{4\lambda^2}\cos\lambda y+\left(\frac{y^2}{4\lambda} -\frac{y}{4\lambda}\right)\sin\lambda y\Bigg\}+\frac{1}{\sin\sigma}\Bigg\{-\frac{2\sigma}{(\lambda^2-\sigma^2)^2}\cos\sigma y+\left(\frac{y}{\lambda^2-\sigma^2}-\frac{1}{2(\lambda^2-\sigma^2)}\right)\sin\sigma y\Bigg\}\Bigg], \tag{4.95}$$

$$A_3(y) = \frac{\phi^2}{2(\lambda^2-\sigma^2)\sin\sigma}\Bigg[\frac{d_1}{2}\Bigg\{\frac{\cos(\sigma-\lambda)y}{2\lambda^2-(\sigma-\lambda)^2}-\frac{\cos(\sigma+\lambda)y}{2\lambda^2-(\sigma+\lambda)^2}\Bigg\}+\frac{d_2}{2}\Bigg\{\frac{\sin(\sigma-\lambda)y}{2\lambda^2-(\sigma-\lambda)^2} +\frac{\sin(\sigma+\lambda)y}{2\lambda^2-(\sigma+\lambda)^2}\Bigg\}+\frac{1}{4\sin\sigma}\Bigg\{\frac{1}{\lambda^2}-\frac{\cos(2\sigma)y}{\lambda^2-2\sigma^2}\Bigg\}\Bigg], \tag{4.96}$$

and the constant e_1, e_2, e_3, e_4 and e_5 are

$$e_1 = \frac{1}{2}\Bigg[\frac{\phi^2}{(\lambda^2-\sigma^2)\sin\sigma}\Bigg\{\frac{d_1^*}{2}\left(\frac{\sin(\sigma+\lambda^*)}{(\sigma+\lambda^*)^3}-\frac{\sin(\sigma-\lambda^*)}{(\sigma-\lambda^*)^3}\right)+\frac{d_2^*}{2}\left(\frac{1}{2(\sigma+\lambda^*)}+\frac{1}{2(\sigma-\lambda^*)} -\frac{1-\cos(\sigma+\lambda^*)}{(\sigma+\lambda^*)^3}-\frac{1-\cos(\sigma-\lambda^*)}{(\sigma-\lambda^*)^3}\right)\Bigg\}\Bigg]+\frac{1}{12}\langle u_w G^*\rangle, \tag{4.97}$$

$$e_2 = \frac{1}{\lambda\sin\lambda}\Bigg\{\left.\frac{dA_1}{dy}\right|_{y=1}+\left.\frac{dA_2}{dy}\right|_{y=1}-\cos\lambda\left(\left.\frac{dA_1}{dy}\right|_{y=0}+\left.\frac{dA_2}{dy}\right|_{y=0}\right)\Bigg\}, \tag{4.98}$$

$$e_3 = -\frac{1}{\lambda}\left(\left.\frac{dA_1}{dy}\right|_{y=0}+\left.\frac{dA_2}{dy}\right|_{y=0}\right), \tag{4.99}$$

$$e_4 = \frac{1}{\sqrt{2}\lambda\sin(\sqrt{2}\lambda)}\left(\left.\frac{dA_3}{dy}\right|_{y=1}-\cos(\sqrt{2}\lambda)\left.\frac{dA_3}{dy}\right|_{y=0}\right), \tag{4.100}$$

$$e_5 = -\frac{1}{\sqrt{2}\lambda}\left.\frac{dA_3}{dy}\right|_{y=0}. \tag{4.101}$$

On solving the system of equations (4.73)–(4.75), one gets,

$$H(y) = \frac{y^9}{12960}-\frac{y^8}{2880}+\frac{y^7}{2240}+\frac{y^6}{17280}-\frac{y^5}{2400}+\frac{y^4}{11520}+\frac{y^3}{24192}+\frac{y^2}{8960}-\frac{13}{453600}. \tag{4.102}$$

Analytical expressions for the functions $I(y)$, $J(y)$, $K(y)$ and $L(y)$ could be obtained by solving the equations (4.76)–(4.84). As the expressions in the concerned equations are too large and complicated to solve analytically, we have solved these equations numerically. Some of those numerical values for a typical case are presented in the table 4.1. From the table it can be observed that the values of the functions of third-order approximations are so small, that they will have negligible contributions in modifying the mean and transverse concentration distributions. So, it would not be a wise and worthy exercise to consider higher order expressions (fourth and higher) in the calculations.

y	$I(y) \times 10^3$	$J(y) \times 10^3$	$K(y) \times 10^3$	$L(y) \times 10^3$
0	$-0.0158 - 0.1727i$	$-0.1161 + 0.0708i$	$-0.0026 + 0.0230i$	$-0.0171 + 0.0026i$
0.25	$-0.0106 - 0.1219i$	$-0.0907 + 0.0787i$	$0.0163 + 0.0369i$	$-0.0151 + 0.0109i$
0.5	$0.0031 + 0.0061i$	$-0.0243 + 0.0710i$	$0.0737 + 0.0527i$	$-0.0055 + 0.0275i$
0.75	$0.0104 + 0.1223i$	$0.0445 + 0.0240i$	$0.1460 + 0.0421i$	$0.0112 + 0.0394i$
1	$0.0098 + 0.1594i$	$0.0727 - 0.0125i$	$0.1805 + 0.0252i$	$0.0211 + 0.0417i$
Average Value (e.g. $\langle I \rangle \times 10^3$)	0	$-0.0230 + 0.0507i$	$0.0812 + 0.0390i$	$-0.0018 + 0.0250i$

Table 4.1: Numerical values of transverse functions for $\delta_s = 1$, where $\phi = 1$ and $T_r = 1$.

Analytical solution for mean concentration up to third-order becomes

$$\begin{aligned}\langle C \rangle &= C^{(0)} + \epsilon \langle C^{(1)} \rangle + \epsilon^2 \langle C^{(2)} \rangle + \epsilon^3 \langle C^{(3)} \rangle \\ &= C^{(0)} + \epsilon Pe\ Re[\langle G(y) \rangle e^{-i\Omega Sct}] \frac{\partial C^{(0)}}{\partial x} + \epsilon^2 Pe^2\ Re[\langle T(y) \rangle e^{-i\Omega Sct} + \langle S(y) \rangle e^{-2i\Omega Sct}] \\ &\quad \times \frac{\partial^2 C^{(0)}}{\partial x^2} + \epsilon^3 Pe^3\ Re[\langle J(y) \rangle e^{-i\Omega Sct} + \langle K(y) \rangle e^{-2i\Omega Sct} + \langle L(y) \rangle e^{-3i\Omega Sct}] \frac{\partial^3 C^{(0)}}{\partial x^3},\end{aligned} \tag{4.103}$$

and third-order transverse concentration will be

$$\begin{aligned}C = C^{(0)} + \epsilon Pe\ [F(y) + Re(G(y) e^{-i\Omega Sct})] \frac{\partial C^{(0)}}{\partial x} + \epsilon^2 Pe^2 [P(y) + Re(Q(y) + T(y) e^{-i\Omega Sct_0} \\ + S(y) e^{-2i\Omega Sct_0})] \frac{\partial^2 C^{(0)}}{\partial x^2} + \epsilon^3 Pe^3 [H(y) + Re(I(y) + J(y) e^{-i\Omega Sct_0} \\ + K(y) e^{-2i\Omega Sct_0} + L(y) e^{-3i\Omega Sct_0})] \frac{\partial^3 C^{(0)}}{\partial x^3}.\end{aligned} \tag{4.104}$$

In the expression of effective dispersion coefficient D_T (Eq. (4.46)), the first term on the R.H.S. (i.e., the constant 1) usually is neglected when compared with the last term of the expression for $Pe > 100$ [18]. It indicates that diffusion in longitudinal direction is neglected in this study by restricting the Peclet number to be high. Peclet number generally becomes very large and high in engineering problems, where the flow becomes advection dominated. Consequently, one can obtain expressions independent of Pe for

mean and real concentrations in a new system $\{\eta/Pe, \langle C\rangle Pe\}$ as

$$\langle C\rangle Pe = C^{(0)}Pe + Re[\langle G(y)\rangle e^{-i(2\pi T_r)\tau}]\frac{\partial(C^{(0)}Pe)}{\partial(\eta/Pe)} + Re[\langle T(y)\rangle e^{-i(2\pi T_r)\tau} + \langle S(y)\rangle \times e^{-i(4\pi T_r)\tau}]\frac{\partial^2(C^{(0)}Pe)}{\partial(\eta/Pe)^2} + Re[\langle J(y)\rangle e^{-i(2\pi T_r)\tau} + \langle K(y)\rangle e^{-i(4\pi T_r)t} + \langle L(y)\rangle e^{-i(6\pi T_r)\tau}] \times \frac{\partial^3(C^{(0)}Pe)}{\partial(\eta/Pe)^3}, \tag{4.105}$$

and

$$C\,Pe = C^{(0)}Pe + [F(y) + Re\{G(y)e^{-i(2\pi T_r)\tau}\}]\frac{\partial(C^{(0)}Pe)}{\partial(\eta/Pe)} + [P(y) + Re\{Q(y) + T(y) \times e^{-i(2\pi T_r)\tau} + S(y)e^{-i(4\pi T_r)\tau}\}]\frac{\partial^2(C^{(0)}Pe)}{\partial(\eta/Pe)^2} + [H(y) + Re\{I(y) + J(y) \times e^{-i(2\pi T_r)\tau} + K(y)e^{-i(4\pi T_r)\tau} + L(y)e^{-i(6\pi T_r)\tau}\}]\frac{\partial^3(C^{(0)}Pe)}{\partial(\eta/Pe)^3}, \tag{4.106}$$

where the parameter T_r represents the ratio of the characteristic time required for vertical mixing to the flow period (T_p) and can be defined [64, 74] as

$$T_r = \frac{T_0}{T_p} = \frac{h^2/D}{2\pi/\omega} = \frac{\Omega Sc}{2\pi}\Big(= \frac{Sc}{\pi\delta_s^2}\Big). \tag{4.107}$$

Here, T_0 is the basic time scale, which can be described as, the time required for the transverse variation of concentration in the vertical direction being smear out through diffusion.

It is concluded from Eq. (4.105) that as $\tau \to \infty$, $\langle C\rangle$ tends to $C^{(0)}$, i.e., transverse mean concentration asymptotically approaches $C^{(0)}$. Hence, for large times, the transverse mean concentration satisfies a diffusion like equation (4.45). In the expression (4.105), the exponential term contributes an additional modification on the mean concentration distribution, which decays with time and does not affect the long-time distribution pattern.

4.4 Results and discussion

In the following subsections, Taylor dispersivity, distributions of mean and transverse concentrations are discussed. The variation of the velocity profile, oscillatory dispersion coefficient and the concentrations depend on the parameters δ_s and Sc. Based on the

assumptions on first time scale (T_0) and the dimensionless angular frequency (Ω), one can get $\Omega^{-1} = O(Sc)$, which implies ${\delta_s}^2 = O(Sc)$. For dispersion to be significant, one may expect that $\delta_s \geqslant O(1)$, equivalently the flow is slow enough for the Stokes boundary layer thickness to be at least comparable with the channel width. Similarly, $\delta_s \ll O(1)$ represents the flow is so fast that the Stokes boundary layer is just a tiny fraction of the channel width. Figure (4.2) shows the variations of the velocity profile given in Eq. (4.8). If the amplitude of oscillation (ϕ) is zero, the velocity profile reduces to a simple shear flow ($u(y) = y$), which is plotted in Fig. (4.2a). Figures (4.2b)–(4.2d) show the variations of oscillatory Couette flow for different values of δ_s when $\phi = 1$ and $T_r = 1$.

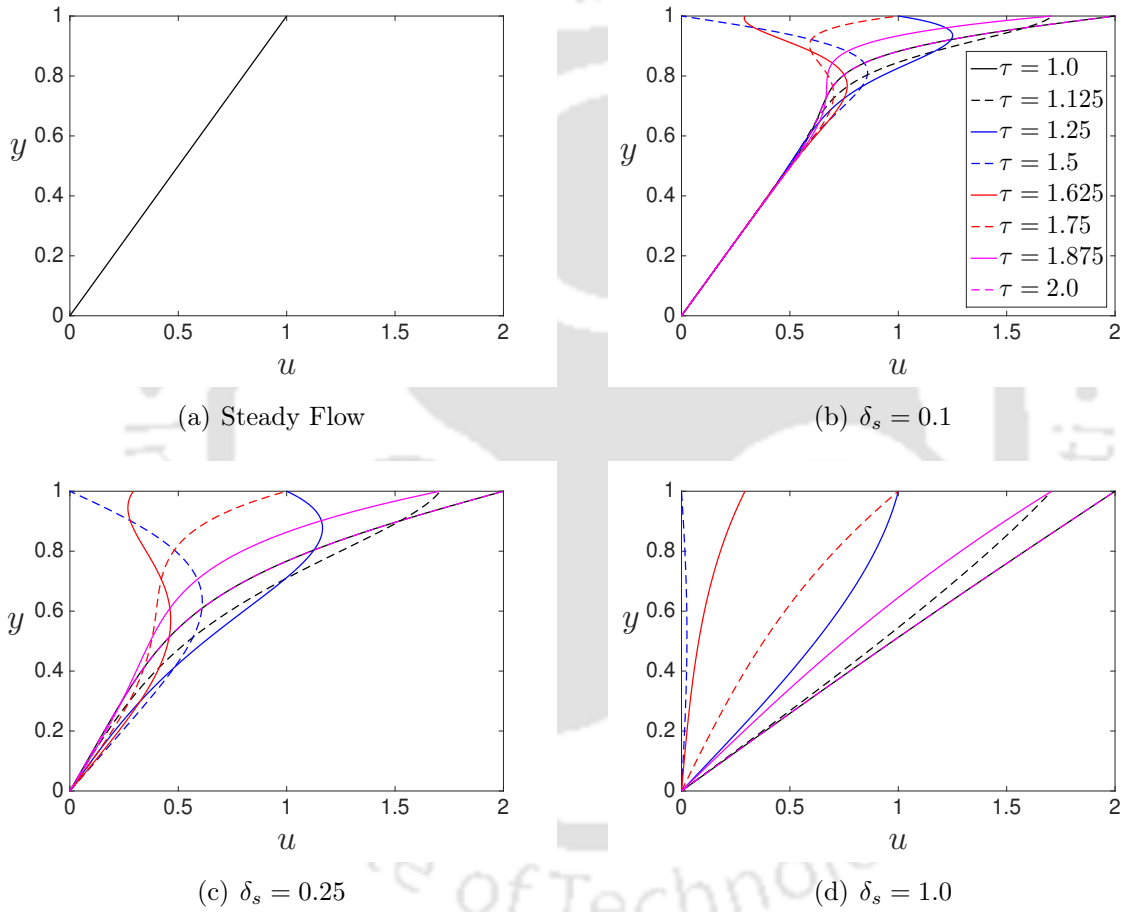

(a) Steady Flow (b) $\delta_s = 0.1$

(c) $\delta_s = 0.25$ (d) $\delta_s = 1.0$

Figure 4.2: Velocity profile of (a) Steady flow, (b - d) Couette flow for different δ_s within one oscillation, where $T_r = 1$.

4.4.1 Dispersivity

From Eqs. (4.47), (4.48), (4.87) and (4.88), the explicit forms for steady and oscillatory components of dispersion coefficient can be written as

$$D_{Ts} = \frac{1}{120}, \tag{4.108}$$

and

$$D_{Tw} = \frac{\phi^2\delta_s^2}{4(Sc-1)} Im\Bigg\{ \frac{\sigma^*}{\lambda^* \sin\sigma^* \sin\sigma} \left(\frac{\sin(\sigma+\lambda^*)}{2(\sigma+\lambda^*)} - \frac{\sin(\sigma-\lambda^*)}{2(\sigma-\lambda^*)} \right) + \frac{\sigma^*(\cos\sigma^* - \cos\lambda^*)}{\lambda^* \sin\lambda^* \sin\sigma^* \sin\sigma} \left(\frac{1-\cos(\sigma+\lambda^*)}{2(\sigma+\lambda^*)} + \frac{1-\cos(\sigma-\lambda^*)}{2(\sigma-\lambda^*)} \right) \Bigg\}, \tag{4.109}$$

where Im stands for the imaginary part.

Here, the value 1/120 for D_{Ts} is in exact agreement with that obtained by Ng and Bai [40] and a good agreement with the value 0.0083, which is the steady-state value of dispersion coefficient obtained by Bandyopadhyay and Mazumder (see Fig. 5 in [6]). The limiting value of D_{Tw} is calculated for $\delta_s = 0$ as the expression of D_{Tw} (Eq. (4.109)) is indeterminate at $\delta_s = 0$. The expression for D_{Tw} is similar to that of Ng and Bai [40] for the case of inert boundaries. Using L'Hospital's rule, one can find the finite limits of D_{Tw} (Eq. (4.109)) at $\delta_s = 0$ and $Sc = 1$.

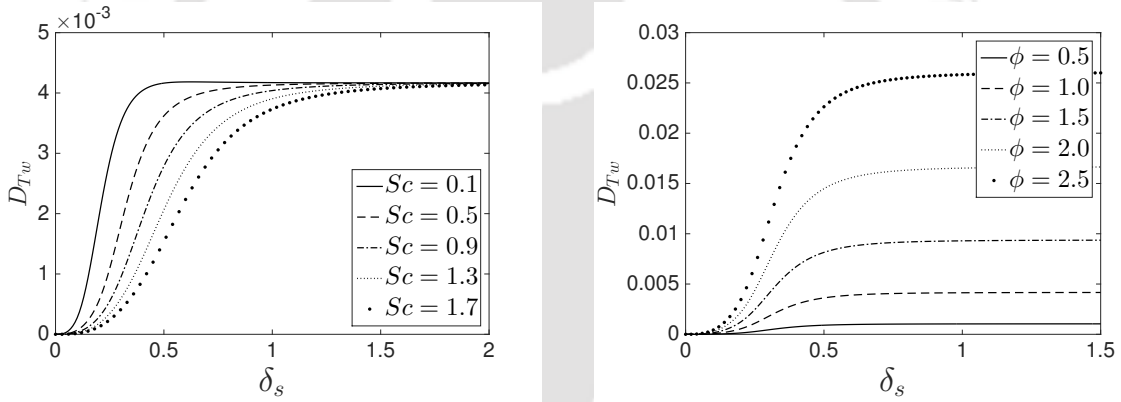

(a) $\phi = 1$ (b) $Sc = 0.5$

Figure 4.3: Variation of oscillatory dispersion coefficient with δ_s for different (a) Sc and (b) ϕ.

The variation of dispersion coefficient D_{Tw} with the oscillation parameter δ_s is illustrated in Fig. (4.3). The figure shows that the dispersion coefficient D_{Tw} increases monotonically with δ_s. Yasuda [74] also observed that dispersion process increases with the increase in δ_s. D_{Tw} increases in δ_s up to unity and for δ_s beyond unity, no significant change in dispersion coefficient is noticed. Behaviour of D_{Tw} with δ_s for different Sc can be seen from Fig. (4.3a). The figure illustrates that with the increase in the value of Sc, the value of D_{Tw} decreases. As Sc increases, the rate of increase in momentum diffusivity is more compared to that in molecular diffusion. So that dispersion for the solute will be less for higher value of Sc. Figure also shows that for $\delta_s \gg 1$, D_{Tw} is independent of Sc. Figure (4.3b) shows that with the increase of ϕ, dispersion coefficient increases. Increase in the amplitude of the upper plate oscillation (ϕ),increases the axial diffusion in

the transport of solute in the flowing fluid. Figure (4.3) also verifies the earlier claim of Ng [38, 39] that $\lim_{\delta_s \gg 1} D_{Tw} = \frac{\phi^2}{2} D_{Ts}$, for $\forall Sc$. So, for $\phi = 1$ and for very slow oscillation, D_{Tw} value becomes $1/240 \sim 0.0042$. It can be observed from Fig. (4.3a) that, for the same situation ($\phi = 1$, $\delta_s \gg 1$), D_{Tw} converges to the above value 0.0042 and is in agreement with Ng's results. One can easily verify that the graphs given in Fig. (4.3b) also follow the relation $\lim_{\delta_s \gg 1} D_{Tw} = \frac{\phi^2}{2} D_{Ts}$.

4.4.2 Different order of asymptotic expansion

From the asymptotic expansion (4.10) we can write the mean and transverse concentration distributions in $\{\eta, y, \tau\}$ coordinates as

$$\langle C(\eta, y, \tau)\rangle = \langle C^{(0)}(\eta, \tau)\rangle + \langle C^{(1)}(\eta, y, \tau)\rangle + \langle C^{(2)}(\eta, y, \tau)\rangle + \langle C^{(3)}(\eta, y, \tau)\rangle + O(\epsilon^4), \quad (4.110)$$

$$C(\eta, y, \tau) = C^{(0)}(\eta, \tau) + C^{(1)}(\eta, y, \tau) + C^{(2)}(\eta, y, \tau) + C^{(3)}(\eta, y, \tau) + O(\epsilon^4), \quad (4.111)$$

where $C^{(0)}(\eta, \tau)$ can be found from Eq. (4.49) and $C^{(i)}(\eta, y, \tau), (i = 1, 2, 3, \cdots)$ are from Eqs. (4.25), (4.51) and (4.72). Basically, $C^{(i)}(\eta, y, \tau)$ represents difference between i^{th} and $(i-1)^{th}$ order approximations.

Figures (4.4) and (4.5) show the longitudinal distribution along the channel calculated as asymptotic expansions from zeroth to third-order. Initially, before $\tau = 3.25$, each order term plays a significant role in the longitudinal distribution. As time proceeds, the contribution of higher order expansion to the distribution diminishes gradually. After $\tau = 3.25$ as shown in figures, higher than the second-order can be truncated without causing much errors. This is also well verified by the tables 4.2 and 4.3, where we have calculated the order percentage [63] to observe the effect of each order expansion. So, after for $\tau > 3.25$, second and third oder approximation graph almost overlapped and difference of them becomes very small. So, it might be enough to evaluate the approximate solutions up to second-order as (for larger $\tau > 5.25$)

$$\langle C(\eta, y, \tau)\rangle = \langle C^{(0)}(\eta, \tau)\rangle + \langle C^{(1)}(\eta, y, \tau)\rangle + \langle C^{(2)}(\eta, y, \tau)\rangle, \quad (4.112)$$

$$C(\eta, y, \tau) = C^{(0)}(\eta, \tau) + C^{(1)}(\eta, y, \tau) + C^{(2)}(\eta, y, \tau). \quad (4.113)$$

4.4.3 Mean concentration distribution

Evolution of mean concentration distribution can be seen from Fig. (4.6), where for $\delta_s = 0.25$ and 1, the longitudinal distribution of third-order mean plotted over one oscillation period. It can be seen from the figure that, time evolution of the curves of mean concentration shows an oscillatory movement along the longitudinal direction. As the so-

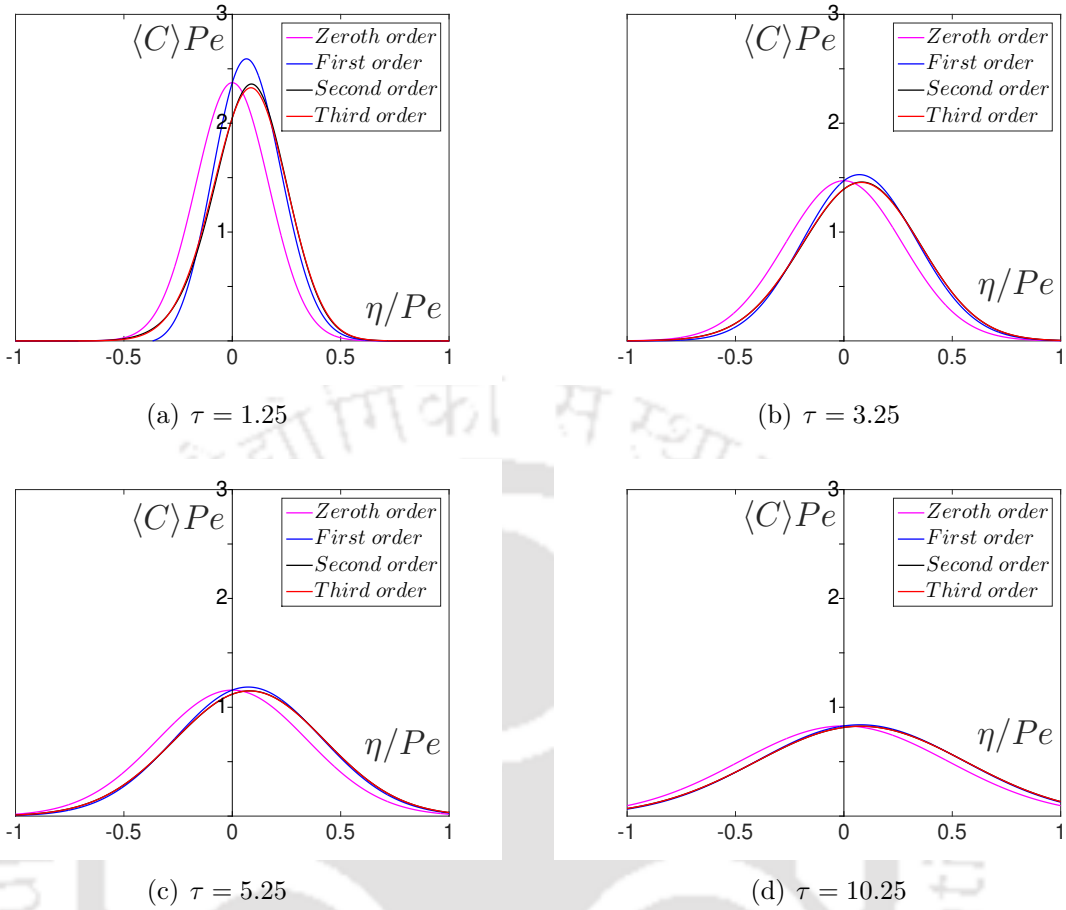

(a) $\tau = 1.25$ (b) $\tau = 3.25$

(c) $\tau = 5.25$ (d) $\tau = 10.25$

Figure 4.4: Longitudinal distribution of mean concentration, calculated as asymptotic expansions from zeroth to third-order.

τ	$\frac{max\{\langle C^{(1)}(\eta,y,\tau)\rangle\}}{C^{(0)}(0,\tau)} \times 100\%$	$\frac{max\{\langle C^{(2)}(\eta,y,\tau)\rangle\}}{C^{(0)}(0,\tau)} \times 100\%$	$\frac{max\{\langle C^{(3)}(\eta,y,\tau)\rangle\}}{C^{(0)}(0,\tau)} \times 100\%$
1.25	27.7823	6.0815	1.6087
3.25	17.2316	2.3392	0.3843
5.25	13.5556	1.4479	0.1871
10.25	9.7031	0.7416	0.0686

Table 4.2: Order percentages for mean concentration, here $\langle C^{(i)}(\eta, y, \tau)\rangle$ represents difference between i^{th} and $(i-1)^{th}$ order approximations of mean concentration.

lute spreads out due to lateral diffusion and advection, the peak of the mean concentration decreases gradually with the increase in time. Such an evolution of mean concentration has also been reported by Jiang and Grotberg [25] for tube flow.

Figure (4.7) shows the difference rate between third-order mean concentration $\langle C\rangle$ and the solution of the Taylor dispersion model C_0 at a fixed axial location $\eta/Pe = 0.25$ for different δ_s. When $\langle C\rangle$ approaches to C_0, in other words, when the difference between these two quantities becomes negligibly small, transverse mean concentration satisfies a one-dimensional diffusion like equation. Figure illustrates that for $\delta_s = 0.25$, after some

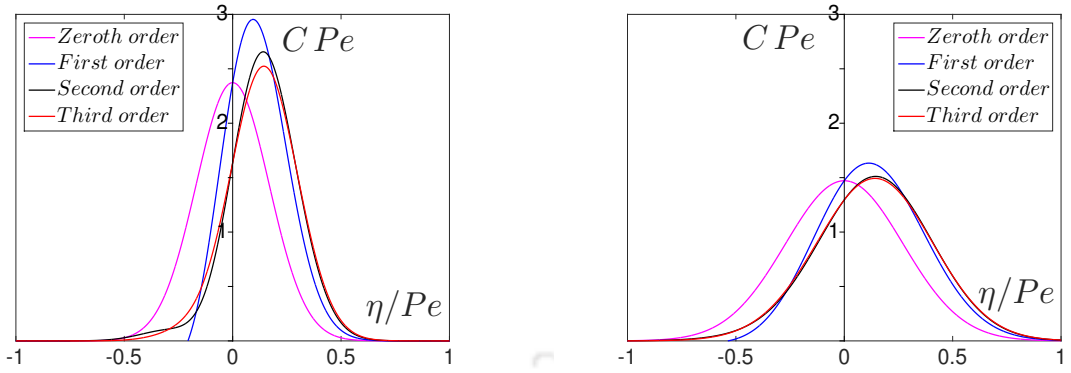

(a) $\tau = 1.25$ (b) $\tau = 3.25$

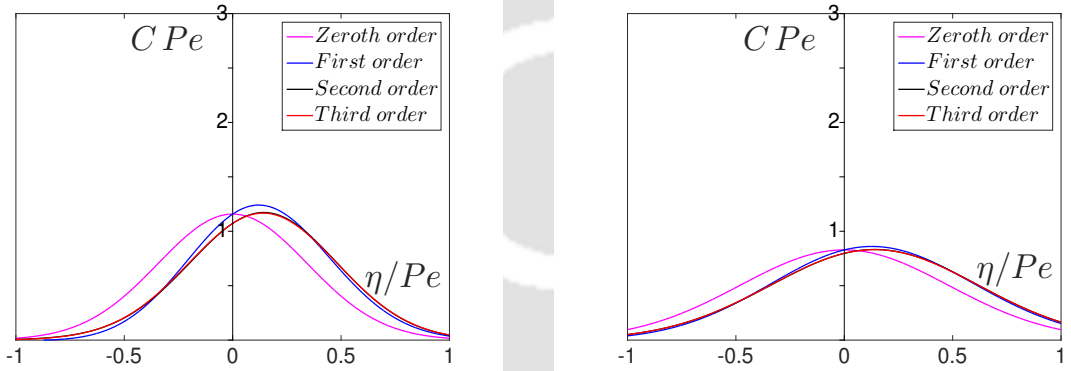

(c) $\tau = 5.25$ (d) $\tau = 10.25$

Figure 4.5: Longitudinal distribution of transverse concentration at oscillatory upper plate (i.e., at $y = 1$), calculated as asymptotic expansions from zeroth to third-order.

τ	$\frac{max\{C^{(1)}(\eta,1,\tau)\}}{C^{(0)}(0,\tau)} \times 100\%$	$\frac{max\{C^{(2)}(\eta,1,\tau)\}}{C^{(0)}(0,\tau)} \times 100\%$	$\frac{max\{C^{(3)}(\eta,1,\tau)\}}{C^{(0)}(0,\tau)} \times 100\%$
1.25	49.4147	13.8498	5.6867
3.25	30.6489	5.3273	1.3586
5.25	24.1105	3.2974	0.6615
10.25	17.2583	1.6890	0.2426

Table 4.3: Order percentages for transverse concentration at $y = 1$, here $C^{(i)}(\eta, 1, \tau)$ represents difference between i^{th} and $(i-1)^{th}$ order approximations of transverse real concentration at $y = 1$.

short time, $\langle C \rangle$ approaches C_0 whereas for the values $\delta_s > 0.25$, the transverse mean takes a long time to reach the Taylor dispersion stage (where difference is negligibly small). The parameter δ_s is increased with the increase in oscillation period of the plate. So, when δ_s value is small, plate oscillation will be fast. For fast oscillation, effects of plate oscillation are restricted in a very thin boundary layer at the upper plate and there is a little effect of plate oscillation on solute except in a thin boundary layer. The effective boundary layer becomes thicker as the value of δ_s increases further. Consequently, the oscillation

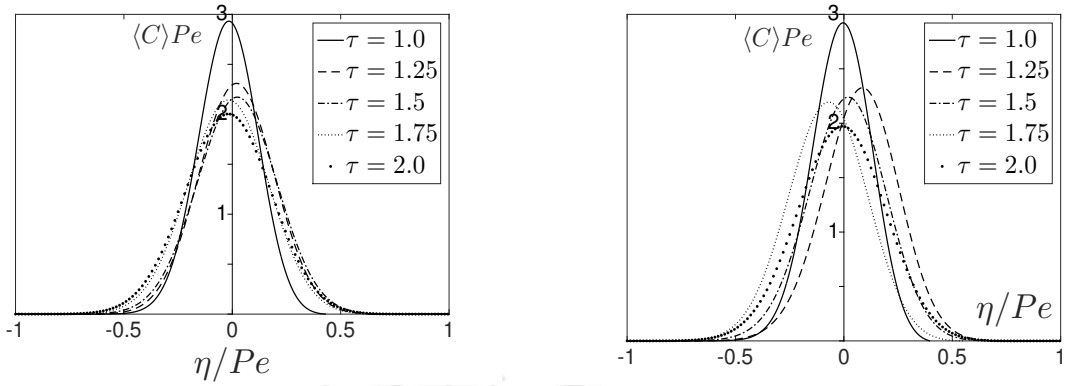

(a) $\delta_s = 0.25$ (b) $\delta_s = 1.0$

Figure 4.6: Longitudinal distribution of mean concentration distribution, where $\phi = 1.0$, $T_r = 1$.

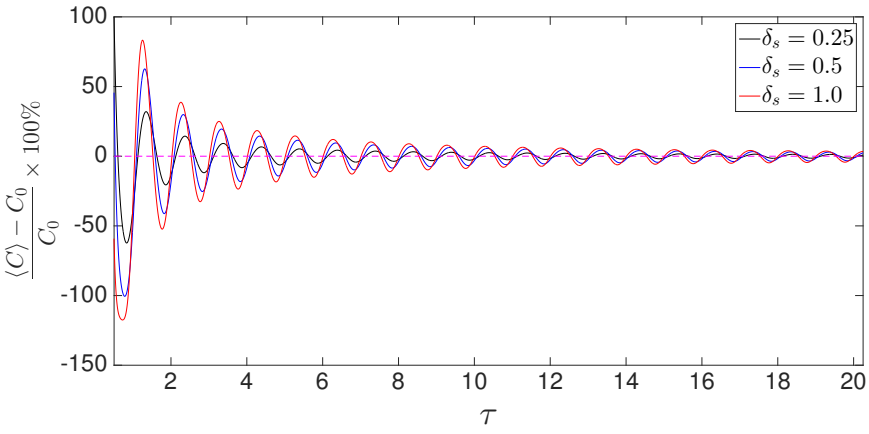

Figure 4.7: Variation of difference rate function of third-order mean with Taylor's mean with time at $\eta = 0.25$ for different δ_s, where $T_r = 1$ (dotted line represents a horizontal line at origin).

of the plate becomes slow but more effective on the solute dispersion. For a fixed δ_s, the amplitude of the difference of two means of the solute cloud gradually decreases as time increases.

4.4.4 Transverse concentration distribution

In order to study the complete solute transport in an oscillatory Couette flow, instead of just mean concentration distribution, we have derived the transverse real concentration (Eq. (4.106)). The accurate two-dimensional concentration distribution and its evolution in oscillatory flows are of essential significance to various applications such as, environmental risk assessment, ecological restoration, etc. Although transverse real concentration was proposed by Gill [18] and Chatwin [9], Wu and Chen [68] first analysed the evolution of it.

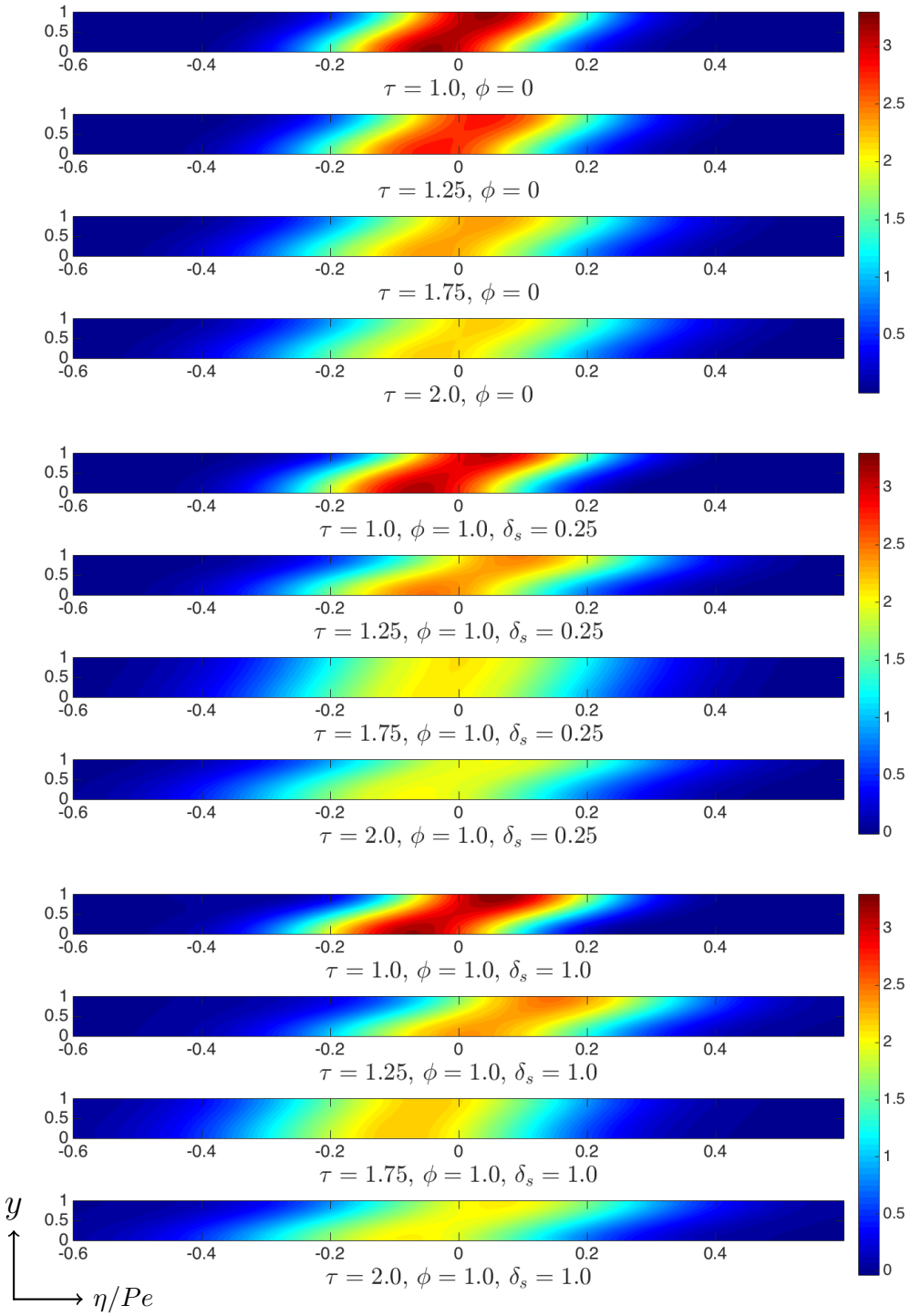

Figure 4.8: Concentration contours for steady and oscillatory flows ($T_r = 1$): horizontal axis represents η/Pe, vertical axis represents y.

The two-dimensional concentration contours are plotted in Fig. (4.8) for steady and oscillatory flows over a period of time. The scalar is injected initially across the line

$\eta = 0$ and dispersed through the channel under the effects of advection and diffusion. The coordinate system in the figure longitudinally moves with the velocity $Pe\,\langle u_s \rangle$, that ensures centroid of the concentration cloud remains at origin with respect to steady state velocity but movement of the centroid can be affected by oscillatory component of the velocity. The first sub figure, shows the concentration distribution for steady state flow, where concentration centroid fixed at origin. The second and third sub figures of Fig. (4.8), show the effect of flow oscillation, where the centroid cloud moves back and forth for fast and slow oscillations. In the downstream, by the influence of upper plate oscillation, the solute near the upper plate moves with higher speed, which creates higher concentration zone near the upper plate. On the other hand, in the upstream, higher concentration zone appears near the stationary lower plate, as movement of the solute is much slower due to slow velocity near the lower plate. It is also noticed that the speed with which the upper plate moves, solute fails to move with same speed and it creates a phase lag between flow velocity and the movement of the solute.

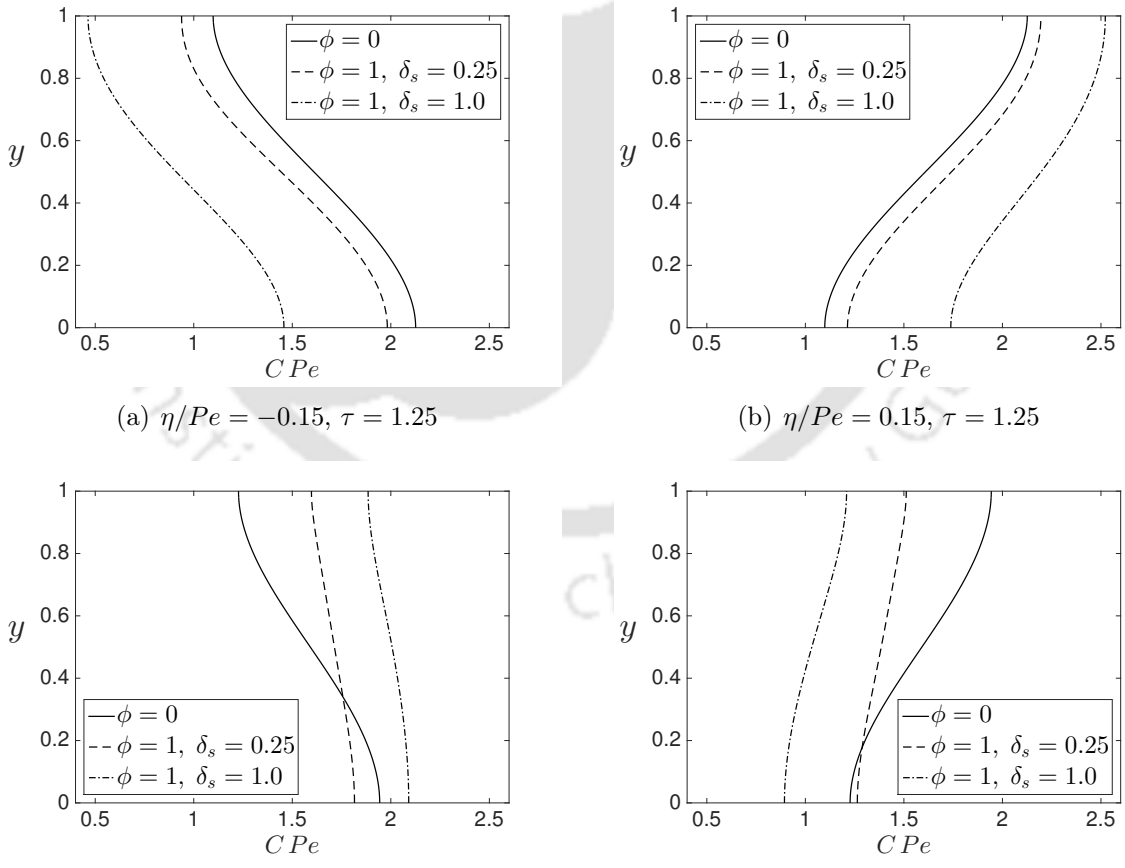

(a) $\eta/Pe = -0.15,\ \tau = 1.25$

(b) $\eta/Pe = 0.15,\ \tau = 1.25$

(c) $\eta/Pe = -0.15,\ \tau = 1.75$

(d) $\eta/Pe = 0.15,\ \tau = 1.75$

Figure 4.9: Transverse variation of concentration distribution by typical cross-sections for steady and oscillatory flows, where $T_r = 1$.

Figure (4.9) illustrates the transverse variation of concentration distribution for steady and oscillatory flows. In order to observe the concentration variations in the upstream and downstream sections properly, two typical cross-sections $\eta = -0.15$ and $\eta = 0.15$ with two different times $\tau = 1.25$ and 1.75 are considered. According to Figs. (4.9a) and (4.9c), for a typical upstream cross-section at $\eta = -0.15$, the concentration increases in the lateral direction from upper plate to lower plate. As pointed out earlier, velocity is slow at an area near the lower plate where longitudinal spreading of solute is very slow, which causes to form a higher concentration zone near the lower plate. The case is reverse across a typical downstream section at $\eta = 0.15$ as plotted in Figs. (4.9b) and (4.9d), the concentration decreases in the lateral direction from the upper plate to the lower plate. This happens because of the velocity difference over the cross-section of the channel. Flow velocity is faster near the oscillatory plate where longitudinal spreading of the scalar substance is fast, which causes higher concentration zone near the oscillatory plate. Initially, the flow is dominated by advection, which results in large concentration variation across the channel at time $\tau = 1.25$. At a later times, lateral diffusion becomes active from oscillatory plate to the stationary plate in the downstream and it becomes reverse in the upstream. This lateral diffusion smears out the concentration variation and makes the distribution uniform across the channel. These results resemble with those obtained by Wu and Chen [67] for open channel flow.

To discuss the uniformity of transverse concentration variations, an indicator $\mathcal{R}$ is adopted (following [67, 68]) as

$$\mathcal{R}(\eta, \delta_s, \tau) = \frac{max(C(\eta, y, \delta_s, \tau)) - min(C(\eta, y, \delta_s, \tau))}{C(0, 0, \delta_s, \tau)} \times 100\%, \tag{4.114}$$

which is the transverse variation in the cross-section against the centroid of the concentration cloud.

Figure (4.10) shows the longitudinal distributions of the transverse concentration variation rates. From the figure, it can be seen that as the solute cloud moves longitudinally from the origin, concentration variation rate increases from zero to a maximum and then decreases to zero again. As the solute moves relatively faster near the oscillatory upper plate of the channel cross-section, maximum variation rate occurs near the upper plate in the downstream. On the other hand, the maximum variation rate occurs near the lower plate in the upstream due to slow movement of solute near lower plate. Figure (4.10a) illustrates the concentration variation rates for simple shear flow. The graph shows that variation rates are symmetrical about the centroid of the solute cloud and maximum variation rate moves away with times from solute centroid. This feature is similar to the results obtained for other steady flows [67]. Transverse variation rates for oscillatory flows with $\delta_s = 0.25$ and 1.0 are depicted in Figs. (4.10b) and (4.10c). Figure (4.10) shows that as δ_s increases, the maximum variation rate also increases. Figure also indicates that

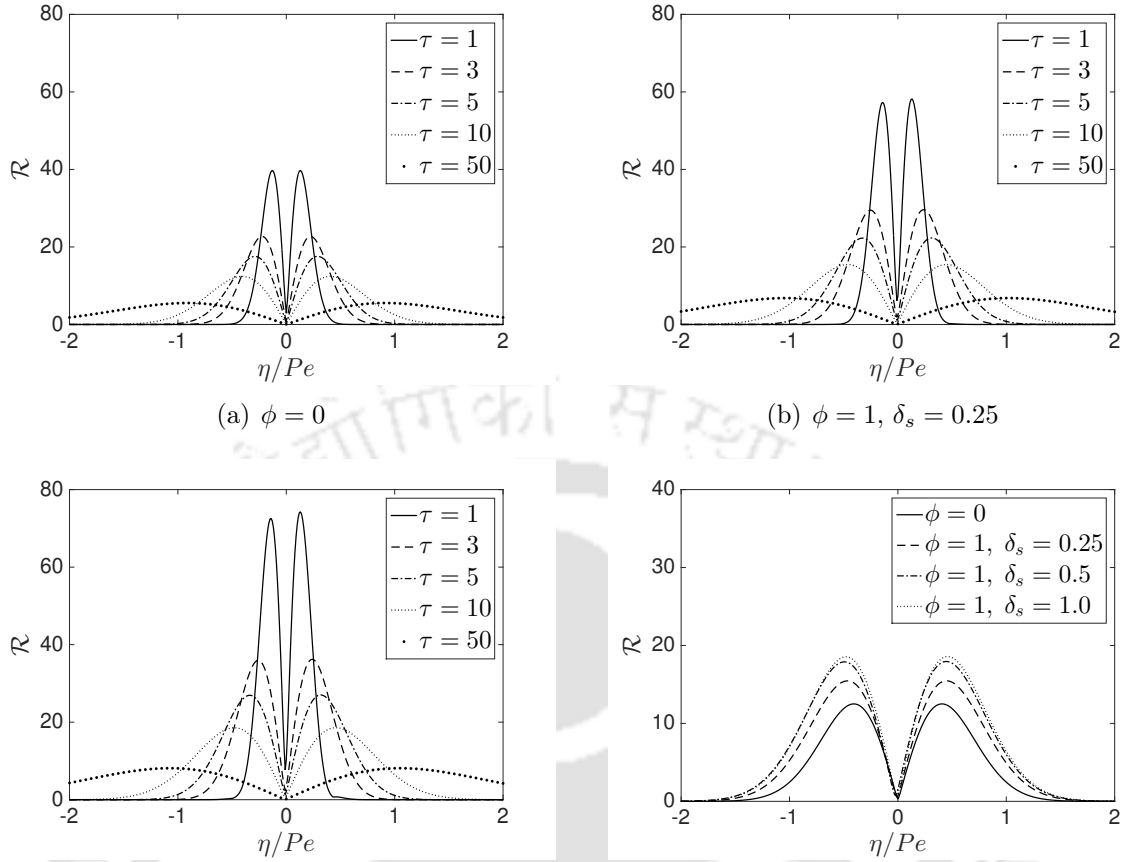

(a) $\phi = 0$ (b) $\phi = 1,\ \delta_s = 0.25$

(c) $\phi = 1,\ \delta_s = 1.0$ (d) $\tau = 10$

Figure 4.10: Longitudinal distribution of transverse concentration variation rates, where $T_r = 1$.

the diminishing of the transverse concentration variation is a large time-scale process, which can be characterized by the dimensionless time as $\tau \sim 10$ (same as for steady state study [67, 68]), compare to the scale of $\tau \sim 1$ suggested by Chatwin [9] for longitudinal normality and that of $\tau \sim 0.1$ by Taylor for dispersion of the mean concentration.

4.5 Conclusions

Multi-scale methods of homogenization is applied to explore the two-dimensional solute transport in an oscillatory Couette flow. Variations of dispersion coefficient with different flow parameters are discussed. Analytical solutions are obtained for the first time for mean and transverse real concentrations up to third-order approximation. By obtaining the mean concentration, the validity of Taylor dispersion model for an oscillatory Couette flow are discussed. This work includes the pattern of transverse real concentration distribution and uniformity over the cross-section of the channel. Some important conclusions are as follows:

1. Dispersion of solute in a flowing fluid increases with the increase in Stokes boundary layer thickness.

2. For slow oscillation of the upper plate, third-order mean will reach Taylor dispersion stage after a long time period compared to the case of fast oscillation of the plate.

3. A time scale up to $10h^2/D$ is suggested to characterize the initial transition stage of the transport process to approach transverse uniformity.

CHAPTER 5

SOLUTE DISPERSION IN AN OSCILLATORY COUETTE FLOW WITH WALL REACTIONS

In the previous chapter the solute dispersion in an oscillatory Couette flow for inert boundary wall is studied. The effects of Stokes boundary layer on solute dispersion are examined. In this following chapter, we discuss about the effects of both reversible and irreversible boundary reactions on oscillatory Couette flow.

5.1 Introduction

There have been many attempts to extend the work of Taylor for oscillatory flows. Dispersion of solute in an oscillatory flow has been studied by Aris [4], Chatwin [9], Smith [59], Mukherjee and Mazumder [34], Ng [37] and others. These studies are limited to inert boundary conditions. Flowing solute may be chemically reactive with the channel wall. The reaction may be homogeneous or heterogeneous. In a homogeneous reaction, the chemical reacts with the flowing fluid and in a heterogeneous reaction, the chemical reacts at the boundary. The latter may be reversible or irreversible. In reversible reaction, solute is assumed to partition between flowing fluid and adsorbing layer. The adsorbed solute again gets back to the flowing fluid. In irreversible reaction, solute totally absorbed into the boundary of the flow geometry. Davidson and Schroter [12], and Phillips and Kaye [47] studied a reversible phase exchange reaction. Mazumder and Das [27], and Jiang and Grotberg [25] have studied the effects of wall absorption in an oscillatory tube flow. Influences of both reversible and irreversible reactions in oscillatory flows have been studied by Ng [38, 39]. Reactions may be linear or non-linear type. Effects of linear reversible or irreversible reactions at the wall on solute dispersion have been investigated by Gupta and Gupta [24], Purnama [49], Sarkar and Jayaraman [55], Mazumder and Mondal [28], Paul and Mazumder [44] and others. Revelli and Ridolfi [52, 53], Paul and

Mazumder [45] have considered the effects of nonlinear chemical reaction on transport coefficients in steady and unsteady flows.

In existing literature on solute transport in oscillatory flows, the main focus was either to obtain the dispersion coefficient or to address the mean concentration distribution. For some environmental or industrial processes, not only the dispersion coefficient or the longitudinal mean concentration, but also the transverse concentration distribution and its uniformity over the cross-section are equally useful. Wu and Chen [67, 68] systemically analysed the transverse uniformity of concentration cloud for laminar steady flows by extending the homogenization technique proposed by Mei et al. [32]. In recent work, Wang and Chen [64] studied the transverse concentration distribution up to first-order approximation for oscillatory flow with inert boundary wall. In this study, an analytical study is presented to explore two-dimensional concentration distribution due to an oscillatory Couette flow, where solute may undergoes reversible and irreversible reactions with the channel bed. Simple analytical expressions are derived for both mean and transverse concentration distributions with the help of multi-scale method of homogenization.

The aim of this chapter is to find the analytical expressions for mean and transverse real concentrations by multi-scale homogenization technique and to explore the evolution of transverse concentration distribution for oscillatory Couette flows. The specific objectives of this work are: (I) to present a multi-scale analysis for the solute dispersion in an oscillatory Couette flow, (II) to obtain all the steady and unsteady components of dispersion coefficients, (III) to obtain analytical expressions for mean and transverse real concentrations up to second-order approximations, (IV) to observe the effects of flow parameters, phase exchange kinetics, bed absorption on dispersion coefficient, mean and transverse concentration distributions, (V) to discuss the uniformity in transverse real concentration over the channel cross-section.

5.2 Formulation of the problem

A laminar, one-dimensional plane Couette flow between two infinite parallel flat plates with a separation width h is considered. The lower plate at $\widehat{y} = 0$ is assumed to be stationary whereas the upper one at $\widehat{y} = h$ oscillates in its own plane with a prescribed velocity

$$\widehat{u}(h, \widehat{t}) = U[1 + \phi Re(e^{-i\omega\widehat{t}})],$$

where U is the steady component of the velocity of the upper plate, ϕ is a factor such that ϕU represents the amplitude of the oscillatory velocity component, ω is the angular frequency of the oscillation, $\widehat{t}$ is time and Re stands for real part. As the flow is influenced

by the oscillation of the upper plate, the velocity profile of the flow can be considered as,

$$\widehat{u}(\widehat{y},\widehat{t}) = \widehat{u}_s + Re(\widehat{u}_w e^{-i\omega\widehat{t}}), \tag{5.1}$$

where $\widehat{u}_s(\widehat{y}) = U\widehat{y}/h$ and $\widehat{u}_w(\widehat{y}) = U\phi\frac{\sin\widehat{\sigma}\widehat{y}}{\sin\widehat{\sigma}h}$ are the steady and oscillatory components of the velocity field respectively. Here $\widehat{\sigma}^2 = i\omega/\nu$ or $\widehat{\sigma} = (1+i)/\widehat{\delta}_s$ and $\widehat{\delta}_s = \sqrt{2\nu/\omega}$ is the thickness of the Stokes boundary layer resulting from the oscillation of the upper plate, where ν is the kinematic viscosity of the fluid.

During the flow some part of the fluid completely absorbed by reversible bed reaction or/and undergoes reversible phase exchange with the channel bed. In the phase where solute flows with the flowing fluid is called mobile or fluid phase and the phase in which the solute retains at the channel bed is termed as immobile phase.

It is assumed that the solute undergoes a reversible phase exchange between mobile and immobile phases. Phase exchange will take place in either forward or backward direction, which can be described by a first-order linear kinetics as

$$\frac{\partial\widehat{C}_s}{\partial t} = k_f\widehat{C} - k_b\widehat{C}_s, \tag{5.2}$$

where $\widehat{C}$ is the concentration (mass of solute per bulk volume of fluid) of the mobile phase, $\widehat{C}_s$ is the concentration (mass of solute per surface area of the channel bed) of the immobile phase. The terms k_f and k_b are the forward and backward rate constants for the sorption reaction respectively. At the equilibrium state, these two phases will have their concentrations in a fixed ratio

$$\widehat{C}_s/\widehat{C} = k_f/k_b = \widehat{\alpha}, \tag{5.3}$$

where $\widehat{\alpha}$ is the partition coefficient or retention parameter that relates the concentrations $\widehat{C}$ and $\widehat{C}_s$. From the equations (5.2) and (5.3) first-order kinetics reversible reaction at the channel bed can be expressed as

$$\frac{\partial\widehat{C}_s}{\partial t} = k(\widehat{\alpha}\widehat{C} - \widehat{C}_s),$$

where $k = k_b$ is the reversible reaction rate constant.

Associated with oscillatory Couette flow, the problem of transport of the substance can be formulated as follows:

$$\frac{\partial\widehat{C}}{\partial\widehat{t}} + \widehat{u}\frac{\partial\widehat{C}}{\partial\widehat{x}} = D\left(\frac{\partial^2\widehat{C}}{\partial\widehat{x}^2} + \frac{\partial^2\widehat{C}}{\partial\widehat{y}^2}\right), \quad 0 < \widehat{y} < h, \tag{5.4}$$

where D, the molecular diffusivity of the substance in the fluid, is assumed to be constant.

The initial and boundary conditions are respectively given as

$$\widehat{C}(\widehat{x},\widehat{y},\widehat{t})|_{\widehat{t}=0}= \frac{Q_m}{h}\delta\Big(\frac{\widehat{x}}{h}\Big) \tag{5.5}$$

$$D\frac{\partial \widehat{C}}{\partial \widehat{y}} = 0, \quad \widehat{y} = h, \tag{5.6}$$

$$D\frac{\partial \widehat{C}}{\partial \widehat{y}} - \widehat{\beta}\widehat{C} = \frac{\partial \widehat{C}_s}{\partial \widehat{t}} = k(\widehat{\alpha}\widehat{C} - \widehat{C}_s), \quad \widehat{y} = 0, \tag{5.7}$$

and

$$\widehat{C}(\widehat{x},\widehat{y},\widehat{t})|_{\widehat{x}=\pm\infty}= 0, \tag{5.8}$$

where Q_m is the released mass and $\delta(\cdot)$ the Dirac delta function.

5.3 Multi-scale Analysis

5.3.1 Scales selection

Associated with two length scales h (channel width) and l (characteristic axial length of the solute cloud), there are three distinct time scales for transport process, i.e., $T_0 = 2\pi/\omega = h^2/D = O(k^{-1})$ as the diffusion time across the width of the channel h, $T_1 = l/U$ as the advection time across the characteristic length l, and $T_2 = l^2/D$ as diffusion time across l.

Time scale for the diffusion time across the width of the channel h:

$$T_0 = 2\pi/\omega = O(h^2/D) = O(k^{-1}).$$

Their ratios are

$$T_0 : T_1 : T_2 = 1 : \frac{1}{\epsilon} : \frac{1}{\epsilon^2},$$

where $\epsilon = \frac{h}{l}$ ($\ll 1$) used as the perturbation parameter.

5.3.2 Dimensionless governing equation and velocity profile

Dimensionless parameters are introduced as

$$x = \frac{\widehat{x}}{l},\ y = \frac{\widehat{y}}{h},\ u = \frac{\widehat{u}}{U},\ t = \frac{\widehat{t}}{h^2/D},\ Pe = \frac{Uh}{D},\ C = \frac{\widehat{C}}{Q_m/h},\ \Omega = \frac{\omega h^2}{\nu},\ Sc = \frac{\nu}{D},\ C_s = \frac{\widehat{C}_s}{Q_m},$$
$$Da = \frac{kh^2}{D},\ \alpha = \frac{\widehat{\alpha}}{h},\ \beta = \frac{\widehat{\beta}l}{D}$$

where Ω is the dimensionless frequency parameter and Sc is the Schmidt number.

The non-dimensional governing equation and boundary conditions can be rewritten as

$$\frac{\partial C}{\partial t} + \epsilon Pe\, u\frac{\partial C}{\partial x} = \epsilon^2\frac{\partial^2 C}{\partial x^2} + \frac{\partial^2 C}{\partial y^2}, \qquad 0 < y < 1, \tag{5.9}$$

$$\frac{\partial C}{\partial y} = 0, \quad y = 1, \tag{5.10}$$

$$\frac{\partial C}{\partial y} - \epsilon\beta C = \frac{\partial C_s}{\partial t} = Da(\alpha C - C_s), \quad y = 0. \tag{5.11}$$

The dimensionless velocity profile is

$$u(y,t) = u_s + Re(u_w e^{-i\Omega Sc\, t}), \tag{5.12}$$

where $u_s(y) = y$ and $u_w(y) = \phi\frac{\sin\sigma y}{\sin\sigma}$ are the steady and oscillatory components of the velocity field respectively. In the expression of u_w, $\sigma = \sqrt{i\Omega}$ or $\sigma = (1+i)/\delta_s$, where $\delta_s = \widehat{\delta}_s/h = \sqrt{2/\Omega}$ is the dimensionless Stokes boundary layer thickness.

5.3.3 Homogenization

For the asymptotic analysis, the homogenization technique of Mei et al. [32] is employed. Based on the time scales mentioned before, fast, medium and slow time variables are introduced accordingly

$$t_0 = t,\ t_1 = \epsilon t,\ t_2 = \epsilon^2 t.$$

The original time derivative becomes, according to the chain rule

$$\frac{\partial}{\partial t} = \frac{\partial}{\partial t_0} + \epsilon\frac{\partial}{\partial t_1} + \epsilon^2\frac{\partial}{\partial t_2}. \tag{5.13}$$

The concentration C is expanded into multiple scales as:

$$C = C^{(0)} + \epsilon C^{(1)} + \epsilon^2 C^{(2)} + O(\epsilon^3), \tag{5.14}$$

where C_n,$(n = 1, 2, 3, \ldots)$ are the developed terms, which are purely oscillatory functions of the short time variable t_0. Substituting (5.13) and (5.14) into (5.9) - (5.11) we have,

$$\left(\frac{\partial C^{(0)}}{\partial t_0} - \frac{\partial^2 C^{(0)}}{\partial y^2}\right) + \epsilon\left(\frac{\partial C^{(0)}}{\partial t_1} + \frac{\partial C^{(1)}}{\partial t_0} + Pe\, u\frac{\partial C^{(0)}}{\partial x} - \frac{\partial^2 C^{(1)}}{\partial y^2}\right) + \epsilon^2\left(\frac{\partial C^{(0)}}{\partial t_2} + \frac{\partial C^{(1)}}{\partial t_1} + \frac{\partial C^{(2)}}{\partial t_0} + Pe\, u\frac{\partial C^{(1)}}{\partial x} - \frac{\partial^2 C^{(0)}}{\partial x^2} - \frac{\partial^2 C^{(2)}}{\partial y^2}\right) + \cdots = 0, \quad 0 < y < 1, \tag{5.15}$$

$$\frac{\partial C^{(0)}}{\partial y} + \epsilon \frac{\partial C^{(1)}}{\partial y} + \epsilon^2 \frac{\partial C^{(2)}}{\partial y} + \cdots = 0, \quad y = 1, \tag{5.16}$$

$$\frac{\partial C^{(0)}}{\partial y} + \epsilon \left(\frac{\partial C^{(1)}}{\partial y} - \beta C^{(0)} \right) + \epsilon^2 \left(\frac{\partial C^{(2)}}{\partial y} - \beta C^{(1)} \right) + \cdots = \frac{\partial C_s^{(0)}}{\partial t_0} + \epsilon \left(\frac{\partial C_s^{(0)}}{\partial t_1} + \frac{\partial C_s^{(1)}}{\partial t_0} \right)$$
$$+\epsilon^2 \left(\frac{\partial C_s^{(0)}}{\partial t_2} + \frac{\partial C_s^{(1)}}{\partial t_1} + \frac{\partial C_s^{(2)}}{\partial t_0} \right) + \cdots = Da(\alpha C^{(0)} - C_s^{(0)}) + \epsilon \Big(Da(\alpha C^{(1)} - C_s^{(1)}) \Big) +$$
$$\epsilon^2 \Big(Da(\alpha C^{(2)} - C_s^{(2)}) \Big) + \cdots, \quad y = 0. \tag{5.17}$$

For leading order ($O(1)$), Eqs. (5.15) and (5.17) give:

$$\frac{\partial C^{(0)}}{\partial t_0} = \frac{\partial^2 C^{(0)}}{\partial y^2}, \qquad 0 < y < 1, \tag{5.18}$$

$$\left. \frac{\partial C^{(0)}}{\partial y} \right|_{y=0} = \left. \frac{\partial C^{(0)}}{\partial y} \right|_{y=1} = 0. \tag{5.19}$$

The general solution of Eq. (5.18) becomes

$$C^{(0)} = C_0^{(0)}(x, t_1, t_2) + \sum_{n=1}^{\infty} Re \left[C_n^{(0)}(x, t_1, t_2) e^{in\pi y} \right] e^{-n^2 \pi^2 t_0}. \tag{5.20}$$

Clearly, for long time evolution, since the series terms die out exponentially quickly because of the exponential decay, $C^{(0)}$ becomes independent of t_0; thus, one can omit the series part and take the solution as,

$$C^{(0)} = C^{(0)}(x, t_1, t_2). \tag{5.21}$$

For first-order ($O(\epsilon)$), Eqs. (5.15) and (5.17) give:

$$\frac{\partial C^{(0)}}{\partial t_1} + \frac{\partial C^{(1)}}{\partial t_0} + Pe\, u \frac{\partial C^{(0)}}{\partial x} = \frac{\partial^2 C^{(1)}}{\partial y^2}, \quad 0 < y < 1, \tag{5.22}$$

$$\frac{\partial C^{(1)}}{\partial y} = 0, \quad y = 1, \tag{5.23}$$

$$\frac{\partial C^{(1)}}{\partial y} - \beta C^{(0)} = \frac{\partial C_s^{(0)}}{\partial t_1} + \frac{\partial C_s^{(1)}}{\partial t_0} = Da(\alpha C^{(1)} - C_s^{(1)}), \quad y = 0. \tag{5.24}$$

Taking time average of these equations w.r.t the fast time variable t_0, we get

$$\frac{\partial C^{(0)}}{\partial t_1} + Pe\, u_s \frac{\partial C^{(0)}}{\partial x} = \frac{\partial^2 \overline{C^{(1)}}}{\partial y^2}, \qquad 0 < y < 1, \tag{5.25}$$

$$\frac{\partial \overline{C^{(1)}}}{\partial y} = 0, \quad y = 1 \tag{5.26}$$

$$\frac{\partial \overline{C^{(1)}}}{\partial y} - \beta C^{(0)} = \alpha \frac{\partial C^{(0)}}{\partial t_1} = Da(\alpha \overline{C^{(1)}} - \overline{C_s^{(1)}}), \quad y = 0, \tag{5.27}$$

where overbar denotes time average w.r.t t_0 as

$$\overline{f} = \frac{\Omega Sc}{2\pi} \int_t^{t+\frac{2\pi}{\Omega Sc}} f dt_0. \tag{5.28}$$

Further, taking a section average of Eq. (5.25) w.r.t the spatial variable y subject to the conditions (5.26) and (5.27), we get

$$\frac{\partial C^{(0)}}{\partial t_1} + Pe \frac{\langle u_s \rangle}{R} \frac{\partial C^{(0)}}{\partial x} + \frac{\beta}{R} C^{(0)} = 0, \tag{5.29}$$

where $R = 1 + \alpha$ is the retardation factor and angle brackets denote section average as

$$\langle v \rangle = \int_0^1 v dy. \tag{5.30}$$

Subtracting (5.22) from (5.29), we get

$$\frac{\partial C^{(1)}}{\partial t_0} + Pe \left[\left(u_s - \frac{\langle u_s \rangle}{R} \right) + Re(u_w e^{-i\Omega Sc t_0}) \right] \frac{\partial C^{(0)}}{\partial x} = \frac{\partial^2 C^{(1)}}{\partial y^2}, \quad 0 < y < 1. \tag{5.31}$$

These equations suggest the following substitutions

$$C^{(1)} = Pe[F(y) + Re(G(y)e^{-i\Omega Sc t_0})] \frac{\partial C^{(0)}}{\partial x} + \beta M(y) C^{(0)}, \tag{5.32}$$

$$C_s^{(1)} = [F_s + Re(G_s e^{-i\omega t_0})] \frac{\partial C^{(0)}}{\partial x} + \beta M_s C^{(0)}, \tag{5.33}$$

where the coefficients $F(y)$, $G(y)$, F_s and G_s are to be found as follows.

On matching with the steady terms associated with $\frac{\partial C^{(0)}}{\partial x}$, the function $F(y)$ is governed by

$$\frac{d^2 F}{dy^2} = u_s - \frac{\langle u_s \rangle}{R} \qquad 0 < y < 1, \tag{5.34}$$

with the following conditions

$$\frac{dF}{dy} = 0, \quad y = 1, \tag{5.35}$$

$$\frac{dF}{dy} = -\frac{\alpha \langle u_s \rangle}{R} = Da(\alpha F - F_s), \quad y = 0, \tag{5.36}$$

and

$$\langle F \rangle = 0. \tag{5.37}$$

Similarly, equating the oscillatory terms associated with $\frac{\partial C^{(0)}}{\partial x}$, one can get

$$\frac{d^2G}{dy^2} + \lambda^2 G = u_w \qquad 0 < y < 1, \tag{5.38}$$

$$\frac{dG}{dy} = 0, \quad y = 1, \tag{5.39}$$

$$\frac{dG}{dy} = -\lambda^2 G_s = Da(\alpha G - G_s), \quad y = 0, \tag{5.40}$$

where

$$\lambda^2 = i\Omega Sc, \qquad or \quad \lambda = Sc^{1/2}\sigma. \tag{5.41}$$

On matching with the steady terms associated with $C^{(0)}$, the function $M(y)$ is governed by

$$\frac{d^2M}{dy^2} = -\frac{1}{R} \quad 0 < y < 1, \tag{5.42}$$

with the following conditions

$$\frac{dM}{dy} = 0, \quad y = 1, \tag{5.43}$$

$$\frac{dM}{dy} = -\frac{1}{R} = Da(\alpha M - M_s) + 1, \quad y = 0. \tag{5.44}$$

For second-order ($O(\epsilon^2)$), Eqs. (5.15)–(5.17) give:

$$\frac{\partial C^{(0)}}{\partial t_2} + \frac{\partial C^{(1)}}{\partial t_1} + \frac{\partial C^{(2)}}{\partial t_0} + Pe\, u\frac{\partial C^{(1)}}{\partial x} = \frac{\partial^2 C^{(0)}}{\partial x^2} + \frac{\partial^2 C^{(2)}}{\partial y^2} \qquad 0 < y < 1, \tag{5.45}$$

$$\frac{\partial C^{(2)}}{\partial y} = 0, \quad y = 1, \tag{5.46}$$

$$\frac{\partial C^{(2)}}{\partial y} - \beta C^{(1)} = \frac{\partial C_s^{(0)}}{\partial t_2} + \frac{\partial C_s^{(1)}}{\partial t_1} + \frac{\partial C_s^{(2)}}{\partial t_0} = Da(\alpha C^{(2)} - C_s^{(2)}), \quad y = 0. \tag{5.47}$$

Averaging Eq. (5.45) w.r.t time variable t_0 followed by space variable y subject to the boundary conditions (5.46), the equation becomes

$$\frac{\partial C^{(0)}}{\partial t_2} + \frac{1}{R}\frac{\partial \langle \overline{C}^{(1)} \rangle}{\partial t_1} + Pe\frac{1}{R}\left\langle \overline{u\frac{\partial C^{(1)}}{\partial x}} \right\rangle + \frac{1}{R}\frac{\partial \overline{C}_s^{(1)}}{\partial t_1} = \frac{1}{R}\frac{\partial^2 C^{(0)}}{\partial x^2} - \frac{\beta}{R}\overline{C}_1(0). \tag{5.48}$$

Subtracting Eq. (5.48) from Eq. (5.45), one can get

$$\frac{\partial C^{(2)}}{\partial t_0}+\frac{\partial C^{(1)}}{\partial t_1}+Pe\left(u\frac{\partial C^{(1)}}{\partial x}-\frac{1}{R}\left\langle\overline{u\frac{\partial C^{(1)}}{\partial x}}\right\rangle\right)-\frac{1}{R}\frac{\partial\langle\overline{C^{(1)}}\rangle}{\partial t_1}-\frac{1}{R}\frac{\partial\overline{C}_s^{(1)}}{\partial t_1}-\frac{\beta}{R}\overline{C}_1(0)$$
$$=\left(1-\frac{1}{R}\right)\frac{\partial^2 C^{(0)}}{\partial x^2}+\frac{\partial^2 C^{(2)}}{\partial y^2},\quad 0<y<1. \tag{5.49}$$

Using (5.12), (5.32) and (5.37), the following terms of (5.49) can be found as,

$$\frac{\partial\langle\overline{C}^{(1)}\rangle}{\partial t_1}=0, \tag{5.50}$$

$$\frac{\partial C^{(1)}}{\partial t_1}=-Pe^2\langle u_s\rangle\Big[F(y)+Re(G(y)e^{-i\Omega Sct_0})\Big]\frac{\partial^2 C^{(0)}}{\partial x^2}, \tag{5.51}$$

$$u\frac{\partial C^{(1)}}{\partial x}=Pe\Big[u_sF+\frac{1}{2}Re(u_wG^*)+Re\{(u_wF+u_sG)e^{-i\Omega Sct_0}\}+\frac{1}{2}Re(u_wGe^{-2i\Omega Sct_0})\Big]$$
$$\times\frac{\partial^2 C^{(0)}}{\partial x^2}+\beta(u_sM+Re(u_wMe^{-i\Omega Sct_0})\frac{\partial C^{(0)}}{\partial x}, \tag{5.52}$$

$$\left\langle\overline{u\frac{\partial C^{(1)}}{\partial x}}\right\rangle=Pe\left[\langle u_sF\rangle+\frac{1}{2}Re\langle u_wG^*\rangle\right]\frac{\partial^2 C^{(0)}}{\partial x^2}+\beta\langle u_sM\rangle\frac{\partial C^{(0)}}{\partial x}, \tag{5.53}$$

$$\frac{\partial\overline{C}_{S1}}{\partial t_1}=-Pe^2F_s\frac{\langle u_s\rangle}{R}\frac{\partial^2 C^{(0)}}{\partial x^2}-Pe\frac{\beta}{R}(F_s+\langle u_s\rangle M_s)\frac{\partial C^{(0)}}{\partial x}-\frac{\beta^2}{R}M_sC^{(0)}, \tag{5.54}$$

where * denotes the complex conjugate.

Substituting these terms in (5.48), one gets

$$\frac{\partial C^{(0)}}{\partial t_2}+Pe\frac{\beta}{R}\left(F(0)+\langle u_sM\rangle-\frac{\langle u_s\rangle M_s}{R}-\frac{1}{R}F_s\right)\frac{\partial C^{(0)}}{\partial x}=\Big\{\frac{1}{R}-Pe^2\Big(\frac{1}{R}\langle u_sF\rangle+\frac{1}{2R}$$
$$\times Re\langle u_wG^*\rangle-F_s\frac{\langle u_s\rangle}{R^2}\Big)\Big\}\frac{\partial^2 C^{(0)}}{\partial x^2}-\frac{\beta^2}{R}\left(M(0)-\frac{M_s}{R}\right)C^{(0)}. \tag{5.55}$$

Multiplying Eq. (5.29) by ϵ, Eq. (5.55) by ϵ^2 and adding them, we obtain

$$\frac{\partial C^{(0)}}{\partial t_0}+\epsilon\frac{\partial C^{(0)}}{\partial t_1}+\epsilon^2\frac{\partial C^{(0)}}{\partial t_2}+\epsilon Pe\left\{\frac{\langle u_s\rangle}{R}+\frac{\epsilon\beta}{R}\left(F(0)+\langle u_sM\rangle-\frac{\langle u_s\rangle M_s}{R}-\frac{1}{R}F_s\right)\right\}\frac{\partial C^{(0)}}{\partial x}$$
$$=\epsilon^2\left\{\frac{1}{R}-Pe^2\left(\frac{1}{R}\langle u_sF\rangle+\frac{1}{2R}Re\langle u_wG^*\rangle-F_s\frac{\langle u_s\rangle}{R^2}\right)\right\}\frac{\partial^2C^{(0)}}{\partial x^2}$$
$$-\epsilon\beta\left(\frac{1}{R}+\epsilon\beta\frac{M_0}{R}-\epsilon\beta\frac{M_s}{R^2}\right)C^{(0)}. \tag{5.56}$$

Using dimensionless variable $\beta_m(\geq 0)=\frac{\widehat{\beta}h}{D}$, Eq. (5.56) can be written, in original time variable, as

$$\frac{\partial C^{(0)}}{\partial t}+\epsilon Pe\left\{\frac{\langle u_s\rangle}{R}+\frac{\beta_m}{R}\left(F(0)+\langle u_sM\rangle-\frac{\langle u_s\rangle M_s}{R}-\frac{1}{R}F_s\right)\right\}\frac{\partial C^{(0)}}{\partial x}=\epsilon^2\left\{\frac{1}{R}-Pe^2\left(\frac{1}{R}\right.\right.$$
$$\left.\left.\times\langle u_sF\rangle+\frac{1}{2R}Re\langle u_wG^*\rangle-F_s\frac{\langle u_s\rangle}{R^2}\right)\right\}\frac{\partial^2C^{(0)}}{\partial x^2}-\beta_m\left(\frac{1}{R}+\beta_m\frac{M(0)}{R}-\beta_m\frac{M_s}{R^2}\right)C^{(0)}. \tag{5.57}$$

Let $\tau=t$ and $\eta=\frac{\widehat{x}}{h}-Pe\,\zeta\,t$, equation becomes

$$\frac{\partial C^{(0)}}{\partial\tau}+Pe\,\zeta\frac{\partial C^{(0)}}{\partial\eta}=D_T\frac{\partial^2C^{(0)}}{\partial\eta^2}-\chi C^{(0)}, \tag{5.58}$$

where

$$\zeta=\frac{\langle u_s\rangle}{R}+\frac{\beta_m}{R}\left(F(0)+\langle u_sM\rangle-\frac{\langle u_s\rangle M_s}{R}-\frac{1}{R}F_s\right), \tag{5.59}$$

$$\chi=\beta_m\left(\frac{1}{R}+\beta_m\frac{M_0}{R}-\beta_m\frac{M_s}{R^2}\right), \tag{5.60}$$

and the Taylor dispersivity

$$D_T=\frac{1}{R}+Pe^2(D_{Ts}+D_{Tw}). \tag{5.61}$$

The term $1/R$ represents the contribution of the effective longitudinal diffusion to Taylor dispersion. The terms D_{Ts} and D_{Tw} are, respectively, the dispersion coefficient components due to the steady and oscillatory flows and can be written as

$$D_{Ts}=-\frac{1}{R}\langle u_sF\rangle+F_s\frac{\langle u_s\rangle}{R^2}, \tag{5.62}$$

$$D_{Tw}=-\frac{1}{2R}Re\langle u_wG^*\rangle. \tag{5.63}$$

Here, the new coordinate system $\{\eta,\tau\}$ allows to view the mass transport from an observer moving at a speed of $Pe\,\zeta$.

The solution of Eq. (5.58) with the initial and boundary conditions given in equations (5.5) and (5.8) is

$$C^{(0)} = \frac{1}{\sqrt{4\pi D_T \tau}} \exp\left(- \frac{\eta^2}{4D_T\tau} - \chi\tau \right), \tag{5.64}$$

which is a longitudinal Gaussian distribution.

Substitution of terms (5.50)–(5.54) in (5.49) gives

$$\begin{aligned}\frac{\partial C^{(2)}}{\partial t_0} + Pe^2\Big[\{(u_s - \frac{\langle u_s\rangle}{R})F - \frac{1}{R}\langle u_s F\rangle\} + \frac{1}{2}Re(u_w G^* - \frac{1}{R}\langle u_w G^*\rangle) + \frac{\langle u_s\rangle}{R^2}F_s + Re[\{(u_s \\ -\frac{\langle u_s\rangle}{R})G + u_w F\}e^{-i\Omega Sct_0}] + \frac{1}{2}Re(u_w G e^{-2i\Omega Sct_0})\Big]\frac{\partial^2 C^{(0)}}{\partial x^2} + \beta Pe\Big[(u_s - \frac{\langle u_s\rangle}{R})M \\ -\frac{1}{R}\langle u_s M\rangle - \frac{F}{R} - \frac{F_0}{R} + \frac{F_s}{R^2} + \frac{\langle u_s\rangle}{R^2}M_s + Re[(u_w M - \frac{1}{R}G)e^{-i\Omega Sct_0}]\Big] \\ \times\frac{\partial C^{(0)}}{\partial x} - \beta^2\left(\frac{M}{R} + \frac{M(0)}{R} - \frac{M_s}{R^2}\right)C^{(0)} = \frac{\partial^2 C^{(2)}}{\partial y^2}.\end{aligned} \tag{5.65}$$

This equation suggests the following substitution,

$$\begin{aligned}C^{(2)} = Pe^2[P(y) + Re(Q(y) + T(y)e^{-i\Omega Sct_0} + S(y)e^{-2i\Omega Sct_0})]\frac{\partial^2 C^{(0)}}{\partial x^2} + \beta Pe[X(y) + Re(\\ Y(y)e^{-i\Omega Sct_0})]\frac{\partial C^{(0)}}{\partial x} + \beta^2 Z C^{(0)}.\end{aligned} \tag{5.66}$$

On matching with the steady terms associated with $\frac{\partial^2 C^{(0)}}{\partial x^2}$, the function $P(y)$ is governed by

$$\frac{d^2P}{dy^2} = (u_s - \frac{\langle u_s\rangle}{R})F + D_{Ts}, \quad 0 < y < 1, \tag{5.67}$$

with the following conditions

$$\frac{dP}{dy} = 0, \quad y = 1, \tag{5.68}$$

$$\frac{dP}{dy} = -\frac{\alpha}{R}\langle u_s F\rangle - \frac{\langle u_s\rangle}{R^2}F_s = Da(\alpha P - P_s), \quad y = 0, \tag{5.69}$$

and

$$\langle P\rangle = 0. \tag{5.70}$$

Similarly, matching with oscillatory non-exponential terms, the governing equation of the function $Q(y)$ becomes,

$$\frac{d^2Q}{dy^2} = \frac{1}{2}(u_w G^* - \frac{1}{R}\langle u_w G^*\rangle), \quad 0 < y < 1, \tag{5.71}$$

with the following conditions

$$\frac{dQ}{dy} = 0, \quad y = 1, \tag{5.72}$$

$$\frac{dQ}{dy} = -\frac{\alpha}{2R}\langle u_w G^* \rangle = Da(\alpha Q - Q_s), \quad y = 0, \tag{5.73}$$

and

$$\langle Q \rangle = 0. \tag{5.74}$$

Similarly, the function $T(Y)$ satisfies the boundary value problem,

$$\frac{d^2T}{dy^2} + \lambda^2 T = (u_s - \frac{\langle u_s \rangle}{R})G + u_w F, \quad 0 < y < 1, \tag{5.75}$$

$$\frac{dT}{dy} = 0, \quad y = 1, \tag{5.76}$$

$$\frac{dT}{dy} = -\frac{\langle u_s \rangle}{R}G_s - \lambda^2 T_s = Da(\alpha T - T_s), \quad y = 0. \tag{5.77}$$

While $S(y)$ satisfies

$$\frac{d^2S}{dy^2} + 2\lambda^2 S = \frac{1}{2}u_w G, \quad 0 < y < 1, \tag{5.78}$$

$$\frac{dS}{dy} = 0, \quad y = 1, \tag{5.79}$$

$$\frac{dS}{dy} = -2\lambda^2 S_s = Da(\alpha S - S_s), \quad y = 0. \tag{5.80}$$

On matching with the steady terms associated with $\frac{\partial C^{(0)}}{\partial x}$, the function $X(y)$ is governed by

$$\frac{d^2X}{dy^2} = (u_s - \frac{\langle u_s \rangle}{R})M - \frac{1}{R}\langle u_s M \rangle - \frac{F}{R} - \frac{F(0)}{R} + \frac{F_s}{R^2} + \frac{\langle u_s \rangle M_s}{R^2}, \quad 0 < y < 1, \tag{5.81}$$

with the following conditions

$$\frac{dX}{dy} = 0, \quad y = 1, \tag{5.82}$$

$$\frac{dX}{dy} = -\frac{\alpha}{R}\langle u_s M \rangle + \frac{F(0)}{R} - \frac{F_s}{R^2} - \frac{\langle u_s \rangle}{R^2}M_s = Da(\alpha X - X_s) + F(0), \quad y = 0, \tag{5.83}$$

and

$$\langle X \rangle = 0. \tag{5.84}$$

On matching with the oscillatory terms associated with $\frac{\partial C^{(0)}}{\partial x}$, the function $Y(y)$ is

governed by

$$\frac{d^2Y}{dy^2} + \lambda^2 Y = -\frac{G}{R} + u_w M, \quad 0 < y < 1, \tag{5.85}$$

$$\frac{dY}{dy} = 0, \quad y = 1, \tag{5.86}$$

$$\frac{dY}{dy} = -\lambda^2 Y_s - \frac{G_s}{R} + G(0) = Da(\alpha Y - Y_s) + G(0), \quad y = 0. \tag{5.87}$$

On matching with the terms associated with $C^{(0)}$, the function $Z(y)$ is governed by

$$\frac{d^2Z}{dy^2} = -\frac{M}{R} - \frac{M(0)}{R} + \frac{M_s}{R^2}, \quad 0 < y < 1, \tag{5.88}$$

$$\frac{dZ}{dy} = 0, \quad y = 1, \tag{5.89}$$

$$\frac{dZ}{dy} = \frac{M(0)}{R} - \frac{M_s}{R^2} = Da(\alpha Z - Z_s) + M(0), \quad y = 0. \tag{5.90}$$

On solving the system of equations (5.34)–(5.44), one gets,

$$F(y) = \frac{1}{6}y^3 - \frac{1}{4R}y^2 - \frac{\alpha}{2R}y + \frac{\alpha}{4R} + \frac{1}{12R} - \frac{1}{24}, \tag{5.91}$$

and

$$G(y) = -\frac{i\phi\delta_s^2}{2(Sc-1)}\left[d_1 \sin(\lambda y) + d_2 \cos(\lambda y) + \frac{\sin(\sigma y)}{\sin\sigma}\right], \tag{5.92}$$

where

$$d_1 = -\left[\frac{\sigma(Da-\lambda^2)}{\lambda\alpha Da}\frac{\sin\lambda}{\sin\sigma} + \sigma\cot\sigma\right]\left[\lambda\cos\lambda + (Da-\lambda^2)\frac{\sin\lambda}{\alpha Da}\right]^{-1}, \tag{5.93}$$

$$d_2 = -\frac{Da-\lambda^2}{\lambda^2\alpha Da}\left[\lambda d_1 + \frac{\sigma}{\sin\sigma}\right], \tag{5.94}$$

and

$$M(y) = -\frac{1}{2R}y^2 + \frac{1}{R}y - \frac{1}{3R}, \tag{5.95}$$

$$F_s = \alpha\left(\frac{\alpha}{4R} + \frac{1}{12R} - \frac{1}{24} + \frac{1}{2DaR}\right), \tag{5.96}$$

$$G_s = -\frac{\phi}{\lambda^2(\lambda^2-\sigma^2)}\left(\lambda d_1 + \frac{\sigma}{\sin\sigma}\right), \tag{5.97}$$

$$M_s = \frac{\alpha}{R}\left(-\frac{1}{3} + \frac{1}{Da}\right). \tag{5.98}$$

Using (5.91)–(5.95), one can find the following

$$\langle u_s F\rangle = -\frac{\alpha}{24R} - \frac{1}{48R} + \frac{1}{80}, \tag{5.99}$$

$$\langle u_s M\rangle = \frac{1}{24R}, \tag{5.100}$$

$$\langle u_w G^*\rangle = \frac{i\phi^2\delta_s^2}{2(Sc-1)}\left\{\frac{{d_1}^*}{\sin\sigma}\left(\frac{\sin(\sigma-\lambda^*)}{2(\sigma-\lambda^*)}-\frac{\sin(\sigma+\lambda^*)}{2(\sigma+\lambda^*)}\right)+\frac{{d_2}^*}{\sin\sigma}\left(\frac{1-\cos(\sigma-\lambda^*)}{2(\sigma-\lambda^*)}+\frac{1-\cos(\sigma+\lambda^*)}{2(\sigma+\lambda^*)}\right)+\frac{1}{\sin\sigma^*\sin\sigma}\left(\frac{\sin(\sigma-\sigma^*)}{2(\sigma-\sigma^*)}-\frac{\sin(\sigma+\sigma^*)}{2(\sigma+\sigma^*)}\right)\right\}, \tag{5.101}$$

and

$$\langle G(y)\rangle = -\frac{i\phi\delta_s^2}{2(Sc-1)}\left[\frac{d_1}{\lambda}(1-\cos\lambda)+\frac{d_2}{\lambda}\sin\lambda+\frac{1-\cos\sigma}{\sigma\sin\sigma}\right]. \tag{5.102}$$

On solving the system of equations (5.67)–(5.90), one gets,

$$P(y) = \frac{1}{180}y^6-\frac{1}{60R}y^5+\left(\frac{1}{96R^2}-\frac{\alpha}{24R}\right)y^4+\left(\frac{\alpha}{24R^2}+\frac{\alpha}{24R}-\frac{1}{144}+\frac{1}{72R}\right)y^3+\left(-\frac{5\alpha}{96R^2}+\frac{\alpha^2}{16R^3}-\frac{1}{96R^2}+\frac{\alpha}{48R^3}+\frac{1}{240R}+\frac{\alpha}{8R^3Da}\right)y^2+\left(\frac{1}{30R}-\frac{\alpha^2}{8R^3}-\frac{1}{80}-\frac{\alpha}{4R^3Da}-\frac{\alpha}{24R^3}-\frac{\alpha}{48R^2}+\frac{\alpha}{24R}-\frac{1}{48R^2}\right)y+\frac{29}{4032}+\frac{\alpha}{12R^3Da}-\frac{3}{160R}-\frac{11\alpha}{480R}+\frac{\alpha}{72R^3}+\frac{5\alpha}{288R^2}+\frac{\alpha^2}{24R^3}+\frac{17}{1440R^2}, \tag{5.103}$$

$$Q(y) = -\frac{1}{2}\left[\frac{\phi^2}{(\lambda^2-\sigma^2)\sin\sigma}\left\{\frac{d_1^*}{2}\left(\frac{\cos(\sigma+\lambda^*)y}{(\sigma+\lambda^*)^2}-\frac{\cos(\sigma-\lambda^*)y}{(\sigma-\lambda^*)^2}\right)+\frac{d_2^*}{2}\left(\frac{y}{\sigma+\lambda^*}+\frac{y}{\sigma-\lambda^*}-\frac{\sin(\sigma+\lambda^*)y}{(\sigma+\lambda^*)^2}-\frac{\sin(\sigma-\lambda^*)y}{(\sigma-\lambda^*)^2}\right)\right\}\right]-\frac{1}{2R}\left(\frac{1}{2}y^2+\alpha y\right)\langle u_w G^*\rangle+e_1, \tag{5.104}$$

$$T(y) = e_2\cos\lambda y+e_3\sin\lambda y+A_1(y)+A_2(y), \tag{5.105}$$

$$S(y) = e_4\cos(\sqrt{2}\lambda)y+e_5\sin(\sqrt{2}\lambda)y+A_3(y), \tag{5.106}$$

$$X(y) = -\frac{1}{30R}y^5+\left(\frac{1}{12R}+\frac{1}{24R^2}\right)y^4+\left(\frac{\alpha}{12R^2}-\frac{1}{18R}-\frac{1}{12R^2}\right)y^3+\left(-\frac{1}{4R^3Da}+\frac{\alpha^2}{8R^3}+\frac{1}{24R}-\frac{\alpha}{24R^3}-\frac{1}{48R^2}+\frac{1}{4R^2Da}-\frac{13\alpha}{48R^2}+\frac{\alpha}{4R^3Da}\right)y^2+\left(-\frac{\alpha}{2R^3Da}-\frac{1}{12R}+\frac{1}{8R^2}-\frac{1}{2R^2Da}+\frac{1}{2R^3Da}-\frac{\alpha^2}{4R^3}+\frac{7\alpha}{24R^2}+\frac{\alpha}{12R^3}\right)y-\frac{31}{720R^2}+\frac{1}{6R^2Da}-\frac{1}{6R^3Da}+\frac{11}{360R}-\frac{\alpha}{36R^3}-\frac{11\alpha}{144R^2}+\frac{\alpha^2}{12R^3}+\frac{\alpha}{6R^3Da}, \tag{5.107}$$

$$Y(y) = e_6\cos\lambda y+e_7\sin\lambda y+A_4(y)+A_5(y), \tag{5.108}$$

$$Z(y) = \frac{1}{24R^2}y^4 - \frac{1}{6R^2}y^3 + \left(\frac{1}{2R^2Da} + \frac{1}{3R^2} - \frac{\alpha}{6R^3} - \frac{1}{2R^3Da}\right)y^2 + \left(-\frac{1}{R^2Da} - \frac{1}{3R^2} + \frac{\alpha}{3R^3} + \frac{1}{R^3Da}\right)y + \frac{1}{3R^2Da} + \frac{4}{45R^2} - \frac{\alpha}{9R^3} - \frac{1}{3R^3Da}, \tag{5.109}$$

where the functions $A_1(y)$, $A_2(y)$, $A_3(y)$, $A_4(y)$ and $A_5(y)$ are

$$A_1(y) = \frac{\phi}{\sin\sigma}\left[\left\{-\frac{\sigma}{(\lambda^2-\sigma^2)^2}y^2 + \frac{\sigma}{R(\lambda^2-\sigma^2)^2}y + \frac{8\sigma^3}{(\lambda^2-\sigma^2)^4} + \frac{4\sigma}{(\lambda^2-\sigma^2)^3} + \frac{\alpha\sigma}{(\lambda^2-\sigma^2)^2} \times\frac{1}{R}\right\}\cos\sigma y + \left\{\frac{1}{6(\lambda^2-\sigma^2)}y^3 - \frac{1}{4R(\lambda^2-\sigma^2)}y^2 - \left(\frac{4\sigma^2}{(\lambda^2-\sigma^2)^3} + \frac{1}{(\lambda^2-\sigma^2)^2} + \frac{\alpha}{2R(\lambda^2-\sigma^2)}\right)y + \frac{2\sigma^2}{R(\lambda^2-\sigma^2)^3} + \frac{1}{2R(\lambda^2-\sigma^2)^2} + \left(\frac{\alpha}{4R} + \frac{1}{12R} - \frac{1}{24}\right) \times\frac{1}{\lambda^2-\sigma^2}\right\}\sin\sigma y\right], \tag{5.110}$$

$$A_2(y) = \frac{\phi}{\lambda^2-\sigma^2}\left[d_1\left\{\left(-\frac{y^2}{4\lambda} + \frac{y}{4\lambda R}\right)\cos\lambda y + \frac{y}{4\lambda^2}\sin\lambda y\right\} + d_2\left\{\frac{y}{4\lambda^2}\cos\lambda y + \left(\frac{y^2}{4\lambda} - \frac{y}{4\lambda R}\right)\sin\lambda y\right\} + \frac{1}{\sin\sigma}\left\{-\frac{2\sigma}{(\lambda^2-\sigma^2)^2}\cos\sigma y + \left(\frac{y}{\lambda^2-\sigma^2} - \frac{1}{2R(\lambda^2-\sigma^2)}\right)\sin\sigma y\right\}\right], \tag{5.111}$$

$$A_3(y) = \frac{\phi^2}{2(\lambda^2-\sigma^2)\sin\sigma}\left[\frac{d_1}{2}\left\{\frac{\cos(\sigma-\lambda)y}{2\lambda^2-(\sigma-\lambda)^2} - \frac{\cos(\sigma+\lambda)y}{2\lambda^2-(\sigma+\lambda)^2}\right\} + \frac{d_2}{2}\left\{\frac{\sin(\sigma-\lambda)y}{2\lambda^2-(\sigma-\lambda)^2} + \frac{\sin(\sigma+\lambda)y}{2\lambda^2-(\sigma+\lambda)^2}\right\} + \frac{1}{4\sin\sigma}\left\{\frac{1}{\lambda^2} - \frac{\cos(2\sigma)y}{\lambda^2-2\sigma^2}\right\}\right], \tag{5.112}$$

$$A_4(y) = -\frac{\phi}{R(\lambda^2-\sigma^2)}\left[d_1\left(-\frac{y}{2\lambda}\cos\lambda y\right) + d_2\left(\frac{y}{2\lambda}\sin\lambda y\right) + \frac{1}{\lambda^2-\sigma^2}\frac{\sin\sigma y}{\sin\sigma}\right], \tag{5.113}$$

$$A_5(y) = \frac{\phi}{R\sin\sigma}\left[\left\{\frac{2\sigma}{(\lambda^2-\sigma^2)^2}(y-1)\right\}\cos\sigma y + \left\{-\frac{1}{2(\lambda^2-\sigma^2)}y^2 + \frac{1}{\lambda^2-\sigma^2}y + 4\sigma^2 \times\frac{1}{(\lambda^2-\sigma^2)^3} + \frac{1}{(\lambda^2-\sigma^2)^2} - \frac{1}{3(\lambda^2-\sigma^2)}\right\}\sin\sigma y\right], \tag{5.114}$$

and the constants e_1, e_2, e_3, e_4, e_5, e_6 and e_7 are

$$e_1 = \frac{1}{2}\Bigg[\frac{\phi^2}{(\lambda^2-\sigma^2)\sin\sigma}\Bigg\{\frac{d_1^*}{2}\left(\frac{\sin(\sigma+\lambda^*)}{(\sigma+\lambda^*)^3}-\frac{\sin(\sigma-\lambda^*)}{(\sigma-\lambda^*)^3}\right)+\frac{d_2^*}{2}\left(\frac{1}{2(\sigma+\lambda^*)}+\frac{1}{2(\sigma-\lambda^*)}\right.$$
$$\left.-\frac{1-\cos(\sigma+\lambda^*)}{(\sigma+\lambda^*)^3}-\frac{1-\cos(\sigma-\lambda^*)}{(\sigma-\lambda^*)^3}\right)\Bigg\}\Bigg]+\frac{1}{2R}\left(\frac{1}{6}+\frac{\alpha}{2}\right)\langle u_w G^*\rangle, \tag{5.115}$$

$$e_2 = \left(\lambda\sin\lambda+\frac{Da}{Da-\lambda^2}\alpha\lambda^2\cos\lambda\right)^{-1}\Bigg[\frac{Da}{Da-\lambda^2}\phi\cos\lambda\Bigg\{\frac{1}{2R\lambda^2(\lambda^2-\sigma^2)}\left(\lambda d_1+\frac{\sigma}{\sin\sigma}\right)$$
$$-\frac{\alpha\lambda^2}{\sin\sigma}\left(\frac{8\sigma^3}{(\lambda^2-\sigma^2)^4}+\frac{2\sigma}{(\lambda^2-\sigma^2)^3}+\frac{\alpha\sigma}{R(\lambda^2-\sigma^2)^2}\right)\Bigg\}+\left.\frac{dA_1}{dy}\right|_{y=1}+\left.\frac{dA_2}{dy}\right|_{y=1}$$
$$-\left(\left.\frac{dA_1}{dy}\right|_{y=0}+\left.\frac{dA_2}{dy}\right|_{y=0}\right)\cos\lambda\Bigg], \tag{5.116}$$

$$e_3 = -\frac{1}{\lambda}\Bigg[\frac{Da}{Da-\lambda^2}\Bigg\{\alpha\lambda^2 e_2-\frac{\phi}{2R\lambda^2(\lambda^2-\sigma^2)}\left(\lambda d_1+\frac{\sigma}{\sin\sigma}\right)+\frac{\phi\alpha\lambda^2}{\sin\sigma}\left(\frac{8\sigma^3}{(\lambda^2-\sigma^2)^4}\right.$$
$$\left.+\frac{2\sigma}{(\lambda^2-\sigma^2)^3}+\frac{\alpha\sigma}{R(\lambda^2-\sigma^2)^2}\right)\Bigg\}+\left.\frac{dA_1}{dy}\right|_{y=0}+\left.\frac{dA_2}{dy}\right|_{y=0}\Bigg], \tag{5.117}$$

$$e_4 = \left(\sqrt{2}\lambda\sin(\sqrt{2}\lambda)+\frac{2Da}{Da-2\lambda^2}\alpha\lambda^2\cos(\sqrt{2}\lambda)\right)^{-1}\Bigg[\left.\frac{dA_3}{dy}\right|_{y=1}-\cos(\sqrt{2}\lambda)\Bigg\{\left.\frac{dA_3}{dy}\right|_{y=0}$$
$$+\frac{2Da}{Da-2\lambda^2}\alpha\lambda^2 A_3(0)\Bigg\}\Bigg], \tag{5.118}$$

$$e_5 = -\frac{1}{\sqrt{2}\lambda}\left[\left.\frac{dC}{dy}\right|_{y=0}+\frac{2Da}{Da-2\lambda^2}\alpha\lambda^2\{e_4+A_3(0)\}\right], \tag{5.119}$$

$$e_6 = \left(\lambda\sin\lambda+\frac{Da}{Da-\lambda^2}\alpha\lambda^2\cos\lambda\right)^{-1}\Bigg[\frac{\phi Da}{R(Da-\lambda^2)}\Bigg\{\frac{1}{\lambda^2(\lambda^2-\sigma^2)}\left(\lambda d_1+\frac{\sigma}{\sin\sigma}\right)$$
$$+\frac{2\alpha\lambda^2\sigma}{(\lambda^2-\sigma^2)^2\sin\sigma}\Bigg\}\cos\lambda+\frac{\phi d_2}{\lambda^2-\sigma^2}\cos\lambda-\left(\left.\frac{dA_4}{dy}\right|_{y=0}+\left.\frac{dA_5}{dy}\right|_{y=0}\right)\cos\lambda$$
$$+\left.\frac{dA_4}{dy}\right|_{y=1}+\left.\frac{dA_5}{dy}\right|_{y=1}\Bigg], \tag{5.120}$$

$$e_7 = \frac{1}{\lambda}\Bigg[\frac{\phi Da}{R(Da-\lambda^2)}\Bigg\{\frac{1}{\lambda^2(\lambda^2-\sigma^2)}\left(\lambda d_1+\frac{\sigma}{\sin\sigma}\right)+\frac{2\alpha\lambda^2\sigma}{(\lambda^2-\sigma^2)^2\sin\sigma}\Bigg\}+\frac{\phi d_2}{\lambda^2-\sigma^2}$$
$$-\frac{Da}{Da-\lambda^2}\alpha\lambda^2 e_6-\left.\frac{dA_4}{dy}\right|_{y=0}-\left.\frac{dA_5}{dy}\right|_{y=0}\Bigg]. \tag{5.121}$$

Analytical solution for mean concentration up to second-order becomes

$$\begin{aligned}\langle C\rangle &= C^{(0)} + \epsilon\langle C^{(1)}\rangle + \epsilon^2\langle C^{(2)}\rangle \\ &= C^{(0)} + \epsilon Pe\ Re[\{\langle G\rangle + \beta_m\langle Y\rangle\}e^{-i\Omega Sct}]\frac{\partial C^{(0)}}{\partial x} + \epsilon^2 Pe^2\ Re[\langle T\rangle e^{-i\Omega Sct} + \langle S\rangle e^{-2i\Omega Sct}] \\ &\quad \times \frac{\partial^2 C^{(0)}}{\partial x^2},\end{aligned} \tag{5.122}$$

and the second-order transverse concentration is

$$\begin{aligned}C = (1+\beta_m M + \beta_m^2 Z)C^{(0)} + \epsilon Pe\ [F + \beta_m X + Re\{(G+\beta_m Y)e^{-i\Omega Sct}\}]\frac{\partial C^{(0)}}{\partial x} + \epsilon^2 Pe^2 \\ \times[P + Re(Q + Te^{-i\Omega Sct_0} + Se^{-2i\Omega Sct_0})]\frac{\partial^2 C^{(0)}}{\partial x^2}.\end{aligned} \tag{5.123}$$

For third-order ($O(\epsilon^3)$), Eqs. (5.15)–(5.17) give:

$$\frac{\partial C^{(1)}}{\partial t_2} + \frac{\partial C^{(2)}}{\partial t_1} + \frac{\partial C^{(3)}}{\partial t_0} + Pe\ u\frac{\partial C^{(2)}}{\partial x} = \frac{\partial^2 C^{(1)}}{\partial x^2} + \frac{\partial^2 C^{(3)}}{\partial y^2}, \quad 0 < y < 1, \tag{5.124}$$

$$\frac{\partial C^{(3)}}{\partial y} = 0, \quad y = 1, \tag{5.125}$$

$$\frac{\partial C^{(3)}}{\partial y} - \beta C^{(2)} = \frac{\partial C_s^{(1)}}{\partial t_2} + \frac{\partial C_s^{(2)}}{\partial t_1} + \frac{\partial C_s^{(3)}}{\partial t_0} = Da(\alpha C^{(3)} - C_s^{(3)}), \quad y = 0, \tag{5.126}$$

Averaging the transport equation of third-order w.r.t. time t_0 and space variable y and combining all the steady terms associated with $\frac{\partial^2 C^{(0)}}{\partial x^2}$, we get the dispersion coefficient $D_{Ts}^{\beta_m}$ as,

$$\begin{aligned}D_{Ts}^{\beta_m} = \beta_m\Bigg[-\frac{P(0)}{R} - \frac{\langle u_s X\rangle}{R} + \frac{P_s}{R^2} + \frac{\langle u_s\rangle X_s}{R^2} + \frac{\langle u_s F\rangle M_s}{R^2} + \frac{\langle u_s M\rangle F_s}{R^2} + \frac{F(0)F_s}{R^2} - \frac{{F_s}^2}{R^3} \\ - \frac{2\langle u_s\rangle F_s M_s}{R^3}\Bigg].\end{aligned} \tag{5.127}$$

Similarly, for oscillatory terms, we get, the dispersion coefficient $D_{Tw}^{\beta_m}$ as,

$$D_{Tw}^{\beta_m} = \beta_m Re\left[\frac{M_s}{2R^2}\langle u_w G^*\rangle - \frac{1}{2R}\langle u_w Y^*\rangle - \frac{1}{R}\left\{Q(0) - \frac{Q_s}{R}\right\}\right]. \tag{5.128}$$

Finally, using these two additional dispersion coefficients in Eq. (5.61) and neglecting the term $1/R$ (the term $1/R$ usually is neglected when compared with the other terms of

the expression for $Pe > 100$), the equation becomes

$$D_T = Pe^2 D_{Ta}, \tag{5.129}$$

where

$$D_{Ta} = D_{Ts} + D_{Tw} + D_{Ts}^{\beta_m} + D_{Tw}^{\beta_m}, \tag{5.130}$$

is the effective overall dispersion coefficient. Now, one can rewrite Eq. (5.64) as,

$$C^{(0)} = \frac{1}{Pe\sqrt{4\pi D_{Ta}\tau}} \exp\left(- \frac{(\eta/Pe)^2}{4D_{Ta}\tau} - \chi\tau \right). \tag{5.131}$$

Using Eq. (5.95) and Eq. (5.98), Eq. (5.60) becomes,

$$\chi = \beta_m \left\{ \frac{1}{R} + \frac{\alpha\beta_m}{R^3}\left(\frac{1}{3} - \frac{1}{Da}\right) - \frac{\beta_m}{3R^2} \right\} \tag{5.132}$$

One can obtain Pe independent expressions for mean and real concentrations from Eqs. (5.122) and (5.123) in a new system $\{\eta/Pe, \langle C\rangle Pe\}$ as

$$\langle C\rangle Pe = C^{(0)}\ Pe + Re[\langle G(y)\rangle + \beta_m \langle Y(y)\rangle e^{-i(2\pi T_r)\tau}] \frac{\partial (C^{(0)}\ Pe)}{\partial(\eta/Pe)} + Re[\langle T(y)\rangle e^{-i(2\pi T_r)\tau} + \langle S(y)\rangle e^{-i(4\pi T_r)\tau}] \times \frac{\partial^2 (C^{(0)}\ Pe)}{\partial(\eta/Pe)^2}, \tag{5.133}$$

and

$$C\ Pe = (1 + \beta_m M(y) + \beta_m^2 Z(y)) C^{(0)}\ Pe + [F(y) + Re\{(G(y) + \beta_m Y(y)) e^{-i(2\pi T_r)\tau}\}] \times \frac{\partial (C^{(0)}\ Pe)}{\partial(\eta/Pe)} + [P(y) + \beta_m X(y) + Re\{Q(y) + T(y) e^{-i(2\pi T_r)\tau} + S(y) e^{-i(4\pi T_r)\tau}\}] \frac{\partial^2 (C^{(0)}\ Pe)}{\partial(\eta/Pe)^2}, \tag{5.134}$$

where $C^{(0)}$ is given by Eq. (5.131) and the parameter T_r represents the ratio of the characteristic time required for vertical mixing to the flow period (T_p) and can be defined as,

$$T_r = \frac{T_0}{T_p} = \frac{h^2/D}{2\pi/\omega} = \frac{\Omega Sc}{2\pi} \left(= \frac{Sc}{\pi\delta_s^2} \right). \tag{5.135}$$

Here, T_0 is the basic time scale, which can be described as the time required for the transverse variation of concentration in the vertical direction to smear out by diffusion.

For significant non-zero exponential decay to occur, the term χ should be positive and

of increasing trend, which implies

$$\beta_m \leq \frac{1}{2}R^2\left(\frac{1}{3}+\frac{\alpha}{Da}\right)^{-1}. \tag{5.136}$$

The equation (5.131) is valid if the effective overall dispersion coefficient D_{Ta} is greater than zero. Using (5.34)–(5.36), (5.62) can be derived as,

$$\begin{aligned} D_{Ts} &= -\frac{1}{R}\left\langle \frac{d^2F}{dy^2}F \right\rangle + F_s\frac{\langle u_s\rangle}{R^2} \\ &= \frac{1}{R}\left\langle \left(\frac{dF}{dy}\right)^2 \right\rangle + \frac{1}{R}\frac{dF}{dy}F\bigg|_{y=0} + F_s\frac{\langle u_s\rangle}{R^2} \\ &= \frac{1}{R}\left\langle \left(\frac{dF}{dy}\right)^2 \right\rangle + \frac{\alpha}{R^3Da}\langle u_s\rangle^2, \end{aligned} \tag{5.137}$$

which is always positive. Using (5.38)–(5.41), (5.63) can be derived as,

$$\begin{aligned} D_{Tw} &= -\frac{1}{2R}Re\left\langle \frac{d^2G}{dy^2}G^* \right\rangle \\ &= \frac{1}{2R}\left\langle \left|\frac{dG}{dy}\right|^2 \right\rangle + \frac{1}{2R}Re\left(\frac{dG}{dy}G^*\bigg|_{y=0}\right) \\ &= \frac{1}{2R}\left\langle \left|\frac{dG}{dy}\right|^2 \right\rangle - \frac{\alpha Da}{2R}|G(0)|^2Re\left(\frac{\lambda^2}{Da-\lambda^2}\right) \\ &= \frac{1}{2R}\left\langle \left|\frac{dG}{dy}\right|^2 \right\rangle + \frac{\alpha Da}{2R}|G(0)|^2\frac{(\Omega Sc)^2}{Da^2+(\Omega Sc)^2}, \end{aligned} \tag{5.138}$$

which is also always positive. So, both the dispersion coefficients D_{Ts} and D_{Tw} are positive definite. Unlike these two, other two coefficients $D_{Ts}^{\beta_m}$ and $D_{Tw}^{\beta_m}$ may not be always positive. In the next section, we shall discuss the behaviours of these absorption-induced dispersion coefficients.

5.4 Results and discussion

5.4.1 Dispersion coefficients

D_{Ts} and D_{Tw}:

The explicit form of the steady state component of dispersion coefficient D_{Ts} can be found from Eq. (5.62) as,

$$D_{Ts} = \frac{1}{120R} + \left(1+3\alpha+\frac{6}{Da}\right)\frac{\alpha}{24R^3}. \tag{5.139}$$

In the inert case ($\alpha = 0$), the dispersion coefficient becomes

$$D_{Ts}|_{\alpha=0} = \frac{1}{120}, \tag{5.140}$$

which is same as that obtained by Ng and Bai [40].

From Eqs. (5.63) and (5.101), one can obtain the explicit form of oscillatory component of dispersion coefficient D_{Tw} as (real part of the last term of Eq. (5.101) is zero),

$$D_{Tw} = \frac{\phi^2\delta_s^2}{4R(Sc-1)} Im\left\{ \frac{{d_1}^*}{\sin\sigma}\left(\frac{\sin(\sigma-\lambda^*)}{2(\sigma-\lambda^*)} - \frac{\sin(\sigma+\lambda^*)}{2(\sigma+\lambda^*)}\right) + \frac{{d_2}^*}{\sin\sigma}\left(\frac{1-\cos(\sigma-\lambda^*)}{2(\sigma-\lambda^*)} + \frac{1-\cos(\sigma+\lambda^*)}{2(\sigma+\lambda^*)}\right)\right\}, \tag{5.141}$$

where Im stands for the imaginary part.

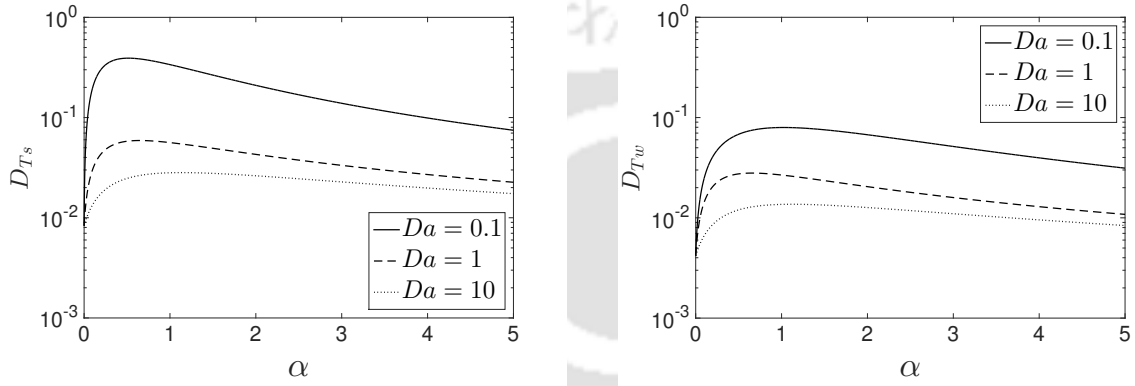

(a) (b) $\delta_s = 1$

Figure 5.1: Variation of dispersion coefficients D_{Ts} and D_{Tw} with α for different Da, where $Sc = 0.1$, $\phi = 1$.

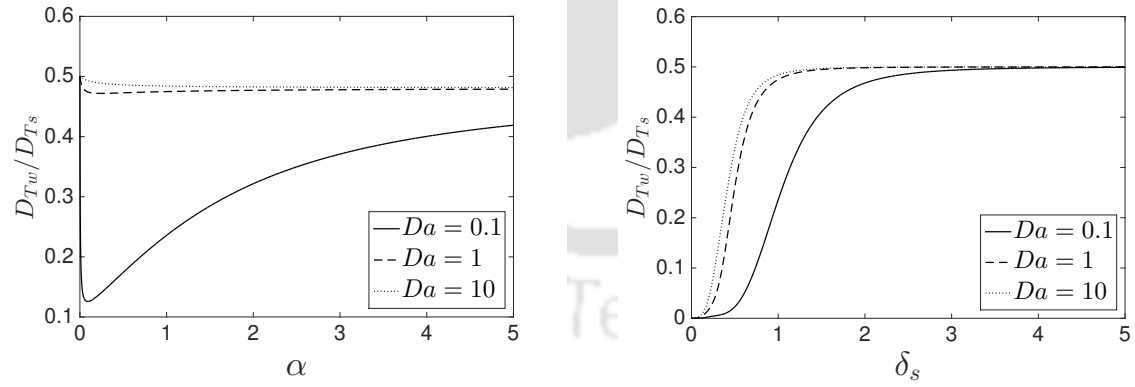

(a) $\delta_s = 1$ (b) $\alpha = 1$

Figure 5.2: Variation of ratio of two dispersion coefficients D_{Ts} and D_{Tw} with α and δ_s respectively for different Da, where $Sc = 0.1$, $\phi = 1$.

Effects of partition coefficient (α) and phase exchange kinetics (Da) on dispersion coefficients D_{Ts} and D_{Tw} are shown in Fig. (5.1). Figure shows that dispersion coefficients increase with the increase of α up to a certain value and then decreases for further increase. The occurrence of this maximum value may be due to bed retention that allows solute to

retain at the channel bed and after a while (depending on Da) it is released back into the flow at the upstream side, by that time the maximum concentration cloud moves from its original position. This creates a long tail of the solute cloud and consequently increases solute dispersion through the channel. Further increase of α beyond a critical value will decrease the dispersion coefficients due to the higher retardation factor, which drags down the ability of solute spreading along the concentration gradient.

The figures show that stronger kinetics or weaker phase exchange rate (i.e., smaller Da) gives rise to larger values of both of the dispersion coefficients. These observations can be verified mathematically.

From Eq. (5.139), the gradient of D_{Ts} at $\alpha = 0$ is

$$\left.\frac{dD_{Ts}}{d\alpha}\right|_{\alpha=0} = \frac{1}{30} + \frac{1}{4Da}, \tag{5.142}$$

which is always positive and is large for small Da. This fact indicates that the curve has a very steep gradient for $Da \ll 1$, which causes sharp increase in dispersion coefficient. Similarly one can observe the same for D_{Tw}. From Fig. (5.1), one can also observe that the value of D_{Ts} is larger than that of D_{Tw}. That can be also noticed from the ratio graph of both the coefficients in Fig. (5.2). Figure (5.2a) shows that the values of the ratio D_{Tw}/D_{Ts} are lie in $0.1-0.5$ and the values of D_{Tw} are comparable with D_{Ts} for large α. The variation of the ratio D_{Tw}/D_{Ts} with δ_s are plotted in Fig. (5.2b). Figure shows that for $\delta_s > 1$, D_{Tw}/D_{Ts} tends to the value 0.5, which verifies the earlier claim of Ng and Bai [40] that for slow oscillation, the oscillatory component of dispersion coefficient is half of steady state dispersion coefficient.

$D_{Ts}^{\beta_m}$ and $D_{Tw}^{\beta_m}$:

Both the coefficients $D_{Ts}^{\beta_m}$ and $D_{Tw}^{\beta_m}$ appear due to absorption at channel bed. It can be seen from Eqs. (5.127) and (5.128) that expression for both the coefficients are linearly proportional to the bed absorption. The value of the bed absorption parameter β_m is taken as unity for plotting figures.

The explicit form of the steady state component of dispersion coefficient due to bed absorption $D_{Ts}^{\beta_m}$ can be found from Eq. (5.127) as,

$$D_{Ts}^{\beta_m} = \beta_m\left(\frac{9}{4R^4Da^2} - \frac{9}{4R^4Da} - \frac{3}{4R^3Da^2} - \frac{1}{6R^5} + \frac{1}{R^5Da} + \frac{31}{60R^4} - \frac{377}{720R^3} + \frac{31}{180R^2} + \frac{91}{60R^3Da} - \frac{4}{15R^2Da} - \frac{3}{2R^5Da^2}\right). \tag{5.143}$$

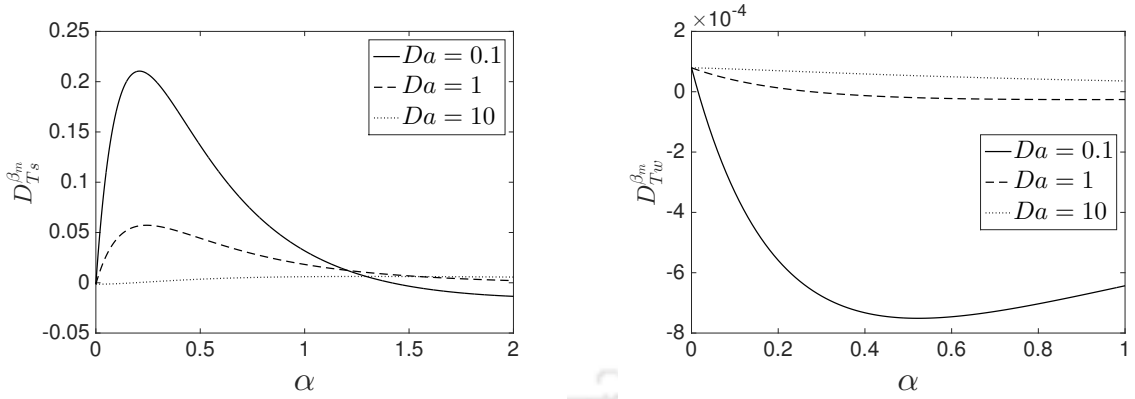

(a) (b) $\delta_s = 0.1$

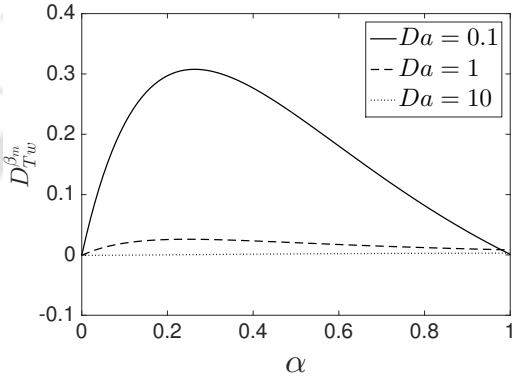

(c) $\delta_s = 1$

Figure 5.3: Variation of dispersion coefficients $D_{Ts}^{\beta_m}$ and $D_{Tw}^{\beta_m}$ with α for different Da, where $Sc = 0.1$, $\phi = 1$.

In the inert case (when $\alpha = 0$, i.e., $R = 1$), the dispersion coefficient $D_{Ts}^{\beta_m}$ becomes

$$D_{Ts}^{\beta_m}\Big|_{\alpha=0} = -\frac{1}{720}\beta_m. \tag{5.144}$$

Effects of bed retention on $D_{Ts}^{\beta_m}$ are shown in Fig. (5.3a). The coefficient is not always positive like the leading order coefficients D_{Ts} and D_{Tw}. $D_{Ts}^{\beta_m}$ is negative for $\alpha = 0$ (Eq. (5.144)). Variations of the graph of $D_{Ts}^{\beta_m}$ are similar to the earlier coefficients, that increases for certain value of α. For very small values of α and Da, the increase is very sharp. These observations can be verified mathematically by finding the gradient of the curve at $\alpha = 0$.

From Eq. (5.143), the gradient of $D_{Ts}^{\beta_m}$ at $\alpha = 0$ is

$$\frac{dD_{Ts}^{\beta_m}}{d\alpha}\Big|_{\alpha=0} = \beta_m\left(-\frac{1}{144} - \frac{1}{60Da} + \frac{3}{4Da^2}\right), \tag{5.145}$$

which indicates that the plot of $D_{Ts}^{\beta_m}$ is more sharper than that of D_{Ts} for very strong kinetics ($Da \ll 1$).

The coefficient $D_{Tw}^{\beta_m}$ can be evaluated from Eq. (5.128) by using (5.73), (5.98), (5.101), (5.104) and (5.108). We have numerically calculated the coefficient $D_{Tw}^{\beta_m}$, as expressions are too long and cumbersome to find out the explicit analytical expression.

Variations of $D_{Tw}^{\beta_m}$ are depicted in Figs. (5.3b) and (5.3c). Figure (5.3b) shows the behaviour of $D_{Tw}^{\beta_m}$ when the flow oscillation is fast. For $\delta_s = 0.1$, which corresponds to fast oscillation of the upper plate, dispersion coefficient diminishes with wall retention for different Da. For fast oscillation, effects of plate oscillation are restricted in a very thin boundary layer at the upper plate and there is a little effect of plate oscillation on solute except in a thin boundary layer, where contribution of velocity shear in solute dispersion is limited and fluid far from the upper plate is not affected by the shear-induced dispersion. Variations of $D_{Tw}^{\beta_m}$ with thicker boundary layer ($\delta_s = 1$) are shown in Fig. (5.3c). Figure shows that unlike the thin boundary layer, the coefficient is increases with wall retention when boundary layer is thick. A thicker boundary layer creates a larger zone, where velocity shear increases the concentration gradient, which in turn increases the solute dispersion. Further increase of α will retard the flow advection and reduces the ability of the solute to move along the concentration gradient, consequently decreases the solute distribution.

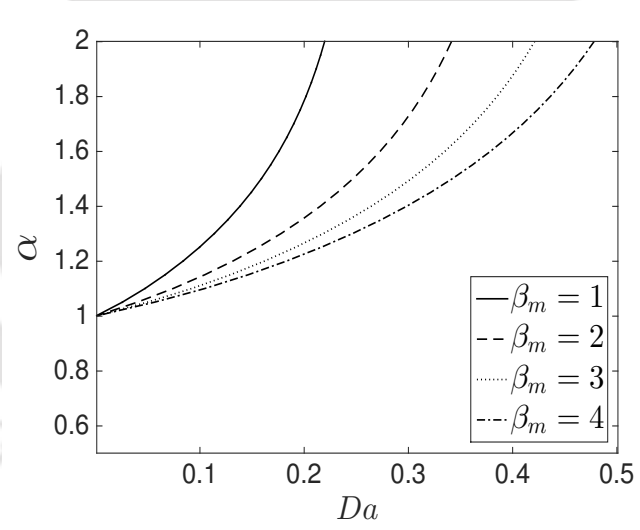

Figure 5.4: Contour of $D_{Ta} = 0$ for different β_m, where $\delta_s = 1$, $Sc = 0.1$, $\phi = 1$. D_{Ta} is positive and negative on the right and the left sides on each contour line respectively.

It is proved that D_{Ts} and D_{Tw} (leading order dispersion coefficients) are both positive definite. Unlike these two, absorption induced dispersion coefficients $D_{Ts}^{\beta_m}$ and $D_{Tw}^{\beta_m}$ can be negative, zero or positive. For Eq. (5.131) to be well defined, we must need the overall effective dispersion coefficient D_{Ta} to be positive. In Fig. (5.4), the contour plots of $D_{Ta} = 0$ are displayed for different β_m. The coefficient D_{Ta} also depends on δ_s, Sc and ϕ. Contour plots are shown here only for $\delta_s = 1$, $Sc = 0.1$ and $\phi = 1$. In this figure, the value of D_{Ta} is positive and negative on the right and the left sides of the corresponding

contour respectively. Figure also shows that the values of D_{Ta} can turn into positive from negative as the bed absorption parameter β_m decreases.

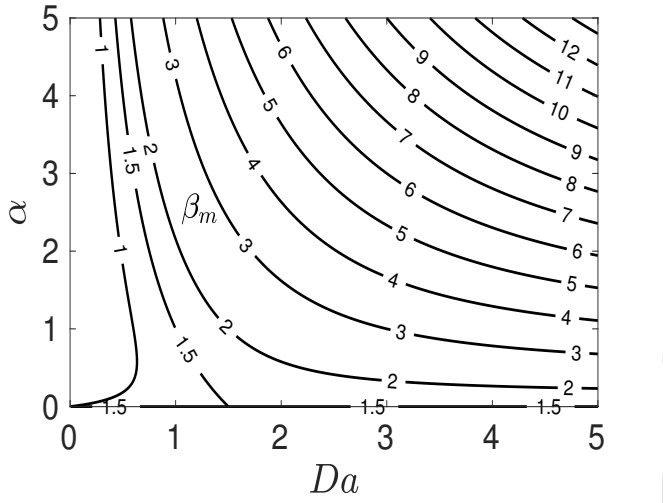

Figure 5.5: Contour of $\beta_m = \frac{1}{2}R^2(\frac{1}{3} + \frac{\alpha}{Da})^{-1}$.

It is mentioned earlier that for significant non-zero exponential decay, the parameters β_m, α and Da must satisfy Eq. (5.136). In Fig. (5.5), the contour for $\beta_m = \frac{1}{2}R^2(\frac{1}{3} + \frac{\alpha}{Da})^{-1}$ is plotted. The region that satisfies Eq. (5.136), is the right upper part of each contour line. Figure shows that more (Da, α) are included in that region when β_m value decreases. In the following part, for evolution of mean and transverse concentration, parameter values that satisfy both $D_{Ta} > 0$ and the equation Eq. (5.136) are considered.

5.4.2 Mean concentration distribution

Longitudinal distributions of the mean concentration in the channel are shown in Fig. (5.6). Figure (5.6a) presents the temporal evolutions of mean concentration for $\delta_s = 1$. The evolution curves of mean concentration move back and forth as a result of flow oscillation, and spread out as a result of lateral diffusion and advection. Figure (5.6b) displays the distribution curves of mean for different values of α. Figure shows that peak value of the mean concentration distribution decreases with the increase of α up to a maximum value as solute dispersion increases in that range. Further increase of α causes the peak value to increase. As large values of α delay the solute transport by slowing down the transport velocity. Variation of longitudinal distribution with Da can be observed from Fig. (5.6c). Figure reveals that for a fixed value of α, peak value of the mean concentration increases as Da increases. For $Da > 1$, the reversible reaction rate is much faster than the diffusion rate. Solute moves back quickly to the fluid from the immobile phase (i.e., the channel bed) and increases the solute concentration in the mobile phase. The result is reverse

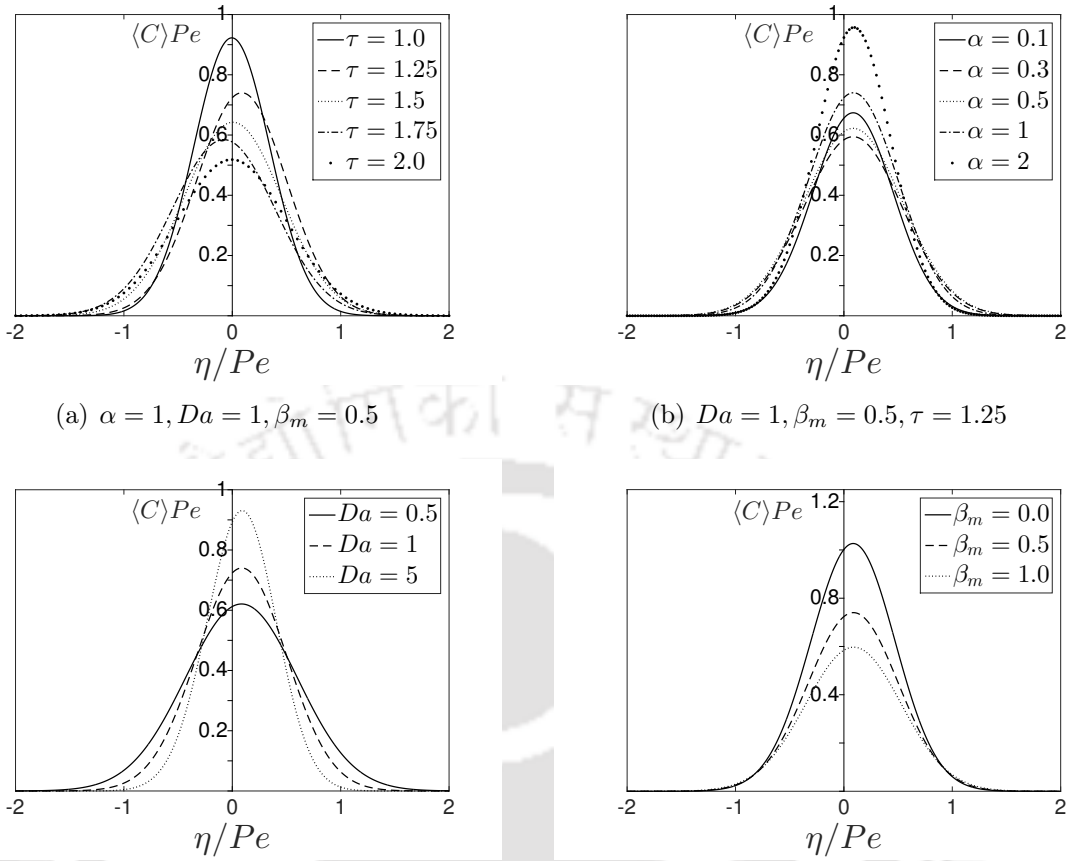

(a) $\alpha = 1, Da = 1, \beta_m = 0.5$ (b) $Da = 1, \beta_m = 0.5, \tau = 1.25$

(c) $\alpha = 1, \beta_m = 0.5, \tau = 1.25$ (d) $Da = 1, \alpha = 1, \tau = 1.25$

Figure 5.6: Longitudinal distribution of mean concentration distribution, where $\delta_s = 1$, $T_r = 1$, $\phi = 1$.

in the case of $Da < 1$, as molecular diffusion rate dominates the reversible reaction rate and makes the mean concentration distribution more blunt and flatter. Effects of β_m on mean concentration are depicted in Fig. (5.6d). Figure shows that with the increase of bed absorption, mean concentration decreases as absorption depletes solute concentration at the channel bed.

5.4.3 Transverse concentration distribution

The two-dimensional concentration contours are plotted in Figs. (5.7) and (5.8) to visualize the effects of bed absorption and retention on real transverse concentration distribution. The scalar is injected initially across the line $\eta = 0$ and dispersed through the channel under the effects of advection and molecular diffusion. The coordinate system in the figure moves longitudinally with the velocity $Pe\,\zeta$, which ensures that the centroid of the concentration cloud remains at the origin with respect to steady state velocity but movement of the centroid can be affected by oscillatory component of the velocity.

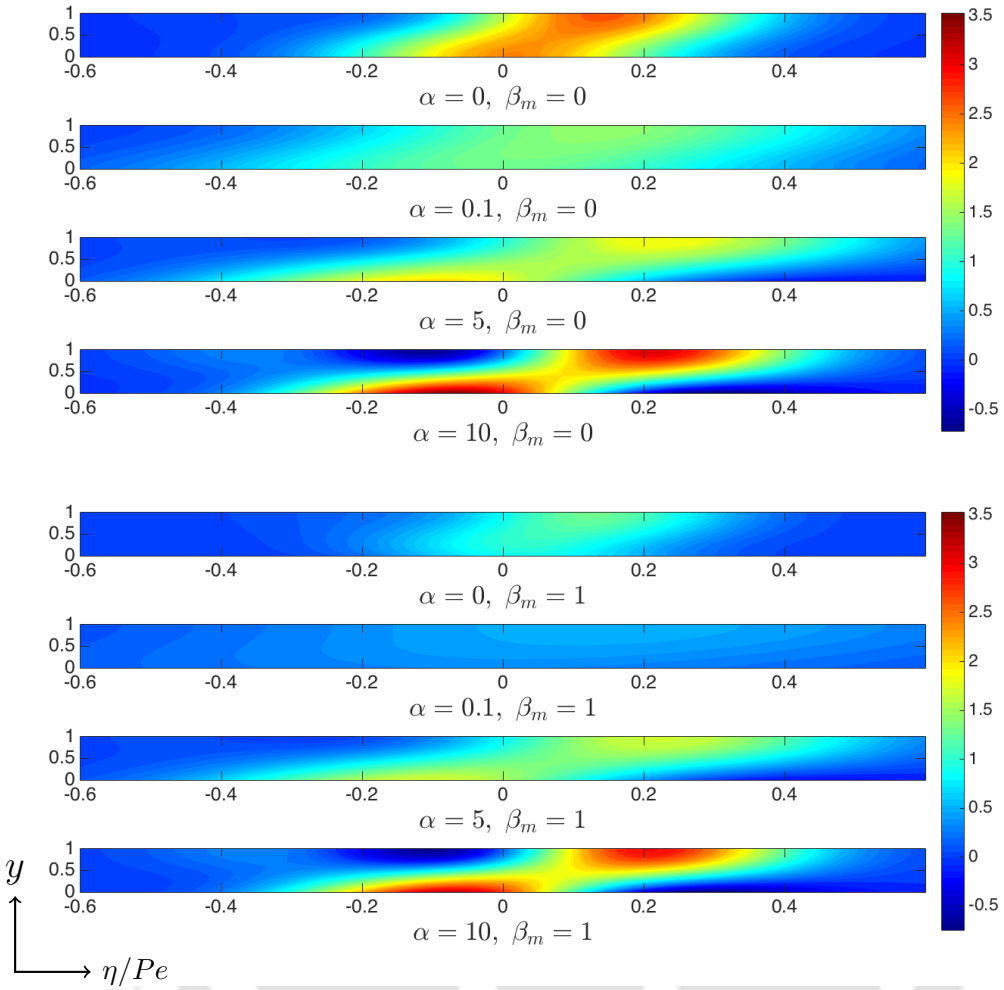

Figure 5.7: Concentration contours at $\tau = 1.25$ for different α, where $Da = 1$, $\delta_s = 1$, $\phi = 1$, $T_r = 1$: horizontal coordinate represents η/Pe, vertical coordinate represents y.

Influences of bed retention on transverse concentration distribution compared to its inert counterpart can be seen from Fig. (5.7). When the channel bed changes from inert (i.e., $\alpha = 0$) to slightly retentive (say, $\alpha = 0.1$), the solute concentration decreases as the channel bed holds some fraction of solute temporally, which allows to enhance the solute dispersion and concentration distribution becomes more dispersed. Further increase of α will retard the flow advection, consequently causes the higher concentration zone in both downstream and upstream sides. From the figure it is also observed that for large α (say, $\alpha = 10$), concentration is higher than that of the flow with inert channel bed owing to higher retention capacity of the channel bed. As bed retention increases, retardation factor reduces the ability of the solute to move along the concentration gradient.

Contour plots in Fig. (5.8) display the effects of phase exchange rate kinetics on two-dimensional concentration distribution. Figure shows that the concentration distribution becomes more dispersed due to slow kinetics (smaller Da), which increases the solute

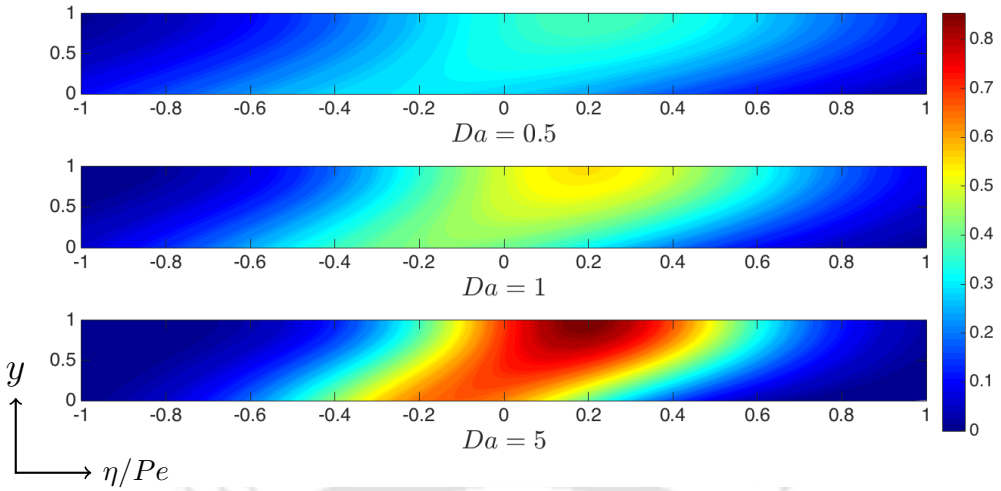

Figure 5.8: Concentration contours at $\tau = 1.25$ for different Da, where $\beta_m = 1$, $\delta_s = 1$, $\phi = 1$, $T_r = 1$: horizontal coordinate represents η/Pe, vertical coordinate represents y.

dispersion in the flow. Further increase of Da increases the solute concentration in the channel as the faster rate of exchange between the channel bed and fluid phase increases solute concentration in the fluid phase.

In order to clearly visualize the solute transport at the channel bed and near the oscillatory plate, concentration distributions at $y = 0$ and $y = 1$ are depicted in Fig. (5.9) for different combinations of α, Da and β_m. Figure exhibits that concentration at upper plate is higher than that at the channel bed for small values of α. With the increase of α, concentration at the channel bed increases faster than that at the upper plate and for higher α, concentration even higher than at the oscillatory upper plate. Bed retention allows for a temporal storage, which increases the solute dispersion more near the channel bed than that at the other parts of the channel. When bed retention is high, it takes large amount of solute from the flow and consequently the retardation factor weighs down the ability of the solute and increase the solute concentration at the channel bed. This increasing effect is strengthen by fast phase exchange rate (larger Da), as storage mass at the channel bed quickly releases the mass to the flow that increases the solute concentration. When bed absorption takes place, it depletes solute more near the channel bed and the solute concentration gets reduced at a faster rate at the channel bed than that at other parts of the channel.

In order to discuss the uniformity of transverse concentration variations, an indicator $\mathcal{R}$ is adopted [68] as

$$\mathcal{R}(\eta, \delta_s, \tau) = \frac{max(C(\eta, y, \delta_s, \tau)) - min(C(\eta, y, \delta_s, \tau))}{C(0, 0, \delta_s, \tau)} \times 100\%, \tag{5.146}$$

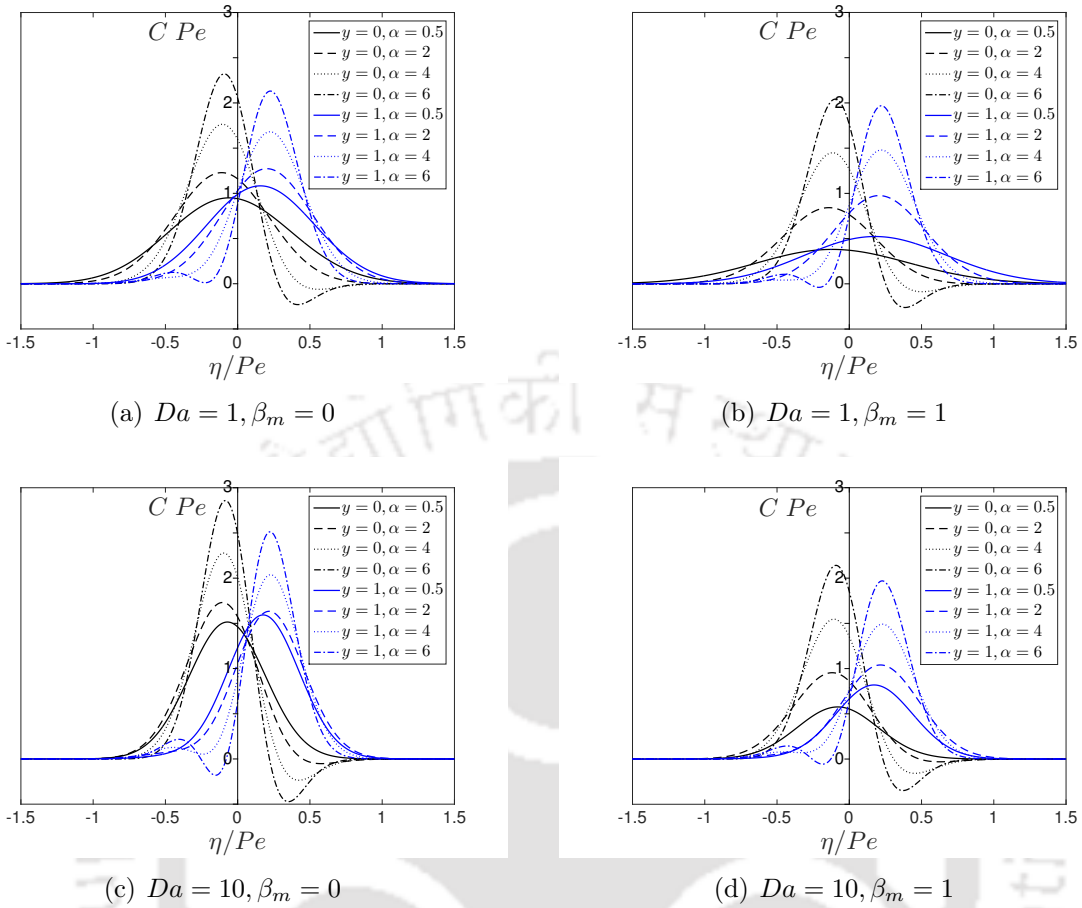

(a) $Da = 1, \beta_m = 0$ (b) $Da = 1, \beta_m = 1$

(c) $Da = 10, \beta_m = 0$ (d) $Da = 10, \beta_m = 1$

Figure 5.9: Concentration distributions at $y = 0$ and $y = 1$, where $\delta_s = 1$, $Tr = 1$, $\tau = 1.25$, $\phi = 1$.

which is the transverse variation in the cross-section against the centroid of the concentration cloud.

Figure (5.10) demonstrates the longitudinal distribution of the transverse concentration variation rate for the oscillatory Couette flow. Effects of retention parameter are plotted in Figs. (5.10a) and (5.10b). Figures reveal that the transverse concentration variation rate decreases when channel bed changes from inert to slightly retentive. Solute dispersion increases with the increase in α and consequently decreases the transverse variation rate. Further increase in α increases the variation rate as strong wall retention increases solute concentration in the flow. In the presence of absorption, the variation rate becomes higher in the downstream whereas in the upstream it becomes lower. In downstream locations, higher concentration appears near the free surface and concentration gets reduced at the channel bed due to bed absorption. This increase in concentration variation rate in the downstream causes increase in the non-uniformity nature of the concentration distribution. On the other hand, in the upstream, initially solute concentration is high at the upstream bed but once bed absorption takes place, the solute concentration

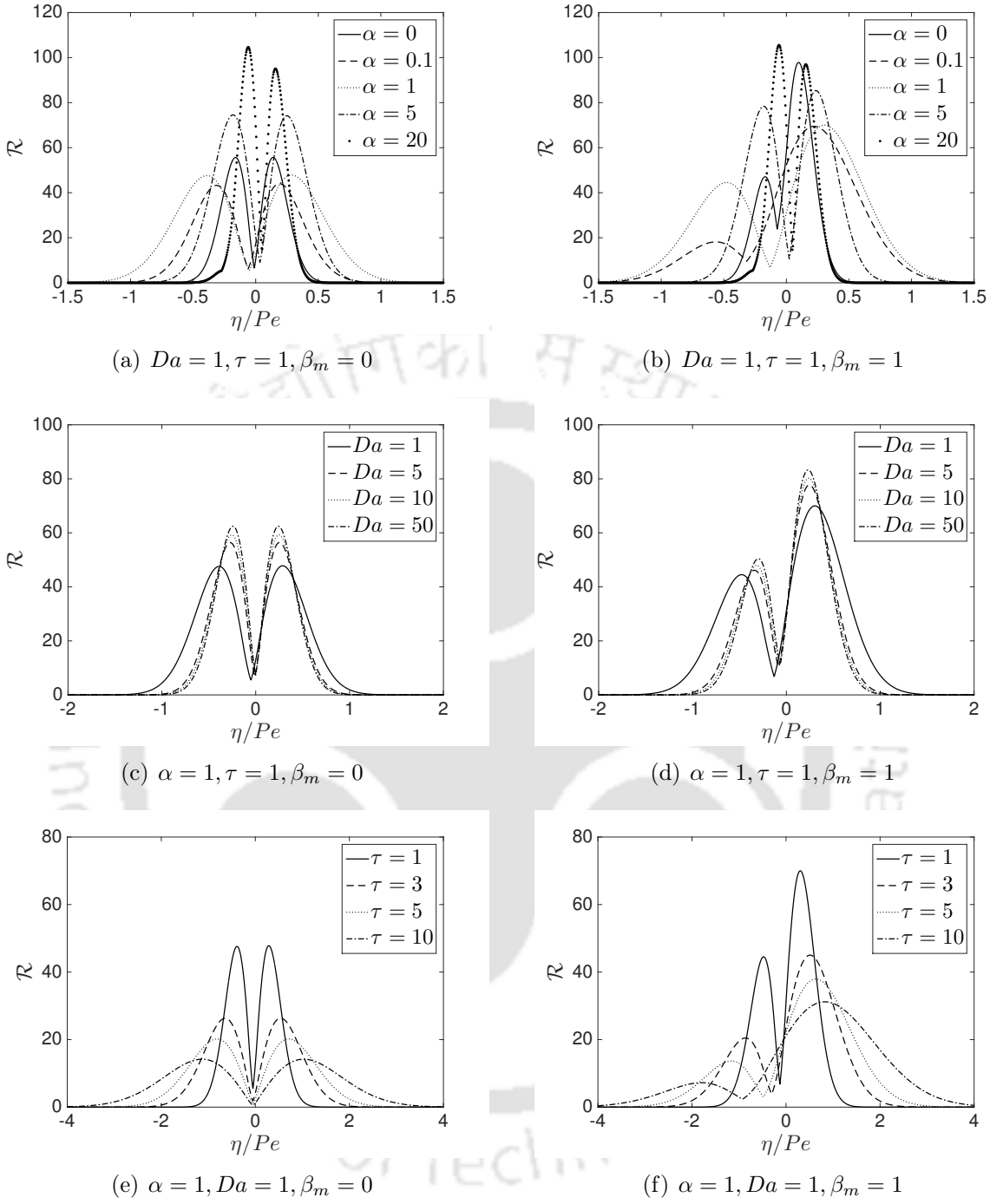

(a) $Da = 1, \tau = 1, \beta_m = 0$ (b) $Da = 1, \tau = 1, \beta_m = 1$

(c) $\alpha = 1, \tau = 1, \beta_m = 0$ (d) $\alpha = 1, \tau = 1, \beta_m = 1$

(e) $\alpha = 1, Da = 1, \beta_m = 0$ (f) $\alpha = 1, Da = 1, \beta_m = 1$

Figure 5.10: Longitudinal distributions of the transverse concentration variation rates, where $\delta_s = 1$, $Tr = 1$, $\tau = 1.25$, $\phi = 1$.

gets reduced near the channel bed and consequently the non-uniformity in the upstream concentration also gets reduced. Increase in bed retention effect increases concentration variation rate and the rate is higher for upstream locations. Figures (5.10c) and (5.10d) display the effects of phase exchange kinetics on transverse variation rates. It is seen from the figure that as Da increases, maximum variation rates on both upstream and down-

stream increase. When Da is large, reversible reaction rate dominates over the diffusion rate and increases the solute concentration in the flow, and also the maximum variation rate. Behaviours of transverse variation rate with time can be seen from Figs. (5.10e) and (5.10f). Peak concentration variation rate decreases with time as solute moves away from its centroid with increasing time.

5.5 Conclusions

Multi-scale methods of homogenization is applied to explore the two-dimensional concentration transport in an oscillatory Couette flow with reversible and irreversible reactions at stationary channel bed. Variations of dispersion coefficient with different flow parameters are studied. Analytical solutions are obtained for mean and transverse real concentrations up to second-order of approximation. This work includes the pattern of transverse real concentration distribution and its uniformity over the cross-section of the channel. Some important observations are as follows:

1. The dispersion coefficients, induced by bed absorption, can be negative unlike other steady or oscillatory dispersion coefficient components.

2. Small retention effect and stronger kinetics lead to a higher value of leading order dispersion coefficients.

3. Concentration at upper plate is higher than that at the channel bed for small retention effect.

4. Concentration at channel bed increases with the increase in retention value and can be higher than the concentration at the oscillatory plate.

5. The transverse concentration variation rate decreases when channel bed changes from inert to slightly retentive. Further, increase in retention parameter increases the variation rate as strong wall retention increases solute concentration in the flow.

6. When bed absorption takes place, the variation rate becomes higher in the downstream than that in the upstream. But for very strong bed retention effect, variation rate can be higher in the upstream compared to that in the downstream.

CHAPTER 6

EFFECTS OF NONLINEAR CHEMICAL REACTIONS ON TRANSPORT COEFFICIENTS

In the previous chapter the solute dispersion in an oscillatory Couette flow reversible and irreversible boundary reactions is studied. In this chapter, we discuss about the effects of nonlinear chemical decay reactions on transport coefficients in an oscillatory Couette flow.

6.1 Introduction

There exist a large number of literature on Taylor dispersion under the effects of either flow oscillation or chemical reaction. Dispersion of solute in an oscillatory flow has been studied by Aris [4], Chatwin [9], Smith [59], Mukherjee and Mazumder [34], Ng [37] and others. Davidson and Schroter [12], and Phillips and Kaye [47] studied a reversible phase exchange reaction. Mazumder and Das [27], and Jiang and Grotberg [25] have studied the effects of wall absorption in an oscillatory tube flow. Reaction may be either homogeneous or heterogeneous. In homogeneous reaction, chemical reacts with the flowing fluid and in heterogeneous reaction, chemical reacts at the boundary. The latter may be reversible (wall retention) or irreversible (wall absorption). Effects of linear reversible or irreversible reactions at the wall on solute dispersion have been investigated by Gupta and Gupta [24], Purnama [49], Sarkar and Jayaraman [55], Mazumder and Mondal [28], Paul and Mazumder [44] and others. In his work, Ng [39] has included a reversible phase exchange along with the wall absorption in an oscillatory pipe flow. Dispersion in oscillatory Couette flow without reaction has been studied by Mazumder and co-workers [6, 43] using a modified moments method. Solute transport in oscillatory Couette flow with sorptive boundaries has been analysed by Ng and Bai [40].

Content of this chapter is published in the journal *Acta Mechanica*, **228** (2017) 2391–2412.

In addition to previously mentioned literature, many exiting studies include only linear (first-order) homogeneous or heterogeneous reaction. A limited number of studies have explored about the case when the reactions are nonlinear. Such studies include the work of Revelli and Ridolfi [52,53]. They have shown the effects of nonlinear chemical reactions on suspended material in sediment-laden turbulent streams. In their recent study, Paul and Mazumder [45] analysed the effects of nonlinear chemical reaction on transport coefficients in steady and oscillatory tube flows. They considered both the homogeneous and heterogeneous nonlinear reaction effects in the flow, but such limited attempts are too deficient considering its vast environmental and biological importance. Still there remains a lot to explore on the effects of higher order chemical reactions on solute transport in other flow geometries.

The proposed study is an important topic from application point of view. As knowledge of the transport coefficients of solute transport under oscillation of boundary is very useful in the hydrodynamic theory of lubrication [7]. The influence of chemical reaction in the study of solute transport has a great significance in blood flow in human arteries [31]. This study also has importance to the shear-driven flows encountered in micro motors, micro channels and other micro fluidic systems [73].

The aim of this chapter is to explore the effects of nonlinear chemical decay phenomena on transport coefficients in an oscillatory Couette flow. A 2-D mathematical model is formulated by taking into account the chemical decay and a phase exchange kinetics between bulk phase (mobile phase) and sorbet boundaries (immobile phases). This is the generalization of the work of Ng and Bai [40] as in this study decay terms are included in both in mobile as well as immobile phase. In this analysis, the decay reaction is (i) nonlinear and (ii) different for the mobile and immobile phases. An 1-D differential model of the cross-sectional averaged concentration of the mobile phase is obtained that provides analytical expressions for three transport coefficients by using mathematical homogenization technique, a powerful way of dealing with multi-scale problems to deduce the effective equations on the larger scale. The work also discusses the effects of different parameters related to this flow on transport coefficients.

6.2 Formulation of the problem

A laminar, one-dimensional plane Couette flow between two infinite parallel flat plates with a separation width h is considered. The lower plate at $\widehat{y} = 0$ is assumed to be stationary whereas the upper one at $\widehat{y} = h$ oscillates in its own plane with a prescribed velocity

$$\widehat{u}(h, \widehat{t}) = U[1 + \phi Re(e^{-i\omega\widehat{t}})],$$

where U is the steady component of the velocity of the upper plate, ϕ is a factor such that ϕU is the amplitude of the oscillatory velocity component, ω is the angular frequency of

the plate oscillation, t is time and Re stands for real part. The velocity profile of the flow can be found as

$$\widehat{u}(\widehat{y},\widehat{t}) = \widehat{u}_s + Re(\widehat{u}_w e^{-i\omega\widehat{t}}), \tag{6.1}$$

where $\widehat{u}_s(\widehat{y}) = U\widehat{y}/h$ and $\widehat{u}_w(\widehat{y}) = U\phi\frac{\sin\widehat{\sigma}y}{\sin\widehat{\sigma}h}$ are the steady and oscillatory components of the velocity field respectively. Here $\widehat{\sigma}^2 = i\omega/\nu$ or $\widehat{\sigma} = (1+i)/\widehat{\delta}_s$ and $\widehat{\delta}_s = \sqrt{2\nu/\omega}$, where ν is the kinematic viscosity of the fluid and $\widehat{\delta}_s$ is the Stokes boundary layer thickness.

Consider the transport of a reactive chemical species through the flow as mentioned above. The chemical is assumed to be completely miscible in the fluid. During the flow, a part of the chemical is retained at the boundary and the rest moves with the fluid. In the phase where chemical flows with the flowing fluid is termed as mobile phase and the phase in which the chemical retains at the boundary is called immobile phase. At the equilibrium state, these two phases will have their concentrations in a fixed ratio

$$\widehat{C}_s/\widehat{C} = \widehat{\alpha},$$

where $\widehat{C}$ is the concentration (mass of chemical per bulk volume of fluid) in the mobile phase, $\widehat{C}_s$ is the concentration (mass of chemical per surface area of wall) in the immobile phase and $\widehat{\alpha}$ is the partition coefficient that relates the concentrations $\widehat{C}$ and $\widehat{C}_s$.

In mobile phase, the chemical is assumed to undergo nonlinear decay reaction with the flowing fluid. So, the transport problem of the reactive chemical can be formulated as

$$\frac{\partial\widehat{C}}{\partial\widehat{t}} + u\frac{\partial\widehat{C}}{\partial\widehat{x}} = D\frac{\partial^2\widehat{C}}{\partial\widehat{x}^2} + D\frac{\partial^2\widehat{C}}{\partial\widehat{y}^2} - \widehat{\mu}\widehat{C}^n, \quad 0 < \widehat{y} < h, \tag{6.2}$$

where D is the molecular diffusivity of the chemical in the fluid assumed to be constant, $\widehat{\mu}$ represents nonlinear decay reaction rate occurring in the bulk flow and n is the corresponding order of that.

In the immobile phase, it is assumed that the chemical undergoes a reversible phase exchange as well as a nonlinear decay reaction, as a result its concentration in the immobile phase ($\widehat{C}_s$) is controlled by phase exchange with mobile phase and also by the decay reaction at the boundary. So, evaluation of immobile phase concentration can be written as,

$$\frac{\partial\widehat{C}_s}{\partial\widehat{t}} = k(\widehat{\alpha}\widehat{C} - \widehat{C}_s) - \widehat{\mu}_s\widehat{C}_s^m,$$

where k is the reversible reaction rate constant, $\widehat{\mu}_s$ and m are the reaction rate and order of the nonlinear decay reaction rate occurring at the boundary respectively.

So, the boundary conditions for Eq. (6.2) at the lower and upper boundaries can be written as,

$$D\frac{\partial\widehat{C}}{\partial\widehat{y}} = \frac{\partial\widehat{C}_{s1}}{\partial\widehat{t}} = k_1(\widehat{\alpha}_1\widehat{C} - \widehat{C}_{s1}) - \widehat{\mu}_{s1}\widehat{C}_{s1}^m, \quad \widehat{y} = 0, \tag{6.3}$$

$$-D\frac{\partial \widehat{C}}{\partial \widehat{y}} = \frac{\partial \widehat{C}_{s2}}{\partial \widehat{t}} = k_2(\widehat{\alpha}_2\widehat{C} - \widehat{C}_{s2}) - \widehat{\mu}_{s2}\widehat{C}_{s2}^{m}, \quad \widehat{y} = h. \tag{6.4}$$

The subscripts 1 and 2 are used to denote quantities associated with the lower and upper boundaries.

6.3 Assumptions

The following assumptions are made to carry out the perturbation analysis:

1. As the fully developed situation is the primary interest in this study, a long time is assumed to be elapsed since the application of the chemical into the flow.

2. Two length scales l and h are considered, where l is the characteristic axial distance for the chemical cloud. Assume that the channel width h is very thin as compared to l, so that the ratio
$$\epsilon = h/l(\ll 1)$$
becomes small enough to use as an ordering parameter.

3. Three distinct time-scales are considered for appreciable effects of diffusion, convection and chemical reaction. In this study, it is assumed that one oscillation period of the flow is sufficient for the diffusion to take place across the entire geometry. This period is considered to be the basic time scale. The reversible phase exchange is assumed to achieve equilibrium locally after a few number of oscillations within this time scale. Therefore, this time scale can be written as,
$$T_0 = 2\pi/\omega = O(h^2/D) = O(k^{-1}).$$
Time scale for advection down the channel is one order of magnitude longer than T_0:
$$T_1 = l/U = T_0/\epsilon.$$
Time scale for axial diffusion/dispersion is two order of magnitude longer than T_0:
$$T_2 = l^2/D = T_0/\epsilon^2.$$
Based on these time scales, one may introduce accordingly
$$t_0 = \widehat{t}, \quad t_1 = \epsilon\widehat{t}, \quad t_2 = \epsilon^2\widehat{t},$$
which are the fast, medium and slow time variables respectively.

4. The Peclet number is equal to the order of unity:

$$Pe \equiv Uh/D = O(1).$$

6.4 Asymptotic Analysis

Initially, one needs to set the terms, involved in the governing equation and boundary conditions, to the same order of magnitude. Let us assume that the lateral diffusion is two order of magnitude greater than the axial diffusion and one order of magnitude greater than the advection. The reactions play an important role in the chemical transport process if the time scale for reactions are comparable with advection. So, the nonlinear reactions occurring in the bulk flow and at the boundaries are all comparable with the advection.

Now inserting the order symbol ϵ in Eqs. (6.2), (6.3) and (6.4) to indicate the relative magnitude of the terms, we have the followings:

$$\frac{\partial \widehat{C}}{\partial \widehat{t}} + \epsilon \widehat{u}\frac{\partial \widehat{C}}{\partial \widehat{x}} = \epsilon^2 D\frac{\partial^2 \widehat{C}}{\partial \widehat{x}^2} + D\frac{\partial^2 \widehat{C}}{\partial \widehat{y}^2} - \epsilon \widehat{\mu}\widehat{C}^n, \qquad 0 < \widehat{y} < h, \tag{6.5}$$

$$D\frac{\partial \widehat{C}}{\partial \widehat{y}} = \frac{\partial \widehat{C}_{s1}}{\partial \widehat{t}} = k_1(\widehat{\alpha}_1\widehat{C} - \widehat{C}_{s1}) - \epsilon \widehat{\mu}_{s1}\widehat{C}_{s1}^m, \qquad \widehat{y} = 0, \tag{6.6}$$

$$-D\frac{\partial \widehat{C}}{\partial \widehat{y}} = \frac{\partial \widehat{C}_{s2}}{\partial \widehat{t}} = k_2(\widehat{\alpha}_2\widehat{C} - \widehat{C}_{s2}) - \epsilon \widehat{\mu}_{s2}\widehat{C}_{s2}^m, \qquad \widehat{y} = h. \tag{6.7}$$

For the asymptotic analysis, the homogenization technique of Mei et al. [32] is employed. The concentrations $\widehat{C}$, $\widehat{C}_{s1}$ and $\widehat{C}_{s2}$ are expanded by the asymptotic expansion, which is first introduced by Fife and Nicholes [14] into multiple scales as:

$$\widehat{C}(\widehat{x},\widehat{y},\widehat{t}) = \widehat{C}^{(0)}(\widehat{x},\widehat{y},t_1,t_2) + \epsilon\widehat{C}^{(1)}(\widehat{x},\widehat{y},t_0,t_1,t_2) + \epsilon^2\widehat{C}^{(2)}(\widehat{x},\widehat{y},t_0,t_1,t_2) + O(\epsilon^3), \tag{6.8}$$

$$\widehat{C}_{s1}(\widehat{x},\widehat{t}) = \widehat{C}_{s1}^{(0)}(\widehat{x},t_1,t_2) + \epsilon\widehat{C}_{s1}^{(1)}(\widehat{x},t_0,t_1,t_2) + \epsilon^2\widehat{C}_{s1}^{(2)}(\widehat{x},t_0,t_1,t_2) + O(\epsilon^3), \tag{6.9}$$

$$\widehat{C}_{s2}(\widehat{x},\widehat{t}) = \widehat{C}_{s2}^{(0)}(\widehat{x},t_1,t_2) + \epsilon\widehat{C}_{s2}^{(1)}(\widehat{x},t_0,t_1,t_2) + \epsilon^2\widehat{C}_{s2}^{(2)}(\widehat{x},t_0,t_1,t_2) + O(\epsilon^3). \tag{6.10}$$

Here, $\widehat{C}^{(n)}$ and $\widehat{C}_{si}^{(n)}$, (i=1,2) are the developed terms, which are purely oscillatory functions of the short time variable t_0.

The original time derivative becomes, according to the chain rule:

$$\frac{\partial}{\partial \widehat{t}} = \frac{\partial}{\partial t_0} + \epsilon\frac{\partial}{\partial t_1} + \epsilon^2\frac{\partial}{\partial t_2}. \tag{6.11}$$

Substituting (6.8)–(6.11) into (6.5)–(6.7), we obtain

$$\left(\frac{\partial \widehat{C}^{(0)}}{\partial t_0} - D\frac{\partial^2 \widehat{C}^{(0)}}{\partial \widehat{y}^2}\right) + \epsilon\left(\frac{\partial \widehat{C}^{(0)}}{\partial t_1} + \frac{\partial \widehat{C}^{(1)}}{\partial t_0} + \widehat{u}\frac{\partial \widehat{C}^{(0)}}{\partial \widehat{x}} - D\frac{\partial^2 \widehat{C}^{(1)}}{\partial \widehat{y}^2} + \widehat{\mu}\widehat{C}^{(0)^n}\right) + \epsilon^2\left(\frac{\partial \widehat{C}^{(0)}}{\partial t_2} + \frac{\partial \widehat{C}^{(1)}}{\partial t_1} + \frac{\partial \widehat{C}^{(2)}}{\partial t_0} + \widehat{u}\frac{\partial \widehat{C}^{(1)}}{\partial \widehat{x}} - D\frac{\partial^2 \widehat{C}^{(0)}}{\partial \widehat{x}^2} - D\frac{\partial^2 \widehat{C}^{(2)}}{\partial \widehat{y}^2} + n\widehat{\mu}\widehat{C}^{(0)^{n-1}}\widehat{C}^{(1)}\right) + \cdots = 0. \tag{6.12}$$

$$D\frac{\partial \widehat{C}^{(0)}}{\partial \widehat{y}} + \epsilon D\frac{\partial \widehat{C}^{(1)}}{\partial \widehat{y}} + \epsilon^2 D\frac{\partial \widehat{C}^{(2)}}{\partial \widehat{y}} + \ldots = \frac{\partial \widehat{C}^{(0)}_{s1}}{\partial t_0} + \epsilon\left(\frac{\partial \widehat{C}^{(0)}_{s1}}{\partial t_1} + \frac{\partial \widehat{C}^{(1)}_{s1}}{\partial t_0}\right) + \epsilon^2\left(\frac{\partial \widehat{C}^{(0)}_{s1}}{\partial t_2} + \frac{\partial \widehat{C}^{(1)}_{s1}}{\partial t_1} + \frac{\partial \widehat{C}^{(2)}_{s1}}{\partial t_0}\right) + \ldots = k_1(\widehat{\alpha}_1\widehat{C}^{(0)} - \widehat{C}^{(0)}_{s1}) + \epsilon\left(k_1(\widehat{\alpha}_1\widehat{C}^{(1)} - \widehat{C}^{(1)}_{s1}) - \widehat{\mu}_{s1}\widehat{C}^{(0)^m}_{s1}\right) + \epsilon^2\left(k_1(\widehat{\alpha}_1\widehat{C}^{(2)} - \widehat{C}^{(2)}_{s1}) - m\widehat{\mu}_{s1}\widehat{C}^{(0)^{m-1}}_{s1}\widehat{C}^{(1)}_{s1}\right) + \ldots \tag{6.13}$$

$$D\frac{\partial \widehat{C}^{(0)}}{\partial \widehat{y}} + \epsilon D\frac{\partial \widehat{C}^{(1)}}{\partial \widehat{y}} + \epsilon^2 D\frac{\partial \widehat{C}^{(2)}}{\partial \widehat{y}} + \ldots = \frac{\partial \widehat{C}^{(0)}_{s2}}{\partial t_0} + \epsilon\left(\frac{\partial \widehat{C}^{(0)}_{s2}}{\partial t_1} + \frac{\partial \widehat{C}^{(1)}_{s2}}{\partial t_0}\right) + \epsilon^2\left(\frac{\partial \widehat{C}^{(0)}_{s2}}{\partial t_2} + \frac{\partial \widehat{C}^{(1)}_{s2}}{\partial t_1} + \frac{\partial \widehat{C}^{(2)}_{s2}}{\partial t_0}\right) + \ldots = k_2(\widehat{\alpha}_2\widehat{C}^{(0)} - \widehat{C}^{(0)}_{s2}) + \epsilon\left(k_2(\widehat{\alpha}_2\widehat{C}^{(1)} - \widehat{C}^{(1)}_{s2}) - \widehat{\mu}_{s2}\widehat{C}^{(0)^m}_{s2}\right) + \epsilon^2\left(k_2(\widehat{\alpha}_2\widehat{C}^{(2)} - \widehat{C}^{(2)}_{s2}) - m\widehat{\mu}_{s2}\widehat{C}^{(0)^{m-1}}_{s2}\widehat{C}^{(1)}_{s2}\right) + \ldots \tag{6.14}$$

For leading order ($O(1)$), Eqs. (6.12)–(6.14) give:

$$\frac{\partial \widehat{C}^{(0)}}{\partial t_0} = D\frac{\partial^2 \widehat{C}^{(0)}}{\partial \widehat{y}^2}, \qquad 0 < \widehat{y} < h, \tag{6.15}$$

$$D\frac{\partial \widehat{C}^{(0)}}{\partial \widehat{y}} = \frac{\partial \widehat{C}^{(0)}_{s1}}{\partial t_0} = k_1(\widehat{\alpha}_1\widehat{C}^{(0)} - \widehat{C}^{(0)}_{s1}), \qquad \widehat{y} = 0, \tag{6.16}$$

$$-D\frac{\partial \widehat{C}^{(0)}}{\partial \widehat{y}} = \frac{\partial \widehat{C}^{(0)}_{s2}}{\partial t_0} = k_2(\widehat{\alpha}_2\widehat{C}^{(0)} - \widehat{C}^{(0)}_{s2}), \qquad \widehat{y} = h. \tag{6.17}$$

By the method of separation of variables, the general solution of Eq. (6.15) becomes

$$\widehat{C}^{(0)} = \widehat{C}^{(0)}_0(\widehat{x}, t_1, t_2) + \sum_{n=1}^{\infty} Re\left[\widehat{C}^{(0)}_n(\widehat{x}, t_1, t_2)e^{i(n\pi/h)\widehat{y}}\right]e^{-(n^2\pi^2 D/h^2)t_0}. \tag{6.18}$$

Evidently for long time evolution, $\widehat{C}^{(0)}$ is independent of t_0, since the series terms die out quickly because of the exponential decay, thus the series part can be canceled out and

the solution becomes

$$\widehat{C}^{(0)} = \widehat{C}^{(0)}(\widehat{x}, t_1, t_2). \tag{6.19}$$

The two boundary conditions (6.16) and (6.17) give

$$\widehat{C}_{s1}^{(0)} = \widehat{\alpha}_1 \widehat{C}^{(0)}, \qquad \widehat{y} = 0, \tag{6.20}$$

$$\widehat{C}_{s2}^{(0)} = \widehat{\alpha}_2 \widehat{C}^{(0)}, \qquad \widehat{y} = h. \tag{6.21}$$

As expected, at the leading order, the mobile phase of the chemical is at local equilibrium with the immobile phase.

For first-order ($O(\epsilon)$), Eqs. (6.12)–(6.14) give:

$$\frac{\partial \widehat{C}^{(0)}}{\partial t_1} + \frac{\partial \widehat{C}^{(1)}}{\partial t_0} + \widehat{u}\frac{\partial \widehat{C}^{(0)}}{\partial \widehat{x}} = D\frac{\partial^2 \widehat{C}^{(1)}}{\partial \widehat{y}^2} - \widehat{\mu}\widehat{C}^{(0)^n}, \qquad 0 < \widehat{y} < h, \tag{6.22}$$

$$D\frac{\partial \widehat{C}^{(1)}}{\partial \widehat{y}} = \frac{\partial \widehat{C}_{s1}^{(0)}}{\partial t_1} + \frac{\partial \widehat{C}_{s1}^{(1)}}{\partial t_0} = k_1(\widehat{\alpha}_1 \widehat{C}^{(1)} - \widehat{C}_{s1}^{(1)}) - \widehat{\mu}_{s1}\widehat{C}_{s1}^{(0)^m}, \qquad \widehat{y} = 0, \tag{6.23}$$

$$-D\frac{\partial \widehat{C}^{(1)}}{\partial \widehat{y}} = \frac{\partial \widehat{C}_{s2}^{(0)}}{\partial t_1} + \frac{\partial \widehat{C}_{s2}^{(1)}}{\partial t_0} = k_2(\widehat{\alpha}_2 \widehat{C}^{(1)} - \widehat{C}_{s2}^{(1)}) - \widehat{\mu}_{s2}\widehat{C}_{s2}^{(0)^m}, \qquad \widehat{y} = h. \tag{6.24}$$

Taking time average of these equations w.r.t. the fast time variable t_0, we get

$$\frac{\partial \widehat{C}^{(0)}}{\partial t_1} + \widehat{u}_s\frac{\partial \widehat{C}^{(0)}}{\partial x} = D\frac{\partial^2 \overline{\widehat{C}^{(1)}}}{\partial \widehat{y}^2} - \widehat{\mu}\widehat{C}^{(0)^n}, \qquad 0 < y < h, \tag{6.25}$$

$$D\frac{\partial \overline{\widehat{C}^{(1)}}}{\partial \widehat{y}} = \frac{\partial \widehat{C}_{s1}^{(0)}}{\partial t_1} = k_1(\widehat{\alpha}_1 \overline{\widehat{C}^{(1)}} - \overline{\widehat{C}_{s1}^{(1)}}) - \widehat{\mu}_{s1}\widehat{C}_{s1}^{(0)^m}, \qquad \widehat{y} = 0, \tag{6.26}$$

$$-D\frac{\partial \overline{\widehat{C}^{(1)}}}{\partial \widehat{y}} = \frac{\partial \widehat{C}_{s2}^{(0)}}{\partial t_1} = k_2(\widehat{\alpha}_2 \overline{\widehat{C}^{(1)}} - \overline{\widehat{C}_{s2}^{(1)}}) - \widehat{\mu}_{s2}\widehat{C}_{s2}^{(0)^m}, \qquad \widehat{y} = h, \tag{6.27}$$

where overbar denotes time average w.r.t. t_0 as

$$\overline{f} = \frac{\omega}{2\pi}\int_{\widehat{t}}^{\widehat{t}+\frac{2\pi}{\omega}} f dt_0. \tag{6.28}$$

Further, taking a section average of Eq. (6.25) w.r.t. the spatial variable y subject to the conditions (6.26) and (6.27), we get

$$\frac{\partial \widehat{C}^{(0)}}{\partial t_1} + \frac{\langle u_s \rangle}{R}\frac{\partial \widehat{C}^{(0)}}{\partial \widehat{x}} + \frac{\widehat{\mu}}{R}\widehat{C}^{(0)^n} = 0, \tag{6.29}$$

where angle brackets denote section average as

$$\langle v\rangle = \frac{1}{h}\int_0^h v d\widehat{y}, \tag{6.30}$$

and

$$R = 1 + (\widehat{\alpha}_1 + \widehat{\alpha}_2)/h, \tag{6.31}$$

is the retardation factor.

Using (6.20) and (6.21) in (6.23) and (6.24) respectively and eliminating $\frac{\partial \widehat{C}^{(0)}}{\partial t_1}$ from (6.22)–(6.24) and (6.29), we get Eqs. (6.22)–(6.24) as

$$\frac{\partial \widehat{C}^{(1)}}{\partial t_0} + \left(u - \frac{\langle \widehat{u}_s\rangle}{R}\right)\frac{\partial \widehat{C}^{(0)}}{\partial \widehat{x}} + \widehat{\mu}\frac{\widehat{\alpha}_1 + \widehat{\alpha}_2}{hR}\widehat{C}^{(0)^n} = D\frac{\partial^2 \widehat{C}^{(1)}}{\partial \widehat{y}^2}, \qquad 0 < \widehat{y} < h, \tag{6.32}$$

$$D\frac{\partial \widehat{C}^{(1)}}{\partial \widehat{y}} = -\widehat{\alpha}_1\frac{\langle \widehat{u}_s\rangle}{R}\frac{\partial \widehat{C}^{(0)}}{\partial \widehat{x}} - \frac{\widehat{\mu}\widehat{\alpha}_1}{R}\widehat{C}^{(0)^n} + \frac{\partial \widehat{C}^{(1)}_{s1}}{\partial t_0} = k_1(\widehat{\alpha}_1\widehat{C}^{(1)} - \widehat{C}^{(1)}_{s1}) - \widehat{\mu}_{s1}\widehat{C}^{(0)^m}_{s1}, \qquad \widehat{y} = 0, \tag{6.33}$$

$$-D\frac{\partial \widehat{C}^{(1)}}{\partial \widehat{y}} = -\widehat{\alpha}_2\frac{\langle \widehat{u}_s\rangle}{R}\frac{\partial \widehat{C}^{(0)}}{\partial \widehat{x}} - \frac{\widehat{\mu}\widehat{\alpha}_2}{R}\widehat{C}^{(0)^n} + \frac{\partial \widehat{C}^{(1)}_{s2}}{\partial t_0} = k_2(\widehat{\alpha}_2\widehat{C}^{(1)} - \widehat{C}^{(1)}_{s2}) - \widehat{\mu}_{s2}\widehat{C}^{(0)^m}_{s2}, \qquad \widehat{y} = h. \tag{6.34}$$

These equations suggest the following substitutions

$$\widehat{C}^{(1)} = [F(\widehat{y}) + Re(G(\widehat{y})e^{-i\omega t_0})]\frac{\partial \widehat{C}^{(0)}}{\partial \widehat{x}} + M(\widehat{y})\widehat{C}^{(0)^n} + N(\widehat{y})\widehat{C}^{(0)^m}, \tag{6.35}$$

$$\widehat{C}^{(1)}_{s1} = [F_{s1} + Re(G_{s1}e^{-i\omega t_0})]\frac{\partial \widehat{C}^{(0)}}{\partial \widehat{x}} + M_{s1}\widehat{C}^{(0)^n} + N_{s1}\widehat{C}^{(0)^m} \tag{6.36}$$

and

$$\widehat{C}^{(1)}_{s2} = [F_{s2} + Re(G_{s2}e^{-i\omega t_0})]\frac{\partial \widehat{C}^{(0)}}{\partial \widehat{x}} + M_{s2}\widehat{C}^{(0)^n} + N_{s2}\widehat{C}^{(0)^m}, \tag{6.37}$$

where, the coefficients $F(\widehat{y}), F_{s1}, F_{s2}, G(\widehat{y}), G_{s1}, G_{s2}, M(\widehat{y}), M_{s1}, M_{s2}, N(\widehat{y}), N_{s1}$ and N_{s2} are to be found as follows.

On matching with the steady terms associated with $\frac{\partial \widehat{C}^{(0)}}{\partial \widehat{x}}$, we find the function $F(\widehat{y})$ is governed by

$$D\frac{d^2F}{d\widehat{y}^2} = \widehat{u}_s - \frac{\langle \widehat{u}_s\rangle}{R}, \qquad 0 < \widehat{y} < h, \tag{6.38}$$

with the boundary conditions

$$D\frac{dF}{d\widehat{y}} = -\widehat{\alpha}_1\frac{\langle \widehat{u}_s\rangle}{R} = k_1(\widehat{\alpha}_1 F - F_{s1}), \qquad \widehat{y} = 0, \tag{6.39}$$

$$-D\frac{dF}{d\widehat{y}} = -\widehat{\alpha}_2\frac{\langle \widehat{u}_s\rangle}{R} = k_2(\widehat{\alpha}_2 F - F_{s2}), \qquad \widehat{y} = h. \tag{6.40}$$

Similarly, equating the oscillatory terms associated with $\frac{\partial \widehat{C}^{(0)}}{\partial \widehat{x}}$, we get

$$D\frac{d^2G}{d\widehat{y}^2} + i\omega G = \widehat{u}_w, \qquad 0 < \widehat{y} < h, \tag{6.41}$$

$$D\frac{dG}{d\widehat{y}} = -i\omega G_{s1} = k_1(\widehat{\alpha}_1 G - G_{s1}), \qquad \widehat{y} = 0, \tag{6.42}$$

$$-D\frac{dG}{d\widehat{y}} = -i\omega G_{s2} = k_2(\widehat{\alpha}_2 G - G_{s2}), \qquad \widehat{y} = h. \tag{6.43}$$

Equating the coefficients of $\widehat{C}^{(0)^n}$, we get

$$D\frac{d^2M}{d\widehat{y}^2} = \widehat{\mu}\frac{\widehat{\alpha}_1 + \widehat{\alpha}_2}{hR}, \qquad 0 < \widehat{y} < h, \tag{6.44}$$

$$D\frac{dM}{d\widehat{y}} = -\frac{\widehat{\mu}\widehat{\alpha}_1}{R} = k_1(\widehat{\alpha}_1 M - M_{s1}), \qquad \widehat{y} = 0, \tag{6.45}$$

$$-D\frac{dM}{d\widehat{y}} = -\frac{\widehat{\mu}\widehat{\alpha}_2}{R} = k_2(\widehat{\alpha}_2 M - M_{s2}), \qquad \widehat{y} = h. \tag{6.46}$$

Equating the coefficients of $\widehat{C}^{(0)^m}$, we get

$$D\frac{d^2N}{d\widehat{y}^2} = 0, \qquad 0 < \widehat{y} < h, \tag{6.47}$$

$$D\frac{dN}{d\widehat{y}} = 0 = k_1(\widehat{\alpha}_1 N - N_{s1}) - \widehat{\mu}_{s1}\alpha_1^m, \qquad \widehat{y} = 0, \tag{6.48}$$

$$-D\frac{dN}{d\widehat{y}} = 0 = k_2(\widehat{\alpha}_2 N - N_{s2}) - \widehat{\mu}_{s2}\alpha_2^m, \qquad \widehat{y} = h. \tag{6.49}$$

For second-order ($O(\epsilon^2)$), Eqs. (6.12)–(6.14) give:

$$\frac{\partial \widehat{C}^{(0)}}{\partial t_2} + \frac{\partial \widehat{C}^{(1)}}{\partial t_1} + \frac{\partial \widehat{C}^{(2)}}{\partial t_0} + \widehat{u}\frac{\partial \widehat{C}^{(1)}}{\partial \widehat{x}} = D\frac{\partial^2 \widehat{C}^{(0)}}{\partial \widehat{x}^2} + D\frac{\partial^2 \widehat{C}^{(2)}}{\partial \widehat{y}^2} - n\widehat{\mu}\widehat{C}^{(0)^{n-1}}\widehat{C}^{(1)}, \qquad 0 < \widehat{y} < h, \tag{6.50}$$

$$D\frac{\partial \widehat{C}^{(2)}}{\partial \widehat{y}} = \frac{\partial \widehat{C}^{(0)}_{s1}}{\partial t_2} + \frac{\partial \widehat{C}^{(1)}_{s1}}{\partial t_1} + \frac{\partial \widehat{C}^{(2)}_{s1}}{\partial t_0} = k_1(\widehat{\alpha}_1\widehat{C}^{(2)} - \widehat{C}^{(2)}_{s1}) - m\widehat{\mu}_{s1}\widehat{C}^{(0)^{m-1}}_{s1}\widehat{C}^{(1)}_{s1}, \qquad \widehat{y} = 0, \tag{6.51}$$

$$-D\frac{\partial \widehat{C}^{(2)}}{\partial \widehat{y}} = \frac{\partial \widehat{C}^{(0)}_{s2}}{\partial t_2} + \frac{\partial \widehat{C}^{(1)}_{s2}}{\partial t_1} + \frac{\partial \widehat{C}^{(2)}_{s2}}{\partial t_0} = k_2(\widehat{\alpha}_2\widehat{C}^{(2)} - \widehat{C}^{(2)}_{s2}) - m\widehat{\mu}_{s2}\widehat{C}^{(0)^{m-1}}_{s2}\widehat{C}^{(1)}_{s2}, \qquad \widehat{y} = h. \tag{6.52}$$

Averaging Eq. (6.50) w.r.t. time variable t_0 followed by space variable $\widehat{y}$ subject to the

boundary conditions (6.51) and (6.52), we get

$$\frac{\partial \widehat{C}^{(0)}}{\partial t_2}+\frac{1}{R}\frac{\partial \langle \overline{\widehat{C}^{(1)}}\rangle}{\partial t_1}+\frac{1}{R}\left\langle \overline{\widehat{u}\frac{\partial \widehat{C}^{(1)}}{\partial \widehat{x}}}\right\rangle+\frac{n\widehat{\mu}}{R}\widehat{C}^{(0)^{n-1}}\langle \overline{\widehat{C}^{(1)}}\rangle+\frac{1}{hR}\left[\frac{\partial \overline{\widehat{C}_{s1}^{(1)}}}{\partial t_1}+\frac{\partial \overline{\widehat{C}_{s2}^{(1)}}}{\partial t_1}\right]=\frac{D}{R}\frac{\partial^2 \widehat{C}^{(0)}}{\partial \widehat{x}^2}. \tag{6.53}$$

Using (6.1), (6.29), (6.35), (6.36) and (6.37), we can get the followings

$$\frac{\partial \langle \overline{\widehat{C}^{(1)}}\rangle}{\partial t_1}=-\frac{\langle F\rangle\langle \widehat{u}_s\rangle}{R}\frac{\partial^2 \widehat{C}^{(0)}}{\partial \widehat{x}^2}-\frac{\widehat{\mu}\langle F\rangle}{R}\frac{\partial \widehat{C}^{(0)^n}}{\partial \widehat{x}}-\frac{\langle M\rangle\langle \widehat{u}_s\rangle}{R}\frac{\partial \widehat{C}^{(0)^n}}{\partial \widehat{x}}-\frac{\langle N\rangle\langle \widehat{u}_s\rangle}{R}\frac{\partial \widehat{C}^{(0)^m}}{\partial \widehat{x}}-\frac{n\widehat{\mu}}{R}\times\langle M\rangle\widehat{C}^{(0)^{2n-1}}-\frac{m\widehat{\mu}}{R}\langle N\rangle\widehat{C}^{(0)^{n+m-1}}, \tag{6.54}$$

$$\left\langle \overline{\widehat{u}\frac{\partial \widehat{C}^{(1)}}{\partial \widehat{x}}}\right\rangle=\left(\langle \widehat{u}_s F\rangle+\frac{1}{2}Re\langle \widehat{u}_w G^*\rangle\right)\frac{\partial^2 \widehat{C}^{(0)}}{\partial \widehat{x}^2}+\langle \widehat{u}_s M\rangle\frac{\partial \widehat{C}^{(0)^n}}{\partial \widehat{x}}+\langle \widehat{u}_s N\rangle\frac{\partial \widehat{C}^{(0)^m}}{\partial \widehat{x}}, \tag{6.55}$$

$$n\widehat{C}^{(0)^{n-1}}\langle \overline{\widehat{C}^{(1)}}\rangle=\langle F\rangle\frac{\partial \widehat{C}^{(0)^n}}{\partial \widehat{x}}+n\langle M\rangle\widehat{C}^{(0)^{2n-1}}+n\langle N\rangle\widehat{C}^{(0)^{n+m-1}}, \tag{6.56}$$

$$\frac{\partial \overline{\widehat{C}_{s1}^{(1)}}}{\partial t_1}=-F_{s1}\frac{\langle \widehat{u}_s\rangle}{R}\frac{\partial^2 \widehat{C}^{(0)}}{\partial \widehat{x}^2}-\frac{\widehat{\mu}}{R}F_{s1}\frac{\partial \widehat{C}^{(0)^n}}{\partial \widehat{x}}-M_{s1}\frac{\langle \widehat{u}_s\rangle}{R}\frac{\partial \widehat{C}^{(0)^n}}{\partial \widehat{x}}-N_{s1}\frac{\langle \widehat{u}_s\rangle}{R}\frac{\partial \widehat{C}^{(0)^m}}{\partial \widehat{x}}-\frac{n\widehat{\mu}}{R}\times M_{s1}\widehat{C}^{(0)^{2n-1}}-\frac{m\widehat{\mu}}{R}N_{s1}\widehat{C}^{(0)^{n+m-1}}, \tag{6.57}$$

$$\frac{\partial \overline{\widehat{C}_{s2}^{(1)}}}{\partial t_1}=-F_{s2}\frac{\langle \widehat{u}_s\rangle}{R}\frac{\partial^2 \widehat{C}^{(0)}}{\partial \widehat{x}^2}-\frac{\widehat{\mu}}{R}F_{s2}\frac{\partial \widehat{C}^{(0)^n}}{\partial \widehat{x}}-M_{s2}\frac{\langle \widehat{u}_s\rangle}{R}\frac{\partial \widehat{C}^{(0)^n}}{\partial \widehat{x}}-N_{s2}\frac{\langle \widehat{u}_s\rangle}{R}\frac{\partial \widehat{C}^{(0)^m}}{\partial \widehat{x}}-\frac{n\widehat{\mu}}{R}\times M_{s2}\widehat{C}^{(0)^{2n-1}}-\frac{m\widehat{\mu}}{R}N_{s2}\widehat{C}^{(0)^{n+m-1}}, \tag{6.58}$$

where * denotes the complex conjugate.

Substitution of these terms in (6.53) gives

$$\frac{\partial \widehat{C}^{(0)}}{\partial t_2}-D_T\frac{\partial^2 \widehat{C}^{(0)}}{\partial \widehat{x}^2}+\zeta_1\frac{\partial \widehat{C}^{(0)^n}}{\partial \widehat{x}}+\zeta_2\frac{\partial \widehat{C}^{(0)^m}}{\partial \widehat{x}}+\chi_1\widehat{C}^{(0)^{2n-1}}+\chi_2\widehat{C}^{(0)^{n+m-1}}=0, \tag{6.59}$$

where

$D_T=\frac{D}{R}+\frac{1}{R}\left\langle F\left(\frac{\langle \widehat{u}_s\rangle}{R}-u_s\right)\right\rangle+\frac{\langle u_s\rangle}{hR^2}(F_{s1}+F_{s2})-\frac{1}{2R}Re\langle u_w G^*\rangle,$

$\zeta_1=\frac{\widehat{\mu}}{hR^2}(\widehat{\alpha}_1\langle F\rangle-F_{s1})+\frac{\widehat{\mu}}{hR^2}(\widehat{\alpha}_2\langle F\rangle-F_{s2})-\frac{1}{R}\left\langle M\left(\frac{\langle \widehat{u}_s\rangle}{R}-\widehat{u}_s\right)\right\rangle-\frac{\langle \widehat{u}_s\rangle}{hR^2}(M_{s1}+M_{s2}),$

$\zeta_2=-\frac{1}{R}\left\langle N\left(\frac{\langle \widehat{u}_s\rangle}{R}-\widehat{u}_s\right)\right\rangle-\frac{\langle \widehat{u}_s\rangle}{hR^2}(N_{s1}+N_{s2}),$

$\chi_1=\frac{n\widehat{\mu}}{hR^2}(\widehat{\alpha}_1\langle M\rangle-M_{s1})+\frac{n\widehat{\mu}}{hR^2}(\widehat{\alpha}_2\langle M\rangle-M_{s2}),$

$$\chi_2 = \frac{n\widehat{\mu}}{R}\langle N\rangle - \frac{m\widehat{\mu}}{R^2}\left(\langle N\rangle + \frac{1}{h}(N_{s1}+N_{s2})\right).$$

6.5 Transport coefficients

Finally, combining the relationships (6.29) and (6.59) we get

$$\frac{\partial \widehat{C}^{(0)}}{\partial \widehat{t}} - D_T\frac{\partial^2 \widehat{C}^{(0)}}{\partial \widehat{x}^2} + \widehat{\zeta}_1\frac{\partial \widehat{C}^{(0)^n}}{\partial \widehat{x}} + \widehat{\zeta}_2\frac{\partial \widehat{C}^{(0)^m}}{\partial \widehat{x}} + \widehat{\zeta}_3\frac{\partial \widehat{C}^{(0)}}{\partial \widehat{x}} + \widehat{\chi}_1\widehat{C}^{(0)^{2n-1}} + \widehat{\chi}_2\widehat{C}^{(0)^{n+m-1}} + \widehat{\chi}_3\widehat{C}^{(0)^n} = 0, \tag{6.60}$$

where $\widehat{\zeta}_3 = \frac{\langle \widehat{u}_s\rangle}{R}$, $\widehat{\chi}_3 = \frac{\widehat{\mu}}{R}$ and other coefficients are same as defined earlier.

Here, $\widehat{\zeta}_i$'s $(i = 1, 2, 3)$ are the effective coefficients for advective terms, $\widehat{\chi}_i$'s $(i = 1, 2, 3)$ are the effective coefficients for the reaction terms and

$$D_T = \frac{D}{R} + \widehat{D}_{Ts} + \widehat{D}_{Tw} \tag{6.61}$$

is the dispersion coefficient, where $\widehat{D}_{Ts}$ and $\widehat{D}_{Tw}$ are respectively the dispersion coefficients due to the steady and oscillatory flows:

$$\widehat{D}_{Ts} = \frac{1}{R}\left\langle F\left(\frac{\langle \widehat{u}_s\rangle}{R} - \widehat{u}_s\right)\right\rangle + \frac{\langle \widehat{u}_s\rangle}{hR^2}(F_{s1}+F_{s2}), \tag{6.62}$$

$$\widehat{D}_{Tw} = -\frac{1}{2R}Re\langle \widehat{u}_w G^*\rangle. \tag{6.63}$$

6.5.1 Dispersion coefficient due to steady flow:

On solving the system of equations (6.38)–(6.40), one can get

$$F(\widehat{y}) = F(0) + \frac{U}{D}\left(\frac{\widehat{y}^3}{6h} - \frac{\widehat{y}^2}{4R} - \frac{\widehat{\alpha}_1\widehat{y}}{2R}\right), \tag{6.64}$$

$$F_{s1} = \widehat{\alpha}_1 F(0) + \frac{\widehat{\alpha}_1}{k_1}\frac{U}{2R}, \tag{6.65}$$

$$F_{s2} = \widehat{\alpha}_2 F(0) + \widehat{\alpha}_2\left(-1 - \frac{4\widehat{\alpha}_1}{h} + \frac{2\widehat{\alpha}_2}{h}\right)\frac{Uh^2}{12RD} + \frac{\widehat{\alpha}_2}{k_2}\frac{U}{2R}, \tag{6.66}$$

where $F(0)$ is an undetermined constant, which will be canceled out to zero. On substituting (6.64)–(6.66) in (6.62) to determine the explicit expression for $\widehat{D}_{Ts}$ as

$$\widehat{D}_{Ts} = \left[1 + 7\frac{\widehat{\alpha}_1}{h} - 3\frac{\widehat{\alpha}_2}{h} + 16\left(\frac{\widehat{\alpha}_1}{h}\right)^2 + 6\left(\frac{\widehat{\alpha}_2}{h}\right)^2 - 8\frac{\widehat{\alpha}_1}{h}\frac{\widehat{\alpha}_2}{h}\right]\frac{U^2h^2}{120R^3D} + \left(\frac{\widehat{\alpha}_1}{k_1} + \frac{\widehat{\alpha}_2}{k_2}\right)\frac{U^2}{4hR^3}. \tag{6.67}$$

6.5.2 Dispersion coefficient due to oscillatory flow:

On solving the system of equations (6.41)–(6.43), $G(y)$ is obtained as,

$$G(\widehat{y}) = -\frac{i\phi USc}{\omega(Sc-1)}\left[a\sin\widehat{\lambda}\widehat{y} + b\cos\widehat{\lambda}\widehat{y} + \frac{\sin\widehat{\sigma}\widehat{y}}{\sin\widehat{\sigma}h}\right], \tag{6.68}$$

where a and b are complex constants, and

$$\widehat{\lambda}^2 = i\omega/D, \quad \text{or} \quad \widehat{\lambda} = Sc^{1/2}\widehat{\sigma}, \tag{6.69}$$

in which $Sc = \nu/D$ is the Schmidt number.

To obtain an explicit expression for $\widehat{D}_{Tw}$, two complex constants a and b are to be determined. Let us first rewrite the boundary conditions (6.42) and (6.43) as

$$G_{s1} = \frac{i\widehat{\xi_1}}{\omega}G,\ D\frac{dG}{dy} = \widehat{\xi}_1 G \qquad \widehat{y} = 0, \tag{6.70}$$

$$G_{s2} = \frac{i\widehat{\xi_2}}{\omega}G,\ -D\frac{dG}{dy} = \widehat{\xi}_2 G \qquad \widehat{y} = h, \tag{6.71}$$

where

$\widehat{\xi_1} = -\frac{i\omega k_1\widehat{\alpha}_1}{k_1 - i\omega}$ and $\widehat{\xi_2} = -\frac{i\omega k_2\widehat{\alpha}_2}{k_2 - i\omega}$.

Now with the help of (6.70) and (6.71), one can get the following values of a and b for different cases.

When reversible kinetic phase exchange reaction is effective only on the lower boundary (i.e., $\widehat{\xi_1} \neq 0$ and $\widehat{\xi_2} = 0$), then

$$a = \left[\frac{D\widehat{\sigma}\widehat{\lambda}}{\widehat{\xi_1}}\frac{\sin\widehat{\lambda}h}{\sin\widehat{\sigma}h} - \widehat{\sigma}\cot\widehat{\sigma}h\right]\left[\widehat{\lambda}\cos\widehat{\lambda}h - \frac{D\widehat{\lambda}^2}{\widehat{\xi_1}}\sin\widehat{\lambda}h\right]^{-1}, \tag{6.72}$$

$$b = \frac{D}{\widehat{\xi_1}}\left(a\widehat{\lambda} + \frac{\widehat{\sigma}}{\sin\widehat{\sigma}h}\right). \tag{6.73}$$

If reversible kinetic phase exchange reaction is effective only on the upper boundary (i.e., $\widehat{\xi_1} = 0$ and $\widehat{\xi_2} \neq 0$), then

$$a = -\frac{\widehat{\sigma}}{\widehat{\lambda}\sin\widehat{\sigma}h}, \tag{6.74}$$

$$b = \left[\frac{D}{\widehat{\xi_2}}\widehat{\sigma}\cot\widehat{\sigma}h + 1 + a\left(\frac{D}{\widehat{\xi_2}}\widehat{\lambda}\cos\widehat{\lambda}h + \sin\widehat{\lambda}h\right)\right]\left[\frac{D}{\widehat{\xi_2}}\widehat{\lambda}\sin\widehat{\lambda}h - \cos\widehat{\lambda}h\right]^{-1}. \tag{6.75}$$

When reversible kinetic phase exchange reaction is effective on both the boundaries

(i.e., $\widehat{\xi}_1 \neq 0$ and $\widehat{\xi}_2 \neq 0$), then

$$\begin{aligned} a = &\left[\frac{D\widehat{\sigma}}{\sin\widehat{\sigma}h}\left(\frac{\cos\widehat{\sigma}h}{\widehat{\xi}_2}+\frac{\cos\widehat{\lambda}h}{\widehat{\xi}_1}\right)+\left(1-\frac{D^2\widehat{\sigma}\widehat{\lambda}}{\widehat{\xi}_1\widehat{\xi}_2}\frac{\sin\widehat{\lambda}h}{\sin\widehat{\sigma}h}\right)\right] \\ &\times\left[\left(-1+\frac{D^2\widehat{\lambda}^2}{\widehat{\xi}_1\widehat{\xi}_2}\right)\sin\widehat{\lambda}h-\left(\frac{1}{\widehat{\xi}_1}+\frac{1}{\widehat{\xi}_2}\right)D\widehat{\lambda}\cos\widehat{\lambda}h\right]^{-1}, \end{aligned} \tag{6.76}$$

$$b = \frac{D}{\widehat{\xi}_1}\left(a\widehat{\lambda}+\frac{\widehat{\sigma}}{\sin\widehat{\sigma}h}\right). \tag{6.77}$$

If reversible kinetic phase exchange reaction is not effective on any of the boundaries (i.e., $\widehat{\xi}_1 = 0$ and $\widehat{\xi}_2 = 0$), then

$$a = -\frac{\widehat{\sigma}}{\widehat{\lambda}\sin\widehat{\sigma}h}, \tag{6.78}$$

$$b = \frac{\widehat{\sigma}(\cos\widehat{\sigma}h-\cos\widehat{\lambda}h)}{\widehat{\lambda}\sin\widehat{\sigma}h\sin\widehat{\lambda}h}. \tag{6.79}$$

Substituting (6.68) into (6.63), we can get an explicit expression for the dispersion coefficient due to oscillatory flow as

$$\begin{aligned} \widehat{D}_{Tw} = \frac{(\phi U)^2 Sc}{2R\omega(Sc-1)} Im\Bigg\{ &\frac{a^*}{\sin\widehat{\sigma}h}\left[\frac{\sin(\widehat{\sigma}-\widehat{\lambda}^*)h}{2(\widehat{\sigma}-\widehat{\lambda}^*)h}-\frac{\sin(\widehat{\sigma}+\widehat{\lambda}^*)h}{2(\widehat{\sigma}+\widehat{\lambda}^*)h}\right] \\ &+\frac{b^*}{\sin\widehat{\sigma}h}\left[\frac{1-\cos(\widehat{\sigma}-\widehat{\lambda}^*)h}{2(\widehat{\sigma}-\widehat{\lambda}^*)h}+\frac{1-\cos(\widehat{\sigma}+\widehat{\lambda}^*)h}{2(\widehat{\sigma}+\widehat{\lambda}^*)h}\right]\Bigg\}, \end{aligned} \tag{6.80}$$

where Im stands for the imaginary part. By L'Hospital's rule one can show that the above expression has a finite limit as $Sc \to 1$.

6.5.3 Effective coefficients for advective and reactive terms:

In transport equation (6.60), $\widehat{\zeta}_i$'s and $\widehat{\chi}_i$'s $(i = 1, 2, 3)$ are the effective coefficients for advective and reactive terms respectively. $\widehat{\zeta}_1$, $\widehat{\chi}_1$ and $\widehat{\chi}_3$ represent the effects of nonlinear reactions in the bulk flow, $\widehat{\zeta}_2$ represents effects of nonlinear reaction at the boundary and coupled effect of both the reactions can be obtained from $\widehat{\chi}_2$.

In order to find the explicit expression for $\widehat{\zeta}_i$'s and $\widehat{\chi}_i$'s $(i = 1, 2, 3)$, first one needs to solve the systems (6.44)–(6.49), which gives

$$M(\widehat{y}) = M(0) + \frac{\widehat{\mu}(\widehat{\alpha}_1+\widehat{\alpha}_2)}{hRD}\frac{\widehat{y}^2}{2} - \frac{\widehat{\mu}\widehat{\alpha}_1}{RD}\widehat{y}, \tag{6.81}$$

$$M_{s1} = \widehat{\alpha}_1 M(0) + \frac{\widehat{\mu}\widehat{\alpha}_1}{Rk_1}, \tag{6.82}$$

$$M_{s2} = \widehat{\alpha}_2 M(0) + \left[\frac{h(\widehat{\alpha}_2 - \widehat{\alpha}_1)}{2D} + \frac{1}{k_2}\right]\frac{\widehat{\mu}\widehat{\alpha}_2}{R}, \tag{6.83}$$

$$N(\widehat{y}) = N(0), \tag{6.84}$$

$$N_{s1} = \widehat{\alpha}_1 N(0) - \frac{\widehat{\mu}_{s1}}{k_1}\alpha_1^m, \tag{6.85}$$

$$N_{s2} = \widehat{\alpha}_2 N(0) - \frac{\widehat{\mu}_{s2}}{k_2}\alpha_2^m. \tag{6.86}$$

To find the undetermined constants $F(0)$, $M(0)$ and $N(0)$, without loss of generality let us take,

$\langle F(\widehat{y})\rangle = \langle M(\widehat{y})\rangle = \langle N(\widehat{y})\rangle = 0$,

which gives,

$F(0) = -\frac{U}{D}\left(\frac{h^2}{24} - \frac{h^2}{12R} - \frac{\widehat{\alpha}_1 h}{4R}\right)$, $M(0) = \frac{\widehat{\mu}\widehat{\alpha}_1 h}{2RD} - \frac{\widehat{\mu}(\widehat{\alpha}_1+\widehat{\alpha}_2)h}{6RD}$ and $N(0) = 0$.

Now, we can find the explicit expression for $\widehat{\zeta}_i$'s and $\widehat{\chi}_i$'s $(i = 1, 2, 3)$ as

$$\widehat{\zeta}_1 = -\frac{\widehat{\mu}Uh^2}{12R^3D}\left[5\frac{\widehat{\alpha}_1^2}{h^2} + 3\frac{\widehat{\alpha}_2^2}{h^2} - 4\frac{\widehat{\alpha}_1\widehat{\alpha}_2}{h^2} + \frac{\widehat{\alpha}_1}{h} - \frac{\widehat{\alpha}_2}{h} + 12\left(\frac{\widehat{\alpha}_1}{h}\frac{D}{k_1h^2} + \frac{\widehat{\alpha}_2}{h}\frac{D}{k_2h^2}\right)\right], \tag{6.87}$$

$$\widehat{\zeta}_2 = \frac{U}{2hR^2}\left[\frac{\widehat{\mu}_{s1}}{k_1}\widehat{\alpha}_1^m + \frac{\widehat{\mu}_{s2}}{k_2}\widehat{\alpha}_2^m\right], \tag{6.88}$$

$$\widehat{\zeta}_3 = \frac{U}{2R}, \tag{6.89}$$

$$\widehat{\chi}_1 = -\frac{n\widehat{\mu}^2h^2}{3R^3D}\left[\frac{\widehat{\alpha}_1^2}{h^2} + \frac{\widehat{\alpha}_2^2}{h^2} - \frac{\widehat{\alpha}_1\widehat{\alpha}_2}{h^2} + 3\left(\frac{\widehat{\alpha}_1}{h}\frac{D}{k_1h^2} + \frac{\widehat{\alpha}_2}{h}\frac{D}{k_2h^2}\right)\right], \tag{6.90}$$

$$\widehat{\chi}_2 = \frac{m\widehat{\mu}}{hR^2}\left[\frac{\widehat{\mu}_{s1}}{k_1}\widehat{\alpha}_1^m + \frac{\widehat{\mu}_{s2}}{k_2}\widehat{\alpha}_2^m\right], \tag{6.91}$$

$$\widehat{\chi}_3 = \frac{\widehat{\mu}}{R}. \tag{6.92}$$

6.5.4 Normalised transport coefficients:

Let us introduce the following normalised variables

$$C^{(0)} = \frac{\widehat{C}^{(0)}}{C_0},\ \alpha_1 = \frac{\widehat{\alpha}_1}{h},\ \alpha_2 = \frac{\widehat{\alpha}_2}{h},\ \xi_1 = \frac{\widehat{\xi}_1 h}{D},\ \xi_2 = \frac{\widehat{\xi}_2 h}{D},\ Da_1 = \frac{k_1h^2}{D},\ Da_2 = \frac{k_2h^2}{D},$$

$$\mu = \frac{\widehat{\mu}}{k}C_0^{n-1},\ \mu_{s1} = \frac{\widehat{\mu}_{s1}}{k_1}h^{m-1}C_0^{m-1},\ \mu_{s2} = \frac{\widehat{\mu}_{s2}}{k_2}h^{m-1}C_0^{m-1},\ \sigma = \widehat{\sigma}h,\ \lambda = \widehat{\lambda}h,\ \delta_s = \frac{\widehat{\delta}_s}{h},$$

where Da_1 and Da_2 are Damkohler numbers for the lower and upper boundaries respectively. In the expression of μ, one assumes $k = k_1$ only when the lower boundary is sorbing, $k = k_2$ only when the upper boundary is sorbing and without loss of generality

$k = k_1 = k_2$ when both the boundaries are sorbing. Using this normalised variables, Eq. (6.60) can be written as,

$$\frac{\partial C^{(0)}}{\partial t} - \left[\frac{D}{R} + D_{Ts}\frac{U^2h^2}{D} + D_{Tw}\frac{U^2h^2}{D}\right]\frac{\partial^2 C^{(0)}}{\partial x^2} + \langle u_s\rangle\zeta_1\frac{\partial C^{(0)^n}}{\partial x} + \langle u_s\rangle\zeta_2\frac{\partial C^{(0)^m}}{\partial x} + \langle u_s\rangle\zeta_3\frac{\partial C^{(0)}}{\partial x} + k\,\chi_1 C^{(0)^{2n-1}} + k\,\chi_2 C^{(0)^{n+m-1}} + k\,\chi_3 C^{(0)^n} = 0, \tag{6.93}$$

where two dispersion coefficients are

$$D_{Ts} = \left[1 + 7\alpha_1 - 3\alpha_2 + 16{\alpha_1}^2 + 6{\alpha_2}^2 - 8\alpha_1\alpha_2\right]\frac{1}{120R^3} + \left(\frac{\alpha_1}{Da_1} + \frac{\alpha_2}{Da_2}\right)\frac{1}{4R^3} \tag{6.94}$$

and

$$D_{Tw} = \frac{\phi^2{\delta_s}^2}{4R(Sc-1)}Im\left\{\frac{a^*}{\sin\sigma}\left[\frac{\sin(\sigma-\lambda^*)}{2(\sigma-\lambda^*)} - \frac{\sin(\sigma+\lambda^*)}{2(\sigma+\lambda^*)}\right] + \frac{b^*}{\sin\sigma}\left[\frac{1-\cos(\sigma-\lambda^*)}{2(\sigma-\lambda^*)} + \frac{1-\cos(\sigma+\lambda^*)}{2(\sigma+\lambda^*)}\right]\right\}. \tag{6.95}$$

The constants a and b are as follows:

When only the lower boundary is sorbing, then

$a = \left[\frac{\sigma\lambda}{\xi_1}\frac{\sin\lambda}{\sin\sigma} - \sigma\cot\sigma\right]\left[\lambda\cos\lambda - \frac{\lambda^2}{\xi_1}\sin\lambda\right]^{-1}$, $b = \frac{1}{\xi_1}\left(a\lambda + \frac{\sigma}{\sin\sigma}\right)$.

When only the upper boundary is sorbing, then

$a = -\frac{\sigma}{\lambda\sin\sigma}$, $b = \left[\frac{1}{\xi_2}\sigma\cot\sigma + 1 + a\left(\frac{1}{\xi_2}\lambda\cos\lambda + \sin\lambda\right)\right]\left[\frac{1}{\xi_2}\lambda\sin\lambda - \cos\lambda\right]^{-1}$.

When both the boundaries are sorbing, then

$a = \left[\frac{\sigma}{\sin\sigma}\left(\frac{\cos\sigma}{\xi_2} + \frac{\cos\lambda}{\xi_1}\right) + \left(1 - \frac{\sigma\lambda}{\xi_1\xi_2}\frac{\sin\lambda}{\sin\sigma}\right)\right]\left[\left(-1 + \frac{\lambda^2}{\xi_1\xi_2}\right)\sin\lambda - \left(\frac{1}{\xi_1} + \frac{1}{\xi_2}\right)\lambda\cos\lambda\right]^{-1}$,

$b = \frac{1}{\xi_1}\left(a\lambda + \frac{\sigma}{\sin\sigma}\right)$.

When none of the boundaries is sorbing, then

$a = -\frac{\sigma}{\lambda\sin\sigma}$, $b = \frac{\sigma(\cos\sigma - \cos\lambda)}{\lambda\sin\sigma\sin\lambda}$.

In all the cases, $\xi_j = \frac{(1-ik_j/\omega)Da_j\alpha_j}{1+(k_j/\omega)^2}$, $k_j/\omega = Da_j{\delta_s}^2/(2Sc)$, where $j = 1, 2$.

Analytical expressions for both the dispersion coefficients obtained here are similar to those obtained by Ng and Bai [40]. This immediately implies that there is no effect of decay reaction on the dispersion coefficients. New findings of this work are advection and reaction coefficients, and their expressions are,

$$\zeta_1 = -\frac{\mu Da}{6R^3}\left[5{\alpha_1}^2 + 3{\alpha_2}^2 - 4\alpha_1\alpha_2 + \alpha_1 - \alpha_2 + 12\left(\frac{\alpha_1}{Da_1} + \frac{\alpha_2}{Da_2}\right)\right], \tag{6.96}$$

$$\zeta_2 = \frac{1}{R^2}\left[\mu_{s1}\alpha_1^m + \mu_{s2}\alpha_2^m\right], \tag{6.97}$$

$$\zeta_3 = \frac{1}{R}, \tag{6.98}$$

$$\chi_1 = -\frac{n\mu^2 Da}{3R^3}\left[\alpha_1^2 + \alpha_2^2 - \alpha_1\alpha_2 + 3\left(\frac{\alpha_1}{Da_1} + \frac{\alpha_2}{Da_2}\right)\right], \tag{6.99}$$

$$\chi_2 = \frac{m\mu}{R^2}\left[\mu_{s1}\alpha_1^m + \mu_{s2}\alpha_2^m\right], \tag{6.100}$$

$$\chi_3 = \frac{\mu}{R}. \tag{6.101}$$

Here, in the expressions of ζ_1 and χ_1 different conditions are used, which are $Da = Da_1$ only when the lower boundary is sorbing, $Da = Da_2$ only when the upper boundary is sorbing and $Da = Da_1 = Da_2$ when both the boundaries are sorbing.

When there is no nonlinear reaction in the bulk flow and at the boundary, i.e., the chemical undergoes only reversible phase exchange with the flowing fluid. All but the coefficient ζ_3 will vanish. As, for this case, $\mu = \mu_{s1} = \mu_{s2} = 0$, so Eq. (6.93) reduces to

$$\frac{\partial C^{(0)}}{\partial t} - \left[\frac{D}{R} + D_{Ts}\frac{U^2h^2}{D} + D_{Tw}\frac{U^2h^2}{D}\right]\frac{\partial^2 C^{(0)}}{\partial x^2} + \langle u_s\rangle\zeta_3\frac{\partial C^{(0)}}{\partial x} = 0, \tag{6.102}$$

where, the coefficients D_{Ts}, D_{Tw} and ζ_3 are same as given by earlier expressions. This equation coincides with the one obtained by Ng and Bai [40] in their work.

When both the decay reactions occurring in the bulk flow and at the boundary are of first-order (linear), i.e., $n = m = 1$, Eq. (6.93) reduces to

$$\begin{aligned}\frac{\partial C^{(0)}}{\partial t} - \left[\frac{D}{R} + D_{Ts}\frac{U^2h^2}{D} + D_{Tw}\frac{U^2h^2}{D}\right]\frac{\partial^2 C^{(0)}}{\partial x^2} + \langle u_s\rangle(\zeta_1+\zeta_2+\zeta_3)\frac{\partial C^{(0)}}{\partial x} \\ +k(\chi_1+\chi_2+\chi_3)C^{(0)} = 0,\end{aligned} \tag{6.103}$$

where, all the coefficients are same as defined earlier. The reaction(K_0) and advection(K_1) coefficients can be written as

$$K_0 = \chi_1 + \chi_2 + \chi_3, \quad K_1 = \zeta_1 + \zeta_2 + \zeta_3, \tag{6.104}$$

which will measure mass depletion and advection speed of the chemical respectively.

6.6 Results and discussions

Three different sorbing cases are analysed with the help of graphs. The cases are defined as follows:

Case 1: only lower boundary is sorbing (i.e., $\alpha_1 > 0$, $\alpha_2 = 0$),

Case 2: only upper boundary is sorbing (i.e., $\alpha_1 = 0$, $\alpha_2 > 0$),

Case 3: both boundaries are sorbing (i.e., $\alpha_1 > 0$, $\alpha_2 > 0$).

The oscillatory dispersion coefficient D_{Tw} depends on δ_s and Sc. The boundary layer thickness parameter δ_s increases with the increase in oscillation period of the plate. Figure (6.1a) shows the variation of D_{Tw} with the Schmidt number Sc for different sorbing cases. Figure shows that for all the cases, D_{Tw} decreases with the increase in Sc. Here, Case 1 shows a sharp decrease in D_{Tw} with increase in Sc and for inert boundaries, D_{Tw} remains invariant against Sc. From Case 3, one can understand that the combined effect of Case 1 and Case 2 reduces the dispersion effects noticeably, particularly when $Sc < 1$. The influence of D_{Tw} with δ_s is shown in Fig. (6.1b). The dispersion coefficient D_{Tw} increases gradually with the increase in δ_s for all the sorbing cases. The enhancement effect of D_{Tw} gradually reduces with increase in δ_s and becomes invariant as the value of δ_s crosses unity.

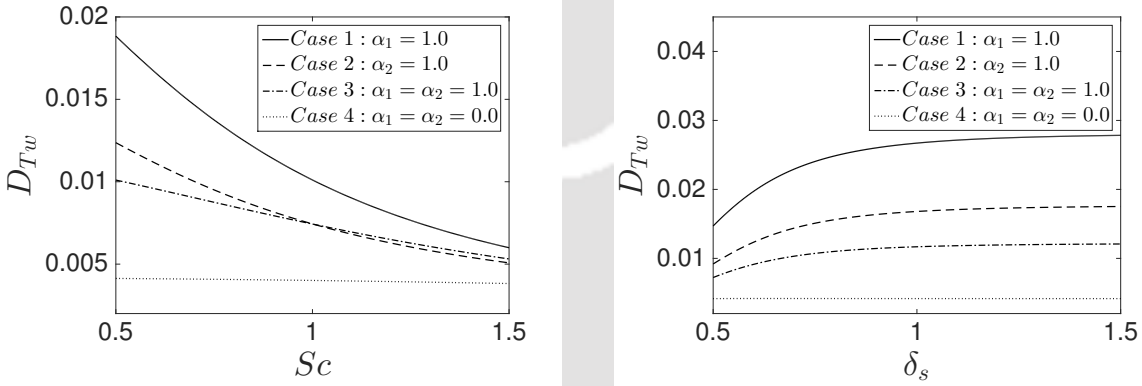

(a) $\delta_s = 1.0$ (b) $Sc = 0.1$

Figure 6.1: Variation of dispersion coefficient D_{Tw} with (a) Schmidt number Sc and (b) oscillation parameter δ_s for various cases, where $Sc = 0.1$, $\phi = 1.0$ and $Da_1 = Da_2 = 1.0$.

The effect of phase partitioning (α) and kinetics (Da) on both the dispersion coefficients D_{Ts} and D_{Tw} are shown in Fig. (6.2) for different sorbing cases. Figures show that stronger kinetics or weaker phase exchange rate (i.e., smaller Da) gives rise to the larger values of both the dispersion coefficients. From the figures one can also observe that the value of D_{Ts} is larger than that of D_{Tw} for all the cases.

Effects of different parameters on different advection and reaction coefficients for all sorbing cases are discussed in the following paragraphs. Without loss of generality, $n = m = 2$ is taken for numerical plotting.

Figure (6.3) shows variations of the reaction coefficient χ_1 , which is associated with the bulk flow reaction, with α_1 or/and α_2 for different degrees of nonlinearity n. Figure (6.3a) depicts phase exchange effects at both lower and upper boundaries. It may be mentioned that at both the boundaries, effects are similar, as χ_1 is symmetric about α_1 and α_2. Figure (6.3b) represents the case when phase exchange effects are active

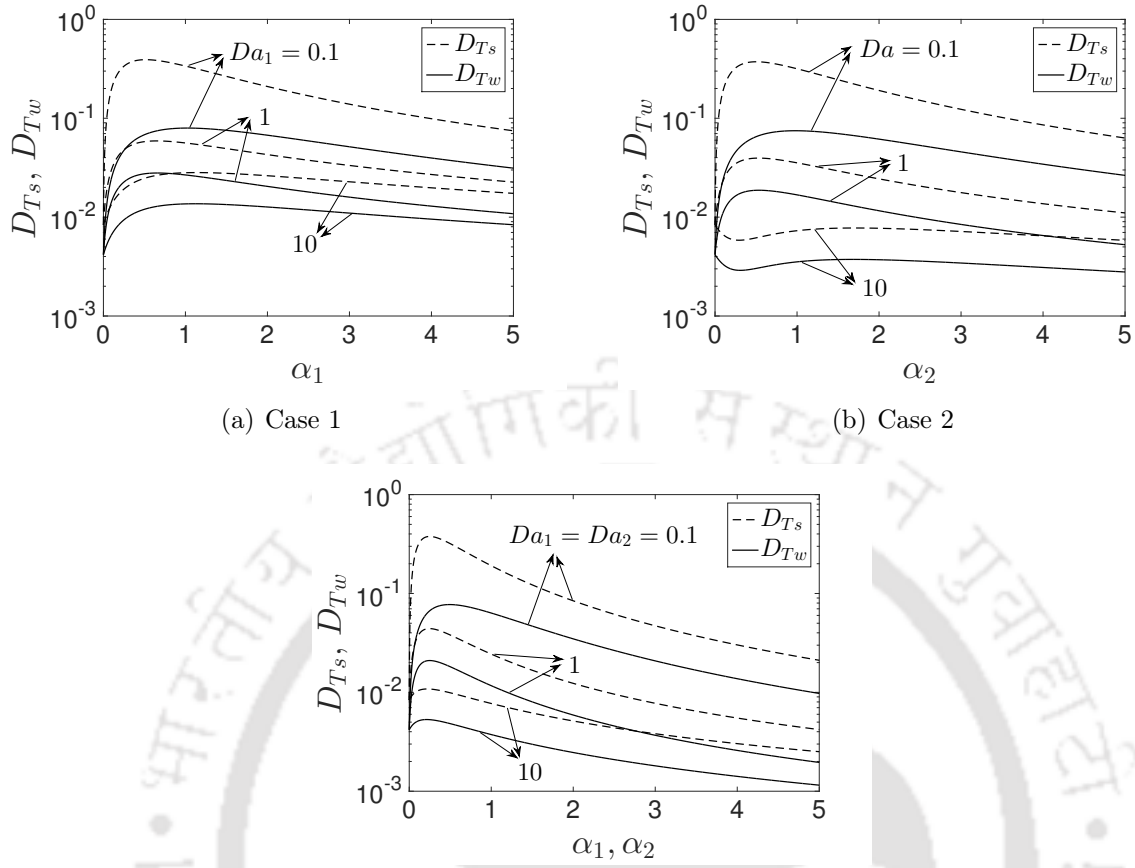

(a) Case 1

(b) Case 2

(c) Case 3

Figure 6.2: Dispersion coefficients D_{Ts} and D_{Tw} as function of α and Da, where $Sc = 0.1$, $\phi = 1.0$ and $\delta_s = 1.0$.

at both boundaries simultaneously. Reaction coefficient χ_1 has no role to play when $n = 0$. For a fixed non-zero value of n, initially the graph of χ_1 decreases sharply to a minimum with increase of α and subsequently it approaches to zero asymptotically . Higher degree of nonlinearity for the decay reaction in the bulk flow reduces the influence of the coefficient χ_1. Similar observation on the reaction coefficient has been reported by Paul and Mazumder [45]. The effects are prominent when α is smaller. Among all the cases, the largest value of the reaction coefficient χ_1 is found in the 3rd case whereas, both Cases 1 and 2 show the lowest one. Figure (6.4) shows the changes of the advection coefficient ζ_2, which is associated with the immobile flow reaction, with α_1 or/and α_2 for different degrees of nonlinearity m. Here, Fig. (6.4a) represents both the cases when one of the boundaries (lower or upper) is sorbing and Fig. (6.4b) represents the case when both the boundaries are sorbing. Figures are showing that advection coefficient increases for $m > 2$ and remain almost stationary for $m \leq 2$ as α increases. Larger degree of nonlinearity for the decay reaction at the boundaries increases the advection speed as α increases.

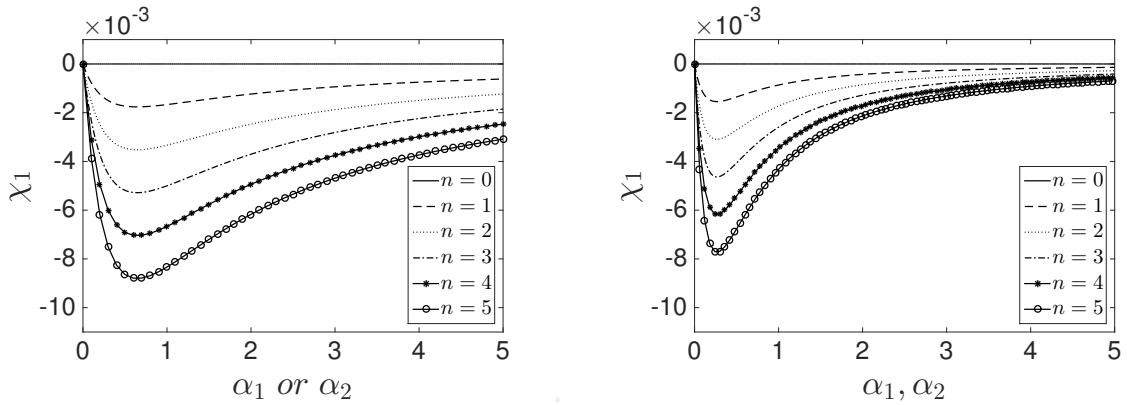

(a) Cases 1 and 2 (b) Case 3

Figure 6.3: The reaction coefficient χ_1 as a function of α for different values of n, where $\mu = 0.1$ and $Da_1 = Da_2 = 1.0$.

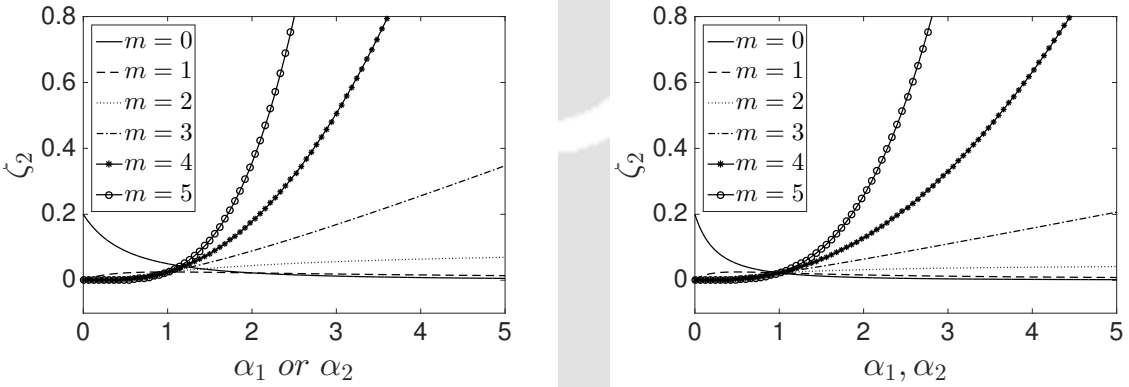

(a) Cases 1 and 2 (b) Case 3

Figure 6.4: The advection coefficient ζ_2 as a function of α for different values of m, where $\mu_{s1} = \mu_{s2} = 0.1$.

The effects on reaction coefficient χ_1 for different values of Da can be seen from Figs. (6.5a) and (6.5b). Figures indicates that stronger kinetics of the phase exchange or smaller Da will give larger value of the reaction coefficient χ_1 for all the cases. For low retention effect, the value of the coefficient χ_1 decreases sharply to a certain value and then increases with the increase in retention effect.

Behaviours of the three transport coefficients χ_1, χ_3 and ζ_1 with nonlinear bulk flow reaction rate μ for different sorbing cases can be seen from Fig. (6.6). Figures (6.6a) and (6.6b) show the variation of χ_1 and χ_3 respectively with reaction rate μ. As χ_1 and χ_3 are symmetric about α_1 and α_2, both Case 1 and Case 2 coincide with each other. In all the cases, χ_1 decreases whereas χ_3 increases monotonically with the increase of bulk flow reaction rate. Among all the cases, Case 3 shows a lower reaction coefficient value. Figure (6.6c) shows the corresponding effects on ζ_1, which decreases monotonically

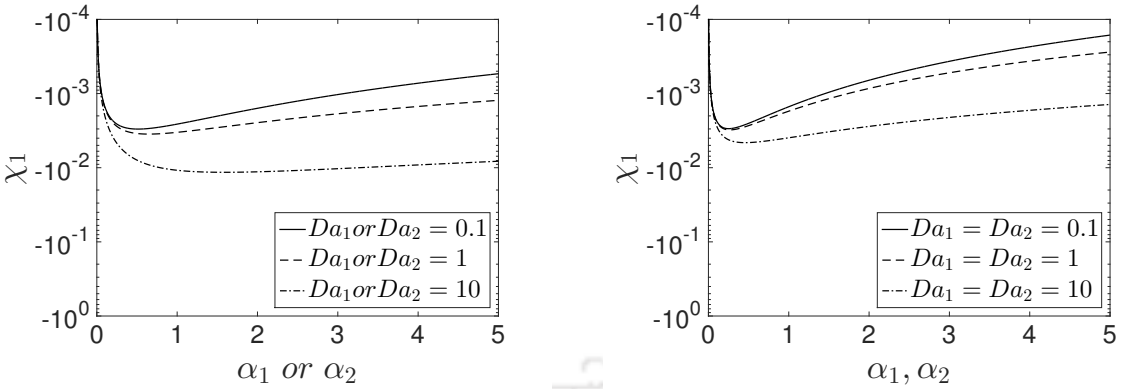

(a) Cases 1 and 2 (b) Case 3

Figure 6.5: The nonlinear reaction coefficient χ_1 as a function of α for different values of Da, where $n = 2$ and $\mu = 0.1$.

as μ increases. Figures show that value of transport coefficients are small when both boundaries are sorbing as the retardation factor is the largest in this case.

Linear variations of the advection coefficient ζ_2 with nonlinear reaction rate μ_{s1} or/and μ_{s2} are presented in Fig. (6.7). Variations of ζ_2 for different sorbing cases are shown in the figure for different values of retention parameter α_i $(i = 1, 2)$. Advection coefficient ζ_2 contributes more for a higher value of the retention parameter and increases monotonically with nonlinear immobile phase reaction rates. The advection coefficient ζ_2 becomes even more active when both the boundaries are sorbing.

When both the reactions, occurring in the bulk flow and at the boundaries, are linear (i.e., $n = m = 1$), the reaction coefficient K_0 and the advection coefficient K_1 are calculated from the expression (6.104). A parameter $\Psi = \mu_{si}/\mu$ $(i = 1, 2)$ is introduced so that $\Psi <, =, > 1$ according to the nonlinear reaction rate constant for the immobile phases is less than, equal to and greater than the corresponding value for the mobile phase respectively. The changes of the reaction coefficient K_0 with the retention parameter α is shown in Figs. (6.8) and (6.9). It is visible from the figures that the reaction coefficient K_0 decreases with α. Figure (6.8) shows the effects of the reaction rates μ, μ_{s1} and μ_{s2} on the reaction coefficient K_0 with the retention parameter α for different sorbing cases. Figures are showing that higher decay reaction rate causes the larger value of reaction coefficient K_0 and it decreases sharply initially and asymptotically approaches to a constant value as α increases. The value of K_0 is smaller in the Case 3 compared to all other sorbing cases. Figure (6.9) shows the variations of the reaction coefficient K_0 with retention parameter α for different values of Da. Figures reveal that strong kinetics of the phase exchange or smaller Da gives a larger reaction coefficient K_0, which is a departure from the one found by Paul and Mazumder [45]. The reason for this discrepancy could be due to difference in geometry. Flow between two parallel infinite plates is considered in the present study

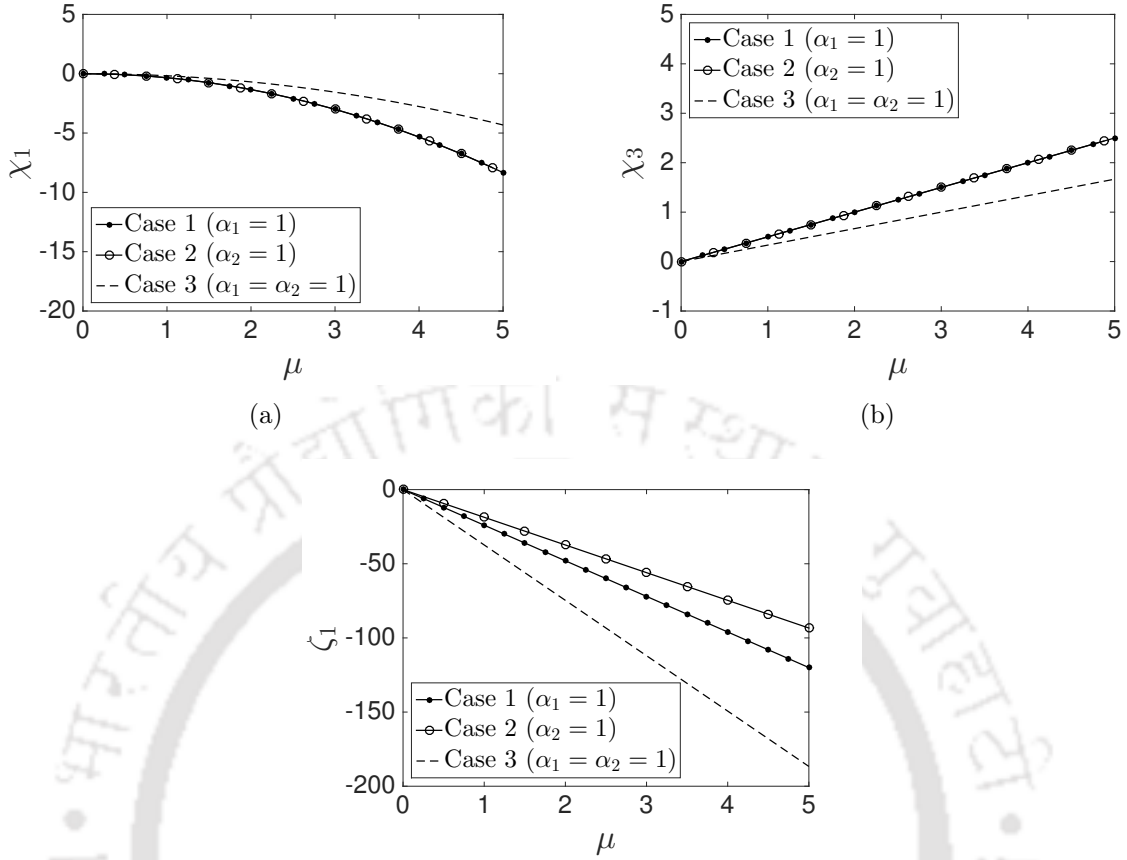

Figure 6.6: The transport coefficients χ_1, χ_3 and ζ_1 as a function of μ for different sorbing cases, where $n = 2$ and $Da_1 = Da_2 = 1.0$.

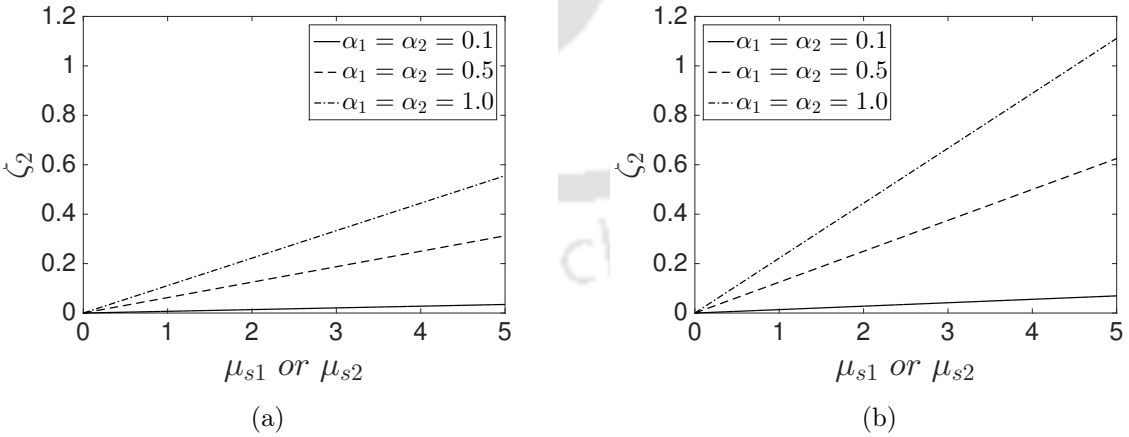

Figure 6.7: The nonlinear advection coefficient ζ_2 as a function of μ_s for different values of α, where $m = 2$ and $\mu = 0.1$.

whereas, pipe flow was studied by them. The case when both boundaries are sorbing shows the smaller value of reaction coefficient K_0.

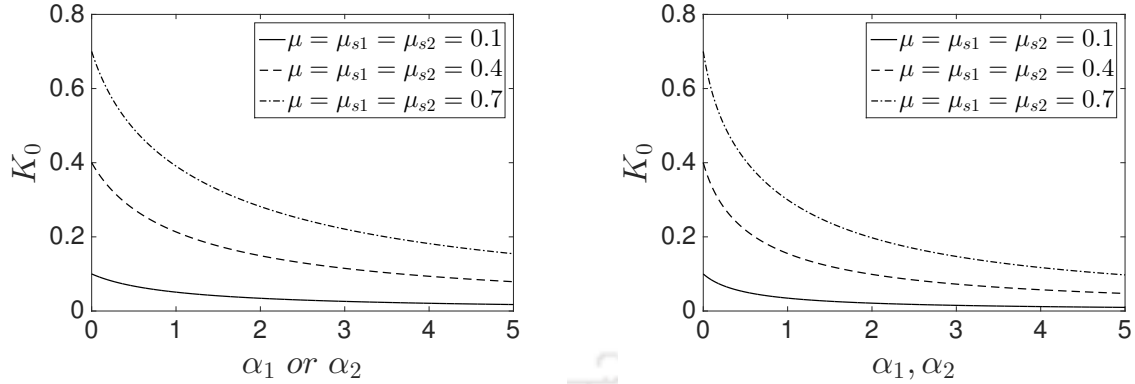

(a) Cases 1 and 2 (b) Case 3

Figure 6.8: The reaction coefficient K_0 as a function of α for different values of μ, where $Da_1 = Da_2 = 1.0$.

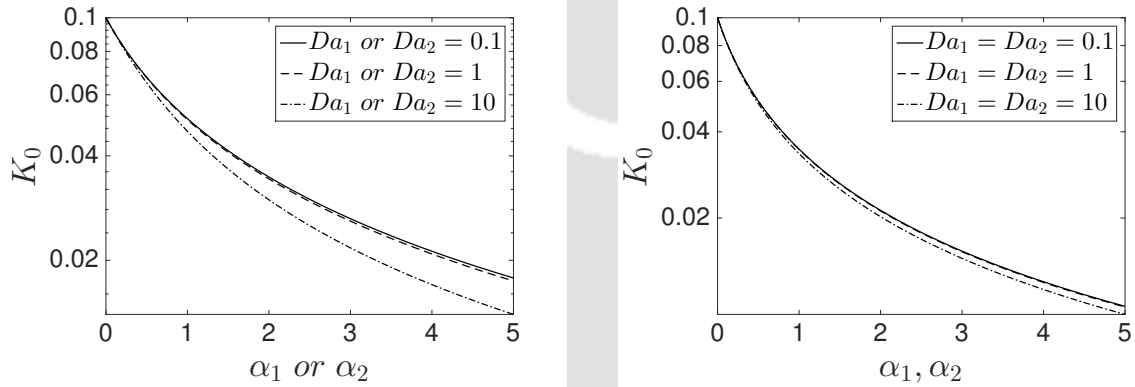

(a) Cases 1 and 2 (b) Case 3

Figure 6.9: The reaction coefficient K_0 as a function of α for different values of Da where $\mu = \mu_{s1} = \mu_{s2} = 0.1$.

Figure (6.10) shows the behaviour of the reaction coefficient K_0 with the ratio of the immobile phase reaction rate to the mobile phase reaction rate Ψ $(= \mu_{si}/\mu,\ i = 1, 2)$. It is clear from the figure that when mobile phase reaction rate μ is fixed for all α, the reaction coefficient K_0 increases monotonically as immobile phase reaction rates μ_{s1} and μ_{s2} increase (increase in Ψ will increase the immobile phase reaction rates for fixed μ) and the figure also indicates that K_0 varies linearly with Ψ when μ is fixed. Figure also shows that decrease in Ψ for fixed immobile reaction rates μ_{s1} and μ_{s2} (i.e., increase in μ) will increase the reaction coefficient. Thus, increase of both the reaction rates increase the mass depletion, as expected.

Similar kind of behaviour as we have seen for the reaction coefficient K_0, can also be observed in the case of the advection coefficient K_1 from Fig. (6.11) when it varies with the retention parameter α for different values of Da. Figures show effects of retention

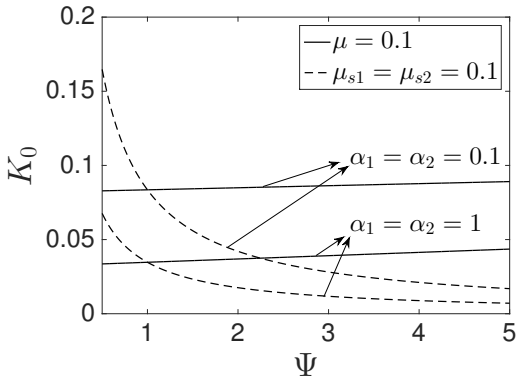

Figure 6.10: Variation of reaction coefficient K_0 with the ratio Ψ for different values of α, where $Da_1 = Da_2 = 1.0$.

parameter on K_1 for different sorbing cases. For all three sorbing cases, it can be seen that the advection coefficient K_1 decreases monotonically with the retention parameter α. In other words, phase exchange can retard the advection speed and this is also observed by Ng and Rudraiah [41]. When the phase exchange rate is very slow (i.e., Da is small), the values of the advection coefficient K_1 becomes larger for all the sorbing cases.

Figure (6.12) shows the nature of the reaction coefficient K_1 with the ratio of the immobile phase reaction rate to the mobile phase reaction rate Ψ. For fixed μ, the reaction coefficient K_1 increases monotonically (like K_0) as immobile phase reaction rates μ_{s1} and μ_{s2} increase. This is not true when immobile phase reaction rates μ_{s1} and μ_{s2} remain fixed and K_1 varies with the mobile phase reaction rate μ. Figure indicates that increase in the immobile reaction rate increases the advection speed but result is opposite for the mobile phase reaction rate. Effect of μ is found to be negligible on K_1 for large values of Ψ. Thus, reaction in immobile phase is more effective compared to reaction in mobile phase. It is remarkable here that K_1 varies almost linearly with Ψ.

6.7 Conclusions

The multi-scale method of homogenization is used to derive an effective transport equation that governs dispersion, advection and reaction phenomena of a chemical species in an oscillatory Couette flow. This study has also investigated the effects of decay, which often affects the fate of solute in the real stream and is very important in forecasting the evolution of pollutants. The main aim of this study is to determine the three transport coefficients associated with the oscillatory Couette flow. In a transverse averaged transport equation, the dispersive, advective and reactive fluxes are mostly controlled by the dispersion, advection and reaction coefficients respectively. So, it is important to learn the variations of those coefficients for different flow parameters. Decay has been considered

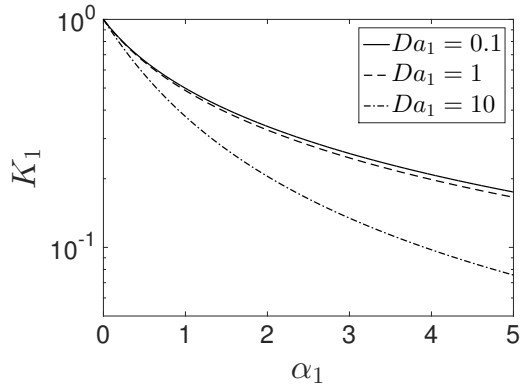

(a) Case 1

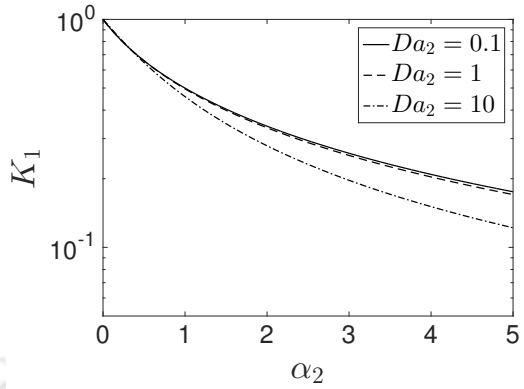

(b) Case 2

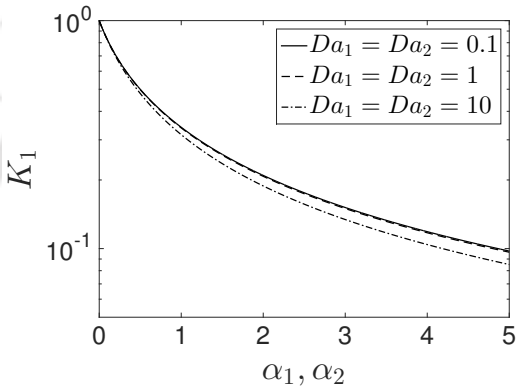

(c) Case 3

Figure 6.11: The advection coefficient K_1 as a function of α for different values of Da, where $\mu = \mu_{s1} = \mu_{s2} = 0.1$.

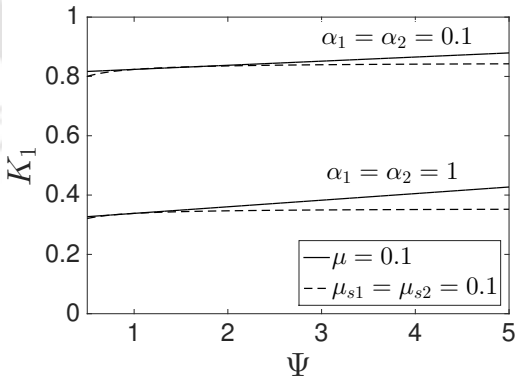

Figure 6.12: Variation of advection coefficient K_1 with the ratio Ψ for different values of α, where $Da_1 = Da_2 = 1.0$.

in both linear and nonlinear cases and with different rates for the mobile and immobile phases.

Analytical expressions are obtained for three transport coefficients. Effects of reten-

tion parameter, phase exchange kinetics and nonlinear decay on transport coefficients are accounted explicitly for different sorbing cases. As a particular case, second-order reactions ($n = m = 2$) are considered in this study for discussion.

Important results found in this work are as follows:

1. Increase in order of nonlinearity in the mobile phase decay reduces the mass depletion in the flow.

2. Increase in order of nonlinearity in the immobile phase decay enhances the advection speed for large retention parameter.

3. Higher decay reaction rates for both in mobile and immobile phases give rise to a large amount of mass depletion.

4. Advection speed decreases by the increase of decay rate in the mobile phase but it increases with the increase of decay rate in the immobile phase.

5. Stronger kinetics or a slower exchange rate leads to larger values of three transport coefficients.

6. Dispersion effects increase with the increase in the boundary layer thickness.

It may be noted that nonlinear decay reactions do not affect the dispersion coefficients as they are independent of the parameters involved in nonlinear decay reactions.

CHAPTER 7

CONCLUSIONS AND FUTURE SCOPE

7.1 Conclusions

This thesis work is to provide analytical expressions for transport coefficients, mean concentration and transverse real concentration. Detailed study of transverse concentration distribution and its uniformity throughout the channel cross-section are also carried out.

An analytical study is presented to explore two-dimensional concentration distribution in an open channel flow with absorbing channel bed. Results show that mean and transverse real concentrations decrease with the increase in bed absorption parameter value. Bed absorption generates large transverse concentration non-uniformity over the channel cross-section, especially in the downstream. Real concentration of the solute over the mean concentration should be preferred to analyse the bed absorption effects more accurately. Our analytical solutions are relatively simpler and easier for post-processing. Results obtained through this study agree well with the analytical solutions of the existing studies.

Unlike the bed absorption, reaction may be reversible in nature. We have analysed the effects of reversible phase exchange kinetics on two-dimensional concentration distribution in an open channel flow, where the solute retains for some time at the channel bed and after that it gets back to the flow depending on phase exchange kinetics. It is noted that as reversible reaction rate (phase exchange rate) increases, the dispersion coefficient decreases, as a result the peak value of mean concentration increases. It is also observed that with the increase in α (retention parameter), dispersion coefficient increases up to a critical value α_m and then it decreases. Therefore, the peak value of mean concentration decreases and the distribution profile of mean concentration becomes flatter and it remains so till α reaches its critical value α_m. Once α crosses its critical value α_m, peak value of mean concentration increases.

An attempt is made to find analytical expressions for mean and transverse real concentrations of a solute by using a multi-scale homogenization technique and to explore the evolution of transverse concentration distribution in oscillatory Couette flows through two inert boundary walls. Results show that dispersion of solute in a flowing fluid increases with the increase in Stokes boundary layer thickness. For slow oscillation of the upper plate, third-order mean of solute concentration reaches Taylor dispersion stage after a long time period compared to that in the case of fast oscillation of the plate. A time scale up to $10h^2/D$ is suggested to characterize the initial transition stage of the transport process to approach transverse uniformity.

To observe the effects of chemical reaction on solute dispersion in an oscillatory Couette flow, we have extended the previous work for chemically reactive boundaries. Here, the solute undergoes reversible and irreversible reactions at the channel bed. It is noticed that dispersion coefficients, induced by bed absorption, can be negative unlike the other steady or oscillatory dispersion coefficient components. Results show that small retention effect and stronger kinetics lead to a higher value of overall dispersion coefficient. It is also seen that concentration at upper plate is higher than that at the channel bed for small retention effect. Concentration at channel bed increases with the increase in retention value and can be higher than the concentration at the oscillatory plate. The transverse concentration variation rate decreases when channel bed changes from inert to slightly retentive. Further, increase in retention parameter increases the variation rate as strong wall retention increases solute concentration in the flow. When bed absorption takes place, the variation rate becomes higher in the downstream than in the upstream. But for very strong bed retention effect, variation rate can be higher in upstream than in the downstream.

As the reaction effect may be nonlinear both in the flow as well as at the boundaries, the final work discusses the effects of non-linear chemical reaction on dispersion coefficients for an oscillatory Couette flow. Results show that increase in order of nonlinearity in the mobile phase decay reduces the mass depletion in the flow. Increase in order of nonlinearity in the immobile phase decay enhances the advection speed for large retention parameter. Higher decay reaction rates for both in mobile and immobile phases give rise to a large amount of mass depletion. Advection speed decreases due to the increase in decay rate in the mobile phase but it increases with the increase in decay rate in the immobile phase. Stronger kinetics or a slower exchange rate leads to larger values of three transport coefficients. It is also observed that dispersion effects become more with the increase in the boundary layer thickness.

7.2 Future scope

Some possible extensions of the present work can be carried out in the future and they are as follows:

- In first two problems, we have obtained the two-dimensional concentration distribution for a steady open channel flow by using multi-scale analysis. Similar work can be done for other steady flows, *e.g.*, tube flow, annular tube flow, packed tube flow, wetland flow.

- In last three problems, the concentration distribution of a solute for an oscillatory Couette flow between two infinite parallel flat plates have been studied. The flow considered here has taken place due to pure oscillation of upper plate with zero pressure gradient of the fluid. This work can be extended by considering periodic pressure gradient to observe the combined effects of plates and pressure pulsation on solute dispersion.

- Multi-scale analysis can be applied in various non-Newtonian fluid models, e.g. Casson model, Carreau model, Carreau–Yasuda model to find the two-dimensional concentration distribution. As recent progress is done to find the transport coefficients and the mean concentration distribution, it may be useful to understand the transport of drug/proteins in plasma in blood flow through the vessels.

BIBLIOGRAPHY

[1] V. Ananthakrishnan, W. Gill, and A. Barduhn. Laminar dispersion in capillaries: Part i. mathematical analysis. *AIChE J.*, 11:1063–1072, 1965.

[2] R. Aris. On the dispersion of a solute in a fluid flowing through a tube. *Proc. R. Soc. Lond. A*, 235:67–77, 1956.

[3] R. Aris. On the dispersion of a solute by diffusion, convection and exchange between phases. *Proc. R. Soc. Lond. A*, 252:538–550, 1959.

[4] R. Aris. On the dispersion of a solute in pulsating flow through a tube. *Proc. R. Soc. Lond. A*, 259:370–376, 1960.

[5] H. Bailey and W. Gogarty. Numerical and experimental results on the dispersion of a solute in a fluid in laminar flow through a tube. *Proc. R. Soc. Lond. A*, 269:352–367, 1962.

[6] S. Bandyopadhyay and B. Mazumder. On contaminant dispersion in unsteady generalised couette flow. *Int. j. eng. sci.*, 37:1407–1423, 1999.

[7] E. Barić and H. Steiner. Extended lubrication theory for generalized couette flow through converging gaps. *Int. J. Heat Mass Transfer*, 99:149–158, 2016.

[8] A. Bournia, J. Coull, and G. Houghton. Dispersion of gases in laminar flow through a circular tube. *Proc. R. Soc. Lond. A*, 261:227–236, 1961.

[9] P. Chatwin. The approach to normality of the concentration distribution of a solute in a solvent flowing along a straight pipe. *J. Fluid Mech.*, 43:321–352, 1970.

[10] P. Chatwin. On the longitudinal dispersion of passive contaminant in oscillatory flows in tubes. *J. Fluid Mech.*, 71:513–527, 1975.

[11] B. Chen. Contaminant transport in a two-zone wetland: dispersion and ecological degradation. *J. Hydrol.*, 488:118–125, 2013.

[12] M. Davidson and R. Schroter. A theoretical model of absorption of gases by the bronchial wall. *J. Fluid Mech.*, 129:313–335, 1983.

[13] E. Evans and C. Kenney. Gaseous dispersion in laminar flow through a circular tube. *Proc. R. Soc. Lond. A*, 284:540–550, 1965.

[14] P. Fife and K. Nicholes. Dispersion in flow through small tubes. *Proc. R. Soc. Lond. A*, 344:131–145, 1975.

[15] H. Fischer. Longitudinal dispersion and turbulent mixing in open-channel flow. *Annu. Rev. Fluid Mech.*, 5:59–78, 1973.

[16] H. Fischer. Mixing and dispersion in estuaries. *Annu. Rev. Fluid Mech.*, 8:107–133, 1976.

[17] H. Fischer, E. List, R. Koh, J. Imberger, and N. Brooks. *Mixing in Inland and Coastal Waters*. Academic Press, New York, 1979.

[18] W. Gill. A note on the solution of transient dispersion problems. *Proc. R. Soc. Lond. A*, 298:335–339, 1967.

[19] W. Gill and V. Ananthakrishnan. Laminar dispersion in capillaries: Part iv. the slug stimulus. *AIChE J.*, 13:801–807, 1967.

[20] W. Gill and R. Sankarasubramanian. Exact analysis of unsteady convective diffusion. *Proc. R. Soc. Lond. A*, 316:341–350, 1970.

[21] W. Gill and R. Sankarasubramanian. Dispersion of a non-uniform slug in time-dependent flow. *Proc. R. Soc. Lond. A*, 322:101–117, 1971.

[22] W. Gill and R. Sankarasubramanian. Dispersion of non-uniformly distributed time-variable continuous sources in time-dependent flow. *Proc. R. Soc. Lond. A*, 327:191–208, 1972.

[23] J. Grotberg, B. Sheth, and L. Mockros. An analysis of pollutant gas transport and absorption in pulmonary airways. *J. Biomech. Eng.*, 112:168–176, 1990.

[24] P. Gupta and A. Gupta. Effect of homogeneous and heterogeneous reactions on the dispersion of a solute in the laminar flow between two plates. *Proc. R. Soc. Lond. A*, 330:59–63, 1972.

[25] Y. Jiang and J. Grotberg. Bolus contaminant dispersion in oscillatory tube flow with conductive walls. *J. Biomech. Eng.*, 115:424–431, 1993.

[26] M. Lighthill. Initial development of diffusion in poiseuille flow. *IMA J. Appl. Math.*, 2:97–108, 1966.

[27] B. Mazumder and S. Das. Effect of boundary reaction on solute dispersion in pulsatile flow through a tube. *J. Fluid Mech.*, 239:523–549, 1992.

[28] B. Mazumder and K. Mondal. On solute transport in oscillatory flow through an annular pipe with a reactive wall and its application to a catheterized artery. *Q. J. Mech. Appl. Math.*, 58:349–365, 2005.

[29] B. Mazumder and S. Paul. Dispersion in oscillatory couette flow with absorbing boundaries. *Int. J. Fluid Mech. Res.*, 35:475–492, 2008.

[30] B. Mazumder and S. Paul. Dispersion of reactive species with reversible and irreversible wall reactions. *Heat Mass Transfer*, 48:933–944, 2012.

[31] D. McDonald. *Blood flow in arteries.* 2nd ed., Edward Arnold, London, 1974.

[32] C. Mei, J. Auriault, and C. Ng. Some applications of the homogenization theory. *Adv. Appl. Mech.*, 32:278–348, 1996.

[33] C. Mei and B. Vernescu. *Homogenization methods for multiscale mechanics.* World scientific, 2010.

[34] A. Mukherjee and B. Mazumder. Dispersion of contaminant in oscillatory flows. *Acta Mech.*, 74:107–122, 1988.

[35] C. Ng. Chemical transport associated with discharge of contaminated fine particles to a steady open-channel flow. *Phys. Fluids*, 12:136–144, 2000.

[36] C. Ng. Dispersion in sediment-laden stream flow. *J. Eng. Mech.*, 126:779–786, 2000.

[37] C. Ng. A time-varying diffusivity model for shear dispersion in oscillatory channel flow. *Fluid Dyn. Res.*, 34:335–355, 2004.

[38] C. Ng. Dispersion in open-channel flow subject to the processes of sorptive exchange on the bottom and air–water exchange on the free surface. *Fluid Dyn. Res.*, 38:359–385, 2006.

[39] C. Ng. Dispersion in steady and oscillatory flows through a tube with reversible and irreversible wall reactions. *Proc. R. Soc. Lond. A*, 462:481–515, 2006.

[40] C. Ng and Y. Bai. Dispersion in oscillatory couette flow with sorptive boundaries. *Acta Mech.*, 178:65–84, 2005.

[41] C. Ng and N. Rudraiah. Convective diffusion in steady flow through a tube with a retentive and absorptive wall. *Phys. Fluids*, 20:073604, 2008.

[42] C. Ng and T. Yip. Effects of kinetic sorptive exchange on solute transport in open-channel flow. *J. Fluid Mech.*, 446:321–345, 2001.

[43] S. Paul and B. Mazumder. Dispersion in unsteady couette–poiseuille flows. *Int. J. Eng. Sci.*, 46:1203–1217, 2008.

[44] S. Paul and B. Mazumder. Transport of reactive solutes in unsteady annular flow subject to wall reactions. *Eur. J. Mech. B-Fluid*, 28:411–419, 2009.

[45] S. Paul and B. Mazumder. Effects of nonlinear chemical reactions on the transport coefficients associated with steady and oscillatory flows through a tube. *Int. J. Heat Mass Transf.*, 54:75–85, 2011.

[46] D. Peaceman and H. Rachford, Jr. The numerical solution of parabolic and elliptic differential equations. *J. Soc. Ind. Appl. Math.*, 3:28–41, 1955.

[47] C. Phillips and S. Kaye. Approximate solutions for developing shear dispersion with exchange between phases. *J. Fluid Mech.*, 374:195–219, 1998.

[48] C. Phillips, S. Kaye, and C. Robinson. Time-dependent transport by convection and diffusion with exchange between two phases. *J. Fluid Mech.*, 297:373–401, 1995.

[49] A. Purnama. Boundary retention effects upon contaminant dispersion in parallel flows. *J. Fluid Mech.*, 195:393–412, 1988.

[50] A. Purnama. The dispersion of chemically active solutes in parallel flow. *J. Fluid Mech.*, 290:263–277, 1995.

[51] G. Ramon, Y. Agnon, and C. Dosoretz. Solute dispersion in oscillating electro-osmotic flow with boundary mass exchange. *Microfluid. Nanofluid.*, 10:97–106, 2011.

[52] R. Revelli and L. Ridolfi. Influence of suspended sediment on the transport processes of nonlinear reactive substances in turbulent streams. *J. Fluid Mech.*, 472:307–331, 2002.

[53] R. Revelli and L. Ridolfi. Transport of reactive chemicals in sediment-laden streams. *Adv. Water Resour.*, 26:815–831, 2003.

[54] R. Sankarasubramanian and W. Gill. Unsteady convective diffusion with interphase mass transfer. *Proc. R. Soc. Lond. A*, 333:115–132, 1973.

[55] A. Sarkar and G. Jayaraman. The effect of wall absorption on dispersion in annular flows. *Acta Mech.*, 158:105–119, 2002.

[56] A. Shankar and A. Lenhoff. Dispersion and partitioning in short coated tubes. *Ind. Eng. Chem. Res.*, 30:828–835, 1991.

[57] R. Smith. Contaminant dispersion in oscillatory flows. *J. Fluid Mech.*, 114:379–398, 1982.

[58] R. Smith. The contraction of contaminant distributions in reversing flows. *J. Fluid Mech.*, 129:137–151, 1983.

[59] R. Smith. Effect of boundary absorption upon longitudinal dispersion in shear flows. *J. Fluid Mech.*, 134:161–177, 1983.

[60] G. Taylor. Dispersion of soluble matter in solvent flowing slowly through a tube. *Proc. R. Soc. Lond. A*, 219:186–203, 1953.

[61] G. Taylor. Conditions under which dispersion of a solute in a stream of solvent can be used to measure molecular diffusion. *Proc. R. Soc. Lond. A*, 225:473–477, 1954.

[62] P. Wang and G. Chen. Solute dispersion in open channel flow with bed absorption. *J. Hydrol.*, 543:208–217, 2016.

[63] P. Wang and G. Chen. Transverse concentration distribution in taylor dispersion: Gill's method of series expansion supported by concentration moments. *Int. J. Heat Mass Transfer*, 95:131–141, 2016.

[64] P. Wang and G. Chen. Concentration distribution for pollutant dispersion in a reversal laminar flow. *J. Hydrol.*, 551:151–161, 2017.

[65] E. Watson. Diffusion in oscillatory pipe flow. *J. Fluid Mech.*, 133:233–244, 1983.

[66] J. Westhaver. Theory of open-tube distillation columns. *Ind. Eng. Chem.*, 34:126–130, 1942.

[67] Z. Wu and G. Chen. Analytical solution for scalar transport in open channel flow: slow-decaying transient effect. *J. Hydrol.*, 519:1974–1984, 2014.

[68] Z. Wu and G. Chen. Approach to transverse uniformity of concentration distribution of a solute in a solvent flowing along a straight pipe. *J. Fluid Mech.*, 740:196–213, 2014.

[69] Z. Wu and G. Chen. Axial diffusion effect on concentration dispersion. *Int. J. Heat Mass Transf.*, 84:571–577, 2015.

[70] Z. Wu, Z. Li, and G. Chen. Multi-scale analysis for environmental dispersion in wetland flow. *Commun. Nonlinear Sci. Numer. Simul.*, 16:3168–3178, 2011.

[71] Z. Wu, L. Zeng, and G. Chen. Analytical modeling for environmental dispersion in wetland. In *Developments in Environmental Modelling*. Elsevier, pp. 251–274 (Chapter 10), 2014.

[72] Z. Wu, L. Zeng, G. Chen, Z. Li, L. Shao, P. Wang, and Z. Jiang. Environmental dispersion in a tidal flow through a depth-dominated wetland. *Commun. Nonlinear Sci. Numer. Simul.*, 17:5007–5025, 2012.

[73] Z. Yang, S. Matsumoto, H. Goto, M. Matsumoto, and R. Maeda. Ultrasonic micromixer for microfluidic systems. *Sens. Actuators A*, 93:266–272, 2001.

[74] H. Yasuda. Longitudinal dispersion due to the boundary layer in an oscillatory current: theoretical analysis in the case of an instantaneous line source. *J. Oceanogr. Soc. Japan.*, 38:385–394, 1982.

[75] H. Yasuda. Longitudinal dispersion of matter due to the shear effect of steady and oscillatory currents. *J. Fluid Mech.*, 148:383–403, 1984.

[76] L. Zeng, G. Chen, H. Tang, and Z. Wu. Environmental dispersion in wetland flow. *Commun. Nonlinear Sci. Numer. Simul.*, 16:206–215, 2011.

[77] L. Zeng, Y. Zhao, B. Chen, P. Ji, Y. Wu, and L. Feng. Longitudinal spread of bicomponent contaminant in wetland flow dominated by bank-wall effect. *J. Hydrol.*, 509:179–187, 2014.

BIODATA

Current Status

Senior research fellow of Department of Mathematics, Indian Institute of Technology Guwahati, Guwahati 781039, India.

Education

- 2010–2012: **Master of Science** (Mathematics)
  Indian Institute of Technology Madras, Chennai, Tamil Nadu, India.
- 2006–2009: **Bachelor of Science** (Honours in Mathematics)
  Bankura Sammilani College, The University of Burdwan, West Bengal, India.

List of Published and Communicated Papers

- Swarup Barik and D. C. Dalal. Influence of nonlinear chemical reactions on the transport coefficients in oscillatory Couette flow. *J. Phys. Conf. Ser.*, 759 (2016) 012080.
- Swarup Barik and D. C. Dalal. On transport coefficients in an oscillatory Couette flow with nonlinear chemical decay reactions. *Acta Mech.* 228 (2017) 2391-2412.
- Swarup Barik and D. C. Dalal. Transverse concentration distribution in an open channel flow with bed absorption: A multi-scale approach. *Commun. Nonlinear Sci. Numer. Simul.* 65 (2018) 1-19.
- Swarup Barik and D. C. Dalal. Multi-scale analysis for concentration distribution in an oscillatory Couette flow. *Proc. R. Soc. Lond. A* 475 (2019) 20180483.
- Swarup Barik and D. C. Dalal. Solute dispersion in an open channel flow with sorptive channel bed. (communicated).